CREEP OF COMPACTED CLAY

JULY 1971 — NUMBER 12

BY

S. V. RAMASWAMY

JHRP

JOINT HIGHWAY RESEARCH PROJECT

PURDUE UNIVERSITY AND

INDIANA STATE HIGHWAY COMMISSION

71-12

Progress Report

CREEP OF COMPACTED CLAYS

TO: J. F. McLaughlin, Director
Joint Highway Research Project

July 7, 1971

File No.: 6-6-6

FROM: H. L. Michael, Associate Director
Joint Highway Research Project

Project No.: C-36-5F

The attached Progress Report titled "Creep of Compacted Clays" is submitted in partial fulfillment of the objectives of the HPR-1 (8), Part II research project titled "Study of Long-Term Deformation of Compacted Cohesive Soil Embankments". The report has been authored by Mr. S. V. Ramaswamy, Graduate Instructor in Research on our staff under the direction of Professor W. H. Perloff.

The objectives of this research was to establish a useful description of the time-dependent stress-strain behavior of compacted cohesive soils which could be incorporated in an analysis of boundary value problems in soil mechanics. Important findings are given in the report which are applicable to this objective.

As this is an HPR project, copies will also be forwarded to the ISHC and the FHWA for review, comment and acceptance.

Respectfully submitted,

Harold L. Michael

Harold L. Michael
Associate Director

HLM:ms

cc: F. L. Ashbaucher
W. L. Dolch
W. H. Goetz
W. L. Grecco
M. J. Gutzwiller
G. K. Hallock
M. E. Harr
R. H. Harrell
M. L. Hayes
E. M. Mikhail
R. D. Miles
J. W Miller
C. F. Scholer
M. B. Scott
W. T. Spencer
N. W. Steinkamp
H. R. J. Walsh
K. B. Woods
E. J. Yoder

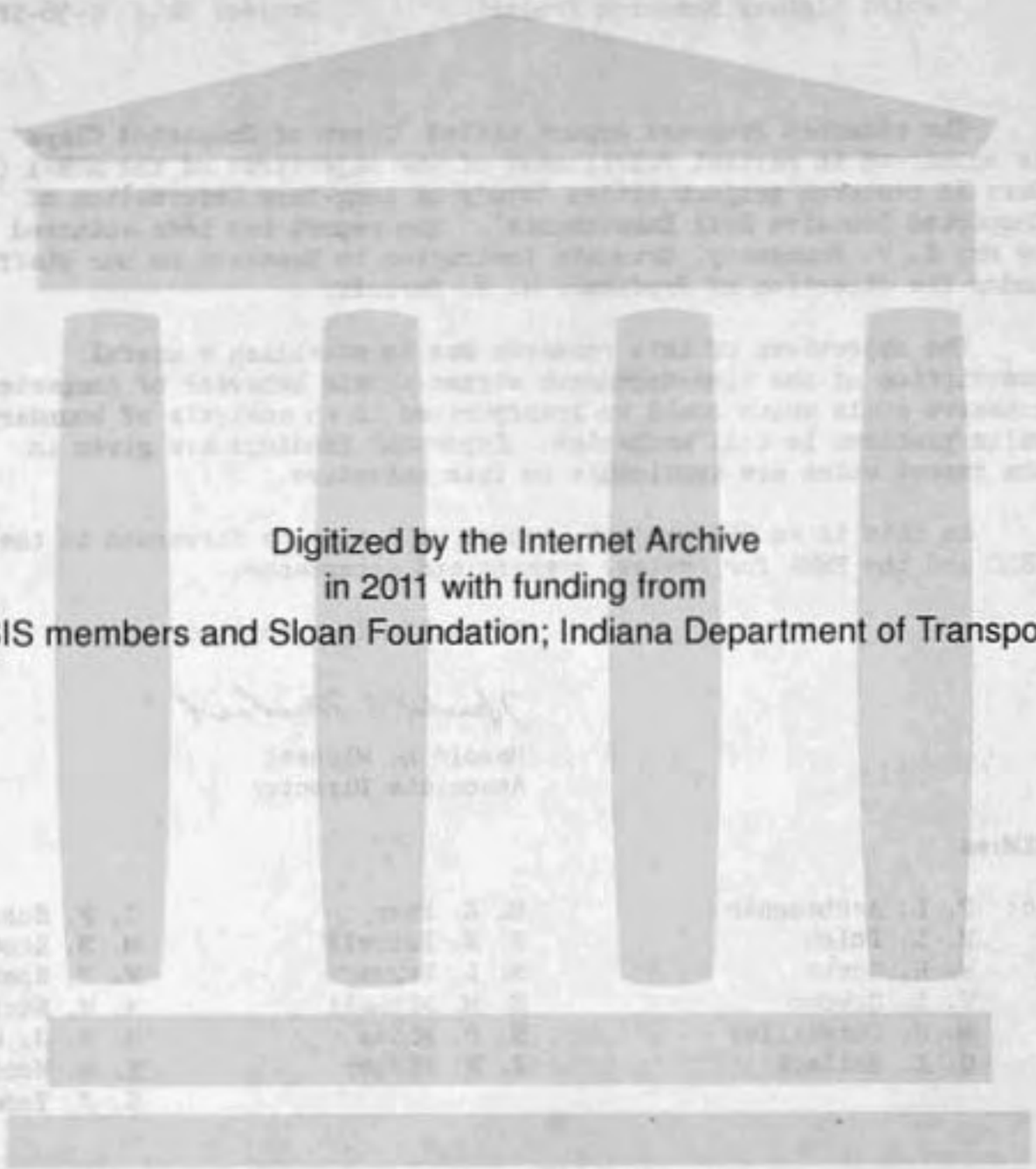

Progress Report

CREEP OF COMPACTED CLAYS

by

S. V. Ramaswamy
Graduate Instructor in Research

Joint Highway Research Project
File: 6-6-6
Project: C-36-5F

Prepared as Part of an Investigation

Conducted by

Joint Highway Research Project
Engineering Experiment Station
Purdue University

in cooperation with the

Indiana State Highway Commission

and the

U.S. Department of Transportation
Federal Highway Administration

Purdue University
Lafayette, Indiana
July 7, 1971

ACKNOWLEDGMENTS

The author wishes to express his sincerest appreciation to his advisor, Dr. W. H. Perloff for his valuable advice, constant encouragement and constructive criticism during the course of this research and in the preparation of this thesis.

The author is deeply indebted to Professor R. A. Schapery for his helpful and stimulating discussions.

Special thanks are due to Mr. W. DeGroff for his invaluable assistance during the experimental work.

The author is very grateful to Joint Highway Research Project for the financial support which made this research possible.

TABLE OF CONTENTS

TABLE OF CONTENTS, cont.

TABLE OF CONTENTS, cont.

LIST OF TABLES

LIST OF TABLES, cont.

LIST OF FIGURES

LIST OF FIGURES, cont.

LIST OF FIGURES, cont.

LIST OF FIGURES, cont.

LIST OF SYMBOLS

A - projected value of strain rate at zero deviator stress on the logarithm strain rate versus deviator stress plot for unit time.

a_σ - stress dependent shift factor.

$B(t)$ - bulk creep compliance

c - the maximum shear creep strain at unit time.

D - deviator stress $(\sigma_1-\sigma_3)$

D_{max} - strength of soil measured at the beginning of creep

$\bar{D}$ - stress level (D/D_{max})

D_o - initial creep compliance

D_1 - linear viscoelastic creep compliance

$D(t)$ - creep compliance

E - modulus of elasticity

$E(t)$ - relaxation modulus

G - shear modulus

$G(t)$ - shear relaxation modulus

g_o, g_1, g_2 - stress dependent shift factors

$J(t)$ - shear creep compliance

J_o' - linear viscoelastic normalized shear creep compliance

LIST OF SYMBOLS, cont.

J_1' - normalized shear creep compliance at one minute

$J'(t)$ - normalized shear creep compliance

$k(t)$ - bulk relaxation modulus

k - linear viscoelastic shear creep compliance

R_1 - stress-strength ratio $(\tau_{oct})/(\tau_{oct})_f$

R_o - τ_m/τ_f, constant

t - any time "t"

v - initial volume

Δv - change in volume

a, b, k_o, k_1, m, n - constants

$\bar{\alpha}$ - value of slope of the mid range linear portion of logarithm strain rate versus deviator stress plot

γ oct - octahedral shear strain

γ max - maximum shear strain

ϵ_1, ϵ_3, ϵ_{kk} - principal strains

ϵ_{ij} $(i \neq j)$ - shear strains

ϵ - axial strain

$\dot{\epsilon}$ - strain rate at any time "t"

ϵ_r - recovery creep strain

ϵ_c - creep strain

$-\epsilon_3/\epsilon_1$ - principal strain ratio

$\bar{\epsilon}$ - volumetric strain $(\epsilon_1+\epsilon_2+\epsilon_3)$

ν - Poisson's ratio

σ_1, σ_2, σ_3, σ_{RR} - principal stresses

LIST OF SYMBOLS, cont.

σ_{ij} $(i \neq j)$ - shear stresses

$\bar{\sigma}$, $(\sigma_{oct})_n$ - spherical stress, $(\sigma_1+\sigma_2+\sigma_3)/3$

σ_r - radial stress

$(\sigma_1-\sigma_3)$ - deviator stress

$(\sigma_1-\sigma_3)_f$ - deviator stress at failure

τ_{oct} - octahedral shear stress

$(\tau_{oct})_f$ - octahedral shear stress at failure corresponding

τ_e, τ_m - constants

ψ, ψ' - reduced time

ABSTRACT

Ramaswamy, S. V., Ph.D., Purdue University, June 1971. Creep of Compacted Clays. Major Professor: William H. Perloff.

The research was initiated to establish a useful description of the time-dependent stress-strain behavior of compacted cohesive soils, which could be incorporated in an analysis of boundary value problems in soil mechanics.

Experimental investigations of time-dependent shear strain characteristics of two compacted cohesive soils under a step deviator stress load were conducted using triaxial compression creep tests. The creep response for the second and subsequent cycles of loading was defined. It was found that the relation between maximum shear strain and time could be expressed in a power law form.

The influence of confining pressure and moisture content were accounted for by expressing the creep parameters of the compacted cohesive soil as a function of the ratio between octahedral shear stress and the octahedral shear stress at failure corresponding to the existing octahedral normal stress. A normalized shear creep compliance which is independent of confining pressure and moisture content was established.

Non-linear viscoelastic constitutive equations based upon the principle of irreversible thermodynamics were found applicable to the description of the creep and recovery response of the compacted cohesive soil in the laboratory. The non-linear effects were time-independent. It was shown that the parameters obtained for the small samples were also valid for large structures, provided that the effective stresses are approximately equal to the applied stresses. In many cases, this condition will be satisfied if the compaction moisture content is below Proctor optimum and the confining pressure does not exceed about 8 kg/cm^2.

A plane strain footing test in which the stress field was different from that existing in the tests used to evaluate the creep parameters was conducted. The footing test was analyzed using the finite element method which took into account the non-linearity and time dependence of the soil behavior. Close agreement between predicted and observed displacements was obtained.

Extension creep tests and hydrostatic compression test results indicated that compacted soils behaved as anisotropic materials. The importance of this effect to the prediction of embankment performance remains to be assessed.

1. INTRODUCTION

Any descriptive model which purports to predict the deformation of a material body subjected to a set of internal and boundary loading must include some description of the material of which the body is composed. Such a description, the material characterization or constitutive law, is necessarily a simplification of reality. But it is important to select a constitutive law containing those factors germane to the problem at hand, since the outcome of an analysis depends to a great extent on this description. For example, simplified assumptions of linear elastic theory have been found extremely useful for computing the distribution of vertical stresses in a cohesive soil mass. But when considering time-dependent deformations of such a mass, however, a time-independent constitutive relation is clearly inapplicable.

Solutions that have been obtained for boundary value problems using nonlinear constitutive relations for saturated or partly saturated earth materials employ parameters pertaining to the particular environmental conditions existing for that problem. Generally, the emphasis in such studies has been more on the analytical method than on the characterization of the material.

In this study an attempt is made to characterize compacted cohesive soil as a nonlinear viscoelastic material. The importance of the failure strength in normalizing the stress-strain behavior under different confining pressures and moisture contents is stressed. The suitability of a generalized constitutive relationship developed on the basis of irreversible thermodynamics for delineating the non-linear time-dependent stress-strain behavior of compacted cohesive soil was studied. Stress dependent viscoelastic parameters obtained from triaxial creep tests were used to predict the time-dependent displacement of a plane strain strip footing, for which the stress field was different from the axisymmetric conditions existing in the laboratory tests.

2. REVIEW OF LITERATURE

2.1 Volume Change Characteristics of Partly Saturated Cohesive Soils

There have been numerous experimental and theoretical investigations of volume change characteristics of saturated clays since Terzaghi published his theory of one-dimensional consolidation. However, consolidation of partly saturated soils has received relatively little attention.

Alpan (1961) introduced a modified time factor ρT in the Terzaghi equation to describe consolidation of partly saturated soils. The factor ρ is a function of degree of saturation, change in volume of pore air and the change in volume of the soil sample. However he did not take into account the change in properties of the fluid and the skeleton during the process of consolidation.

Yoshimi and Osterberg (1963) performed extensive experiments on the one-dimensional compression of partly saturated soils. They concluded that there was virtually no outflow of pore water during compression, even when the degree of saturation was about ninety per cent. Since the pore water movement was negligible, the time rato of compression was governed by the rheological characteristics of the soil skeleton. Hence the time rate of compressive

strain was independent of the drainage conditions or thickness of the specimen, but did depend on the stress increment ratio.

Teerawong (1963) investigated consolidation of soils compacted dry of optimum[1]. He assumed that the air voids in the soil specimen were completely interconnected and only air escaped from the soils during consolidation. He obtained an expression for time-dependent compression taking into account the compressibility of air, solubility of air in water, and assuming viscous resistance only for the soil skeleton. Danielson (1963) extended this work to include permanent shearing resistance of the skeleton as well as viscous response.

Barden (1965) developed a series of nonlinear partial differential equations for the one-dimensional consolidation of partly saturated soils, the range of degree of saturation varying from zero to one hundred per cent. Based on the degree of saturation, he classified any particular consolidation process into one of five idealized processes from extremely dry clays (degree of saturation less than fifty per cent) to very wet clays (degree of saturation greater than ninety per cent). To solve the equations, he assumed linear relationships between pore water pressure and permeability, between pore water pressure and density of pore

---

1. Optimum moisture content is not unique for a particular soil, but is dependent on the type and amount of compactive effort used.

fluid and between pore water pressure and porosity. His results suggest that for clays compacted wet of optimum, the variation in permeability during consolidation has a more important effect on the process than the compressibility of the pore fluid.

The importance of degree of saturation to air permeability was shown by Langfelder, Chen and Justice (1968) who found that the air permeability of cohesive soils was affected by water content, dry density, and the method of compaction. The changes in air permeability as water content was increased were small on the dry side of optimum water content, until the water content reached the optimum moisture content, when it became essentially zero. They concluded that as the water content increased, the connecting necks between larger air pores tended to close and the continuous passage for air to flow through ceases to exist. The phenomenon of occlusion takes place and the air permeability becomes negligible. But as Matyas (1969) has pointed out, three of the five soils tested in the above program exhibited some permeability to air at compaction water contents at or beyond optimum water content. Hence it is evident that air permeability may be small at optimum water content but not essentially zero. The comments of Yoshimi and Osterberg (1963) that one cannot exclude the possibility that near the optimum water content the air voids can be partly

interconnected and partly isolated, seem particularly valid in this respect.

Toriyama and Sawada (1968) studied the one-dimensional consolidation characteristics of partly saturated soils compacted wet of optimum. They derived an equation which takes into account the compressibility of the pore fluid, changes in permeability with degree of saturation and effective stress, as well as changes in compressibility of the skeleton with effective stress. They solved the derived equation numerically, and found that the pore water pressure set up by loading depended on the compressibility of the soil skeleton and the degree of saturation.

The existence of air in addition to water in the pores of partly saturated soils makes the study of their behavior extremely complicated. Furthermore, relatively few experimental investigations concerning volume change characteristics have been undertaken. The analytical efforts have been concerned with describing soil response under one-dimensional conditions. Without further information, however, the results of one-dimensional analyses and experiments cannot be extrapolated to the more general problem of interest herein.

2.2 Pore Pressure in Compacted Soils

Hilf (1956) conducted an extensive study of the pore fluid pressures in partly saturated soils and was the first

to measure directly the negative pore water pressure in compacted soils. He developed the axis translation technique to permit measurement of capillary pressures less than one atmosphere below zero gage, and found a large negative pore water pressure in soils compacted near the optimum water content. The axis translation technique, described in detail by Hilf (1956), has been extensively used since then.

Lambe (1961) investigated the variation of the magnitude of negative pore water pressure in compacted cohesive soils with degree of saturation. He concluded that the degree of saturation was an important factor in the magnitude of negative pore water pressure and that there was a marked decrease in the magnitude of the negative pressure as the degree of saturation was increased to one hundred per cent.

Olsen and Langfelder (1965) have reported negative pore pressures as low as -100 psi for plastic clays compacted two per cent dry of optimum water content. Samples of Grundite clay compacted at 127 psi had pore water pressures lower than -250 psi when the moisture contents were only five per cent less than the optimum moisture content. They also pointed out that consideration of the osmotic pressures near clay particle surfaces lead to the conclusion that the actual pore water pressures in unsaturated soil varied from approximately -1 atmosphere to high positive values.

Schuurmann(1966) assumed that pore air formed bubbles in pore water and obtained a relation between the pore air pressure u_a and the pore water pressure u_w. He showed that as the air bubble size decreased, there is an increase in the value of $(u_a - u_w)$.

Matyas and Radhakrishna (1968) subjected cylindrical samples to all round pressure and to zero radial strain (K_o) loading. They concluded that the principle of effective stress was not adequate to explain the volumetric behavior of partly saturated soils subjected to different stress paths.

Except for the influence of the degree of saturation on the magnitude of initial negative pore water pressure, the influence of other factors like pore size distribution is unknown. Furthermore, neither the magnitude of developed pore water pressure in response to loading, nor the relationship between effective stresses and mechanical behavior of unsaturated compacted clays is understood. Thus, the applicability of the effective stress principle to such materials cannot be demonstrated at the present time.

2.3 Shear Deformation Studies of Cohesive Soils

Rheological models which can be visualized as linear springs in combination with linear or nonlinear dashpots have been extensively used to characterize the time-dependent shear deformation behavior of clays. Murayama

and Shibata (1961) analyzed results of a number of triaxial creep tests taking into account the effect of temperature. Christensen and Wu (1964) have made use of the rate process theory of Eyring to determine the parameters of their rheological model and this gives a fairly accurate description of the creep behavior of clays under some ranges of loading.

Various experimental studies have been conducted to develop an understanding of the basic mechanisms contributing to the shearing resistance of soils and the factors that control the time-dependent responses to stress and strain. Mitchell (1964) used the rate process theory to relate the shearing resistance of soils in triaxial compression tests to frictional and cohesive parameters, effective stress, soil structure, rate of strain and temperature. He showed that his derived equation yielded reasonable results if reasonable values were assumed for the unknown parameters.

Mitchell and Campanella (1963) and Mitchell et. al. (1969) developed a working hypothesis based on the rate process theory, which relates creep rate to soil properties and applied stress. However the practical utility of the expressions developed by them remains doubtful, since they have not indicated any reliable method for accurately evaluating the various parameters involved in their equations.

Singh and Mitchell (1968) proposed a simple phenomenological relationship for the stress-strain-time behavior of soils, valid for a range of creep stresses varying from 30 per cent to 90 per cent or more of the initial strength, as follows:

$$\dot{\epsilon} = Ae^{\bar{\alpha}\bar{D}}(t_1/t)^m \qquad (2\text{-}1)$$

where

$\dot{\epsilon}$ = strain rate at any time t;

A = projected value of strain rate at zero deviator stress on the logarithm strain rate versus deviator stress plot for unit time;

α = value of slope of the mid-range linear portion of logarithm strain rate versus deviator stress plot;

$\bar{\alpha}$ = αD_{max};

D_{max} = strength of soil measured at the beginning of creep;

$\bar{D}$ = stress level = D/D_{max};

D = deviator stress $(\sigma_1 - \sigma_3)$;

t_1 = unit time;

t = any time, t;

m = slope of logarithm strain rate versus logarithm time.

According to them the same basic form of relationship is applicable, irrespective of whether the clays are undisturbed or remolded, wet or dry, normally consolidated

or overconsolidated, or tested drained or undrained. But most of the data presented pertained to undrained tests and secondary compression part of the drained tests. Walker (1969) has questioned the validity of the proposed three parameter equation for the entire spectrum of macroscopic response of clay structure to an applied stress system. He felt that the parameters A, α, and m are likely to be functions of the testing conditions. He concluded that any generalized relationship should include all the variables involved in the deformation process (i.e.) volumetric strain, shear strain and pore water pressure and their variation with applied stress and time.

Lara-Tomas (1962) subjected hollow cylindrical specimens of compacted soil to constant shear stresses and studied their creep behavior. He concluded that suitable rheological models can be evolved to fit the data.

Perloff (1966) conducted extensive triaxial creep tests on compacted cohesive soils and obtained a relation between the shear strain and time as follows:

$$(\epsilon_1 - \epsilon_3) = at^b \qquad (2\text{-}2)$$

where

ϵ_1 = axial strain,

ϵ_3 = lateral strain;

a,b = constants;

He concluded that "b" could be taken as essentially constant, irrespective of stress-level, confining pressure and moisture content and that by expressing "a" as a function of the ratio between the stress level and the failure stress, the effects of moisture content and confining pressure could be removed.

Pagen and Jagannath (1967, 1968) concluded that compacted cohesive soils can be treated as linear viscoelastic materials within a given range of stress and strain depending on the environmental condition and compaction methods.

They expressed the strain-time response by the relation

$$\epsilon = ct^m \qquad (2\text{-}3)$$

where

ϵ = axial strain;

t = time;

c, m = constants.

Sankaran (1966) conducted one-dimensional consolidation tests on saturated soils, and triaxial creep tests on partly saturated soils. Based on his test results, he proposed a generalized stress-strain-time relationship for compacted soils relating octahedral shear stress and octahedral shear strain.

For principal stresses applied to the coordinate directions, the octahedral shear stress is,

$$\tau_{oct} = \frac{1}{3}\left[(\sigma_1-\sigma_2)^2 + (\sigma_2-\sigma_3)^2 + (\sigma_3-\sigma_1)^2\right]^{\frac{1}{2}} \qquad (2\text{-}4)$$

since $\sigma_2 = \sigma_3$ in both the triaxial and one-dimensional consolidation tests,

$$\tau_{oct} = \frac{\sqrt{2}}{3}(\sigma_1 - \sigma_3) . \qquad (2\text{-}5a)$$

Also

$$\tau_{max} = \frac{1}{2}(\sigma_1 - \sigma_3) \qquad (2\text{-}5b)$$

Similarly the octahedral shear strain and maximum shear strain are, respectively,

$$\gamma_{oct} = \frac{2\sqrt{2}}{3}(\epsilon_1 - \epsilon_3) \qquad (2\text{-}6a)$$

and

$$\gamma_{max} = (\epsilon_1 - \epsilon_3) \qquad (2\text{-}6b)$$

So it is obvious that a relationship postulated between octahedral shear stress and shear strain is equally valid for the maximum shear stress and strain. In one dimensional consolidation both volumetric strain and shear strain can be expressed in terms of axial strain as follows:

$$\text{volumetric strain} = \frac{\Delta V}{V} = \epsilon_1 + \epsilon_2 + \epsilon_3 = \epsilon_1 \qquad (2\text{-}7)$$

since $\epsilon_2 = \epsilon_3 = 0$

$$\gamma_{max} = \epsilon_1 - \epsilon_3 = \epsilon_1 \qquad (2\text{-}8)$$

Hence it appears that additional experimental evidence is needed to make critical checks on the generality of the proposed relationships.

Use of Linear Viscoelasticity

There has been a recent emphasis on applications of the principles of viscoelasticity to represent the time-dependent nature of cohesive soils. Elastic concepts of soil behavior have proved extremely useful in the determination of stress distribution within the soil mass under various loading conditions. Application of concepts of viscoelasticity is the logical next step if soil is considered as a material having time-dependent properties.

By using the principle of superposition, the linear viscoelastic behavior of any material can be expressed by hereditary integrals. For example, in the case of uniaxial stresses and strains,

$$\varepsilon(t) = \int_{-\infty}^{t} D(t-\tau) \frac{d\sigma(\tau)}{d\tau} d\tau \qquad (2\text{-}9)$$

or

$$\sigma(t) = \int_{-\infty}^{t} D(t-\tau) \frac{d\varepsilon(\tau)}{d\tau} d\tau \qquad (2\text{-}10)$$

where

$D(t-\tau)$ = uniaxial creep compliance function;

$E(t-\tau)$ = uniaxial relaxation modulus function;

ε, σ, t = uniaxial strain, uniaxial stress, and time, respectively.

These integral equations are known as Duhamel integrals and have long been known in mathematics. Each of these equations can be derived from the other, based on the assumption that

$$\varepsilon(\tau) = 0; \quad \sigma(\tau) = 0 \quad \tau < 0 \tag{2-11}$$

Then it can be shown

$$E(0)\, D(t) = 1 + \int_{0^+}^{t} D(\tau)\, \frac{dE(t-\tau)}{d(t-\tau)}\, d\tau \tag{2-12}$$

where

$E(0)$ = initial value of the relaxation modulus;

$D(t)$ = creep compliance.

It is obvious that the above equation holds even if D and E are interchanged.

Considering a uniaxial compression creep test with constant stress σ_o applied at $t = 0$ to an initially unstressed and unstrained body, i.e.,

$$\sigma(0^-) = \varepsilon(0^-) = 0 \tag{2-13}$$

then

$$\varepsilon(t) = \sigma_o\, D(0) + \sigma_o \int_{0^-}^{t} \frac{dD(t-\tau)}{d(t-\tau)}\, d\tau \tag{2-14}$$

In a general state of stress and strain in three dimensions for an isotropic medium, two operators are required to describe the stress-strain relationship for a linear viscoelastic material (Lee, 1956). Generally in viscoelastic analysis, to separate the volumetric and distortional responses, they are chosen as the bulk relaxation modulus (or bulk creep compliance) and the shear relaxation modulus (or bulk creep compliance). The general stress-strain-time equations can be written as,

$$\sigma_{ij} = 3[K(0)\,\varepsilon_{kk}(t) - \int_0^t \varepsilon_{kk}(\tau)\,\frac{dK(t-\tau)}{d(t-\tau)}\,d\tau]\,\delta_{ij} + 2[G(0)\,\varepsilon_{ij}(t) - \int_0^t \varepsilon_{ij}(t)\,\frac{dG(t-\tau)}{d(t-\tau)}\,d\tau] \quad (2\text{-}15)$$

or

$$\varepsilon_{ij} = \tfrac{1}{3}\,[B(0)\,\sigma_{kk}(t) - \int_0^t \sigma_{kk}(\tau)\,\frac{dB(t-\tau)}{d(t-\tau)}\,d\tau]\,\delta_{ij} + \tfrac{1}{2}\,[J(0)\,\sigma_{ij}(t) - \int_0^t \sigma_{ij}(\tau)\,\frac{dJ(t-\tau)}{d(t-\tau)}\,d\tau] \quad (2\text{-}16)$$

where

K = the bulk relaxation modulus;

G = the shear relaxation modulus;

B = the bulk creep compliance;

J = the shear creep compliance;

σ_{ij} = component of the stress tensor;

ε_{ij} = component of the strain tensor;

δ_{ij}, Kronecker delta = $\begin{matrix} 0 \\ 1 \end{matrix}\Big]\begin{matrix} i \neq j \\ i \neq j \end{matrix}$

repeated subscript implies summation over entire range.

Nonlinear Viscoelastfcity

Many viscoelastic materials encountered in engineering applications do not exhibit linear behavior. Some polymers and concrete respond nonlinearly at high strains, while soils show marked nonlinearity even at low stresses and

strains (Mitchell et al, 1968). The integral representation of constitutive equations can still be used and the nonlinear functional can be written (Leaderman, 1962) for uniaxial loading as,

$$\sigma(t) = \int_{-\infty}^{t} E(t-\tau) \frac{dg[e(\tau)]}{d\tau} d\tau \qquad (2\text{-}17)$$

where

$g[e(\tau)]$ = a function of the history of strain "e";

$E(t)$ = relaxation function.

One other way of integral representation (Soussou and Moavenzadeh, 1970), in which the kernal is modified, is

$$\sigma(t) = \int_{-\infty}^{t} E(t-\tau),\ e(\tau) \frac{de(\tau)}{d\tau} d\tau \qquad (2\text{-}18)$$

where

the relaxation function is a function of $(t-\tau)$ and $e(\tau)$.

One of the most widely used representatives for nonlinear viscoelastic behavior is that of Green and Rivlin (1957). For the uniaxial, isotropic case, for instance, creep response can be written as the sum of multiple integrals:

$$\sigma(t) = E_o\sigma(t) + \sum_{n=1}^{\infty} \int_{\infty}^{t} \cdots \int_{\infty}^{t} K_n(t-\tau_1, \ldots t-\tau_n)$$

$$\varepsilon(\tau_1)\ldots\varepsilon(\tau_n)\, d\tau_1 \ldots d\tau_n \qquad (2\text{-}19)$$

where

σ = uniaxial stress;

ϵ = uniaxial strain;

k_n = scalar relaxation functions;

E_o = measures the instantaneous stress.

For practical purposes only a finite number of terms can be used in this multiple integral expansion and hence this is mostly used for weakly nonlinear materials.

Thermodynamic Approach

The thermodynamics of irreversible processes has been made use of by Biot (1958) to develop a theory of linear irreversible phenomena. He derived the linear equations governing the general inhomogeneous thermodynamic system which is in the neighborhood of a stable equilibrium state. He showed that they can be used to derive linear stress-strain equations of anisotropic, isothermal, viscoelastic materials and to deduce variational principles.

Schapery (1964, 1966a, 1966b, 1969a, 1969b) has extended the use of thermodynamic concepts applied by Biot to derive constitutive equations for nonlinear viscoelastic materials. His theory (1969a, 1969b) is developed using stress as independent state variables and the state of strain is expressed in stress and temperature histories. Introduction of special forms of entropy production and Gibbs free energy based on observed nonlinear response of the materials enabled him to derive constitutive equations

of a single integral type similar to the Boltzmann superposition integral with the nonlinear material properties expressed as functions of stress and temperature. This leads to relations in which the only time-dependent parameters entering are the linear viscoelastic creep compliances. For the one-dimensional, isothermal case of uniaxial loading the nonlinear constitutive equation can be written as (Schapery, 1969a),

$$\varepsilon(t) = g_o D_o \sigma + g_1 \int_0^t \Delta D(\psi-\psi') \frac{dg_2\sigma}{d\tau} d\tau \qquad (2\text{-}20)$$

where

D_o, $\Delta D(\psi)$ = components of linear viscoelastic creep compliance;

ψ = the reduced time defined by

$$\psi = \int_0^t \frac{dt'}{a_\sigma} \quad a_\sigma > 0 \qquad (2\text{-}20a)$$

$$\psi' = \psi(\tau) = \int_0^\tau \frac{dt'}{a_\sigma} \quad a_\sigma > 0 \qquad (2\text{-}20b)$$

where

$$a_\sigma = f[\sigma(t')]$$

and the material properties g_o, g_1, g_2 are functions of stress only.

Schapery (1969b) and Lou and Schapery (1969) have used creep and recovery data to evaluate these properties, by means of a graphical procedure. These stress dependent

roperties have specific thermodynamic significance;
hanges in g_o, g_1 and g_2 reflect third and higher order
ependence of the Gibbs energy on the applied stress and
$_\sigma$ arises from similar higher order effects in both
ntropy production and free energy.

2.4 Solution of Boundary Value Problems for Earth Materials

Analytical solutions have been obtained for various
oundary value problems of interest in soil engineering
ased on linear elasticity or viscoelasticity. But it is
xtremely difficult to obtain a closed form solution for
boundary value problem, if the real boundaries and actual
oading conditions existing in the field have to be taken
nto account. If in addition, the soil properties also
ary either in space or with time, the solution becomes
till more difficult.

Some of the difficulties in obtaining realistic
olutions to actual problems can be overcome by resorting
o numerical methods. The more versatile methods can take
nto consideration the actual boundary conditions, soil
roperties and spatial variation in soil properties. A
umped parameter model was used to solve the problem of a
trip footing on an idealized elastic-plastic soil (Hoeg,
t al, 1968). This model generated central finite difference
pproximations to the differential equations of equilibrium.

Another approach, the finite element method is extremely versatile for solving stress and deformation problems in the field and has been extensively dealt with in the literature (Wilson, 1965; Zienkiewicz and Cheung, 1967). Numerous soil mechanics and rock mechanics problems have been analyzed using this approach. These include: the stresses and deformations within an earth embankment constructed of compacted clay having nonlinear stress-strain characteristics (Clough and Woodward, 1967); the problem of a circular footing resting on homogeneous layer of clay having nonlinear stress-strain characteristics (Girijavallabhan and Reese, 1968); the problem of a strip footing and also a circular footing resting on two layers of clays, each having different nonlinear stress-strain characteristics (Radhakrishnan and Reese, 1969; Desai and Reese, 1970); the problem of initial deformation of a strip footing resting on saturated clay having bilinear stress-strain characteristics and a yield strength dependent on the orientation of principal stresses (D'Appolonia and Lambe, 1970); the problem of deformation of tunnels within a rock mass (Perloff, 1969). The finite element method has also been used to solve problems, where the material properties are time-dependent. Zienkiewicz et al (1968) have used this method to solve some problems in concrete and rock structures in which the materials were considered to be linear

viscoelastic. Their method can also be applied to non-linear viscoelastic materials.

It is to be pointed out that in almost all the work referred to in the previous paragraph, the emphasis was more on the mode of analysis than on the material characterization. Each problem has been treated as an individual, isolated case and virtually no attempt was made to enumerate a realistic constitutive relationship for the material, applicable to environmental conditions other than the problem considered. It is felt that accurate delineation of material characteristics have to be given more importance than has been the case hitherto if realistic predictions are to be obtained in soil mechanics field problems.

2.5 Objective of Study

From the brief review presented it appears that a generalized stress-strain-time relation for compacted clays, suitable for prediction of the response of a body of such material to imposed loadings is not available at the present time. It is the objective of this study to develop such a generalized constitutive relation for compacted clays, and to demonstrate its applicability to the prediction of behavior of a mass of material subjected to boundary loads.

3. EXPERIMENTAL PROCEDURE FOR CREEP TESTS

3.1 Soils Studied

Two commercially available soils, "Edgar Plastic Kaolin (EPK)" and "Grundite" were used in this study. The kaolin is a moderately well crystallized kaoline mined in Edgar, Florida by the Edgar Plastic Kaolin Company. The grundite was processed by the Illinois Clay Products Company and its clay fraction is primarily illite (Olsen and Langfelder, 1965). The classification properties are given in Table 1 and in Figure 3-1.

One of the advantages in using such commercially mined soils of this type is that large quantities of the material with minimal variation of the material properties can be obtained.

3.2 Preparation of Soil

Batches of soil were prepared by mixing about 3000 grams of soil (kaolin or grundite) with the required amount of water for the desired moisture content in a "liquid-solids twin shell Blender" manufactured by the Patterson-Kelley Company for about 20 minutes (Figure 3-2). The mixed soil was then stored in air tight plastic bags or containers in a one hundred per cent humitidy room for

Table 1

Classification Properties of Grundite and Edgar Plastic Kaolin

	Grundite	Edgar Plastic Kaolin
Liquid Limit (%)	56.0	59.0
Plastic Limit (%)	32.0	37.0
Plasticity Index (%)	24.0	22.0
Specific Gravity of Solids	2.79	2.6
Clay Fraction (% < 0.002 mm)	64.0	81.0

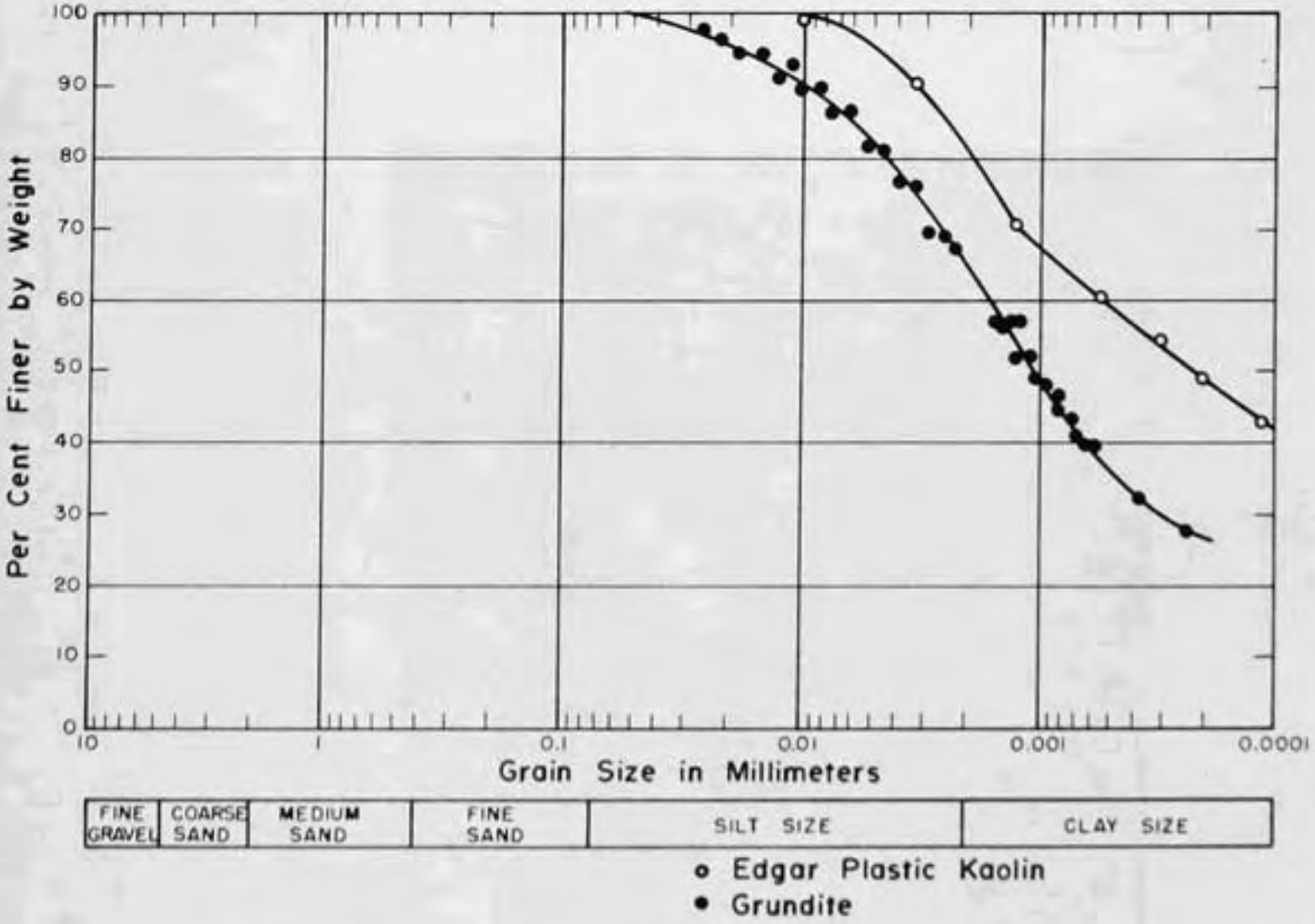

Figure 3.1 - Grain Size Distribution for Edgar Plastic Kaolin and Grundite (Perloff, 1966)

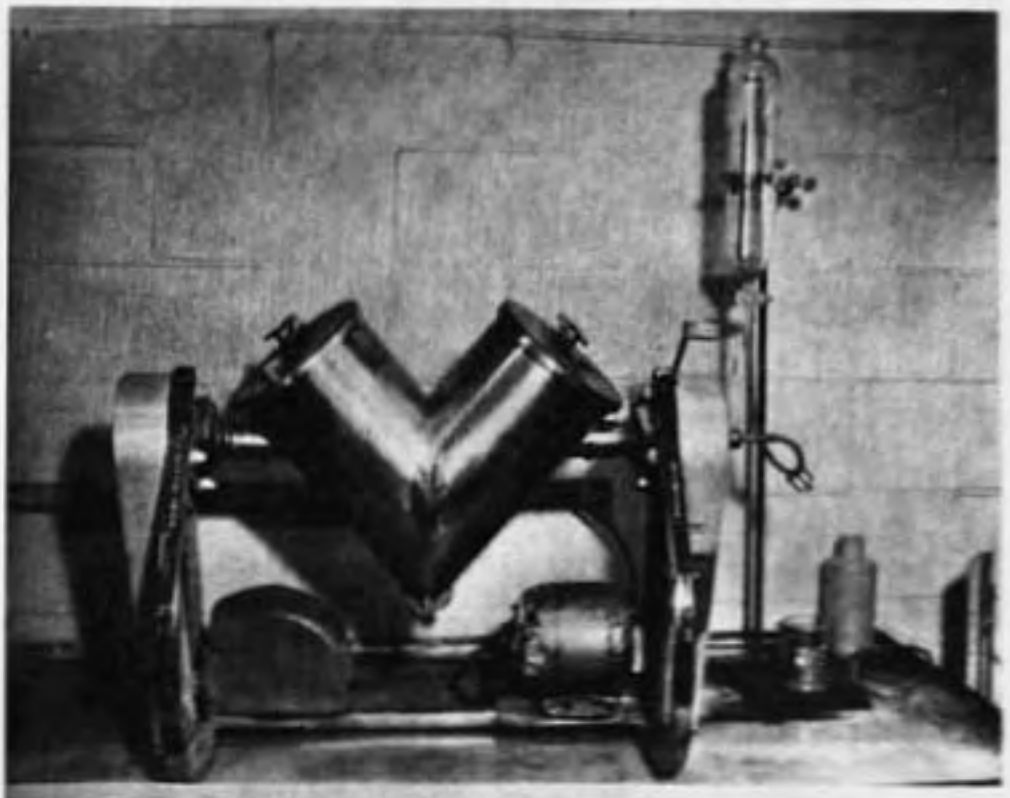

Figure 3-2. Liquid-Solids Twin Shell Blender.

about a week to allow for migration and uniform distribution of moisture content throughout the soil.

3.3 Preparation of Compacted Specimens

Test specimens for the triaxial creep tests were 2.81 inches high and 1.31 inches in diameter and were prepared at the desired moisture content by both kneading and impact compaction.

Kneading compaction was accomplished with a Harvard miniature compaction equipment (Figure 3-3). Specimens were compacted in five layers with 20 tamps of the spring loaded compactor per layer. Compactive forces varied from twenty to sixty pounds. The impact compaction was performed with a special drop hammer weighing 3.62 pounds and falling ten inches (Figure 3-3). The specimens were prepared in three layers with total compactive efforts ranging from 30 to 135 blows. Impact and kneading compaction curves for both grundite and EPK are shown in Figures 3-4, 3-5, 3-6 and 3-7.

The amount of soil to be added to each layer was predetermined by preliminary trials. The sides of the compaction mold were lubricated with silicone oil to facilitate extrusion of the compacted specimen with the least disturbance. The top of each layer was scarified before the succeeding layer was compacted. After being extruded from the mold the sample was weighed and placed in a polythene plastic sandwich bag, which was then coated with a mixture of paraffin wax and petrolatum. The compacted specimens were stored in

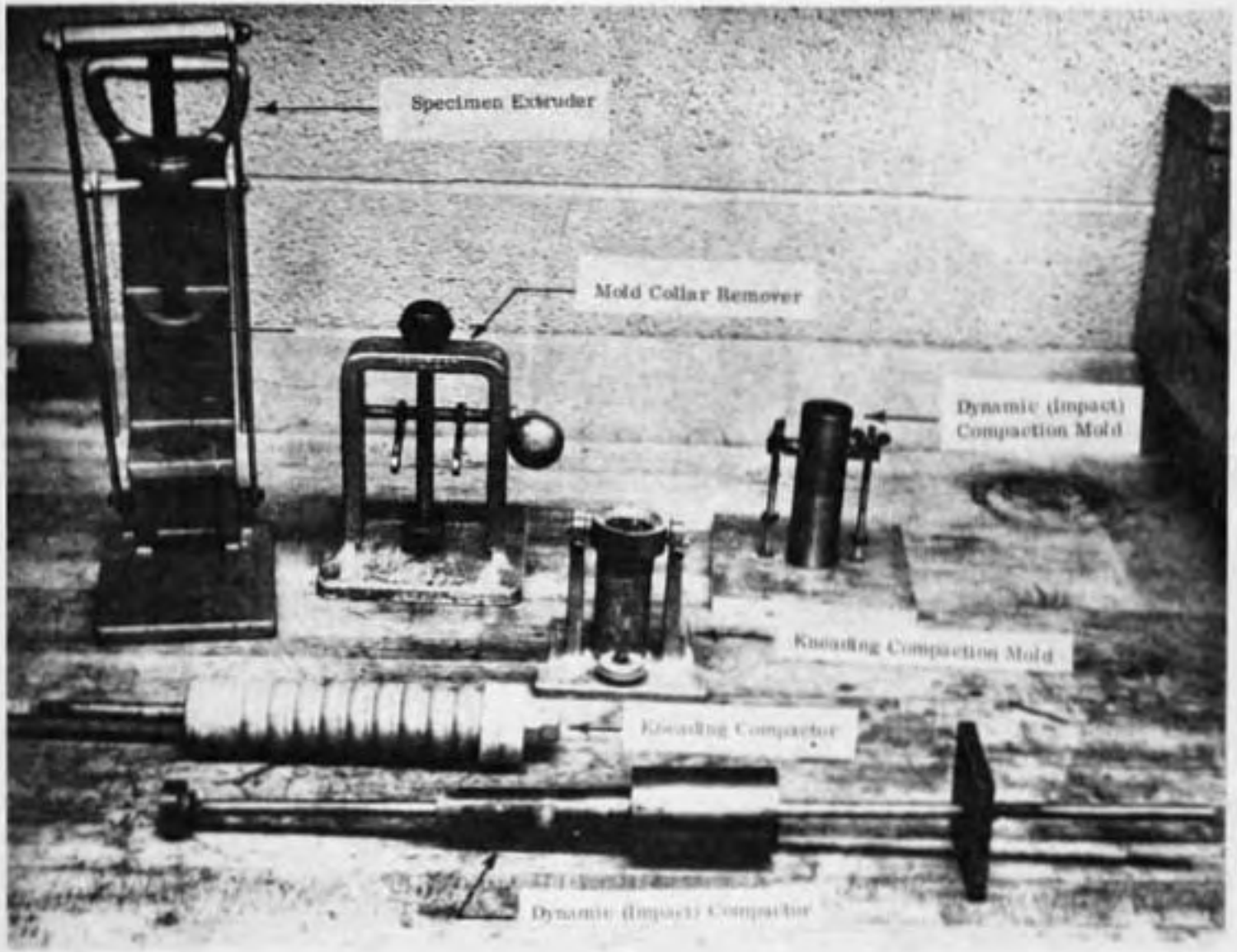

Figure 3-3. Compaction Apparatus.
(Perloff, 1966)

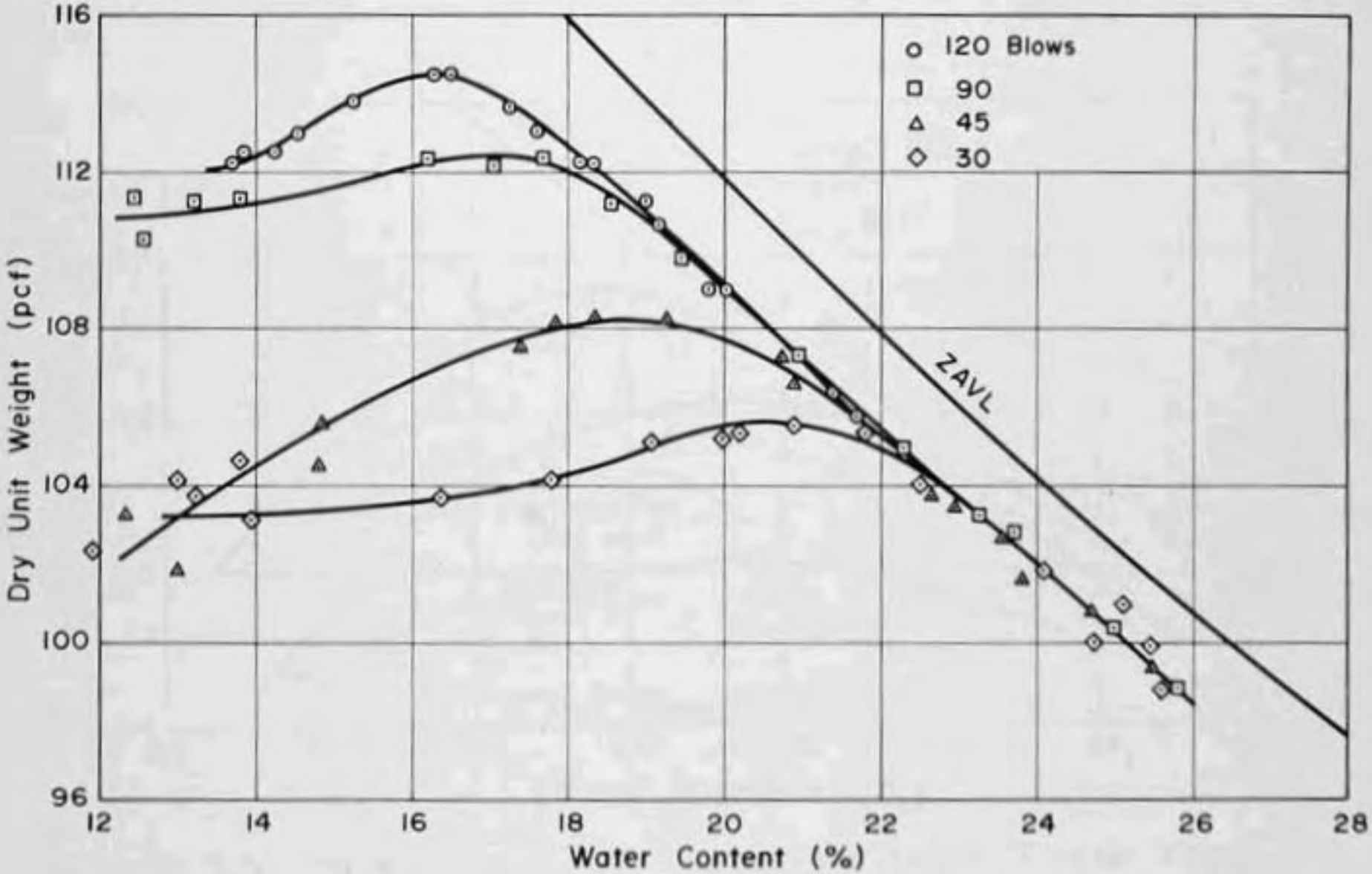

Figure 3.4 - Impact Compaction Curves for Grundite
(Perloff, 1966)

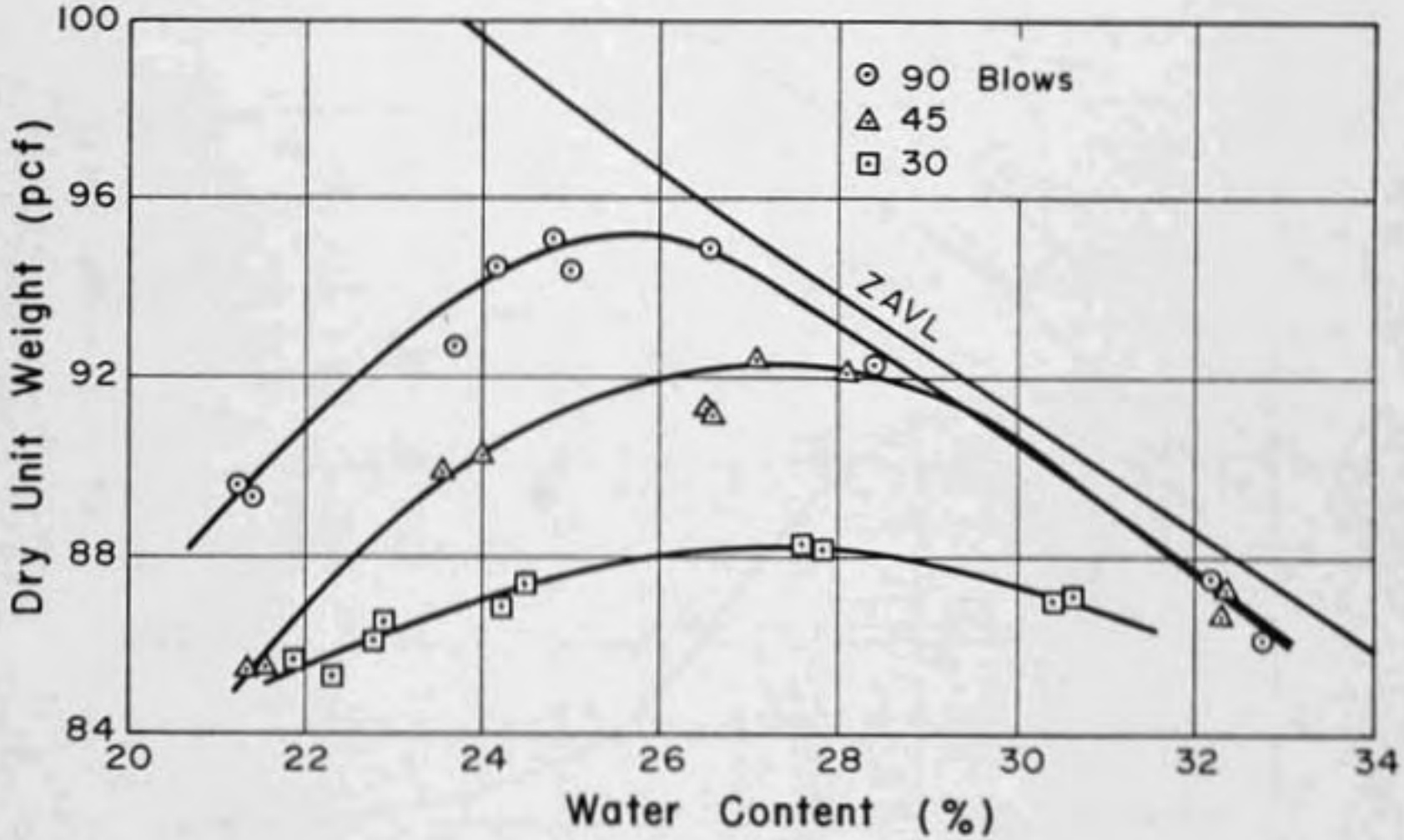

Figure 3.5 - Impact Compaction Curves for Edgar Plastic Kaolin (Perloff, 1966)

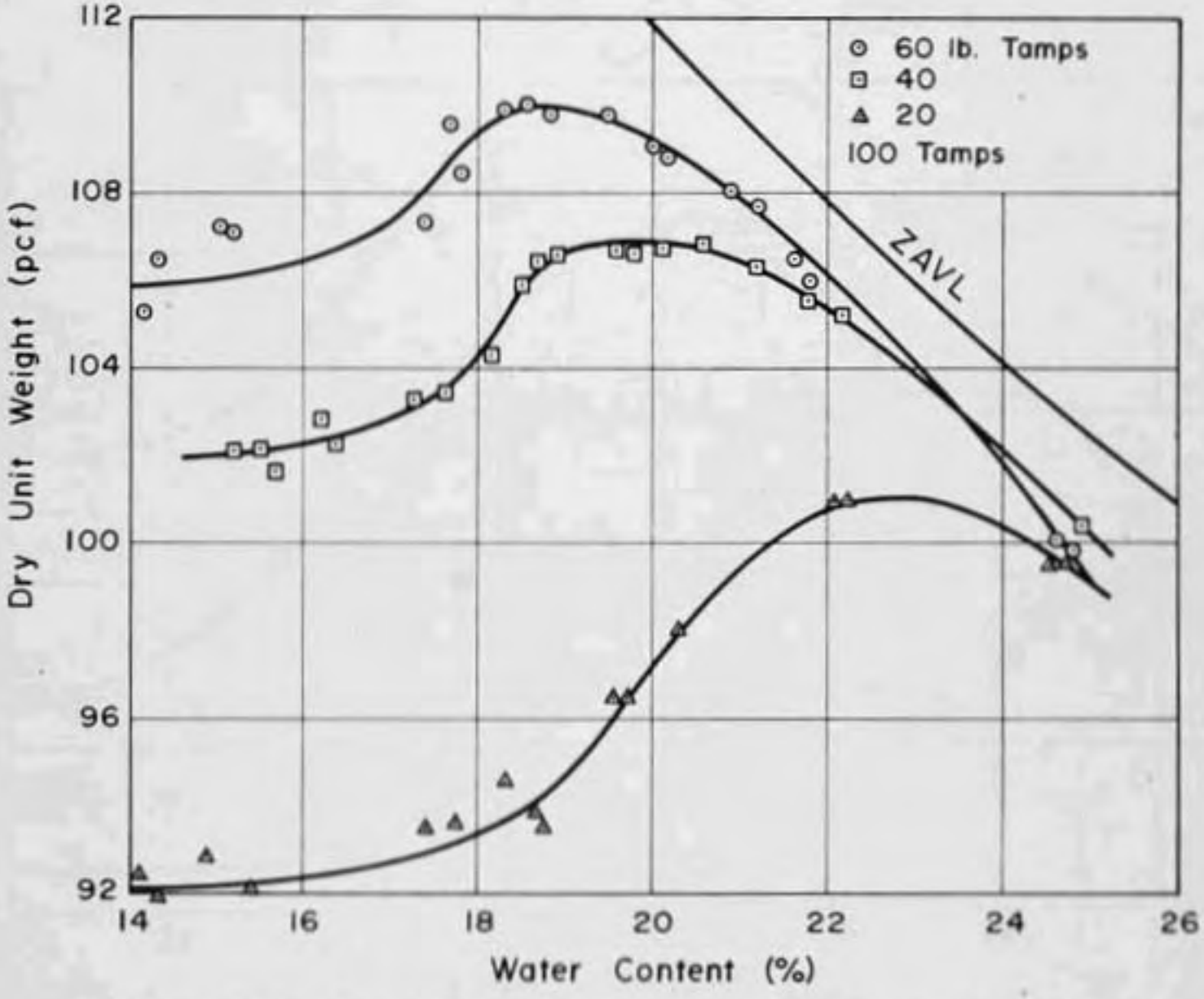

Figure 3.6 - Kneading Compaction Curves for Grundite (Perloff, 1966)

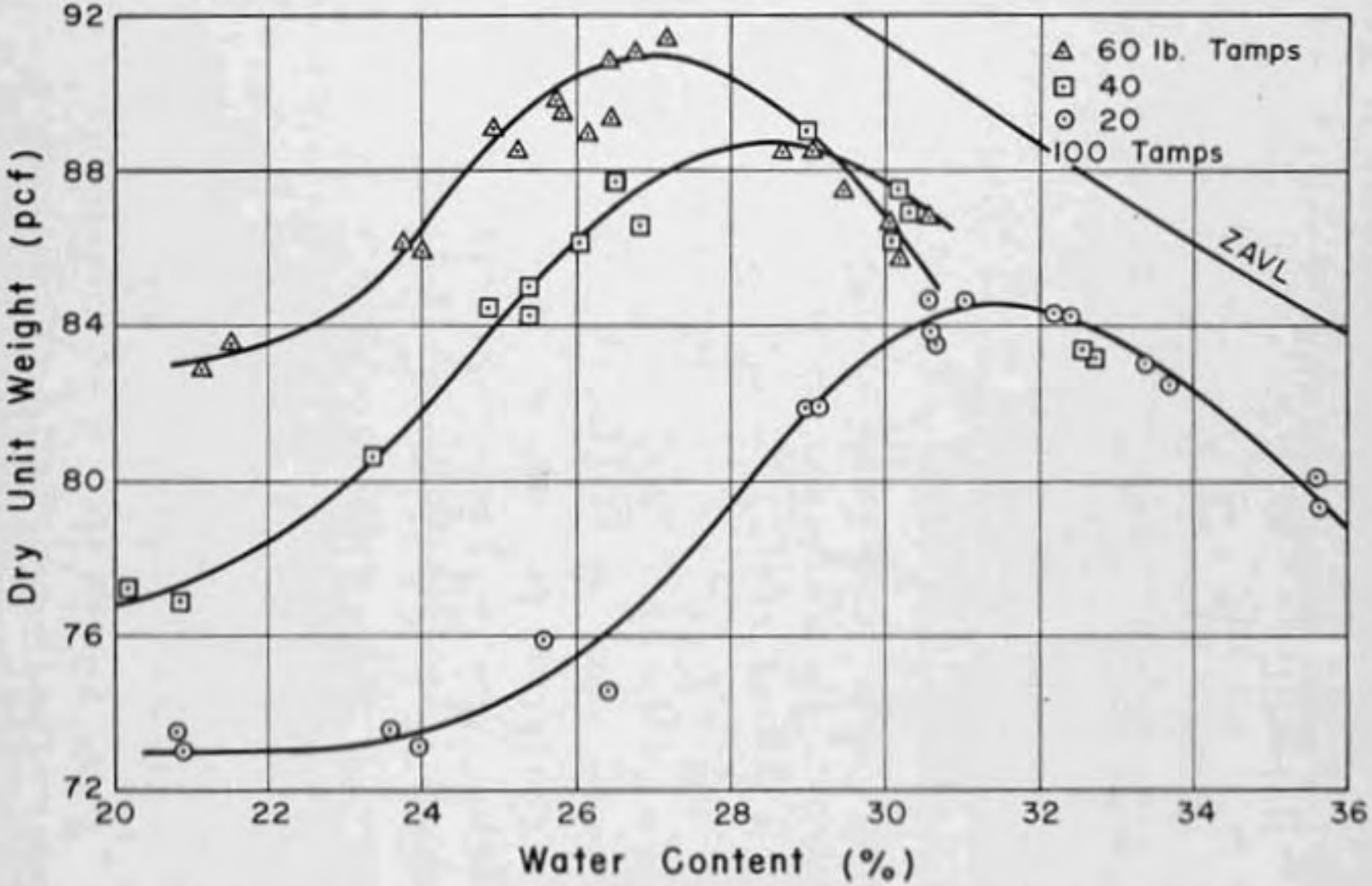

Figure 3.7 - Kneading Compaction Curves for Edgar Plastic Kaolin
(Perloff, 1966)

desiccator jars for at least ten days; the bottom of the desiccator jars were filled with water to ensure one hundred per cent humidity.

The various laboratory compaction procedures mentioned above have been developed basically to simulate a compaction as similar as practicable to the ones used in the field. Various investigators have compared the salient properties between field and laboratory compacted samples. Walker and Holtz (1953) simulated the sheepsfoot compaction method in the laboratory by a special apparatus, and their results indicated that the moisture-dry density curves obtained by the standard laboratory impact compaction methods are similar to those obtained by sheepsfoot compaction. Casagrande and Hirschfield (1960) have shown that by altering the number of layers and number of blows per layer in the Harvard miniature compaction apparatus, a laboratory moisture-density curve can be fitted to the field curve. Holtz and Ellis (1963) conducted laboratory shear tests on compacted soil specimens cut from blocks obtained in the field, as well as on specimens of the soil molded by the standard impact method. Their tests indicated that the strengths of soils compacted by the standard laboratory and field methods are quite close, perhaps even within range of experimental errors. Based on their study of the results of tests conducted at Waterways Experiment Station (1949), Wahls and Langfelder (1967) felt that the stress strain

characteristics of kneading compacted samples would be similar to field compacted samples.

Specimens for laboratory studies on compacted cohesive soils are generally obtained by compacting them in layers by static, kneading or impact methods (Leonards, 1955; Seed et. al, 1960; Casagrande and Hirschfield, 1960; Barden and Sides, 1970). In this study impact and kneading compaction methods were chosen with the belief that the results would be generally applicable to field structures.

3.4 Experimental Apparatus

Triaxial compression equipment in which both axial and radial displacement could be recorded as continuous functions of time was developed by Perloff (1966). Figure 3-8 shows the salient details of the setup. Some of the important accessaries of the assembly are described below.

The triaxial compression chamber used in this study was of "Norwegian" variety manufactured by Geonor (Andresén and Simons, 1960). The confining pressure was applied to the chamber fluid, water, by a small piston-loaded constant pressure cell. An approximately one-half inch deep layer of oil was mafntained at the top of the cell in order to lubricate the vertical piston with which the axial load was applied to the specimen. The piston was lapped in a rotating ball bearing bushing which was continuously rotated by a small motor via a flexible cable.

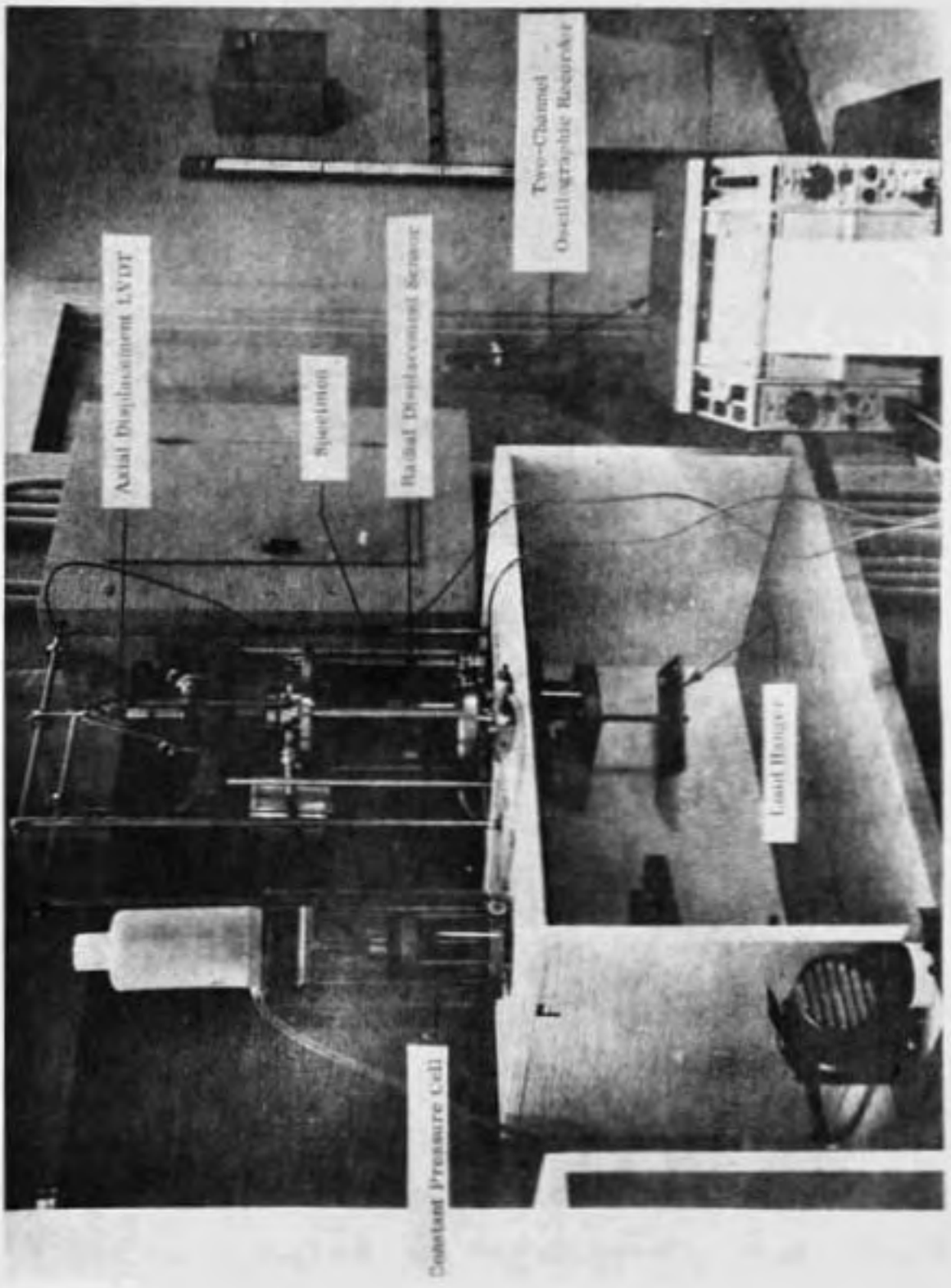

Figure 3-8. Experimental Set Up For Creep Tests. (Sankaran, 1966)

The triaxial cell was mounted on a loading frame in such a manner that an axial load could be applied to the piston by placing weights on the load hanger. This permitted compensation of the upward pressure on the piston due to chamber pressure as well as application of additional axial load for creep testing. In order to apply a step load nearly instantaneously, and yet smoothly without impact, the required weights were supported just above the load hanger by four posts which extend from a plate attached to a hydraulic jack underneath the load hanger. The weights were lowered until they were almost in contact with the loading hanger, at which point the jack piston was fixed in position. At the instant of loading the hydraulic pressure release valve in the jack was opened and the weights contacted the load hanger, applying the load through the piston to the specimen.

The axial or vertical deformation of the specimen was determined by measuring the vertical movement of the cross-bar which applied loads to the piston of the triaxial compression chamber. The sensor utilized was a Daytronic model 103C - 200 linear variable differential transformer (LVDT). This device converts displacements into an electrical signal which can be continuously recorded.

The radial deformation in the specimen was measured by a device which is a modification of one suggested by Bishop and Henkel (1962). A schematic diagram of the radial

displacement sensor is shown in Figure 3-9. A photograph of the device mounted on the base of the triaxial compression cell prior to the placing of the outer chamber is shown in Figure 3-10. The main feature of this device was an International Resistance Company miniature LVDT which converts movement of the two arms in contact with the specimen into an electrical output signal. The stiffness of the spring in the LVDT assembly as well as the tension of the rubber bands could be adjusted so that pressure exerted by the pads on the specimen is sufficient to maintain contact during the testing. The hinges at the junction of the supporting rod and brass collars were lubricated with a thin machine oil to ensure the free movement of the movable arm.

The recording equipment used was a two channel "Oscillo/riter" manufactured by Texas Instruments, Inc. The recording unit excited the axial and radial displacement LVDT and also modulated the signals transmitted by them. The modulated signals were recorded on a two-channel strip chart, so that a continuous record of both the axial and radial displacements was obtained.

3.5 Testing Procedure for Creep Tests

Both the axial and radial displacement LVDT's were calibrated before the start of each creep test. The compacted specimen was then removed from the dessicator,

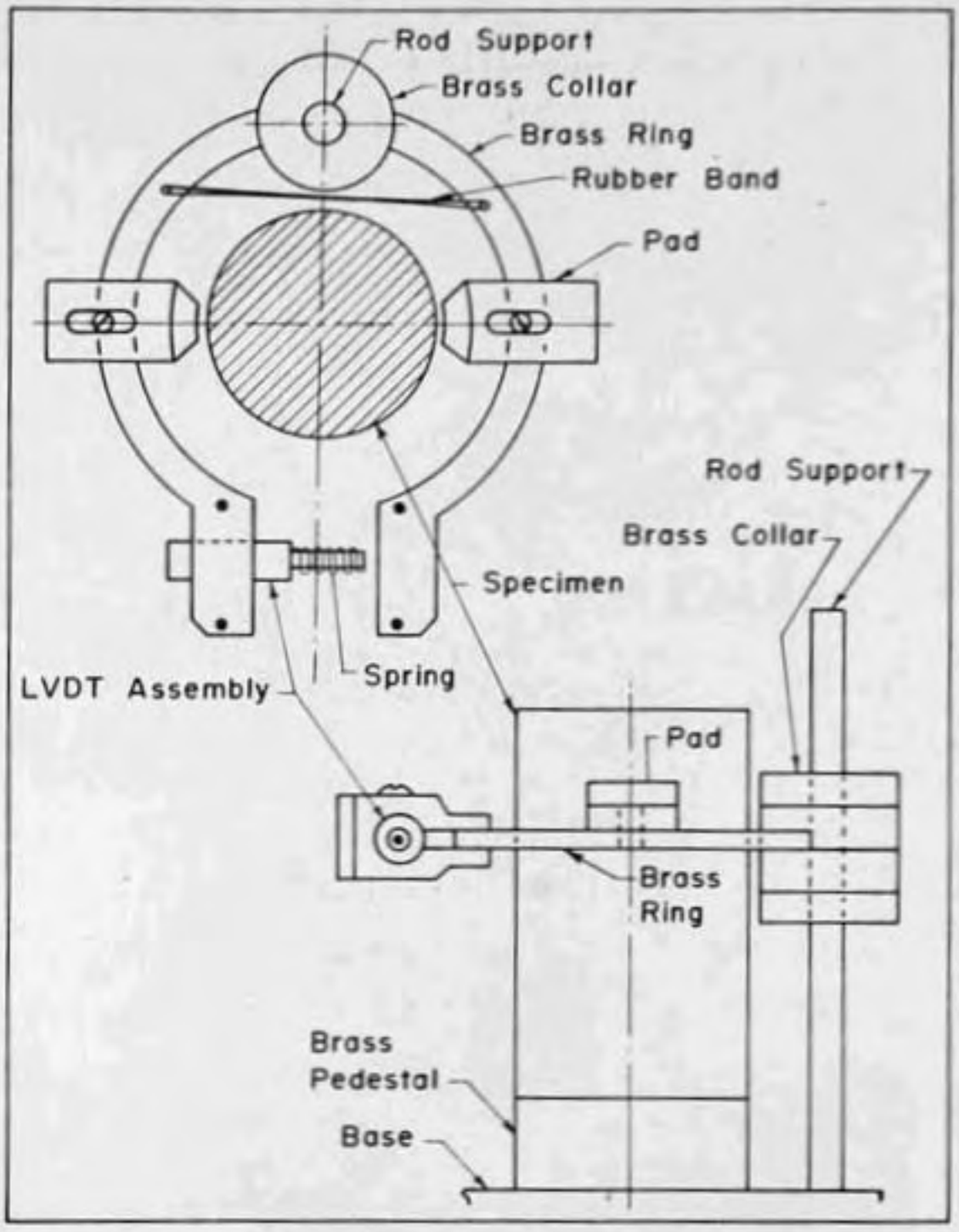

Figure 3.9 - Schematic Diagram of Radial Displacement Sensor and Specimen on Triaxial Cell Base (Perloff, 1966)

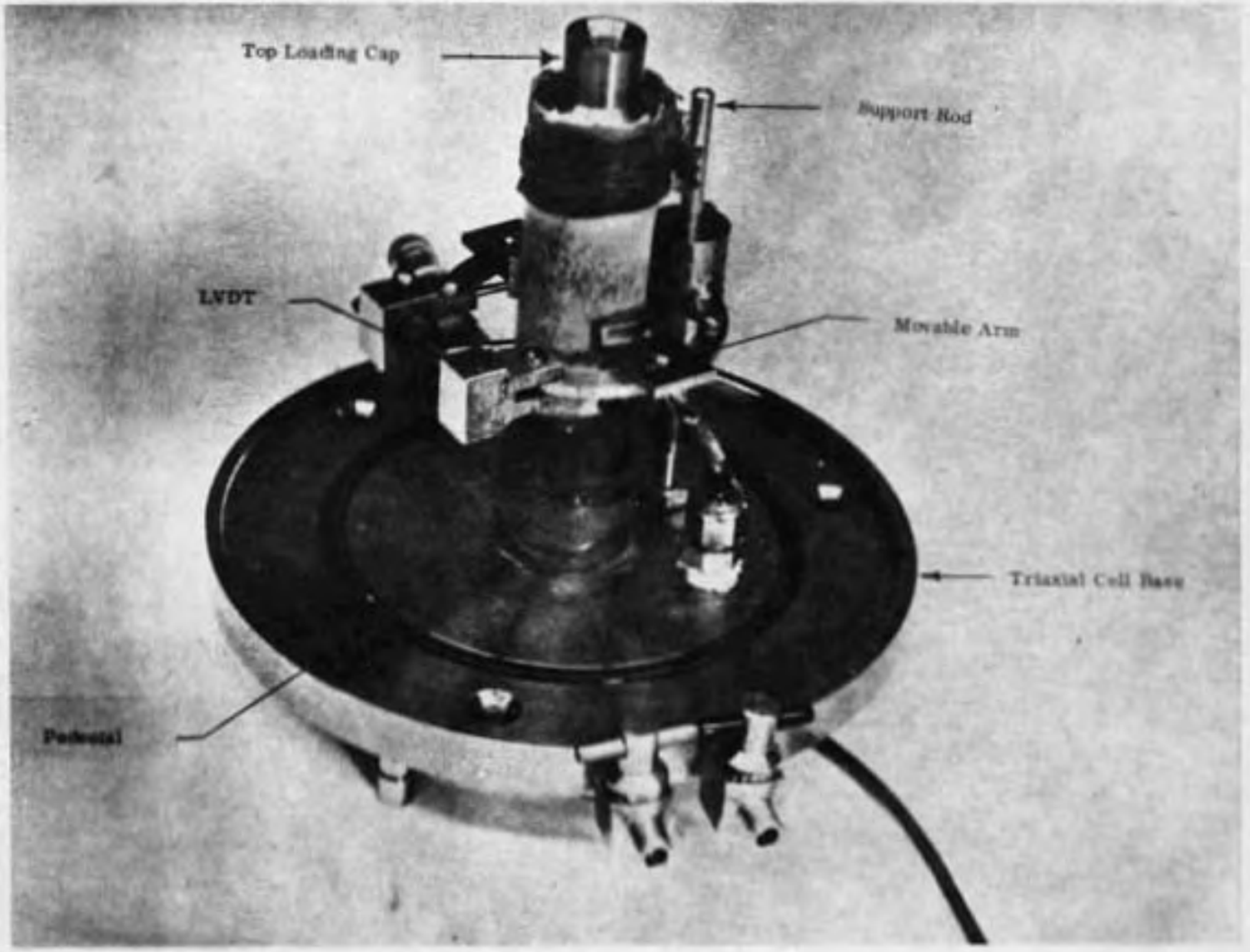

Figure 3-10. Radial Deformation Sensor and Creep Specimen in Position.
(Perloff, 1966)

stripped of its protective plastic cover and placed on a porous stone resting on top of the pedestal of the triaxial cell base. A latex protective membrane 0.006 cm thick was placed around the specimen with a special former designed for this purpose (Figure 3-11). After the top loading cap was placed on the specimen, the rubber membrane was firmly attached to the cap and bottom pedestal with rubber tie strips and silicone grease.

The radial displacement sensor was mounted on the base of the cell. The LVDT assembly was so adjusted that the deformation occurring during the test could be recorded on the strip chart, since it could not be adjusted after the application of the confining pressure to the compression chamber. The outer chamber was then attached to the base of the cell, filled with distilled water and centered on the loading frame. The axial displacement sensor was then mounted on the chamber and its position adjusted so that the deformation occurring during the test could be recorded on the strip chart.

The desired confining pressure was applied to the chamber fluid and, simultaneously, sufficient axial load was placed on the triaxial chamber load hanger to counteract the uplift pressure on the piston. Consolidation was permitted through the open valves connected to the pedestal at the base of the specimen. When deformation due to confining pressure had almost ceased, the desired additional

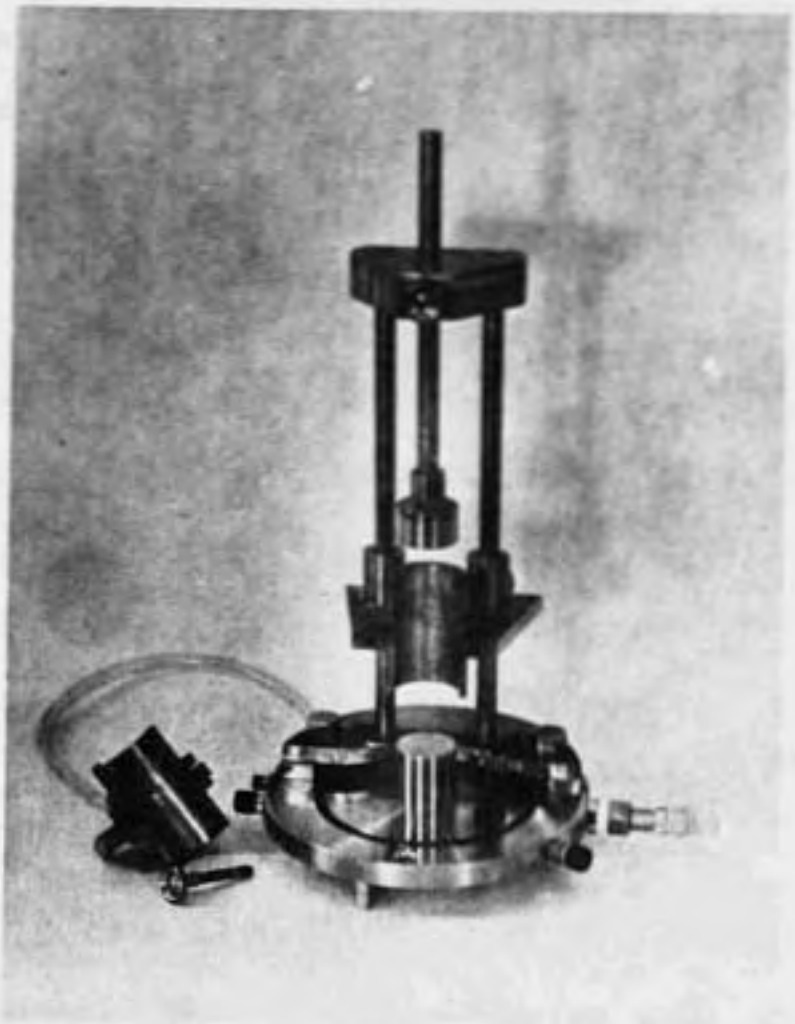

Figure 3-11. Special Former for Mounting the Specimen on Base of Triaxial Cell.
(Perloff, 1966)

axial stress was applied to the piston, as described earlier. This load was left on for the appropriate length of time, generally for one hour, and then removed. The specimen was then allowed to relax for half an hour, by which time essentially all rebound following load removal was completed. For each load level two such cycles of creep and relaxation were generally performed and a continuous record of deformations during the operation was obtained. After the last load and unload cycle, the specimen was failed in compression.

During consolidation and subsequent creep of the specimen during the drained tests, the drainage lines were kept open, and it is possible that a moisture loss of small magnitude occurred through them. However, since the duration of creep tests was only about one hour in most of the experiments, it is unlikely that the change affected the strain readings appreciably.

3.6 Strength Determination

A Model 56 Wykeham Farrance compressive loading device of one ton capacity, in which load was applied at a constant rate of ram movement, was used in determining the strength of samples. Axial displacement was measured with a Federal Dial Gage, Model C8IS-C graduated to 0.001 inch. The displacement rate generally used in testing was 0.03 inches per minute, giving an average axial strain rate

slightly higher than one per cent per minute. Time to failure varied from about 2.5 minutes to about 25 minutes, depending upon the compaction conditions and confining pressure. After each sample was tested to failure, its water content was determined.

4. RESULTS AND DISCUSSION OF CREEP TESTS

4.1 Parameters of Interest

In a general state of stress and strain in three dimensions, for an isotropic material two functionals are needed to establish the relation between the stress tensor and strain tensor.

As has been indicated in section 2-3, many materials respond differently to volumetric and shear effects. Hence it is useful to consider the stresses at a point as the superposition of the spherical stress $\bar{\sigma}$ and the deviatoric stresses $\sigma_{11} - \bar{\sigma}$, $\sigma_{22} - \bar{\sigma}$ and $\sigma_{33} - \bar{\sigma}$ (Figure 4-1). As the sum of the normal stresses in the latter is equal to zero, these stresses produce no volume change if the material is isotropic, nondilatant and not too strongly nonlinear; they produce only distortion. Similarly strain at a point can be thought of as being the sum of pure volume change with no distortion, and a pure distortion with no change in volume. The stress and strain system can be written as

$$\begin{bmatrix} \sigma_{11} & \sigma_{12} & \sigma_{13} \\ \sigma_{21} & \sigma_{22} & \sigma_{23} \\ \sigma_{31} & \sigma_{32} & \sigma_{33} \end{bmatrix} = \begin{bmatrix} \bar{\sigma} & 0 & 0 \\ 0 & \bar{\sigma} & 0 \\ 0 & 0 & \bar{\sigma} \end{bmatrix} + \begin{bmatrix} \sigma_{11}-\bar{\sigma} & \sigma_{12} & \sigma_{13} \\ \sigma_{21} & \sigma_{22}-\bar{\sigma} & \sigma_{23} \\ \sigma_{31} & \sigma_{32} & \sigma_{33}-\bar{\sigma} \end{bmatrix} \quad (4\text{-}1)$$

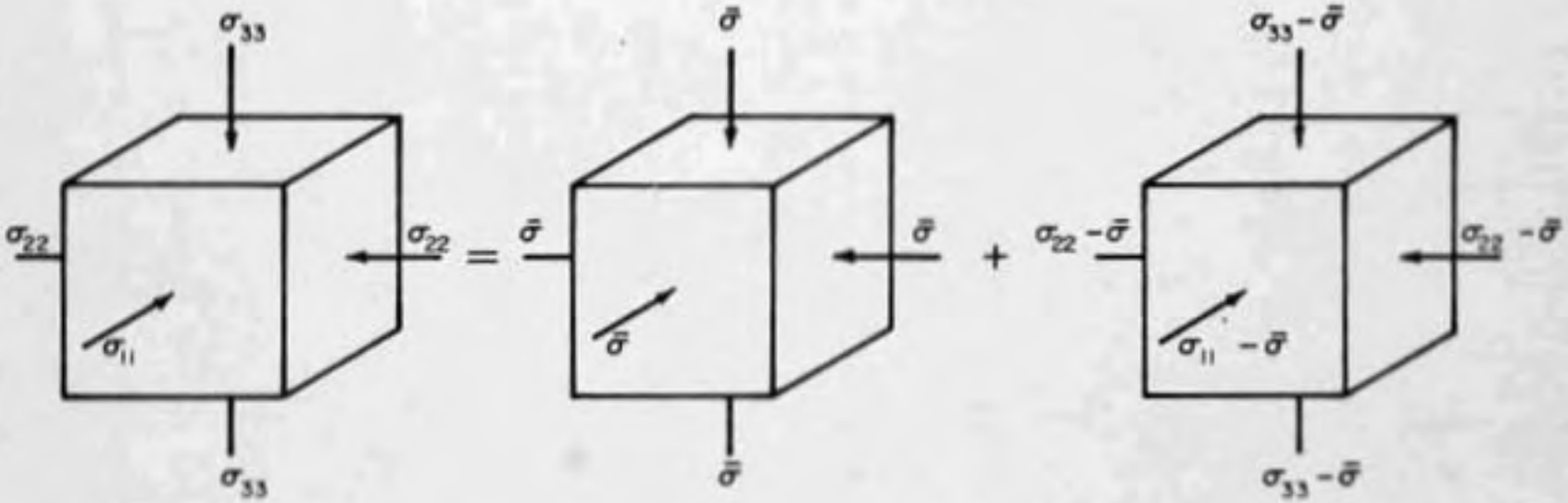

a)-Principal Stresses b)-Spherical Component c)-Deviatoric Component

Figure 4.1 - Decomposition of The State of Stress at a Point into Spherical and Deviatoric Components

$$\begin{bmatrix} \epsilon_{11} & \epsilon_{12} & \epsilon_{13} \\ \epsilon_{21} & \epsilon_{22} & \epsilon_{23} \\ \epsilon_{31} & \epsilon_{32} & \epsilon_{33} \end{bmatrix} = \begin{bmatrix} \bar{\epsilon} & 0 & 0 \\ 0 & \epsilon & 0 \\ 0 & 0 & \bar{\epsilon} \end{bmatrix} + \begin{bmatrix} \epsilon_{11}-\bar{\epsilon} & \epsilon_{12} & \epsilon_{13} \\ \epsilon_{21} & \epsilon_{22}-\bar{\epsilon} & \epsilon_{23} \\ \epsilon_{31} & \epsilon_{32} & \epsilon_{33}-\bar{\epsilon} \end{bmatrix} \quad (4\text{-}2)$$

where

$$\bar{\sigma} = \frac{1}{3}(\sigma_{11} + \sigma_{22} + \sigma_{33})$$

$$\bar{\epsilon} = \frac{1}{3}(\epsilon_{11} + \epsilon_{22} + \epsilon_{33})$$

It is useful, where possible, to represent these tensors by scalar parameters. The spherical stress tensor is often represented by the octahedral normal stress and the deviatoric stress tensor by the octahedral shear stress. Such a simplification is useful only if the material is assumed non-dilatant and isotropic. These assumptions have been made herein, as in other analytical studies (Clough and Woodward, 1967; Girijavallaban and Reese, 1968).

In the previous discussions of the triaxial test, homogeneous stress and strain states within the specimen have been assumed. Thus, the specimen is treated as having "point-like" attributes and the material response, which pertains to a material point, can be determined from the measurements of the response of the gross specimen. But actually the radial deformation of the cylindrical specimen is likely to be restrained by the development of friction with the end plates and as a consequence, inhomogeneity in stress and strain conditions within the sample will be

introduced. Experimental results indicate that the end restraint leads to nonuniform stresses and strains within the specimen both for cohesive and cohesionless soils (Shockley and Ahlvin, 1960; Roscoe, et. al., 1963; Truesdale and Rusin, 1963; Januskevicius and Vey, 1965; Barden and McDermott, 1965; Kraft, 1965). A homogeneous state of stress and strain within the sample can be approached by using lubricated end caps of larger diameter than the specimen, which allows for more nearly free expansion at the top and the bottom (Rowe and Barden, 1964; Januskevicius and Vey, 1965; Duncan and Dunlop, 1968; Kirkpatrick and Belshaw, 1968).

Different kinds of special testing equipment have been developed to obtain homogeneous stress conditions in the soil sample during testing (Sowers, 1963), but with only partial success. Ko and Scott (1967) fabricated equipment to apply a uniform stress across each boundary at a cubical sample. But according to Bell (1968), edge restraint may cause inhomogeneity in this apparatus also. Roscoe and his co-workers developed a new triaxial apparatus (1970) and some experimental results obtained with it have been reported.

However homogeneous conditions can be generally assumed to prevail in the triaxial test whenever,

1) the length to diameter ratio is sufficiently large (Bishop and Green, 1965; Duncan and Dunlop,

1968; Perloff and Pombo, 1969)

2) the strains are small (Rowe and Barden, 1964; Duncan and Dunlop, 1968);

3) the diameter of the lubricated end plates are larger than the specimen (Rowe and Barden, 1964; Januskevicius and Vey, 1965; Kirkpatrick and Belshaw, 1968).

In the triaxial creep tests that were conducted during this investigation, the length to diameter ratio was always greater than two, the strains were generally less than one per cent and the diameter of the top loading cap was 1.41 inches while the diameter of the specimen was 1.31 inches. Hence it is felt that homogeneous stress and strain conditions within the specimen can be reasonably assumed for these tests.

4.2 Characterization of Time-Dependent Nature of the Soils Tested

In Figure 4-2 the maximum shear strain obtained during typical triaxial compression creep tests on impact compacted specimens is plotted against time for various stress levels. It is to be noted that in the triaxial creep tests, the octahedral shear strain is a scalar multiple of the maximum shear strain (Equation 2-6a). For the duration of the test period, the creep curves appear as straight lines in a logarithmic plot. Thus the relation between maximum shear (distortional) strain and time can be expressed as,

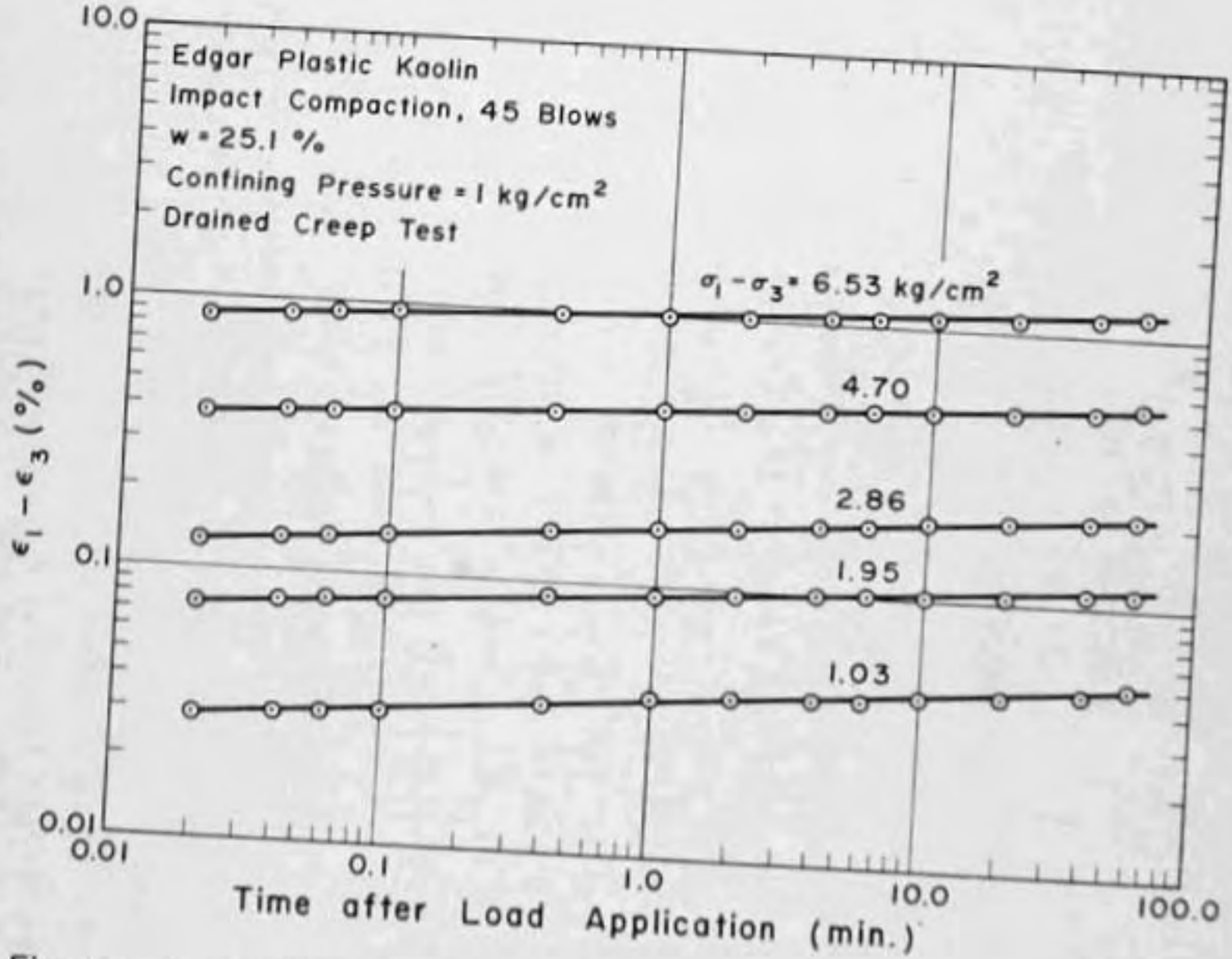

Figure 4.2 - Relation Between Maximum Shear Strain and Time
(Ramaswamy and Perloff, 1970)

$$(\varepsilon_1 - \varepsilon_3)\,(t) = ct^n \qquad (4\text{-}3)$$

where

$(\varepsilon_1-\varepsilon_3)(t)$ = maximum shear strain at time t;

$\varepsilon_1(t)$ = axial strain at time t;

$\varepsilon_3(t)$ = radial strain at time t;

t = time elapsed after the application of load;

c,n = constants.

As discussed by Perloff (1966), this form of relation appears to be valid whether the sample was tested drained or undrained; whether it was the first loading or subsequent loadings, whether the sample was confined or unconfined; for all stress levels, for all moisture contents, for all types of compaction that were used in this study and for duration of creep up to 1000 minutes (Figure 4-3). These results are in general agreement with those obtained for uniaxial measurements on saturated clays by Singh and Mitchell (1968, 1969) and Murayama and Shibata (1961) as well as torsional shear tests on compacted clays by Lara-Tomas (1962). Bishop (1969) has conducted drained constant stress level tests on undisturbed clays, the test duration being up to 1000 days. Some of his test results showed that power law representation is valid during the entire time range, while other tests indicated only a limited period of applicability. He attributes this sudden

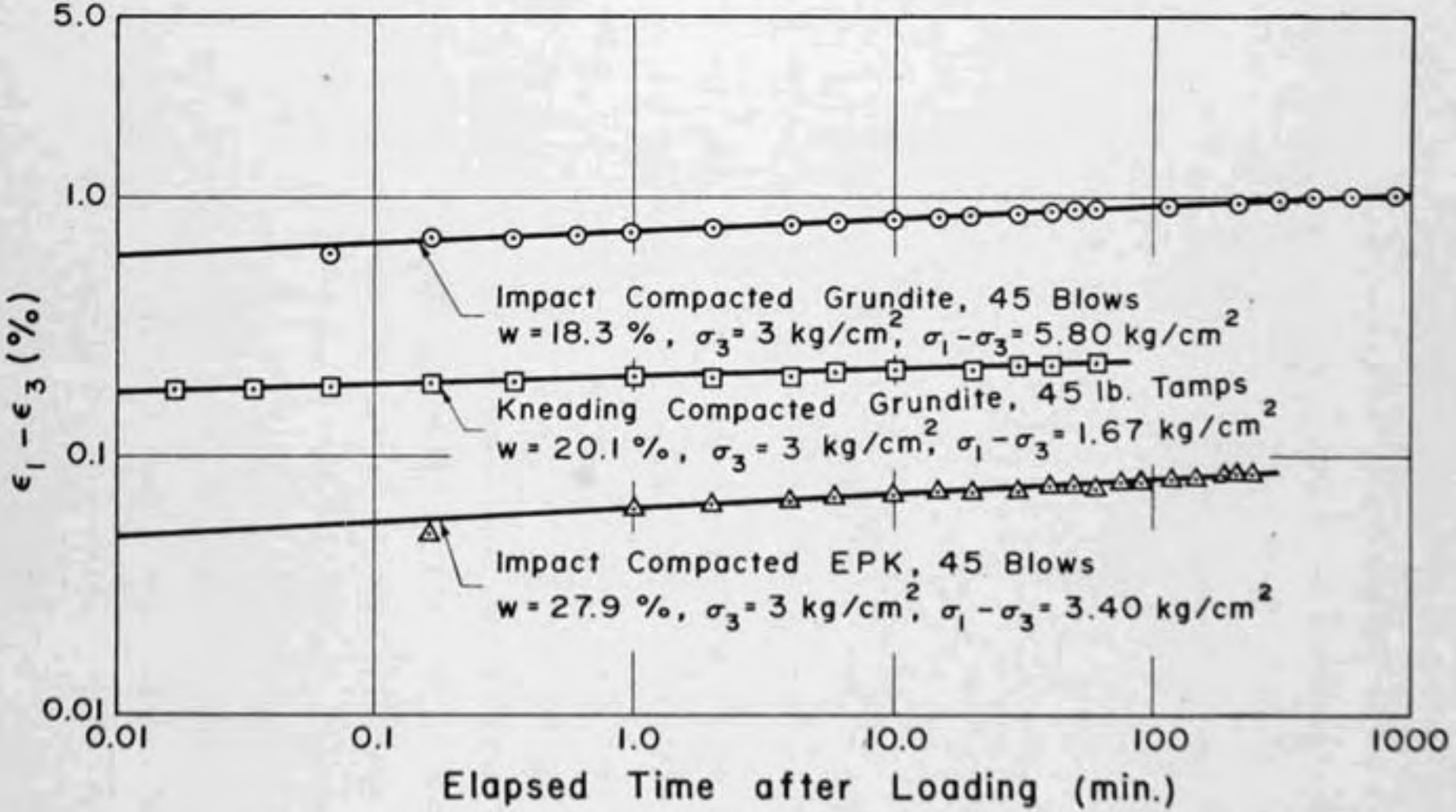

Figure 4.3 - Confined Creep Test Results (Perloff, 1966)

increase of strain rate after a certain period of creep loading to the fundamental modification of the soil structure. Such structural changes are unlikely to take place in compacted clay.

Equation 4-3 implies that the shear creep compliance can be expressed as

$$J(t) = \Delta J(t) \qquad (4-4)$$

instead of the usual

$$J(t) = J(0) + \Delta J(t)$$

where

$J(0)$ = initial value of compliance (t=0)

$\Delta J(t) = J(t) - J(0)$ = transient component of compliance.

Figure 4-4 shows the variation of creep compliance with time at various stress levels for EPK. It is clear that the power law representation of the shear creep compliance is valid within the time range used in the test program.

A complete material characterization can be given for a homogeneous, isotropic, non-dilatant material by describing one other material parameter. For a triaxial compression creep test in which the lateral pressure remains fixed, the negative of the ratio between lateral strain and axial strain at any time can be usefully thought of as the equivalent Poisson's ratio at that time. This ratio constitutes the second parameter required.

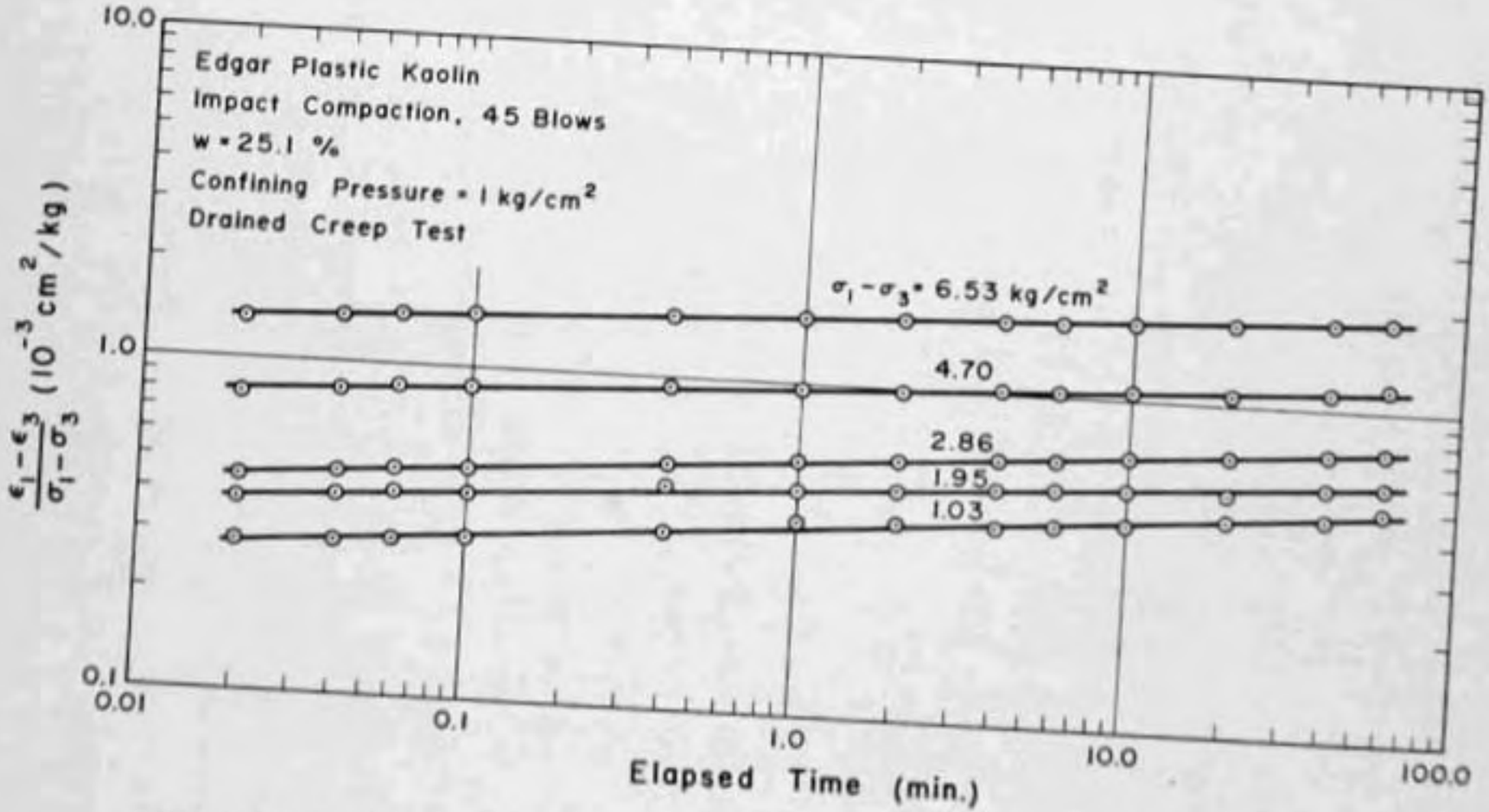

Figure 4.4 - Shear Creep Compliance as a Function of Time
(Data from Ramaswamy and Perloff, 1970)

The relation between the equivalent Poisson's ratio (the principal strain ratio in a compressive creep test) and time for various stress levels is shown for a typical test in Figure 4-5. At lower stress levels the principal strain ratio decreased with increase in time; but as the shear stress level increased, its value increased with time. This trend appeared to be true for all the tests that were conducted during this study, irrespective of test conditions. However, increase or decrease in value at a particular stress level with time was comparatively small. Hence it is believed reasonable to assume that the equivalent Poisson's ratio is for practical purposes, independent of time.

4.3 Effect of Loading History on Creep Behavior

It was shown by Perloff (1966) that the shear strain induced by the load application is substantially larger for initial loading than for the succeeding cycles, even though the straight line logarithmic relationship between shear strain and time appeared to be valid for all cycles. Figure 4-6 shows the results of four loading and unloading cycles of a test in which an EPK sample was subjected to eight loading and unloading cycles. The figure shows that for a limited number of cycles, the difference between total strains at the end of two successive cycles of load application become progressively less as the number of cycles is increased. Investigations on the effects of

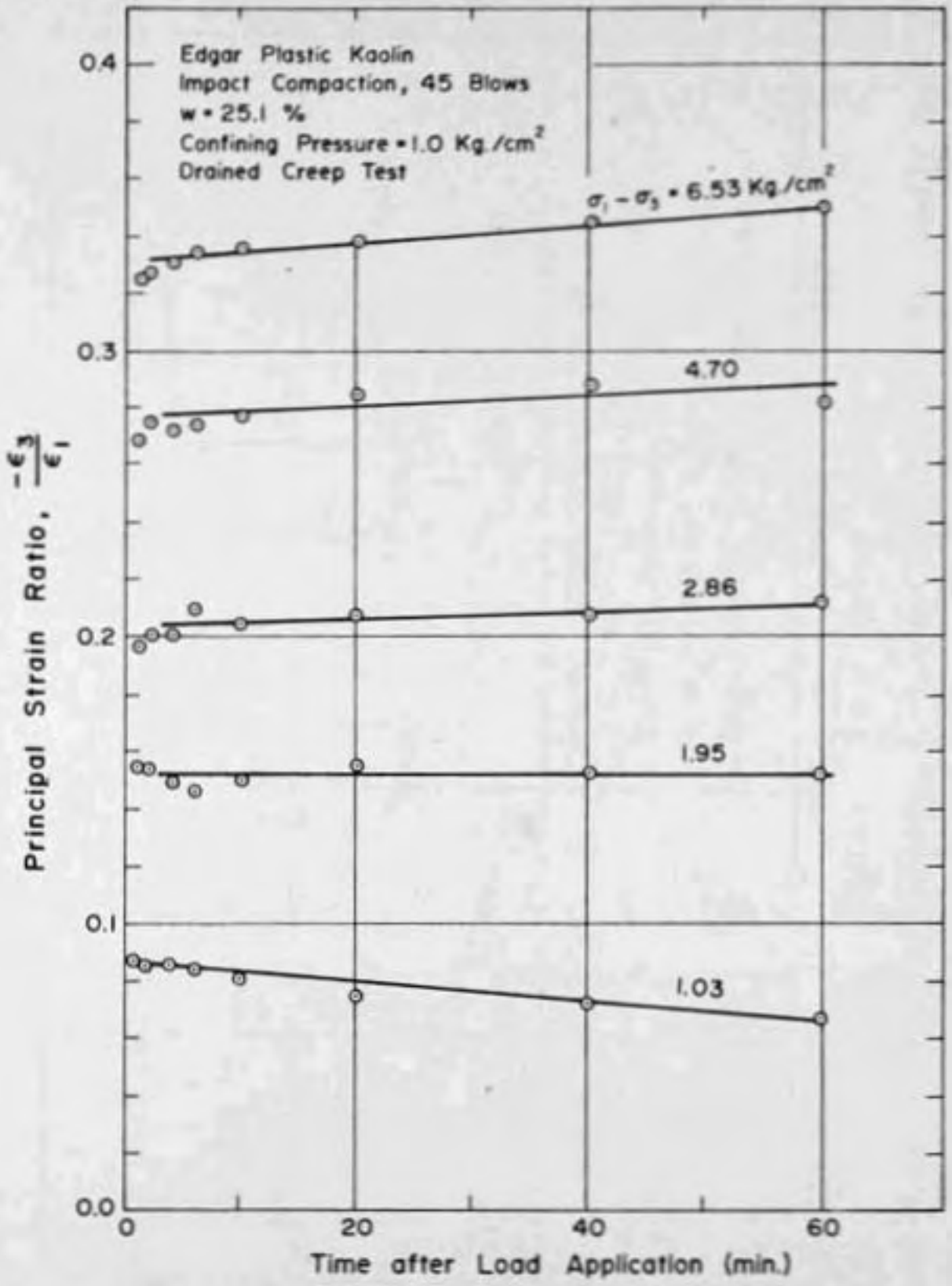

Figure 4.5 - Relation Between Principal Strain Ratio and Time

(Ramaswamy and Perloff, 1970)

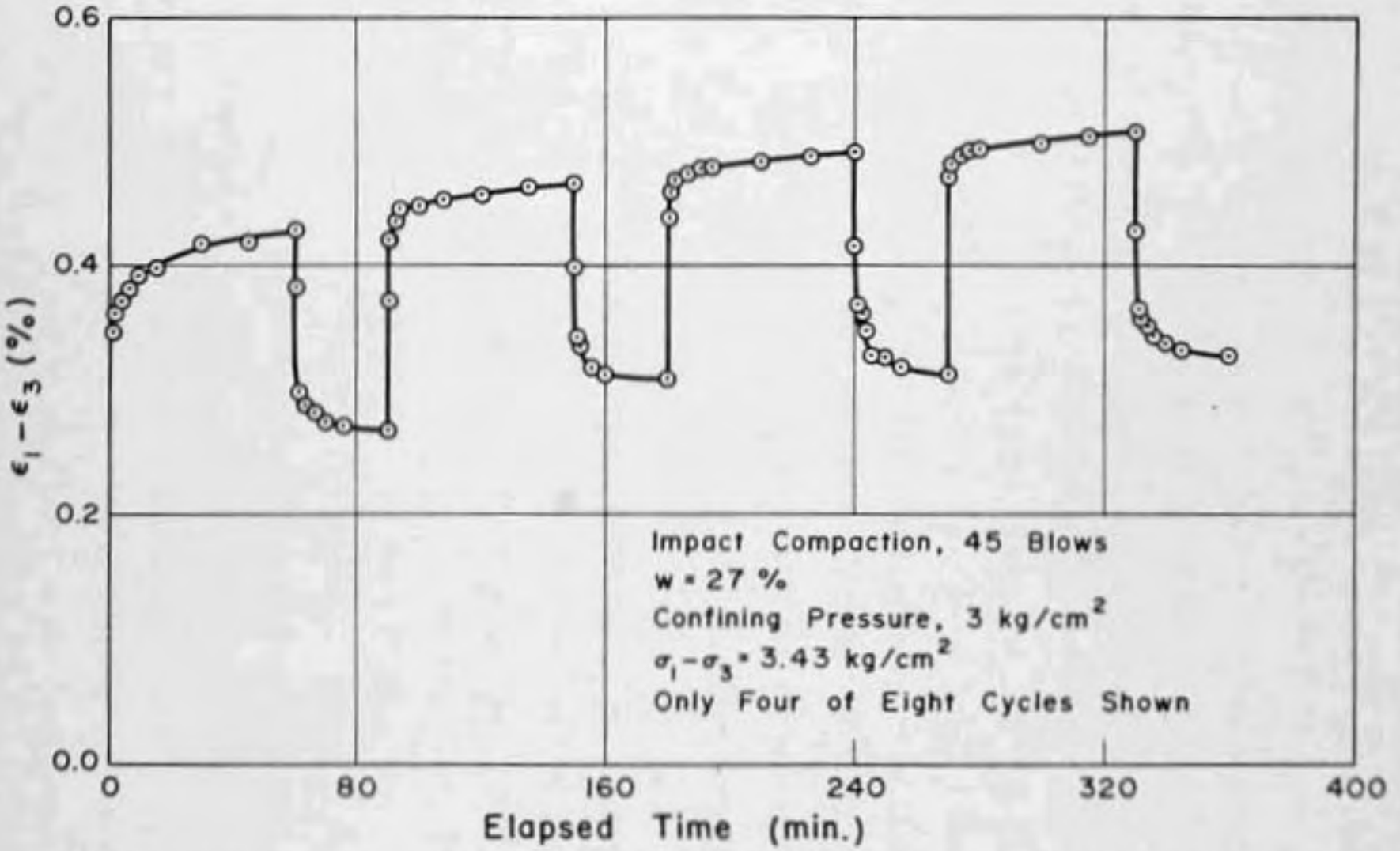

Figure 4.6 - Results of Confined Creep Test on EPK (Perloff, 1966)

repeated loadings on the deformation characteristics of compacted cohesive soils indicate a similar trend (Seed, et al, 1955).

It is also seen that the shear strain response is substantially lower in succeeding cycles than for the initial loading. Figure 4-7 shows this more clearly. The shear strain for each cycle and time are adjusted to zero at the instant of load application. Thus the net change in strain during each cycle of loading can be readily compared. The larger strain in the first loading cycle is evident. A similar result was observed by Lara-Tomas (1962). This result appeared applicable irrespective of the duration of the first loading cycle and the length of the unloading period between load cycles.

Similar results have been reported in the extensive investigations carried out on the deformation and strength characteristics of compacted cohesive soils subjected to repeated loads (Seed, et. al., 1955; Seed and Chan, 1958; Larew and Leonards, 1962). It has been found that the deformation under the first application of load was much greater than for the subsequent applications of load, irrespective of the duration of the first loading. For instance, the frequency of load applications in the investigations of Seed, et. al. (1955) varied from 3 to 20 cycles per minute. They state that a general relationship may exist, between the deformation after one application

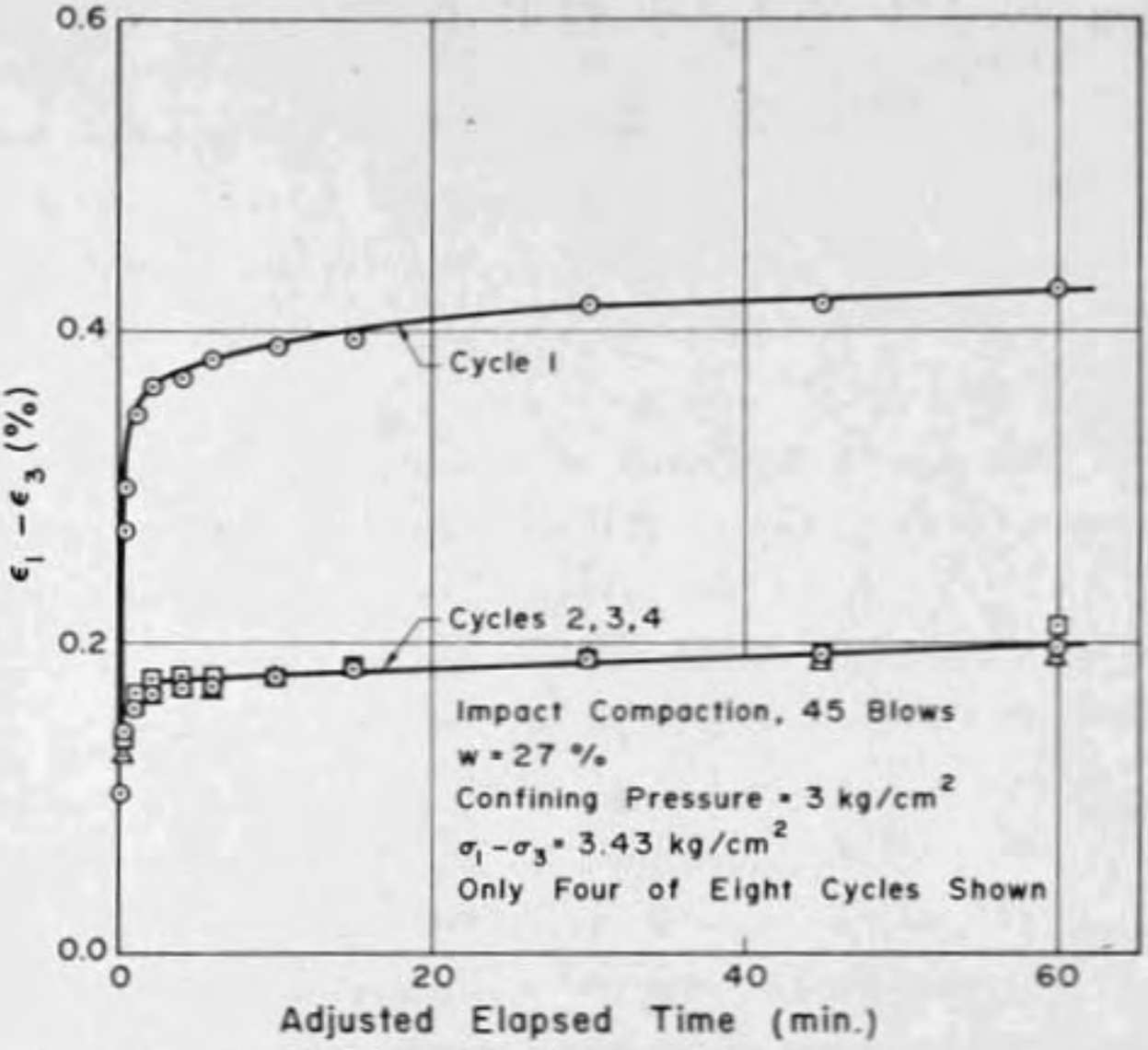

Figure 4.7 - Net Strains for Individual Cycles of Confined Creep Test on EPK (Perloff, 1966)

of a given stress level and the residual deformation after any number of applications of the same stress level.

During field compaction, a loose earth lift is spread over compacted layer and rolled. The compaction of the loose lift induces only a small amount of compaction in the layers below. (Johnson and Salleberg, 1960). The stresses imposed by the rolling of the loose soil on the compacted layers below may be substantial, depending on the ratio between the diameter of the compaction device and the depth (Sowers and Gulliver, 1955). Hence it is felt that the compaction of the loose lift by rolling approximates to an initial repetitive loading of a limited number of cycles on the compacted layer below it.

It was not clear, however, whether the above conclusions were valid when the initial load was applied for only a very short duration of time. Hence triaxial creep tests were performed wherein the duration of the first cycle of loading was limited to one minute. The specimen was then allowed to relax for fifteen minutes and then reloaded. Figures 4-8 and 4-9 show the results of tests on two similar specimens, one of which was subjected to the short first load cycle described above, the other of which experienced the conventional one-hour first load followed by a one-half hour unload period. Other conditions of testing for the two samples were identical.

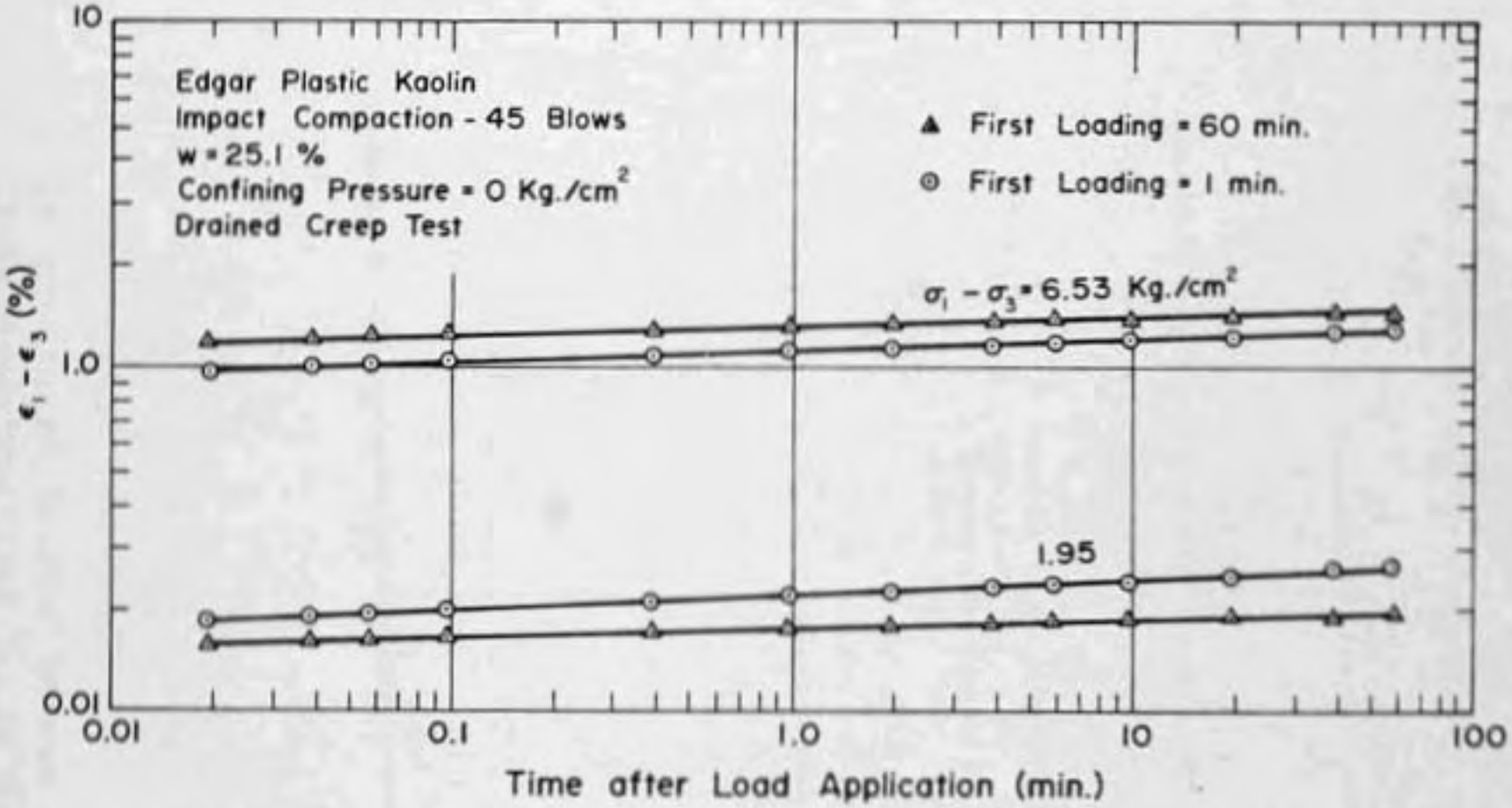

Figure 4.8 - Comparison of Relation Between Maximum Shear Strain and Time During Second Load Cycle, for First Loading Periods of one Minute and one Hour

(Ramaswamy and Perloff, 1970)

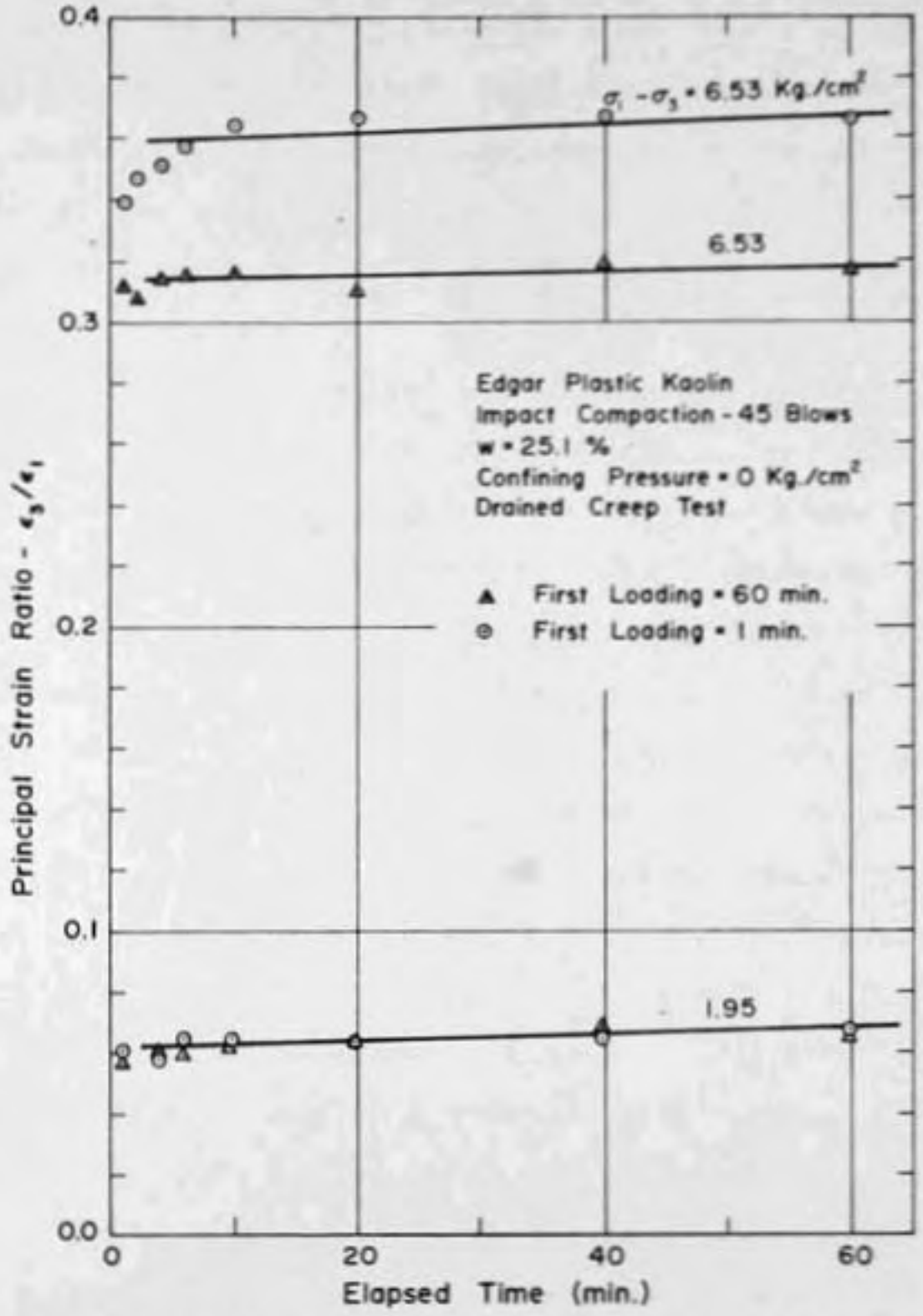

Figure 4.9 - Comparison of Relation Between Principal Strain Ratio and Time During Second Load Cycle, for First Loading Periods of one Minute and one Hour

(Ramaswamy and Perloff, 1970)

The figures show the second cycle responses for the two specimens. It is seen that the responses are similar and the difference between these two cases is small enough to be attributed to sample-to-sample variation. Hence it can be concluded that the response in second and subsequent cycles do not depend on the duration of the first loading cycle.

In order to determine what loading condition was of interest in the prediction of creep deformations of a compacted fill, it is useful to consider, for example, an earth embankment of fifty feet in height. Assuming the unit weight of soil mass as 110 pounds per cubic foot, the maximum vertical stress will be approximately 40 psi. When the soil is compacted in the field, the contact pressure will be approximately 250 psi under a sheeps foot roller. The vertical normal pressure reduces rapidly with depth since the dimensions of the sheeps foot are relatively small. If the foot size is assumed to be 8" x 0.7", the vertical pressure will be less than 50 psi when the depth exceeds two inches. But the sheeps foot exerts a punching action and it can be reasonably expected that the soil mass in the compacted layer will be at a depth less than 2 inches at one time or another during the compaction process. This implies that the compacted layer is subjected to a number of cycles of greater or

equal magnitude than the subsequent dead load stress that will be imposed. Hence it would seem reasonable to use the response due to second and subsequent loadings in the analysis. Consequently all further results will be reported for second or subsequent cycles of loading.[1]

Perloff (1966) has reported that the creep response of a compacted specimen subjected to one of a series of loads is essentially equivalent to that experienced under a single load of the same magnitude. He conducted two series of comparative creep tests to determine if a single specimen subjected to a series of stresses would behave in the same fashion as a number of identical specimens each of which was subjected to a single stress level. Figure 4-10 shows the creep curves for the second loading cycle for EPK, in which the soil was subjected to a series of stress levels. The results of a few tests on similar specimens for which the applied stress is the only creep stress to which the soil was subjected are also shown. The figure indicates that the results of the test in which the soil has been subjected to a series of loads

---

1. It is recognized that the first cycle of creep loading in this investigation is not the equivalent of expected field loading, and that the effects of a confined creep test on the compacted cohesive soil may be different from the repetitive loading of a limited number of cycles.

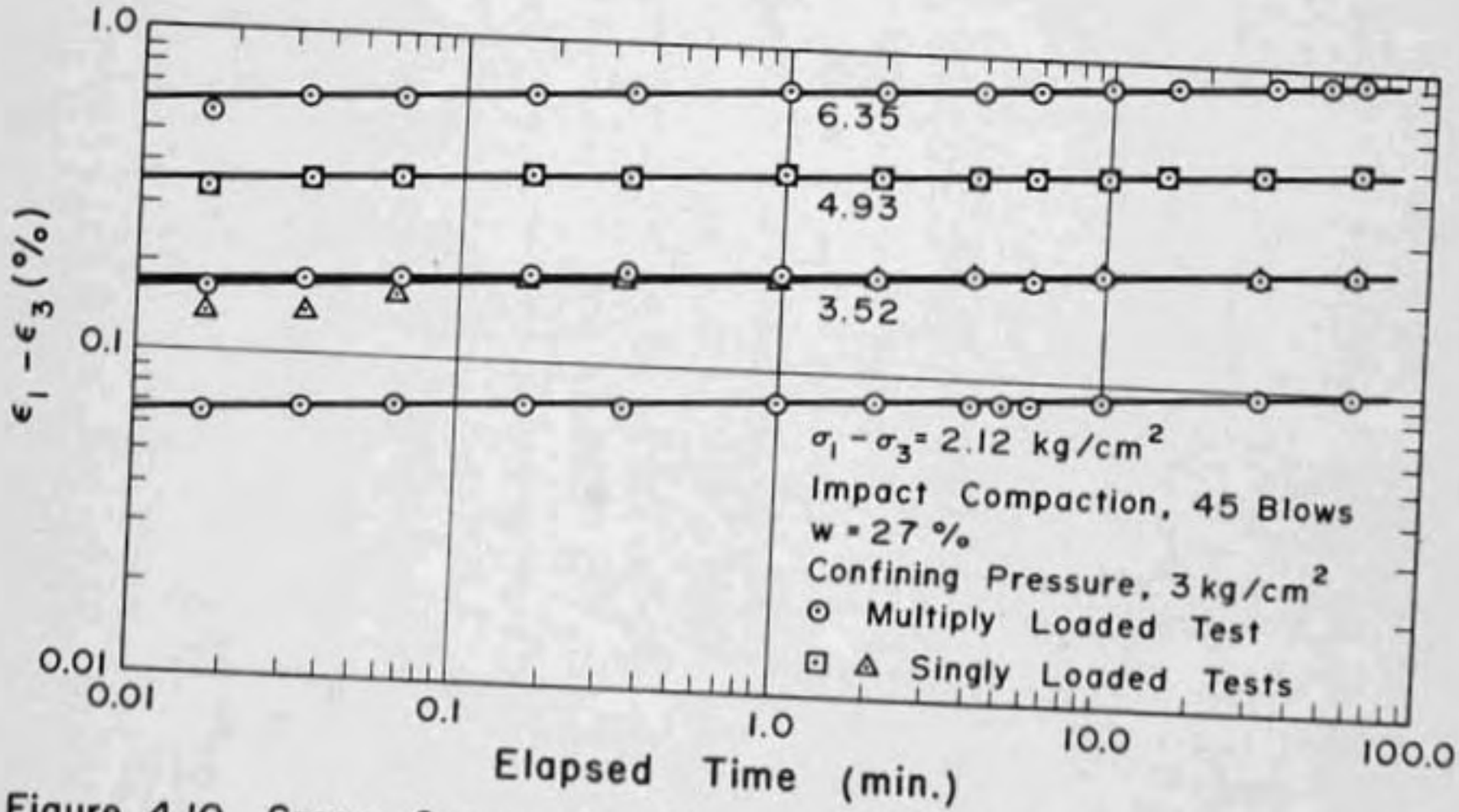

Figure 4.10 - Creep Curves for Singly and Multiply Loaded Specimens of EPK (Perloff, 1966)

are essentially similar to those from tests in which each load is applied to a separate soil specimen. This implies that the behavior under a given stress level is not influenced by the previous stresses experienced by the specimen, so long as the stress level is larger than those preceding. Hence the standard test procedure was modified so that a single specimen was used for each load series.

4.4 Effect of Stress Level, Confining Pressure and Moisture Content on Creep Behavior

Figures 4-11 and 4-12 indicate the influence of stress level and confining pressure on the magnitude of creep parameters c, the principal strain ratio and n for Edgar plastic kaolin and grundite. It is seen that the magnitude of c increases in a non-linear manner with increase in stress level. The magnitude of principal strain ratio also increases with stress level while n appears to be independent of stress level. The confining pressure does not influence the creep parameters in such a marked manner. At a particular stress level the magnitudes of c and the principal strain ratio decrease as the confining pressure increases while n remains unaffected.

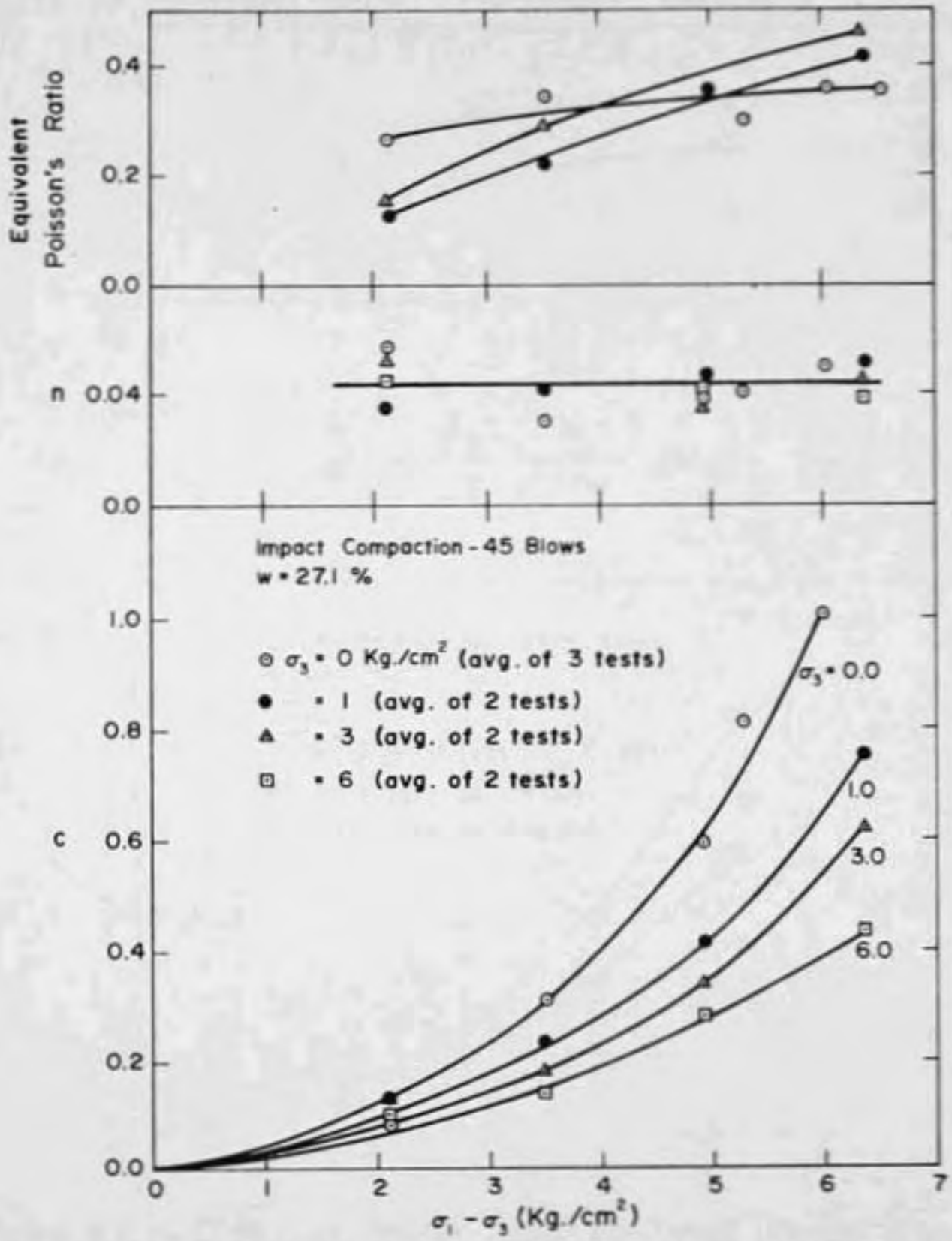

Figure 4.11 - Effect of Stress Level on Creep Parameters for EPK (Data from Perloff, 1966)

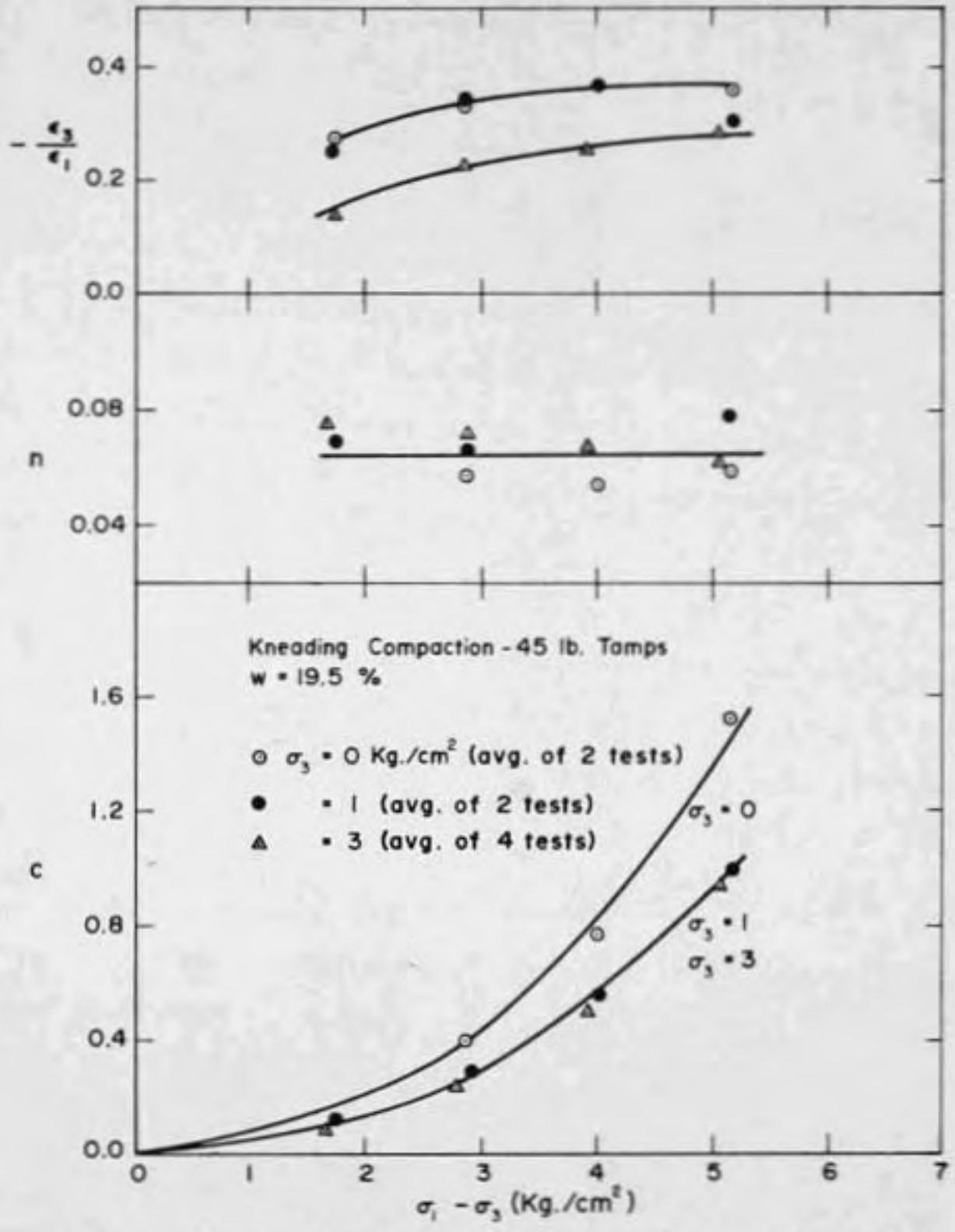

Figure 4.12 - Effect of Stress Level on Creep Parameters for Grundite (Data from Perloff, 1966)

To verify the above results, constant strain rate triaxial compression tests with lateral measurements were performed on a specimen that had already undergone creep testing. The equivalent Poisson's ratio calculated at various stages of the test is shown in Figure 4-13. Also shown are the results for the creep test performed prior to constant strain rate testing. The good agreement is evident.

The influence of moisture content on the magnitude of creep parameters for Grundite is shown in Figures 4-14 and 4-15 for two compactive efforts. It is seen that even though the value of c increases linearly with increase in stress level at low moisture contents, its behavior is highly nonlinear at or above optimum moisture content. The value of principal strain ratio is higher at moisture contents above optimum and increases with increase in stress level. The magnitude of n is essentially independent of moisture content.

4.5 Correlation of Creep Response to Failure Strength

It has been shown previously (Perloff, 1966) that the creep response as characterized by the parameter c could be described usefully as a function of the stress ratio

$$(\sigma_1 - \sigma_3)/(\sigma_1 - \sigma_3)_f \qquad (4\text{-}6)$$

where

$(\sigma_1 - \sigma_3)$ = principal stress difference;

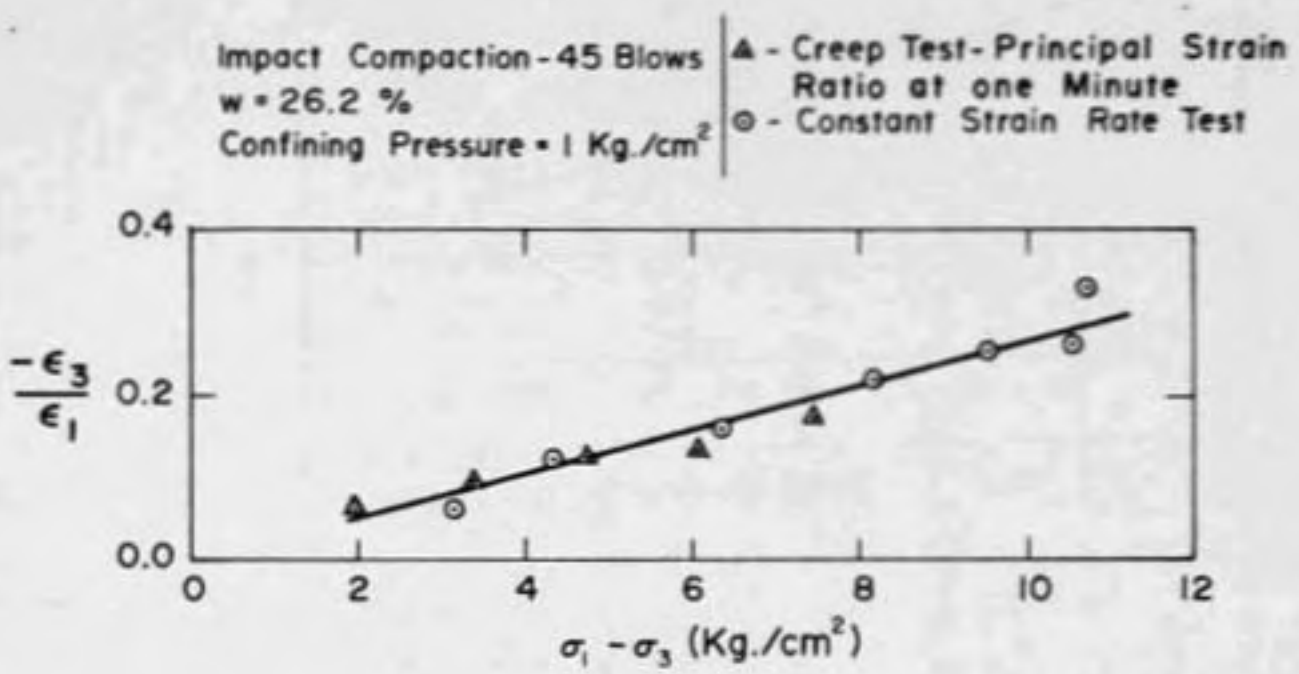

Figure 4.13 - Effect of Stress Level on Principal Strain Ratio for EPK

(Ramaswamy and Perloff, 1970)

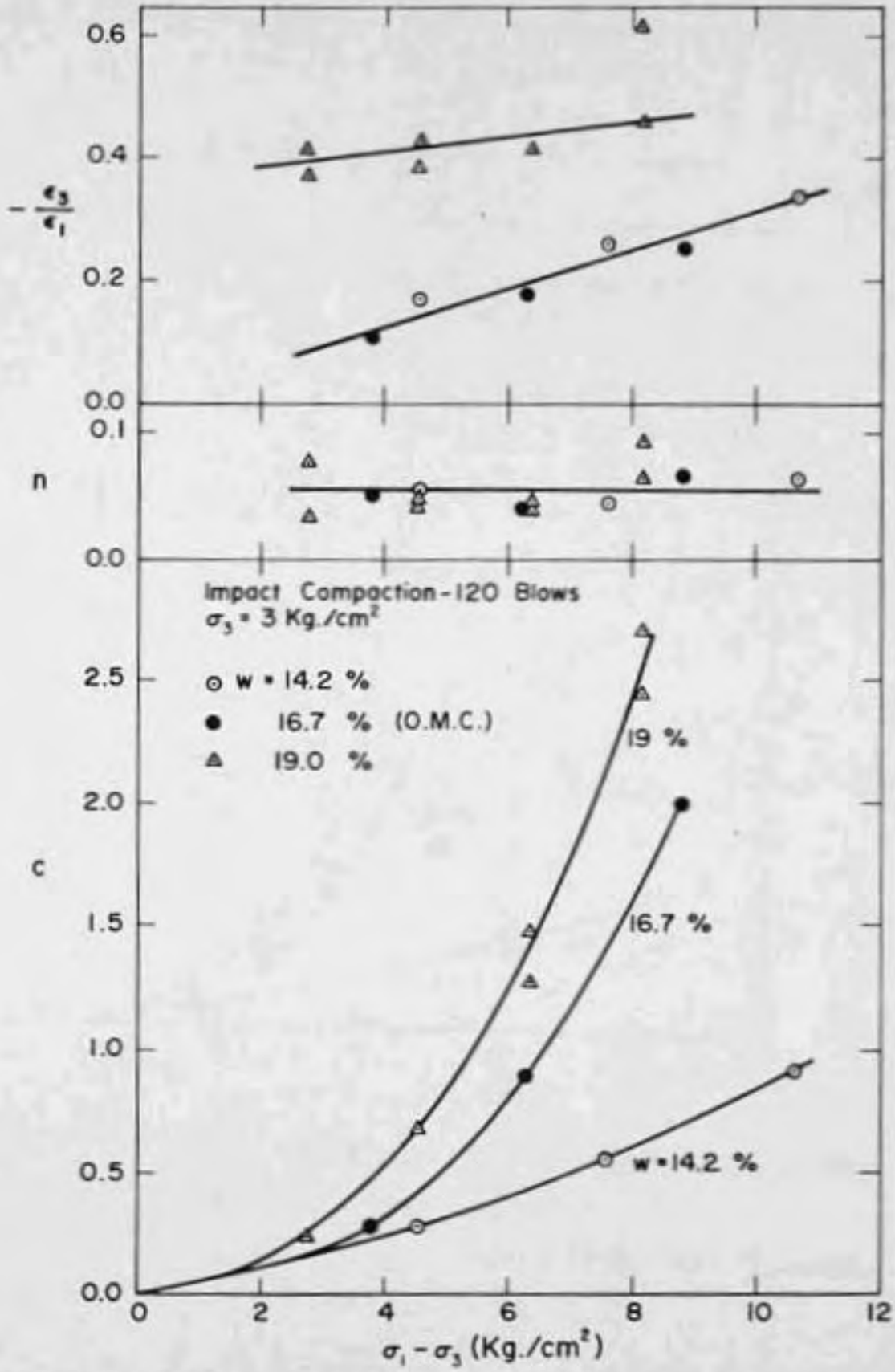

Figure 4.14 - Effect of Moisture Content on Creep Parameters for Grundite
(Data from Perloff, 1966)

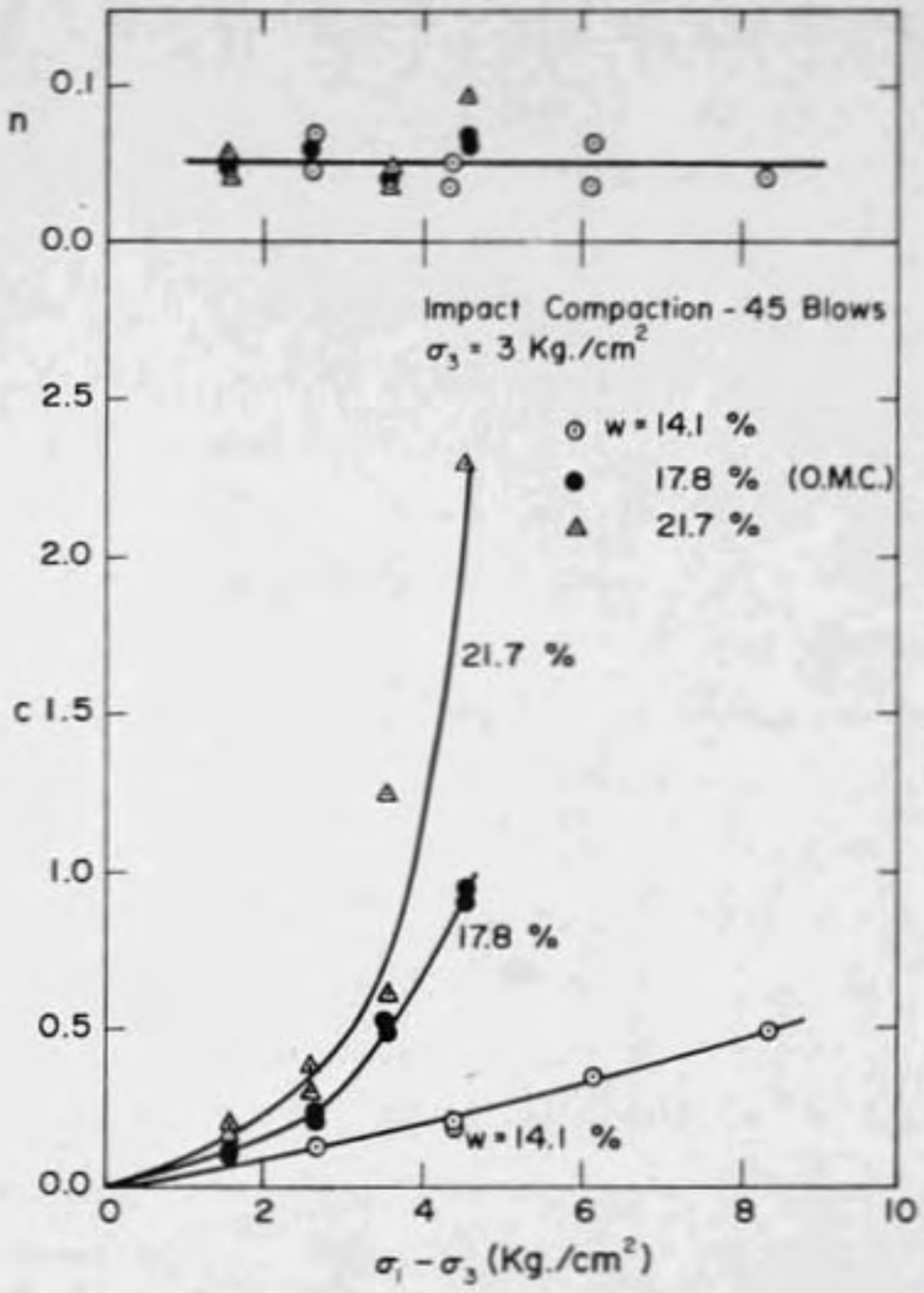

Figure 4.15 - Effect of Moisture Content on Creep Parameters for Grundite

(Data from Perloff, 1966)

$(\sigma_1 - \sigma_3)_f$ = principal stress difference at failure .

When this was done, it was found that the effects of water content and confining pressure were approximately accounted for.

The failure stress, $(\sigma_1 - \sigma_3)_f$, used in the above expression is that corresponding to the confining pressure, σ_3, at which the test was performed. Its magnitude, however, is a function of the type of testing. That is, in the triaxial test the confining pressure is also equal to the initial octahedral normal stress. As the applied loads are increased there is, in general, a corresponding increase in octahedral normal stress. If the shearing resistance is a function of confinement, there will be a concomitant increase in the failure strength as the octahedral normal stress increases. So the use of the shear strength corresponding to the normal stress acting at the moment of failure seems more realistic than using the failure stress corresponding to the initial normal stresses.

The question then arises as to what form the failure criterion should take. There have been many attempts to determine an appropriate theory of failure for soils (Kirkpatrick, 1957; Wu, et al, 1963; Bishop, 1966; Ko and Scott, 1968). On the basis of these investigations and others, it appears that the complete state of stress is important in determining failure conditions for soils.

Newmark (1960) has suggested a failure criterion in terms of stresses and strains in the octahedral plane, which incorporate all components of the stress and strain tensors. The form of this criterion adopted in this study is

$$(\tau_{oct})_f = c^* + (\sigma_{oct})_f \tan \phi^* \qquad (4.7)$$

where

$(\tau_{oct})_f$ = the octahedral shear stress at failure;

$(\sigma_{oct})_f$ = octahedral normal stress at failure;

c^* = intercept on the τ-axis;

ϕ^* = slope of the failure envelope.

This is equivalent to an extended form of Von Mises theory of yielding and has also been proposed by Drucker and Prager (1952) as an extension of the conventional Mohr-Coulomb criterion.

Figure 4-16 shows the relation between $(\sigma_1 - \sigma_3)_f$ and octahedral normal stress at failure. It is to be noted that $(\tau_{oct})_f$ is proportional to $(\sigma_1 - \sigma_3)_f$ in the triaxial creep tests (Equation 2-4). Using this relation the creep parameters in Figure 4-12 are replotted in Figure 4-17 as a function of the octahedral stress-strength ratio, $(\tau_{oct})/(\tau_{oct})_f$. The figure clearly indicates that by plotting c as a function of the stress-strength ratio, the effect of confining pressure, for grundite, can be approximately accounted for. Figures 4-18 and 4-19 show

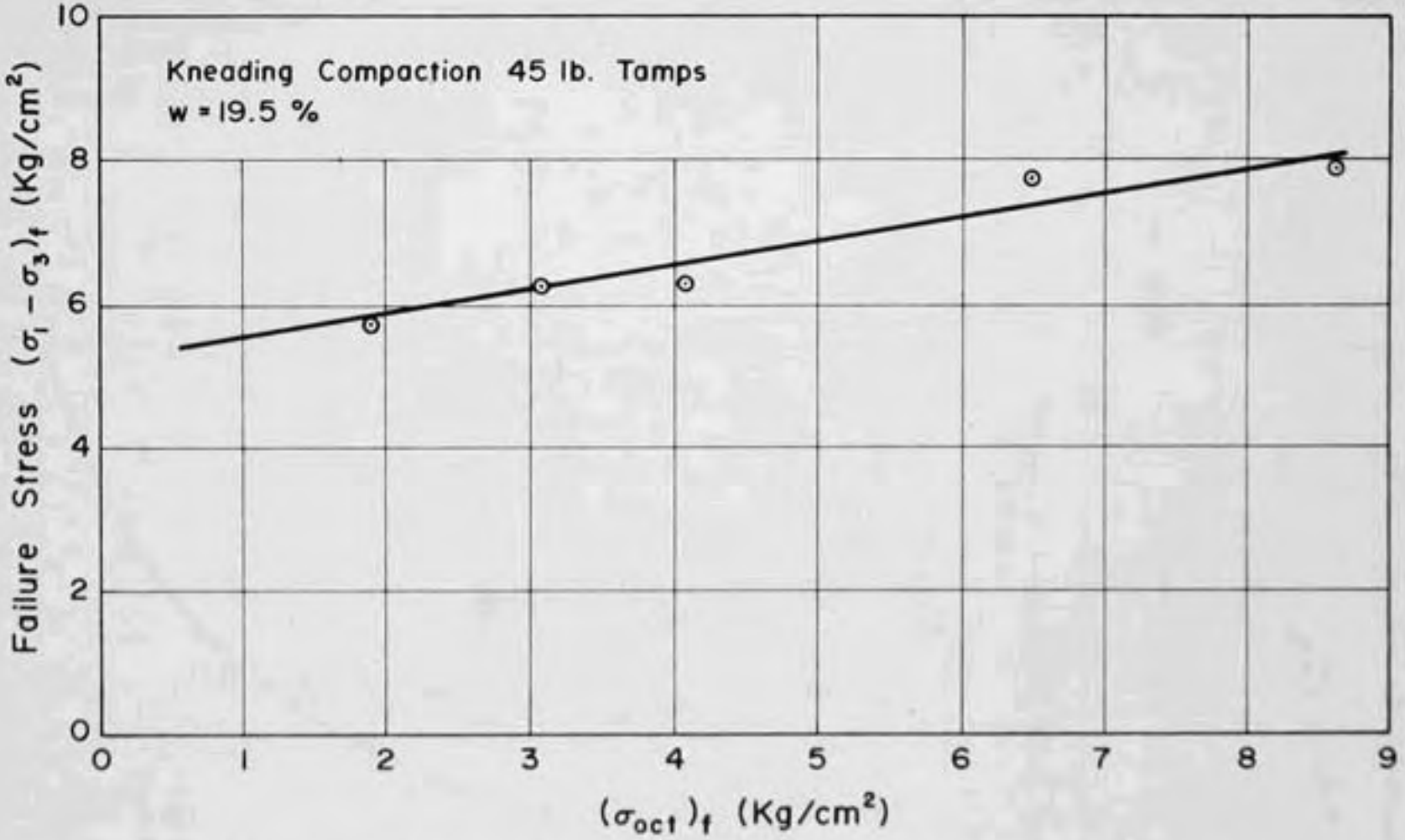

Figure 4.16- Effect of Octahedral Normal Stress on $(\sigma_1 - \sigma_3)_f$ for Grundite (Data from Perloff, 1966)

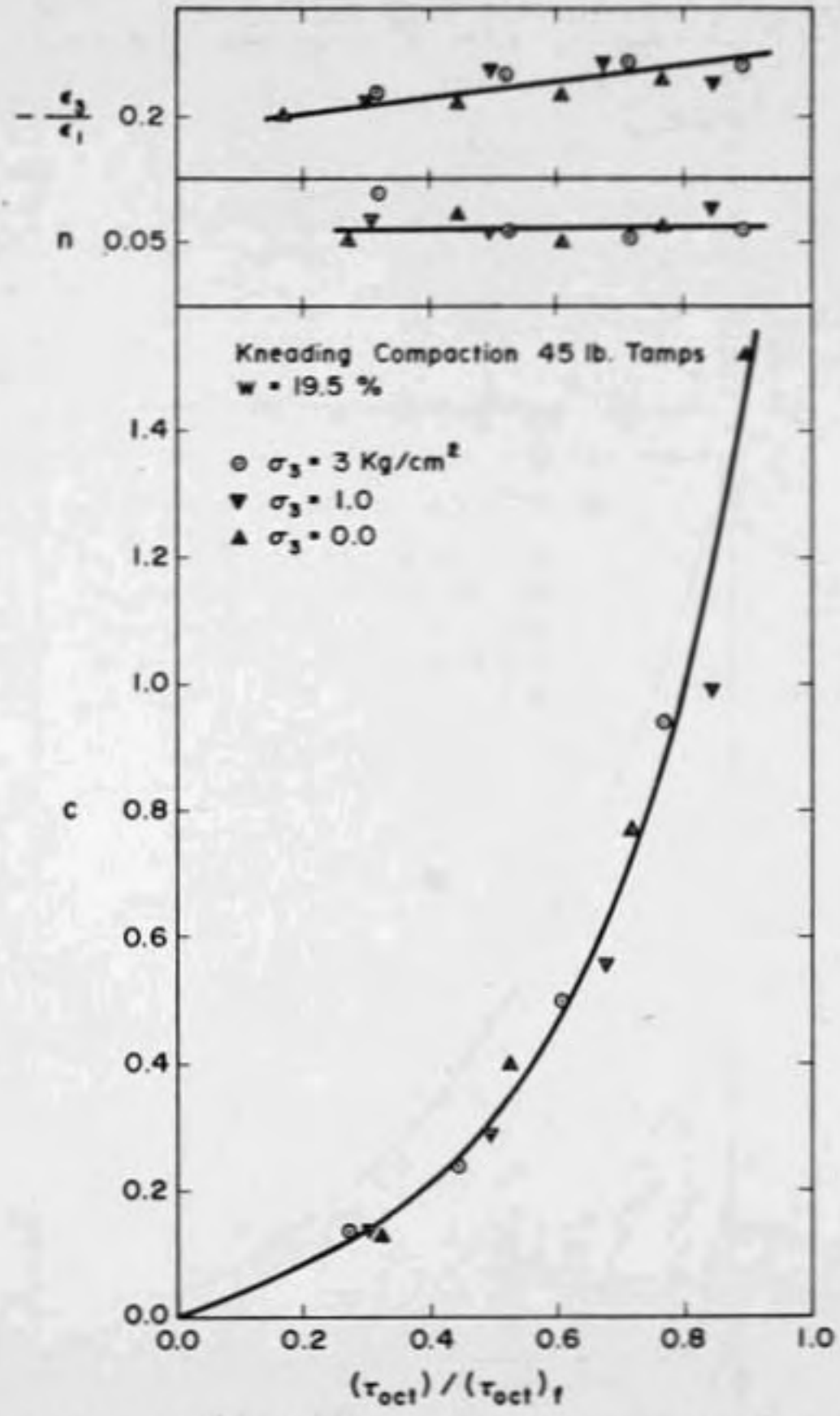

Figure 4.17 - Effect of Stress-Strength Ratio on Creep Parameters for Grundite

(Data from Perloff, 1966)

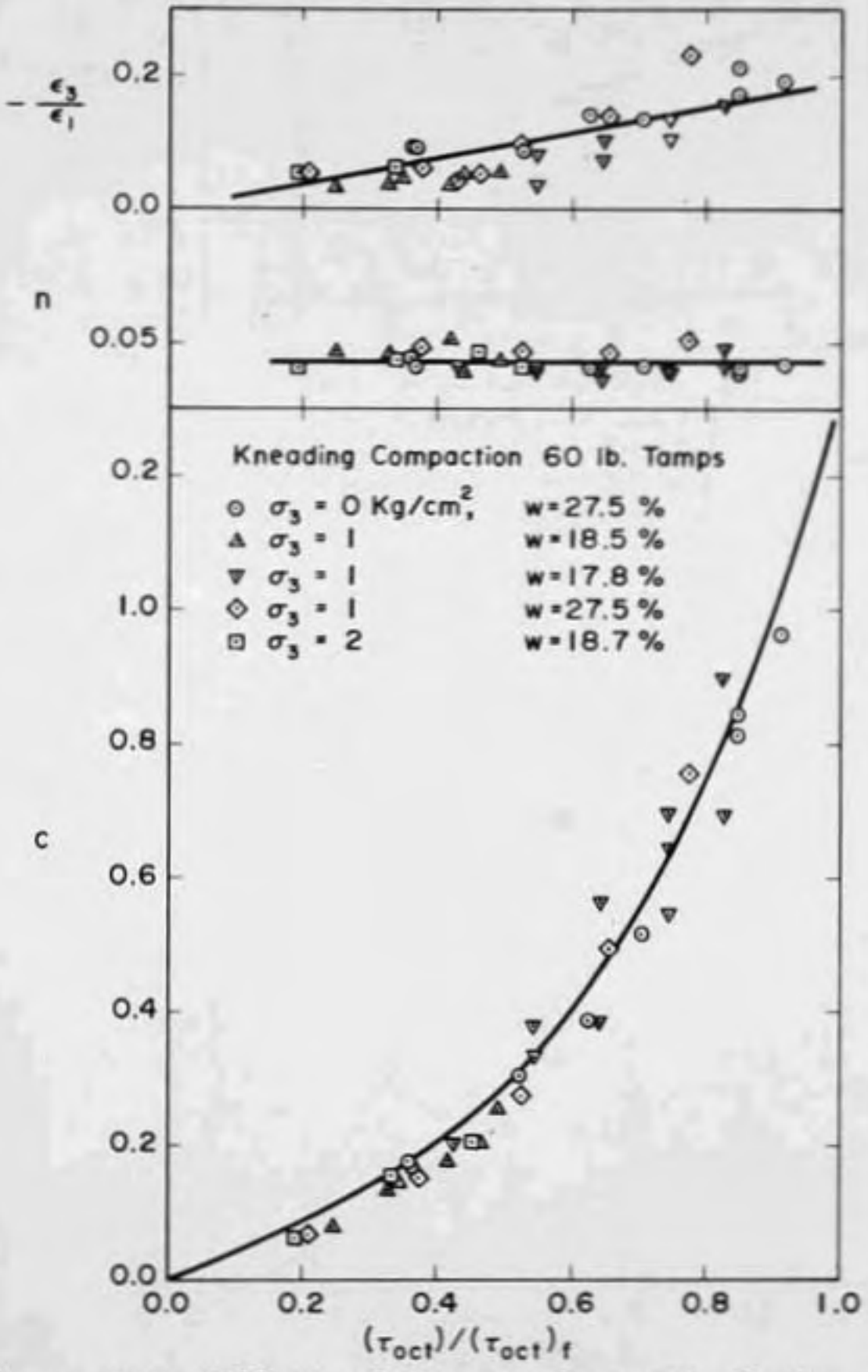

Figure 4.18 - Effect of Stress-Strength Ratio on Creep Parameters for EPK
(Data from Ramaswamy and Perloff, 1970)

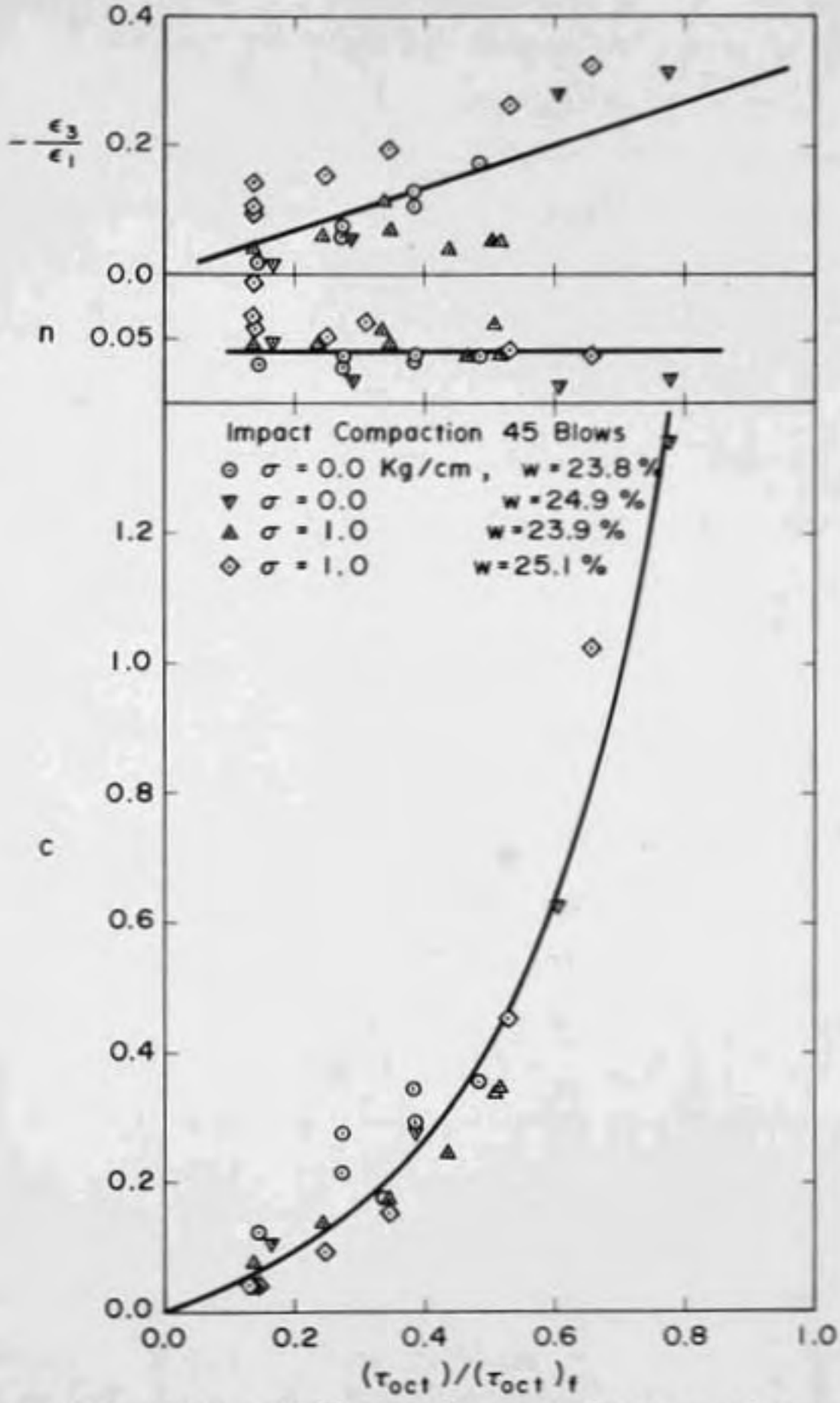

Figure 4.19 - Effect of Stress - Strength Ratio on Creep Parameters for EPK

(Data from Ramaswamy and Perloff, 1970)

similar relation for Edgar plastic kaolin for both impact and kneading compaction. It is seen that the principal strain ratio increases with increasing values of stress-strength ratio, while n is essentially independent of the magnitude of $(\tau_{oct})/(\tau_{oct})_f$.

4.6 Scaling Effect

The parameters for the compacted soil are obtained from the triaxial creep tests conducted on small specimens. The question then arises whether they can be directly applied to the analysis of prototype structures. When the specimens are small in comparison with the actual soil mass, possibility of scaling effect must be considered.

Deformation of a compacted cohesive soil is a continuous process with time. The main factors that may contribute to controlling the rate of time-dependent deformation are:

1. escape of air through the pores;
2. compression of air within the pores;
3. dissolution of air in water;
4. escape of water through the pores;
5. redistribution of water within the pores; and
6. deformation of the soil structure itself.

Relevant information available on the volume change and shear deformation characteristics of compacted cohesive soils is summarized in the following.

1. There is no expulsion of water from the compacted

soil under load, even when the degree of saturation is very high (Yoshimi and Osterberg, 1963; Danielson, 1963).

2. Substantial negative pore pressures exist in the capillaries of the partly saturated soil (Hilf, 1956; Lambe, 1961; Olson and Langfelder, 1965).
3. The negative pore water pressures existing in the capillaries of compacted soil are likely to be greater than the loadings used in the creep deformation studies (Yoshimi and Osterberg, 1963; Olsen and Langfelder, 1965).
4. When the soil is compacted at optimum or dry of optimum water content, the pores are interconnected and the soil will be permeable to air (Teerawong, 1963; Yoshimi and Osterberg, 1963; Langfelder, et al, 1968).
5. The rheological characteristics of the soil skeletal structure is the most dominant factor influencing the time-dependent shear deformation behavior of compacted cohesive soils (Yoshimi and Osterberg, 1963; Danielson, 1963; Barden, 1965).

Immediately after loading there is excess air and water pressure induced in the partly saturated sample, but since the induced water pressure is generally far less than the negative pore water pressure existing in the soil, there will be no escape of water (Yoshimi and Osterberg, 1963).

It is difficult to predict the redistribution of water in the pores due to pressure gradients caused by the loading. However the volume change involved in this process is likely to be negligible. So the increase in pore water pressure due to loading has little influence in the deformation of partly saturated soils.

The distribution of pores will probably be the same irrespective of sample size, since similar methods are used in the compaction processes. So for the same increase in pressure, the compression of air in the entrapped voids and the dissolution of air in water will be the same irrespective of the sample size. Hence there will be no scaling effect due to these factors.

The rheological properties of the soil are not likely to alter with increase or decrease in size, since the soil skeleton will possess the same basic properties in both cases. Thus there is no scale effect for this factor either.

The excess pore air pressure has to be dissipated in the course of time. The time taken for dissipation is likely to be very small in the laboratory specimen, due to the fact that length of drainage path is small and the permeability to air is relatively high. As the sample size is increased, the length of drainage path also increases. In large samples it is possible that the induced air pressure may be an influential factor in the time-dependent behavior of compacted cohesive soils. So it was decided to investigate the effect

of drainage on stress-strain-time response of the specimen.

Two series of tests were conducted to determine the effects of partial drainage and no drainage, and the responses were compared with the regular creep tests which were fully drained. The zero drainage case corresponds to the case of an infinite drainage length. In the first series, samples were consolidated to the required pressure and then the drainage valves were closed when the creep loads were applied. This can be considered equivalent to partial drainage. In the second series unconfined samples were tested. Instead of a porous stone, a plexiglas disc was placed at the bottom of the specimen and the drainage valves were kept closed during the test. This is a completely undrained case. In both series filter drains were not used and it was assumed that there was no diffusion of air through the membrane.

As illustrated in Figure 4-20, the relation

$$(\varepsilon_1 - \varepsilon_3)(t) = ct^n \qquad (4\text{-}3)$$

is valid for any drainage case. It is also seen that the principal strain ratio is independent of time as shown in Figure 4-21. Figures 4-22 and 4-23 show the comparison between undrained and partly drained cases with the fully drained case. The variations of parameter c and equivalent Poisson's ratio with stress-strength ratio was essentially the same in the test series irrespective of drainage conditions. It is evident that the response of compacted

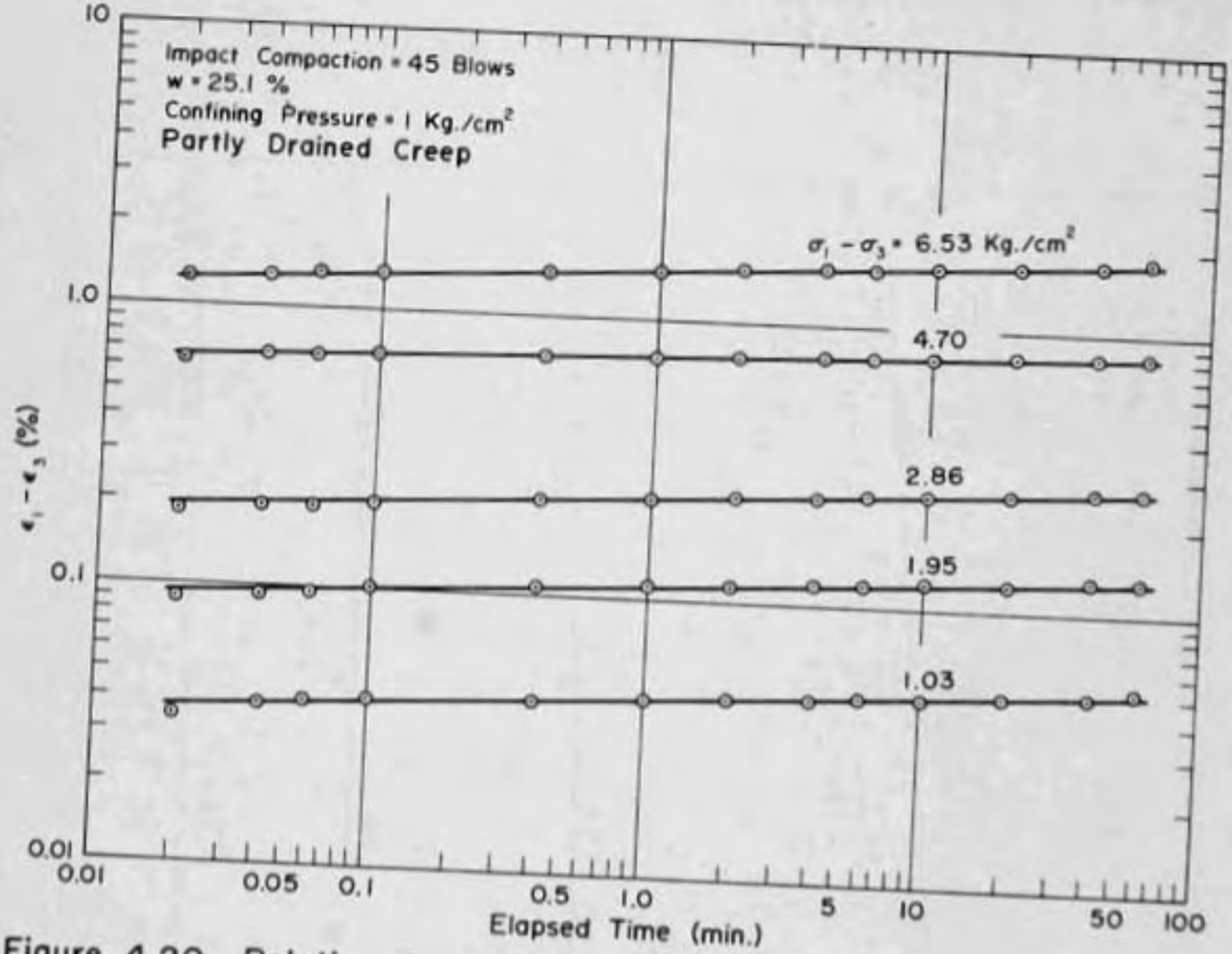

Figure 4.20 - Relation Between Maximum Shear Strain and Time for EPK (Ramaswamy and Perloff, 1970)

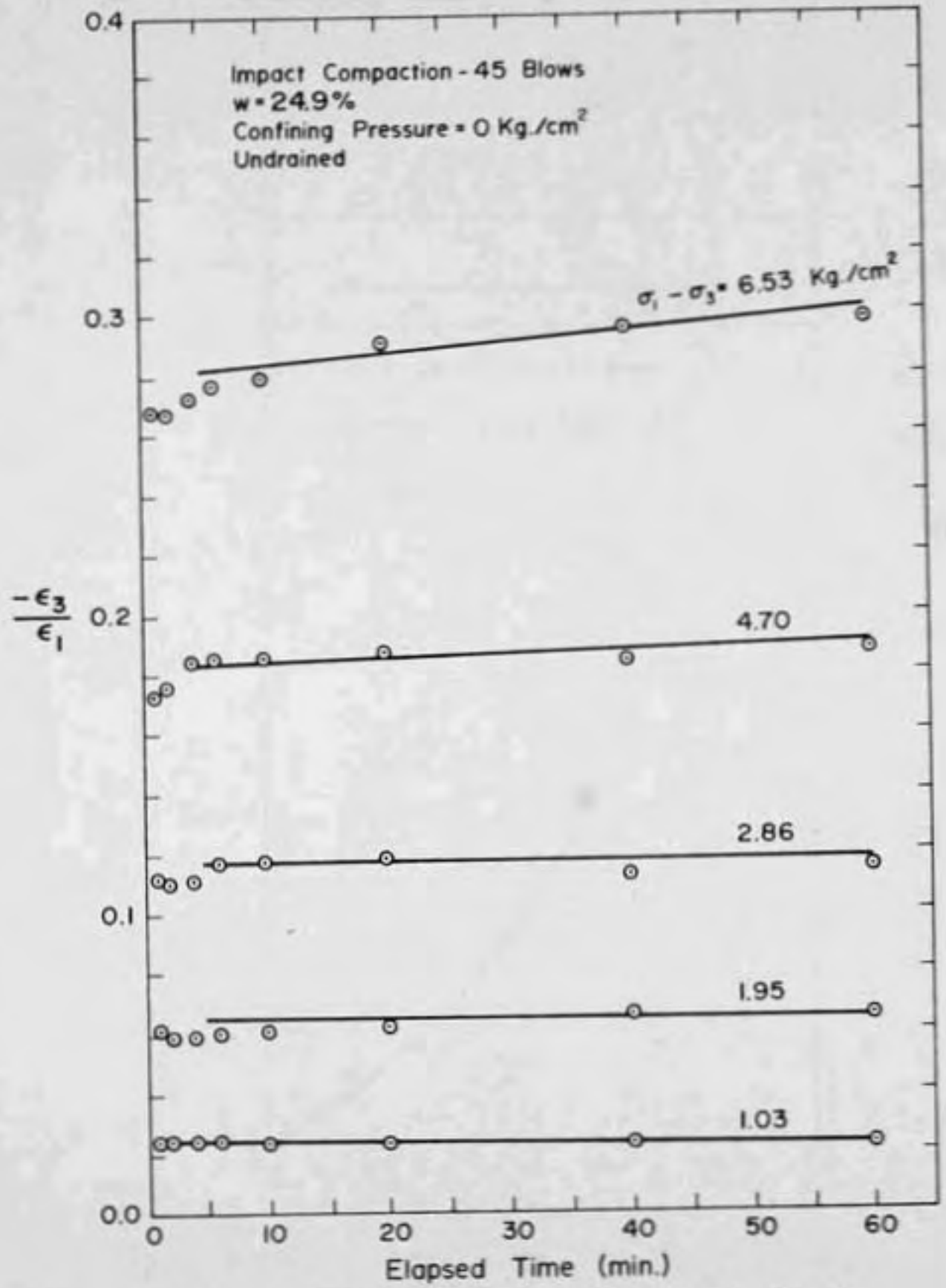

Figure 4.21 - Relation Between Principal Strain Ratio and Time for EPK
(Ramaswamy and Perloff, 1970)

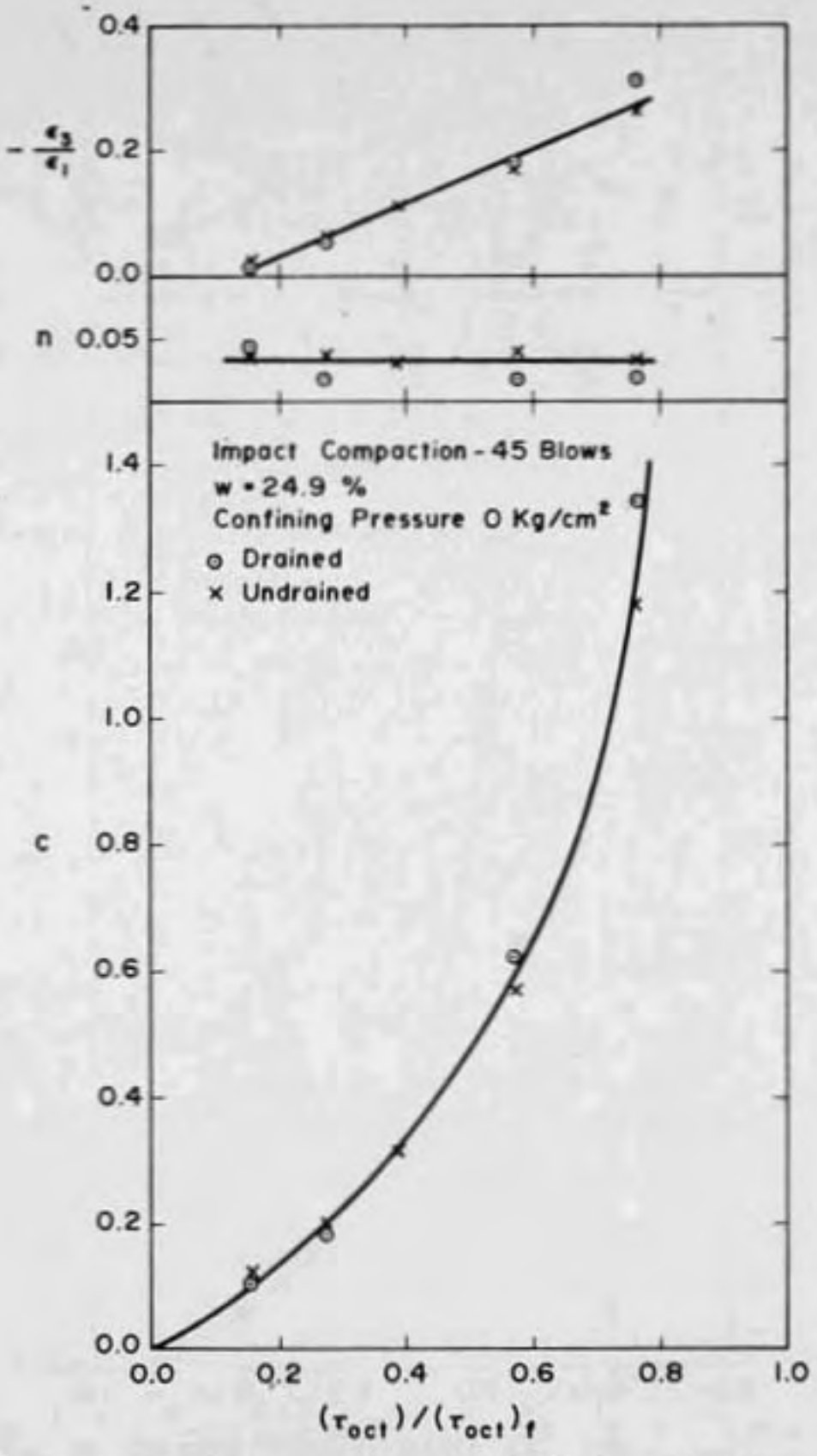

Figure 4.22 - Comparison of Effects of Stress - Strength Ratio for Drained and Undrained Creep Tests on EPK
(Data from Ramaswamy and Perloff, 1970)

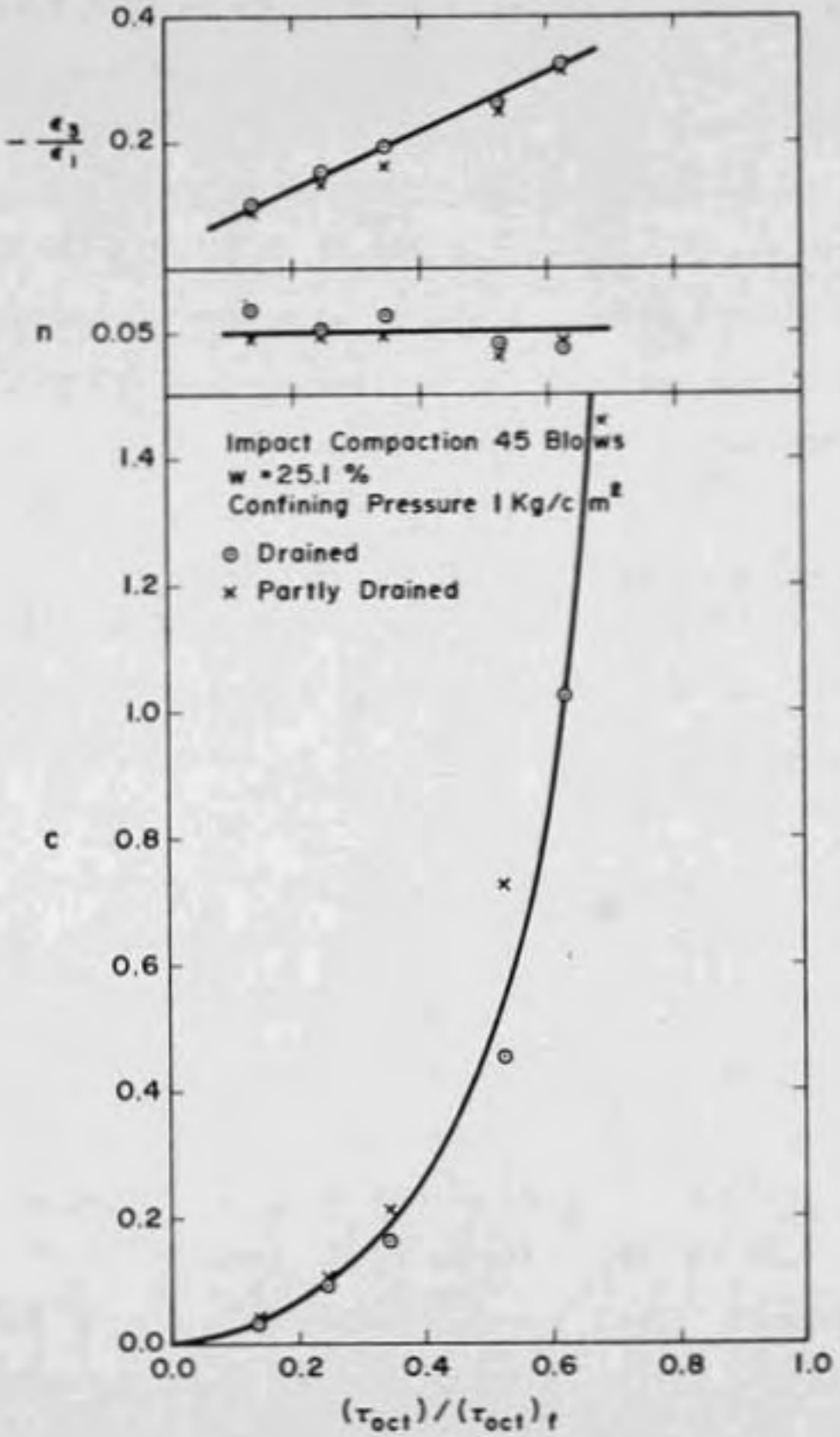

Figure 4.23 - Comparison of Effects of Stress-Strength Ratio for Drained and Partly Drained Creep Tests on EPK
(Data from Ramaswamy and Perloff, 1970)

cohesive soil under load is essentially independent of the length of the drainage path. Hence it is concluded that pore air pressure does not affect significantly the time-dependent behavior of partly saturated cohesive soil in the range of stresses used, and the mechanical properties are independent of the size of the soil mass considered in testing. But it is to be pointed out that the moisture content was two per cent dry of optimum. An approximate determination of the induced air pressure was made assuming that the entire volume change was due to the compression of air in the voids. It was found that the maximum induced air pressure was only about 1.5 psi. The conclusion is reasonable in view of the small magnitude of induced air pressure due to applied loads.

However experimental creep parameters may not be valid as the degree of saturation approaches one hundred per cent and air voids tend to become isolated. For example, if the hydrostatic confining pressure on a compacted cohesive soil specimen is increased and no drainage is permitted, the pressure is transmitted partly to the entrapped air. This air is reduced in volume at constant temperature according to Boyle's law and is partially dissolved in water according to Henry's law. Hence the degree of saturation will tend to increase significantly. But there is no definite information regarding the relation between the increase in degree of saturation and buildup of pore

water pressure. Casagrande and Hirschfield (1960) have done extensive investigations on the pore pressure buildup in the compacted cohesive soil subjected to various stress conditions. They concluded that the pore pressure development in specimens compacted to a given unit weight is principally a function of the water content and the total major principal stress. However, Yoshimi and Osterberg (1963) found no expulsion of water from compacted samples in a one-dimensional consolidation test even when the degree of saturation was as high as 97.0 per cent.

It is clear that the placement moisture content and the stresses to which the soil is to be subjected in the field have to be known before one can properly model the field behavior. The total stresses within the embankment can be computed with sufficient accuracy (Perloff, et. al, 1967). But moisture control is either lacking or applied in a number of ways, depending upon the project. Substantial pore pressure build up have been observed in earth embankments during construction (Gould, 1959; Gibbs, et. al, 1960). Walker and Holtz (1953) have investigated the practical limits within which the moisture content in the compacted fill can be varied, using the "limiting moisture concept" and the results of one-dimensional consolidation tests. The placement moisture content should neither be so low as to cause extensive settlement on saturation nor be so high as to cause a large increase in

pore water pressures during construction. They recommended a moisture content of 2 per cent less than the optimum as a suitable value. But Leonards and Narain (1964) advocated the use of at least optimum moisture content in earth dams to avoid a brittle material response and transverse cracking.

In the present investigation calculation for an impact compacted sample under a confining pressure of 1 kilogram per square centimeter indicated that the degree of saturation increased from 92.3 per cent to 93.3 per cent under a stepwise increase of deviator stress to 6.53 kilograms per square centimeter; the influence of confining pressure was not taken into account. Previous investigations have indicated (Sankaran, 1966) that there is no loss of moisture at similar stress levels. So, based on the present test results and the results of other investigators, a conservative upper limit for the major principal stress of about 8 kilograms per square centimeter (Casagrande and Hirschfield, 1960) can be set for the validity of the proposed parameters for a cohesive soil compacted at optimum moisture content. This works out to be the maximum vertical stress at the base of an embankment of 120 feet in height. However, this is an arbitrary limit, and for each soil the allowable major principal total stress is bound to vary with method

of compaction, placement moisture content and the existing drainage.

4.7 Generalized Stress-Strain-Time Relationship

Attempts to establish a comprehensive stress-strain-time relationship for cohesive soils have all been generalized from relatively simple testing conditions. The most common testing procedure used is the triaxial compression test, in which radial symmetry exists. The test results obtained in this study are compared with those of other investigations to verify the validity of the proposed relationships.

Lara-Tomas (1961) applied a constant torsional shear stress on a hollow cylindrical compacted soil sample and measured the shear deformation with time. The applied shear stress was the maximum shear stress, and proportional to the octahedral shear stress. He plotted logarithm of strain rate against logarithm of time and concluded that,

$$\frac{d\gamma}{dt} = at^{-m} \qquad (4\text{-}8)$$

in which

γ = shear strain

a, m = constants

t = time in minutes.

On integration of Equation 4-8,

$$\gamma(t) = \gamma_o + \frac{at^{-m+1}}{-m+1} \qquad (4\text{-}9)$$

Setting

$$\gamma = (\varepsilon_1 - \varepsilon_3)$$

$$n = -m+1$$

$$c = \frac{a}{-m+1}$$

$$\gamma_o = 0$$

Equation 4-9 becomes

$$\varepsilon_1 - \varepsilon_3 = ct^n \qquad (4\text{-}10)$$

This suggests that Lara-Tomas's (1962) results are consistent with those presented herein. A direct comparison with his findings is shown in Figure 4-24, in which the logarithm of strain rate is shown as a linear function of logarithm of time for creep tests on EPK. As the shear stress is increased, the straight line has a tendency to move up, the value of m being almost the same, independent of stress level. These results are similar to those obtained by Lara-Tomas (1962).

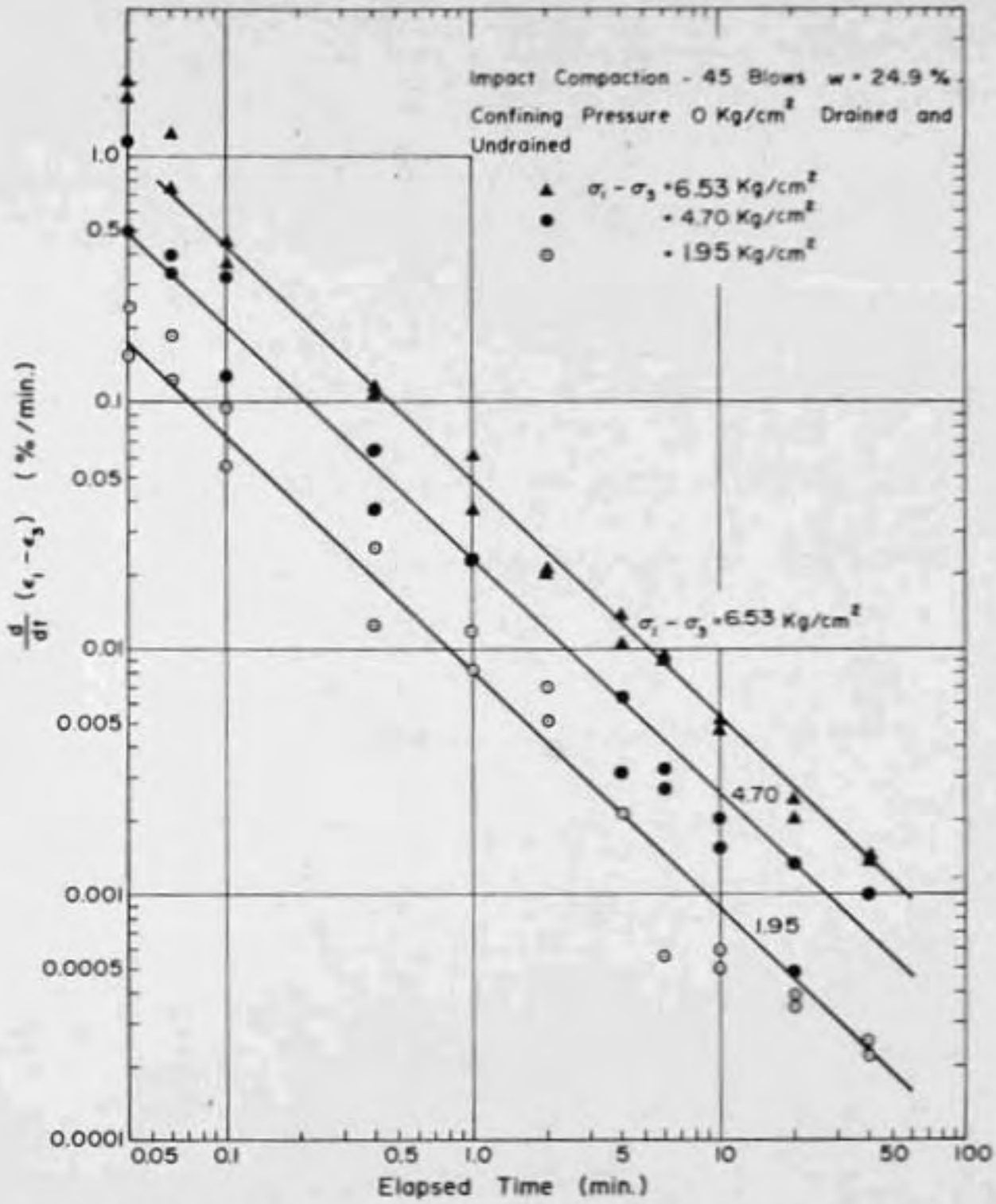

Figure 4.24 - Relation Between Shear Strain Rate and Time at Various Stress Levels for EPK
(Ramaswamy and Perloff, 1970)

Similar results were obtained by Mitchell et. al. (1969) for measured axial strains of saturated clay specimens subjected to triaxial compression creep testing under constant cell pressure. (Equation 2-1) Because radial strains are proportional to axial strains for saturated specimens, their results also support those presented herein.

The results obtained by Pagen and Jagannath (1967, 1968) are also consistent with the representation proposed.

4.8 Non-linear Viscoelastic Material Characterization

It has already been indicated that the response of many types of non-linear viscoelastic materials can be expressed in a form similar to that for linear viscoelastic behavior. For example, for uniaxial loading,

$$\varepsilon(t) = g_o D_o \sigma + g_1 \int_0^t \Delta D(\psi - \psi') \frac{dg_2\sigma}{d\tau} d\tau \qquad (2\text{-}20)$$

Because the logarithm of the creep compliance is a linear function of the logarithm of time, it is necessary to use both creep and recovery data to determine the magnitude of, g_o, g_1, g_2 and a_σ which are stress dependent parameters (Schapery, 1969a, 1969b; Lou and Schapery, 1969).

For a two-step uniaxial loading test,

$$\sigma = \begin{cases} 0, & t < 0 \\ \sigma_a, & 0 < t < t_a \\ \sigma_b, & t_a < t < t_b \end{cases} \tag{4-11}$$

where σ_a and σ_b are constant stresses. Then from Equation 4-11 for $0 < t < t_a$, using the Dirac delta function for $d\sigma/dt$,

$$\epsilon = [g_o^a D_o + g_1^a g_2^a \Delta D(\psi)] \sigma_a \tag{4-12}$$

or

$$\epsilon = D_n^a \sigma_a \tag{4-13}$$

in which

$$\psi = \frac{t}{a_o^a}$$

and D_n^a is the nonlinear uniaxial creep compliance for the stress σ_a. The strain for $t_a < t < t_b$ is

$$\epsilon = g_o^b D_o \sigma_b + g_1^b [g_2^a \sigma_a \Delta D(\psi_b) + (g_2^b \sigma_b - g_2^a \sigma_a) \Delta D(\psi_a)] \tag{4-14}$$

in which

$$\psi_a = \frac{t - t_a}{a_\sigma^b}$$

$$\psi_b = \frac{t_a}{a_\sigma^a} + \frac{t - t_a}{a_\sigma^b} .$$

The superscripts on the material parameters indicate the stress at which they are to be evaluated.

These equations can be used to evaluate the stress dependent parameters ε_o, ε_1, ε_2 and a_σ. For a creep and recovery test

$$\sigma_a = \sigma_1 - \sigma_3 \tag{4-15}$$

$$\sigma_b = 0 \tag{4-16}$$

Combining equations 4-13, 4-14, 4-15, 4-16 and expressing in terms of shear strains, the creep strain is

$$(\varepsilon_1-\varepsilon_3)(t) = J_n(\sigma_1-\sigma_3) = [\varepsilon_o J_o + \varepsilon_1 \varepsilon_2 \Delta J(\psi)] (\sigma_1-\sigma_3) \tag{4-17}$$

in which

$\Delta J(\psi)$ is the linear shear creep compliance,

J_o is the initial (time independent) component of the shear creep compliance,

J_n is the non-linear shear creep compliance at shear stress level $(\sigma_1 - \sigma_3)$.

From this expression, the time dependent component of the shear creep compliance can be obtained as

$$\Delta J_n = J_n - \varepsilon_o J_o = \varepsilon_1 \varepsilon_2 \Delta J(\psi) \tag{4-18}$$

or

$$\log (\Delta J_n) = \log (\varepsilon_1 \varepsilon_2) + \log \Delta J(\psi) \tag{4-19}$$

Thus, in general, if log (ΔJ_n) is plotted as a function of log (t), curves at different stress levels should be parallel. Using the reference linear viscoelastic compliance curve as a "master curve", the others can be shifted to it. The amount of horizontal (t) shift is equal to log a_σ and the vertical shift is log ($g_1 g_2$).

If, however, the lines at different stress levels are not only parallel but also straight, as indicated by the test results on compacted cohesive soils (Figure 4-4), unique values for a_σ and $g_1 g_2$ cannot be obtained from creep data alone. Recovery data must also be used.

Denoting the recovery shear strain by ϵ_r,

$$\epsilon_r = (\epsilon_1 - \epsilon_3)_{recovery}$$

the recovery curve for unloading at $t = t_a$ can be obtained from Equation 4-14, since $g_1^b = 1$ for $\sigma_b = 0$. In terms of shear parameters this gives

$$\epsilon_r = g_2 (\sigma_1 - \sigma_3) [\Delta J(\psi_b) - J(\psi_b - \psi_a)] \qquad (4\text{-}20)$$

in which

$$\psi_b = \frac{t_a}{a_\sigma} + t - t_a, \quad ; \quad \psi_a = \frac{t_a}{a_\sigma}$$

For the compacted clays tested it is apparent from Equation 4-3 that

$$J_o = 0 \ , \quad \Delta J(\psi) = k\psi^n \qquad (4\text{-}21)$$

in which k is a constant and is equal to the linear shear creep compliance. Then the creep strain at $t = t_a$ is

$$(\varepsilon_1-\varepsilon_3)_c = \Delta\varepsilon_c = g_1 g_2 k \left(\frac{t_a}{a_\sigma}\right)^n (\sigma_1-\sigma_3) \qquad (4\text{-}22)$$

and the recovery strain is .

$$\varepsilon_r = g_2(\sigma_1-\sigma_3)\, k[\phi_b^n - (\phi_b-\phi_a)^n] \qquad (4\text{-}23)$$

The ratio between Equations 4-22 and 4-23 is

$$\frac{\varepsilon_r}{\Delta\varepsilon_c} = \frac{1}{g_1}\,[(1 + a_\sigma\lambda)^n - (a_\sigma\lambda)^n] \qquad (4\text{-}24)$$

in which

$$\lambda = \frac{t - t_a}{t_a}$$

Taking the logarithm of Equation 4-24,

$$\log\left(\frac{\varepsilon_r}{\Delta\varepsilon_c}\right) = -\log(g_1) + \log[(1+a_\sigma\lambda)^n-(a_\sigma\lambda)^n] \qquad (4\text{-}25)$$

It is evident from Equation 4-25 that a graphical shifting procedure can be applied to recovery data to determine a_σ and g_1 for different stress levels. A reference curve of normalized recovery strain $(\varepsilon_r/\Delta\varepsilon_c)$ is plotted against λ on double logarithmic paper by letting $a_\sigma = g_1 = 1$ in Equation 4-24 for appropriate values of n. Figure 4-25 shows normalized recovery strain curves for several values of n. The reference curve is the normalized recovery strain for a

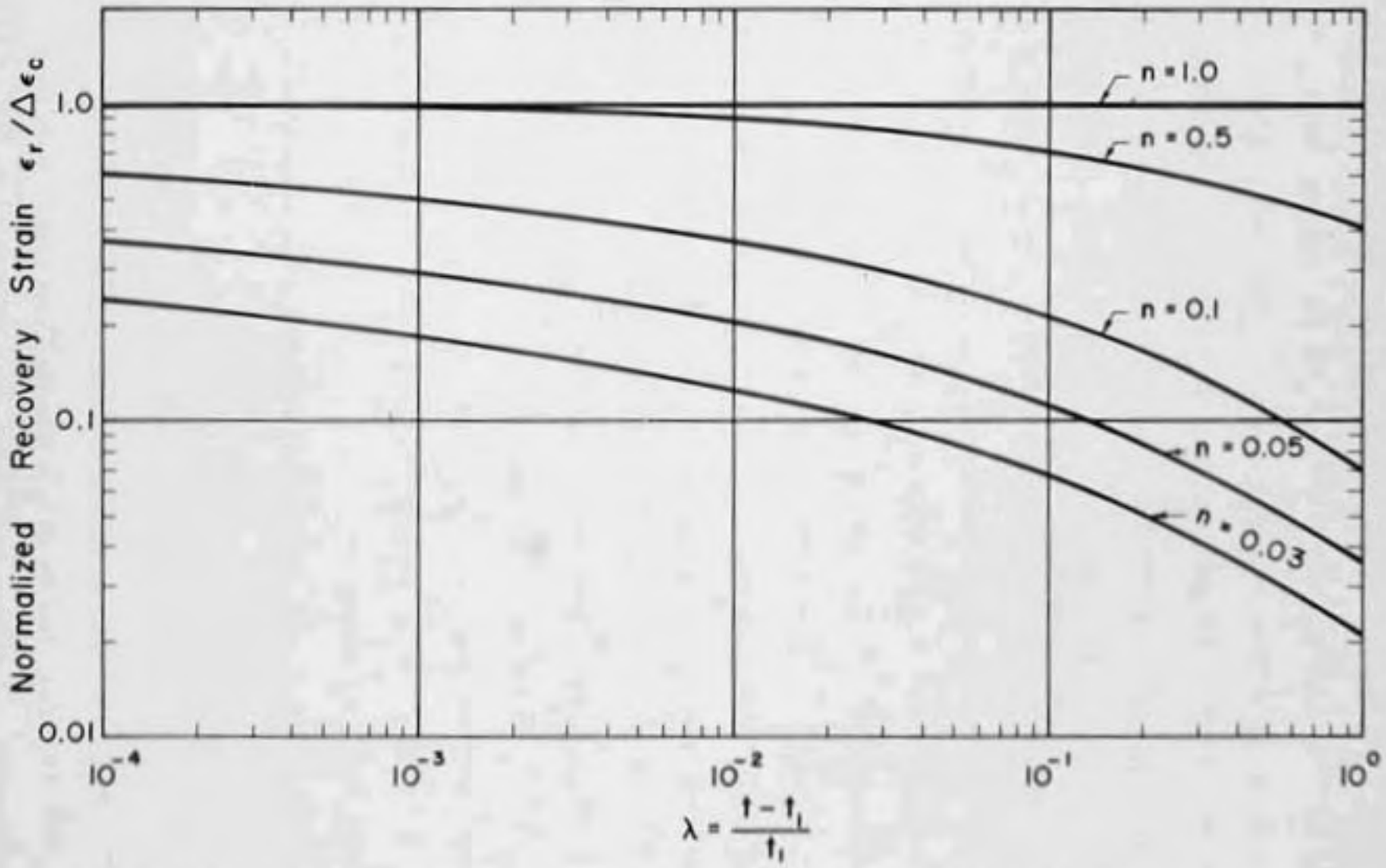

Figure 4.25 - Normalized Recovery Curve for $D(t) = D_1 t^n$

linear viscoelastic material. The normalized recovery curve for each stress level can be superimposed on the reference linear viscoelastic curve by translating it along the two axes. The amount of horizontal shift (λ) to the left, and the vertical shift ($\varepsilon_r/\Delta\sigma_c$) up are equal to log a_σ and log g_1 respectively. Since the curves are not generally straight lines, unique values of a_σ and g_1 can be obtained. When the linear viscoelastic creep compliance is known, the magnitude of g_2 can be determined from creep curves. Knowing the values of a_σ, g, and k, different values of g_2 can be substituted in Equation 4-17 until the predicted creep curve coincides with the actual creep curve. Hence all the values that are needed to characterize the material at a particular stress level can be obtained.

In applying the above non-linear viscoelastic formulation to the behavior of compacted cohesive soils, the effect of confining pressure and the moisture content can be accounted for it the creep strain is expressed as a function of the stress-strength ratio. Therefore it is convenient to define a normalized creep compliance J'(t), as

$$J'(t) = \frac{\gamma_{oct}(t)}{[(\tau_{oct})/(\tau_{oct})_f]} \qquad (4\text{-}26)$$

The actual shear creep compliance can be obtained by dividing the normalized shear creep compliance by the octahedral shear stress at failure corresponding to the existing octahedral normal stress.

A series of creep and recovery tests for EPK, compacted by kneading, are presented to show that the non-linear viscoelastic relationships are applicable to compacted cohesive soil. The procedure adopted was to determine the stress dependent parameters g_1, g_2 and a_σ for a particular specimen and to use them in predicting the creep and recovery response of other specimens compacted by the same method.

Figure 4-26 shows the normalized master recovery strain curve for the sample. From this figure, the magnitudes of a_σ and g_1 at each stress level were obtained. It was found that even at the lowest stress levels the values of g_1 and a_σ were not equal to one. Hence the linear viscoelastic stress level was lower than the lowest stress level used. So a method had to be devised to determine the magnitude of the normalized linear viscoelastic creep compliance.

One of the expressions that can be used to describe the creep compliance is (Thorkildson, 1958)

$$D_n = \frac{\sinh(\sigma/\sigma_e)}{\sigma/\sigma_e} D_o + \frac{\sinh(\sigma/\sigma_m)}{\sigma/\sigma_m} D_1 t^n \qquad (4\text{-}27)$$

where

σ_e, σ_m D_1 and n are parameters for a particular material.

For compacted cohesive soils, the equation can be modified to express the normalized shear creep compliance as,

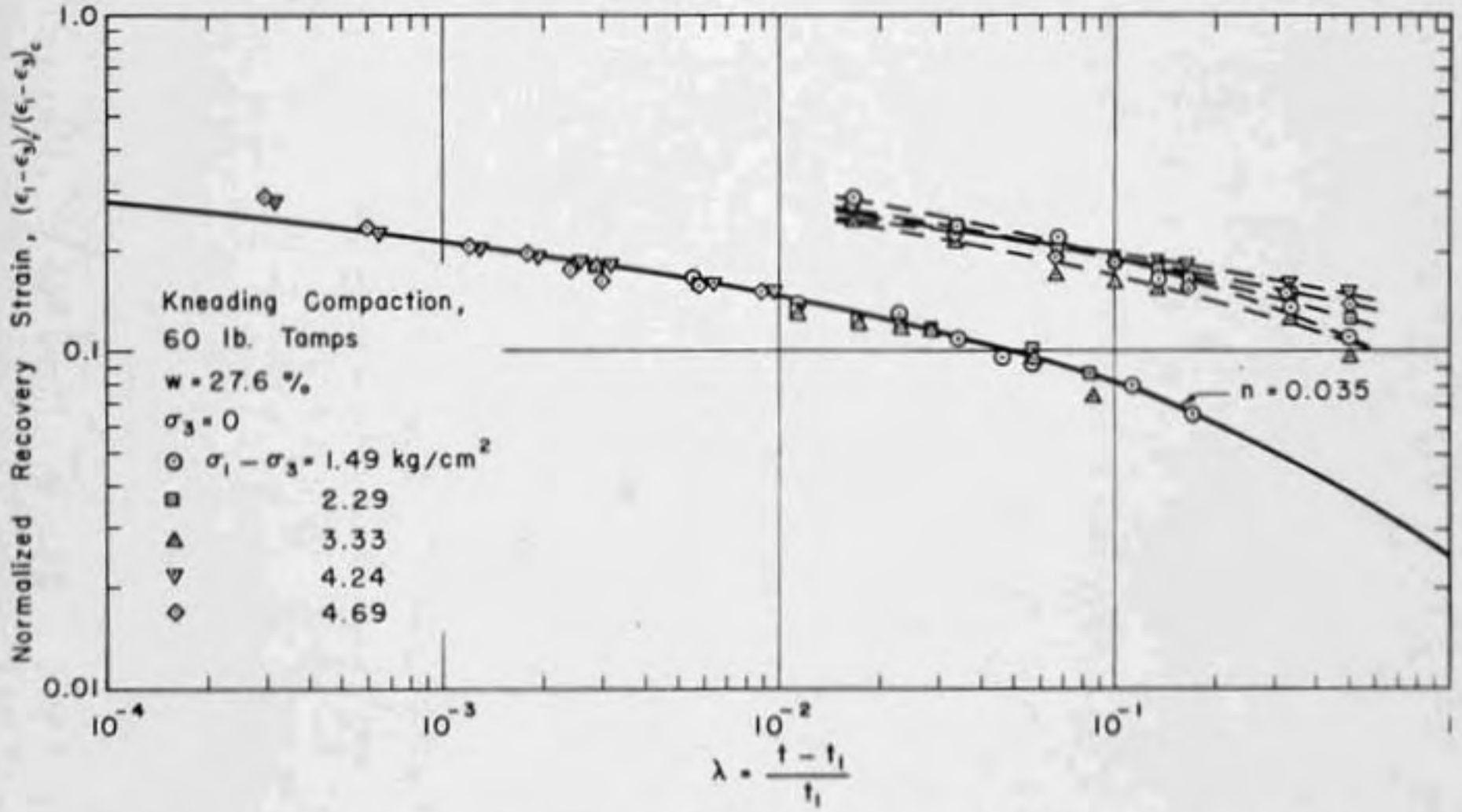

Figure 4.26 - Determination of Shift Factors a_σ and g_1 for EPK
(Data from Ramaswamy and Perloff, 1970)

$$J'(t) = \frac{\sinh (R_1/R_o)}{(R_1/R_o)} \; J'_o \; t^n \qquad (4\text{-}28)$$

where

$R_1 = \tau_{oct}/(\tau_{oct})_f$;

R_o = constant for the particular material;

J'_o = the normalized linear shear creep compliance.

Also,

$$\frac{\varepsilon_1 \varepsilon_2}{a_\sigma^n} = \frac{\sinh (R_1/R_o)}{(R_1/R_o)} \qquad (4\text{-}29)$$

The octahedral shear strain at any time can be written as

$$\gamma_{oct}(t) = \frac{\sinh (R_1/R_o)}{(R_1/R_o)} \; J'_o \; t^n \; R_1 \qquad (4\text{-}30)$$

The values of J'_o and R_o are obtained by fitting Equation 4-30 to the plot of octahedral shear strain at one minute as a function of the stress-strength ratio by the method of least squares. The curves shown in Figures 4-17, 4-18 and 4-19 are actually obtained from Equation 4-30 for t = 1 minute.

The magnitude of ε_2 can be obtained from Equation 4-29:

$$\varepsilon_2 = \frac{\sinh (R_1/R_o)}{(R_1/R_o)} \cdot \frac{a_\sigma^n}{\varepsilon_1} \qquad (4\text{-}31)$$

Figure 4-27 shows the effect of the stress strength ratio on the magnitudes of non-linear viscoelastic parameters for an unconfined kneading compacted specimen of moisture content 27.5 per cent. The fact that a shifting procedure can be conveniently applied to obtain the parameters a_σ and g_1 is itself an indication that the proposed nonlinear viscoelastic constitutive law can be applied to compacted cohesive soils. Figure 4-27 was used to obtain the creep parameters for predicting the creep response of some other samples with different moisture contents and confining pressures. The creep strain for the instantaneous step loading is

$$(\varepsilon_1-\varepsilon_3)(t) = \frac{3}{2\sqrt{2}}\ \gamma_{oct} = \frac{3}{2\sqrt{2}}\ g_1 g_2\ (\frac{t}{a_\sigma})^n\ J'_o R_1 \qquad (4\text{-}32)$$

Figure 4-28 shows the predicted and experimental creep curves. The points shown are the measured data, the solid lines are the predicted relations. The maximum deviation was found to be eight per cent.

The data of Figure 4-27 were also used to predict both creep and recovery response for specimens at various confining pressures. The recovery strain is

$$(\varepsilon_1-\varepsilon_3)_r = \frac{3}{2\sqrt{2}}\ (\gamma_{oct})_r$$

$$= \frac{3}{2\sqrt{2}}\ \frac{(\gamma_{oct})_c}{g_1}\ [(1+a_\sigma\lambda)^n - (a_\sigma\lambda)^n] \qquad (4\text{-}33)$$

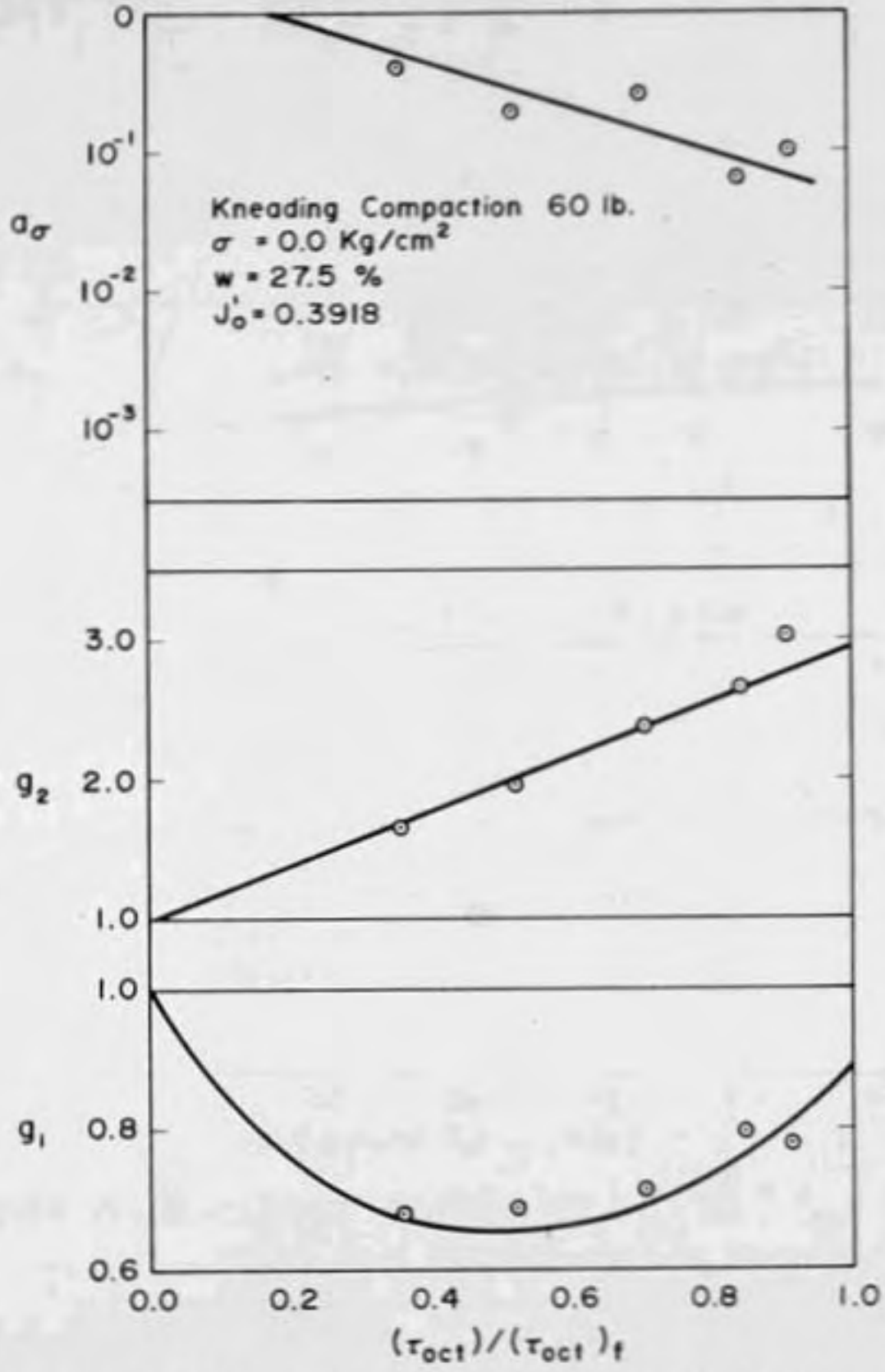

Figure 4.27 - Effect of Stress Strength Ratio on Nonlinear Viscoelastic Parameters for EPK

(Data from Ramaswamy and Perloff, 1970)

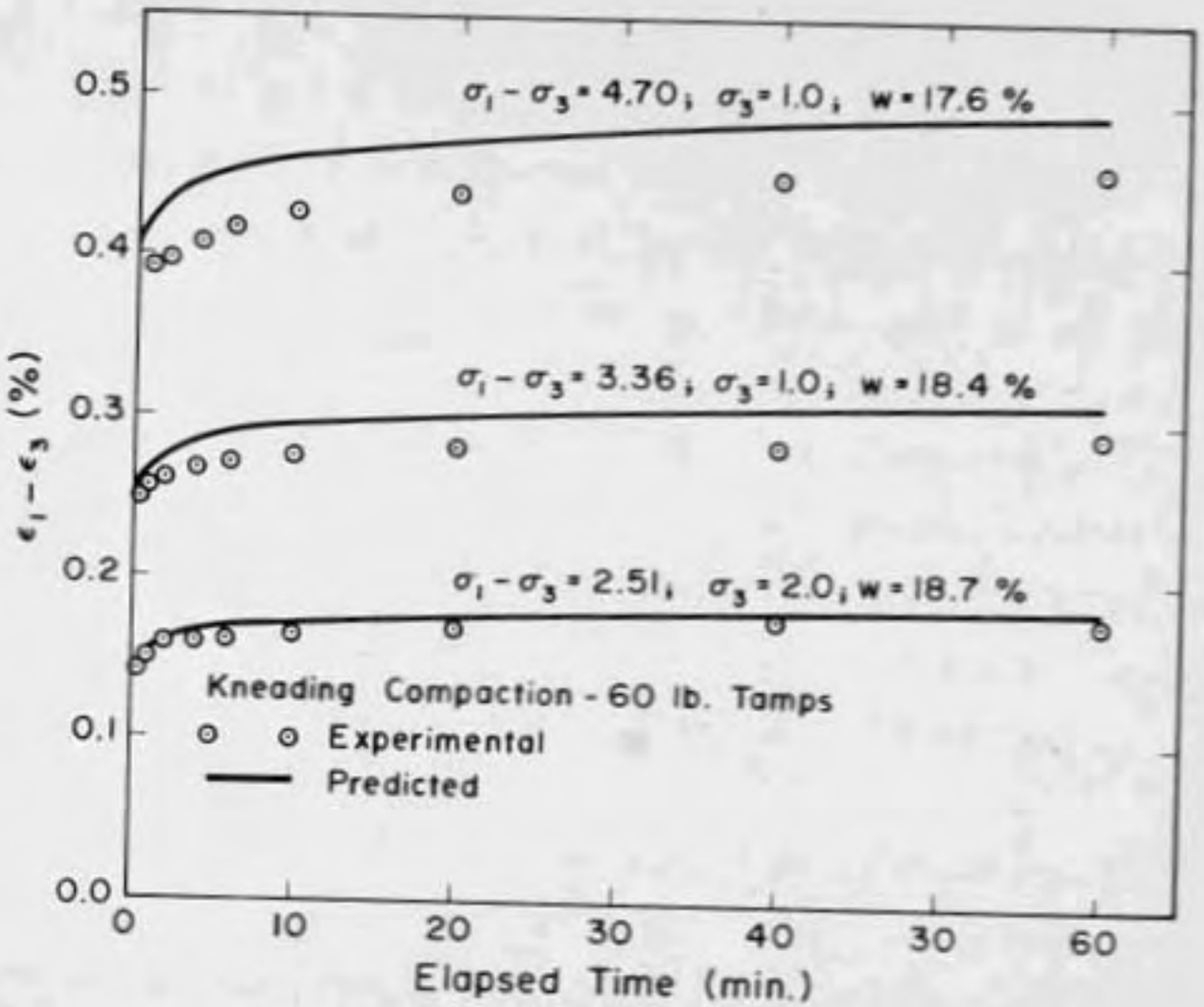

Figure 4.28 - Creep Curve for EPK
(Data from Ramaswamy and Perloff, 1970)

The comparison between predicted and measured strains is shown in Figure 4-29. The points show the measured strains; the solid lines are the results predicted from Equations 4-32 and 4-33.

4.9 Effects of Anisotropy

During the compaction process, clay particles are likely to develop a preferred orientation perpendicular to the major principal stress direction. Hence the question arises as to whether the compacted clay will be anisotropic in its strength and stress-strain characteristics. To determine the extent of the anisotropic behavior of compacted cohesive soils, two series of triaxial extension creep tests were conducted, in which the direction of major principal stress was parallel to the plane of compaction. The soil tested was EPK and both impact and kneading compaction were used.

For these tests the Norwegian triaxial shear equipment was modified so that the diameter of the loading piston was the same as that of the sample. Thus an increase in fluid pressure around the sample would not affect the axial stress.

The triaxial extension tests were conducted undrained. The sample was set up in a generally similar manner as in compression creep tests. Confining pressure was applied by means of the constant pressure cell. However the

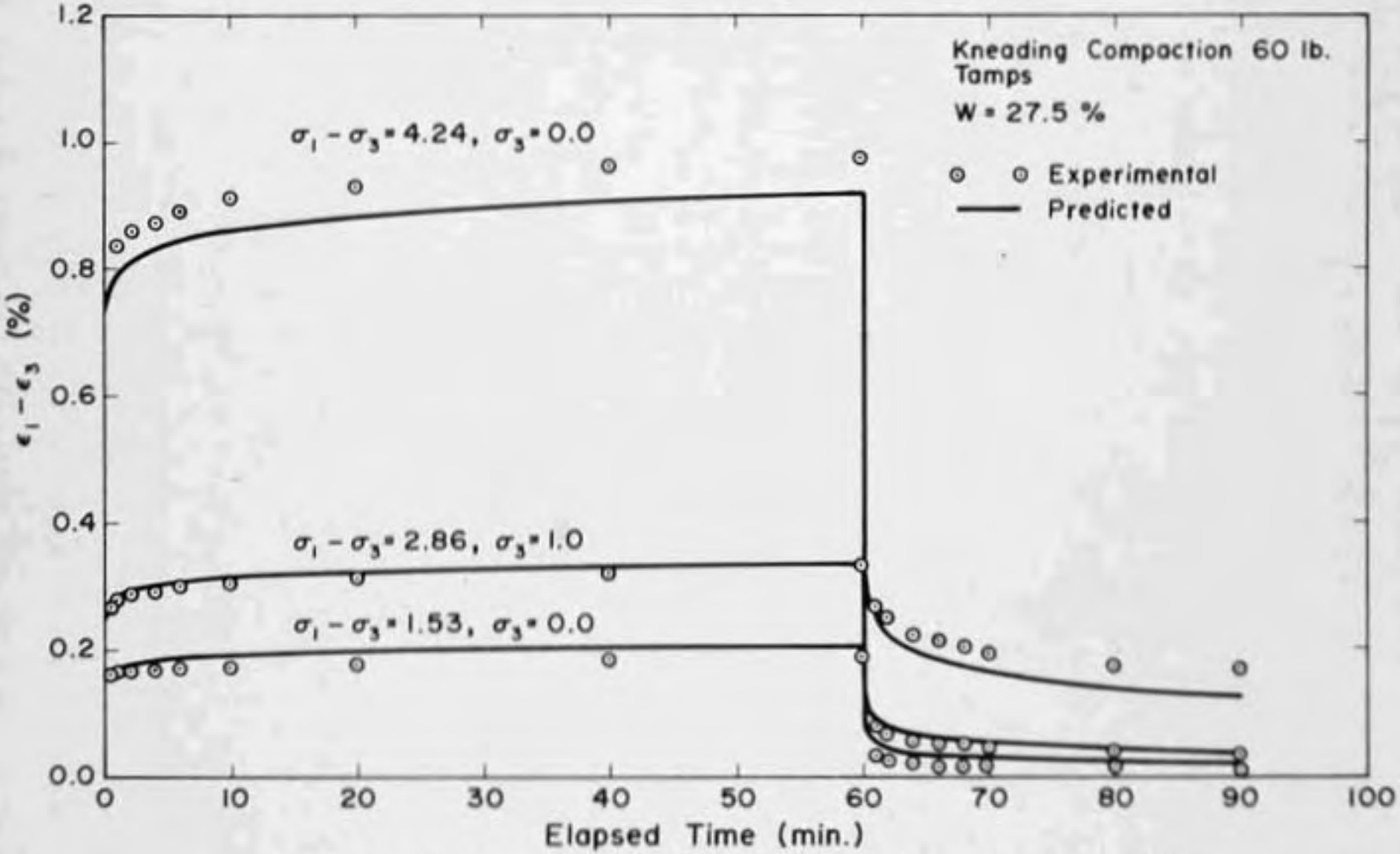

Figure 4.29 - Creep and Recovery Curves for EPK
(Data from Ramaswamy and Perloff, 1970)

specimens are undrained since a plexiglas disc was used at the bottom of the specimen, instead of the porous stone. In the initial tests it was found that the application of confining pressure sometimes lifted the specimen off the base. Hence "Duco Cement" was used to create a bond between the base pedestal and the plexiglas disc, as well as between the disc and the soil. After the deformations had almost ceased, the lateral stress which was the major principal stress, was increased to the required level.

When the lateral stress was applied, the triaxial cell itself deformed resulting in the movement of the top cap of the cell, which was the reference for measurement of axial deformation. Hence a correction had to be applied. This was done by conducting an extension test on a steel cylinder at the same stress levels applied in the extension test; also they were too small to produce any deformation in the steel sample. Hence the movement of the axial deformation gauge was entirely due to the triaxial cell. Two tests were conducted and the average of the two was used to correct the extension test data on the compacted soil sample.

Since the major principal stresses in the extension test are the lateral stresses, the magnitude of the equivalent Poisson's ratio is not equal to the ratio between the principal strains. Its value at a particular time t can be obtained by noting that for isotropic linear

elastic behavior:

$$\Delta\varepsilon_1 = \frac{1}{E}\left[\Delta\sigma_1 - \mu(\Delta\sigma_2 + \Delta\sigma_3)\right] \qquad (4\text{-}34)$$

and

$$\Delta\varepsilon_3 = \frac{1}{E}\left[\Delta\sigma_3 - \mu(\Delta\sigma_1 + \Delta\sigma_2)\right] \qquad (4\text{-}35)$$

For the triaxial extension test

$$\Delta\sigma_2 = \Delta\sigma_1 = \Delta\sigma_r \qquad (4\text{-}36$$

and

$$\Delta\sigma_3 = \Delta\sigma_a - 0 \qquad (4\text{-}37)$$

In these expressions the Δ indicates an incremental value after consolidation under an all-round pressure. Substituting Equations 4-36 and 4-37 into Equations 4-34 and 4-35, and dividing,

$$\frac{\Delta\varepsilon_3}{\Delta\varepsilon_1} = \frac{-2\mu}{1-\mu} \qquad (4\text{-}38)$$

or

$$\mu = \frac{-\Delta\varepsilon_3}{2\Delta\varepsilon_1 - \Delta\varepsilon_3} \qquad (4\text{-}39)$$

This expression was used to determine the equivalent Poisson's ratio at time t from the extension test results.

Figure 4-30 shows the typical results of an extension test series conducted on compacted Edgar Plastic Kaolin (EPK). It also indicates that the relation between maximum

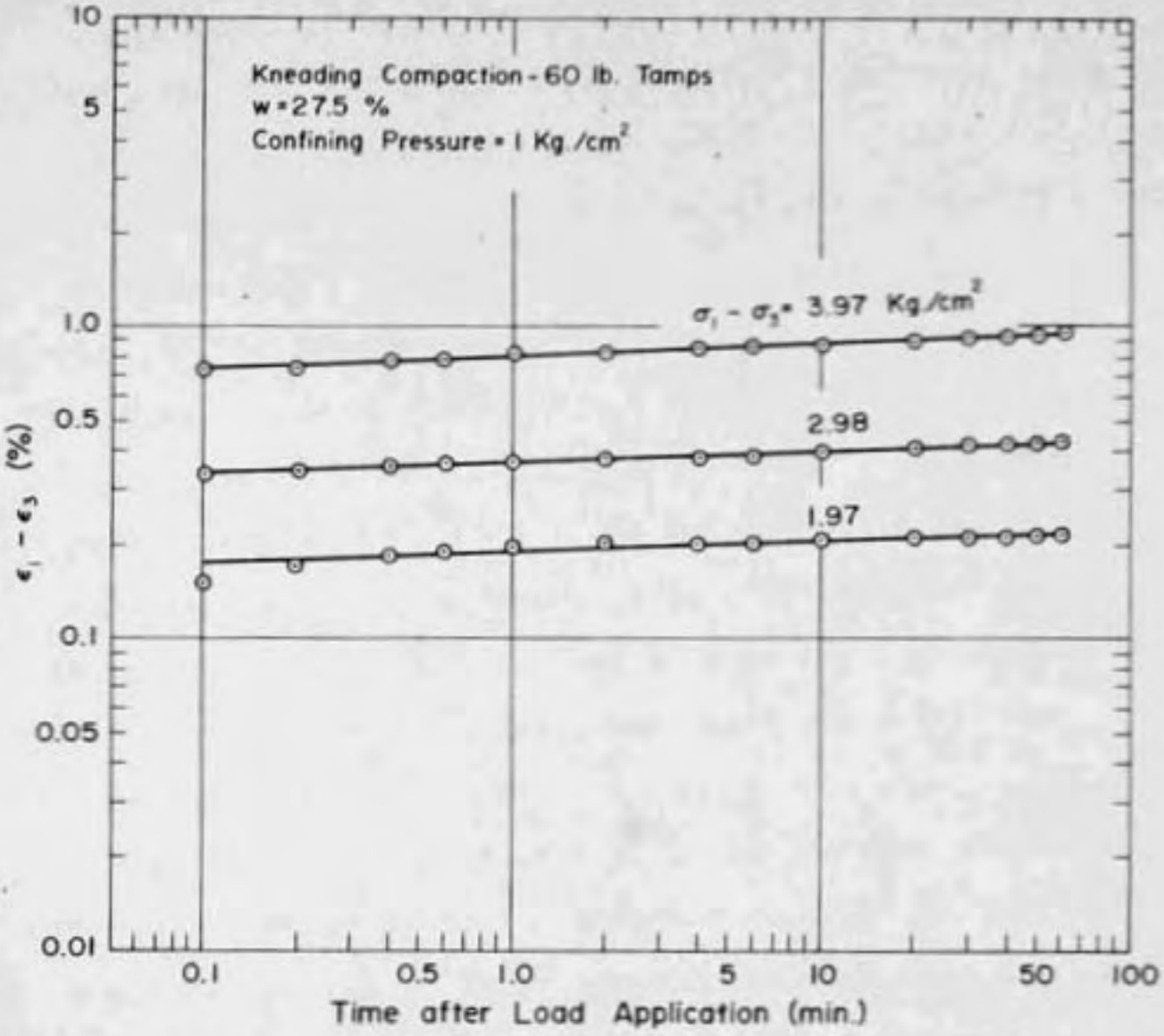

Figure 4.30 - Relation Between Maximum Shear Strain and Time for Extension Creep Tests on EPK

(Ramaswamy and Perloff, 1970)

shear strain and time in an extension test can be represented by Equation 4-3.

As shown in Figure 4-31 the magnitude of the equivalent Poisson's ratio was independent of time at a particular stress level. The influence of stress level on the equivalent Poisson's ratio was minor. However, the magnitude of the equivalent Poisson's ratio was greater than previously noted in the compression creep tests, even exceeding 0.5 as shown in Figure 4.33.

Figures 4-32 and 4-33 show the comparison between drained compression creep tests and undrained extension tests for two types of compaction. At low shear stress levels the magnitudes of c are similar for the two tests. But at higher stress levels, the magnitude c for the extension tests was higher.

Due to limitations on the maximum chamber pressure, it was not possible to increase the stresses to failure in extension tests. Hence the results could not be compared at equal stress-strength ratios. From an inspection of the figures, it seems probable that even if the strength ratio has been used, c would have been larger for the extension tests at higher stress ratios. As shown in Figures 4-32 and 4-33, the magnitude of n was independent of the stress system and shear stress level.

Figure 4-34 shows the results of an isotropic consolidation test conducted on a grundite specimen. If the

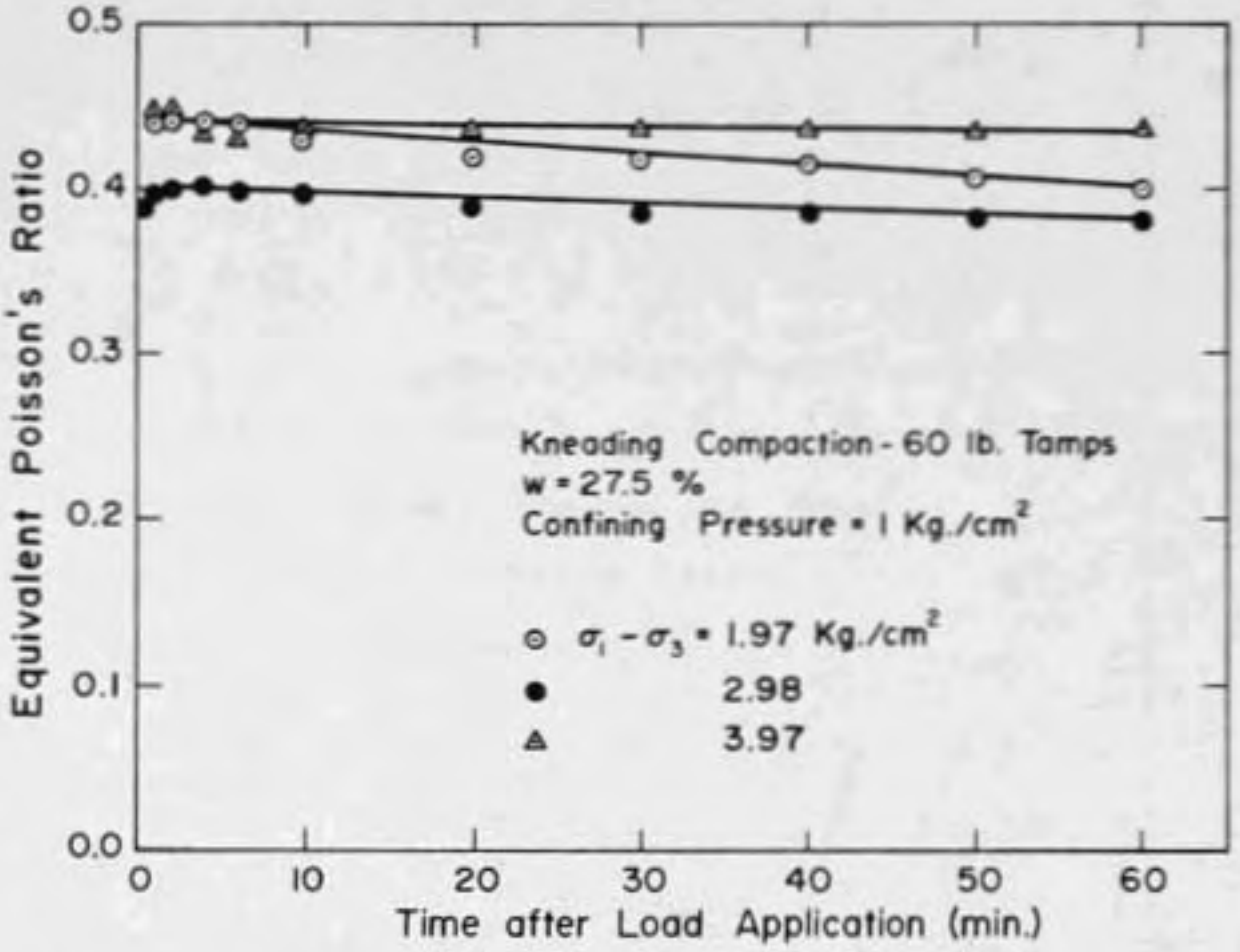

Figure 4.31 - Relation Between Equivalent Poisson's Ratio and Time for Extension Tests on EPK

(Ramaswamy and Perloff, 1970)

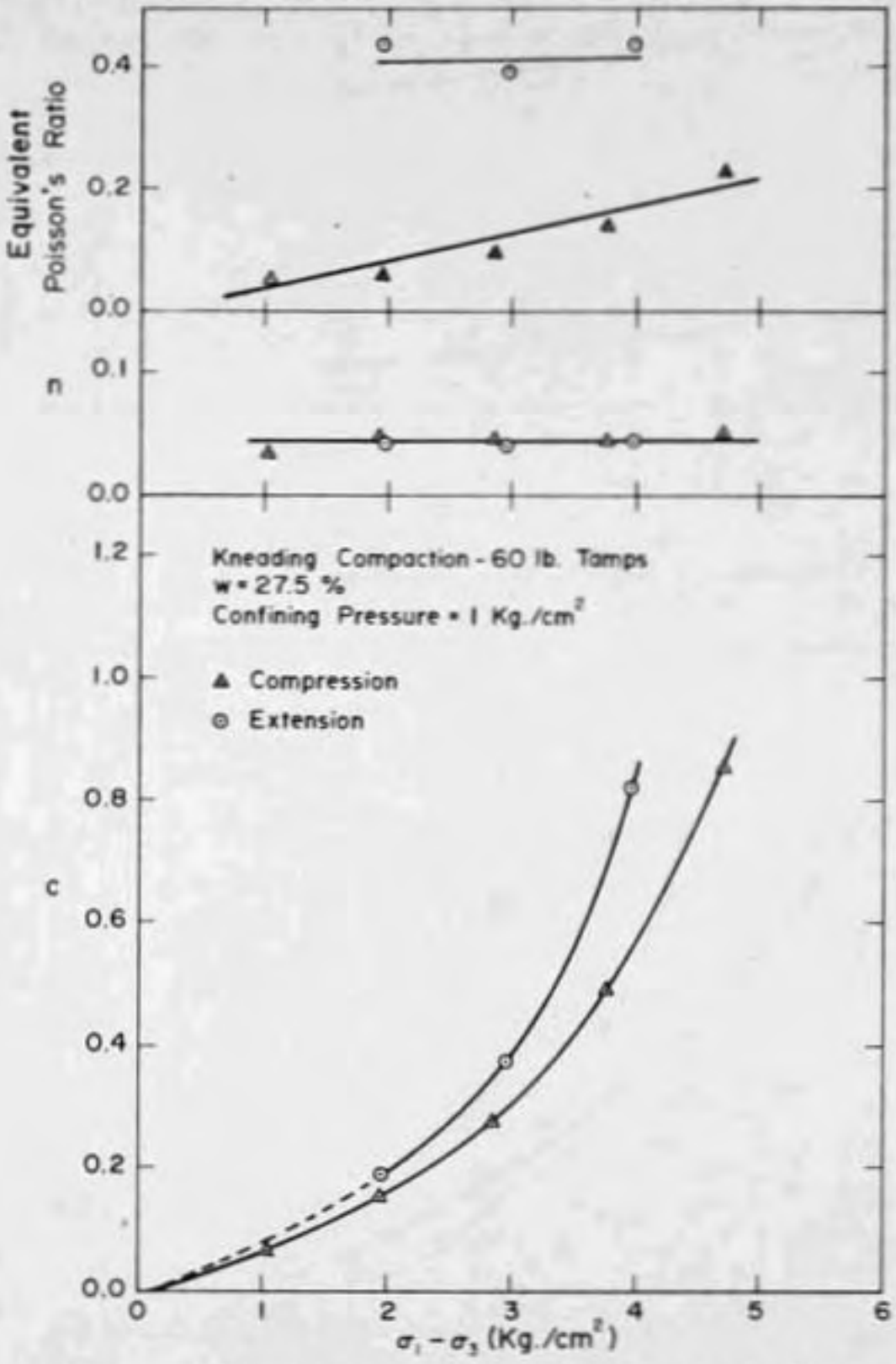

Figure 4.32 - Comparison of Effect of Stress Level on Creep Parameters Between Compression and Extension Creep Tests. (Ramaswamy and Perloff, 1970)

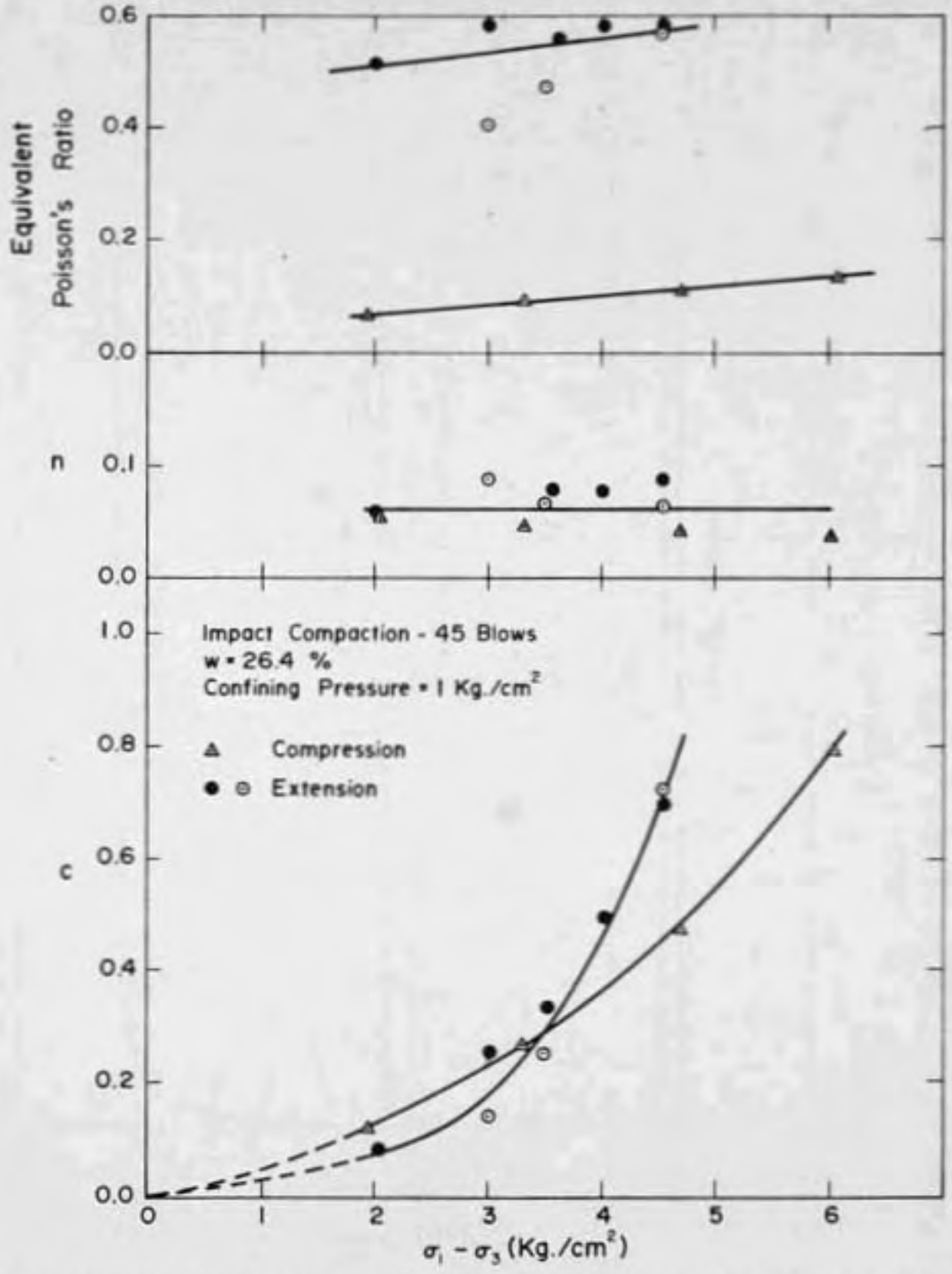

Figure 4.33 - Comparison of Effect of Stress Level on Creep Parameters Between Compression and Extension Tests for E P K

(Ramaswamy and Perloff, 1970)

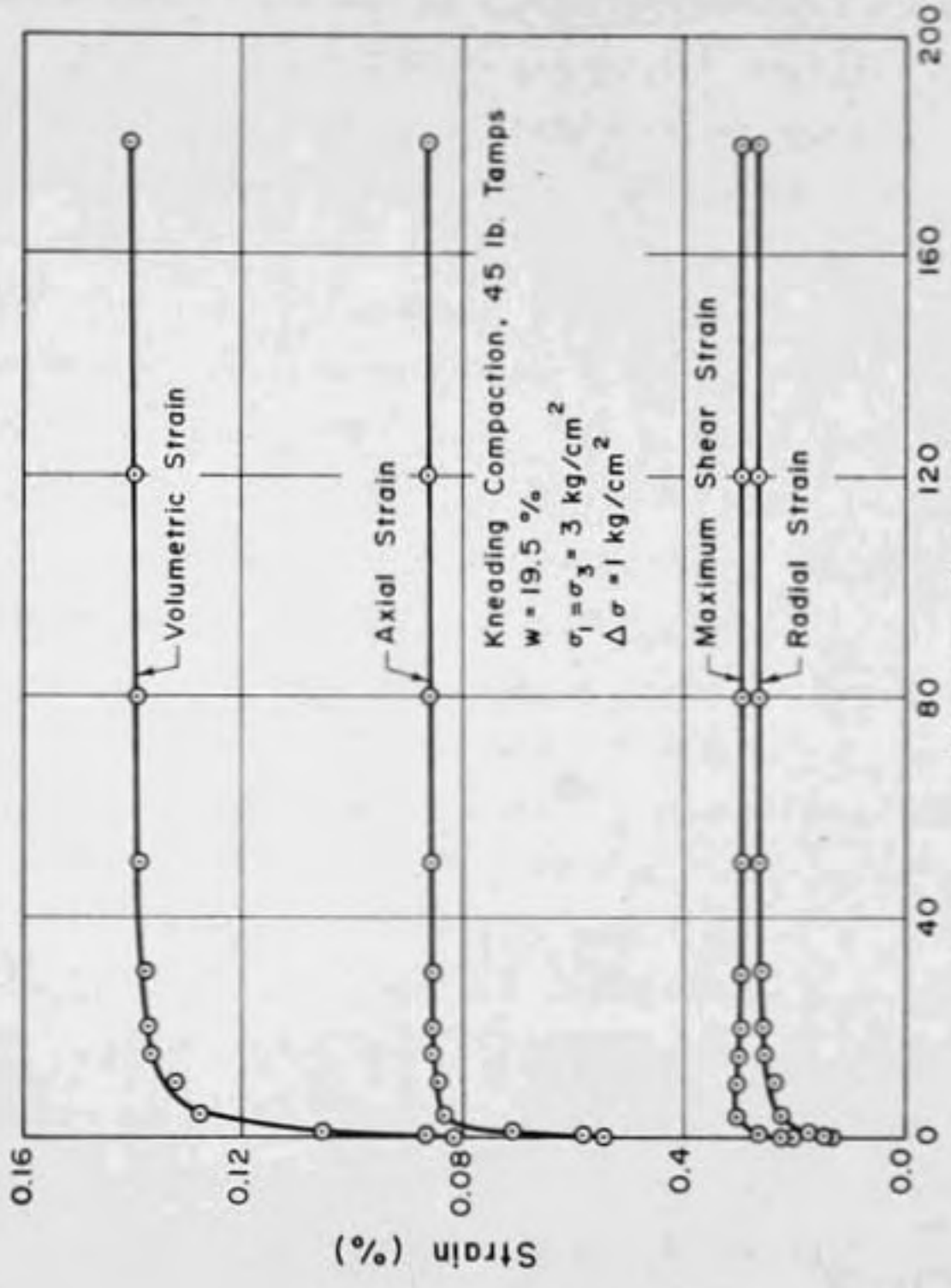

Figure 4.34 - Triaxial Consolidation Results for Grundite (Perloff, 1966)

material had been isotropic, only volumetric strain should have been observed. But it is seen that a shear strain also occurs in response to an applied spherical stress.

The results cited above suggest that the soil behaves in an anisotropic manner. The implication of anisotropic response is that a minimum of five parameters or functions are required to describe the mechanical behavior of the simplest anisotropic material. It was not possible to evaluate the necessary parameters from the extension and compression test results alone. Also, doubts have been expressed about comparing the results of extension and compression tests on a triaxial specimen to obtain the necessary parameters for soils (Roscoe, et. al., 1963).

However the following comparison may be of use in evaluating the influence of anisotropic behavior in the proposed analysis. The modulus of elasticity at one minute was calculated for both extension and compression tests, assuming the material to be isotropic. The ratio between the modulus calculated for the extension test and that for the compression test at the same stress level varied from 0.8 to 1.8. This ratio may roughly be assumed to be the ratio between the modulus in the horizontal direction and that in the vertical direction. Barden (1963) has pointed out that the ratio between moduli is much more important than the values of Poisson's ratios in computing surface settlements. Also it is not clear

what degree of anisotropy would be produced in the field by action of the compaction equipment. Hence it was deemed reasonable to assume isotropic behavior for the soil in this analysis.

5. LABORATORY STRIP FOOTING TEST

5.1 Planning of Test

The constitutive relationship for the compacted cohesive soils was determined by means of axisymmetric creep tests in which two of the principal stresses were held constant during the test, while the third was increased. Very rarely does this condition exist in the field since, in general all stress components will be changing simultaneously during loading. Thus, it was necessary to investigate whether the proposed constitutive law was valid under more general stress conditions. This was done by applying it to a boundary value problem for which a solution could be obtained. The problem considered was the case of a long strip footing, uniformly loaded at the surface of a mass of compacted clay.

The test was performed in an aluminum box 6 inches x 6 inches and 9 inches deep, where the soil was compacted to a depth of about 3 inches. The box was constructed of 1/4 inch thick aluminum plates and suitably braced. The inside of the box was coated with silicon oil to minimize the effects of friction during compaction. A steel strip 5.5 inches long, 1/2 inch wide and 1/4 inch thick was used for the strip footing. The footing had a length to width

ratio of 11 and the width of the box was 12 times the width of the footing. A space of 1/4 inch was left between the end of the footing and the edge of the box to prevent side restraint.

5.2 Loading

Loads were applied using a lever-type consolidation loading frame. A vertical steel rod 1/2 inch in diameter and 7 inches in length with a spherical seat at one end was attached to the middle of the footing. Steel plates were welded to this rod and the top of the footing strip to provide additional stiffness to the assembly. The shaft was passed through an oiled bronze bushing to reduce friction. The bushing was supported by a steel plate attached to the top of the box. The steel plate could be moved laterally so that the entire assembly could be made vertical. Figure 5-1 is a schematic diagram of the box and the footing. The footing was loaded through the steel ball in the consolidation frame. The vertical displacement of the footing with time was measured by a dial gage and a LVDT similar to the one used for axial deformation measurements in the creep tests. The dial gage used was a Federal model E3B5 with a least count of 0.0001 inch. Figure 5-2 shows the details of the strip footing and the entire test setup is shown in Figure 5-3.

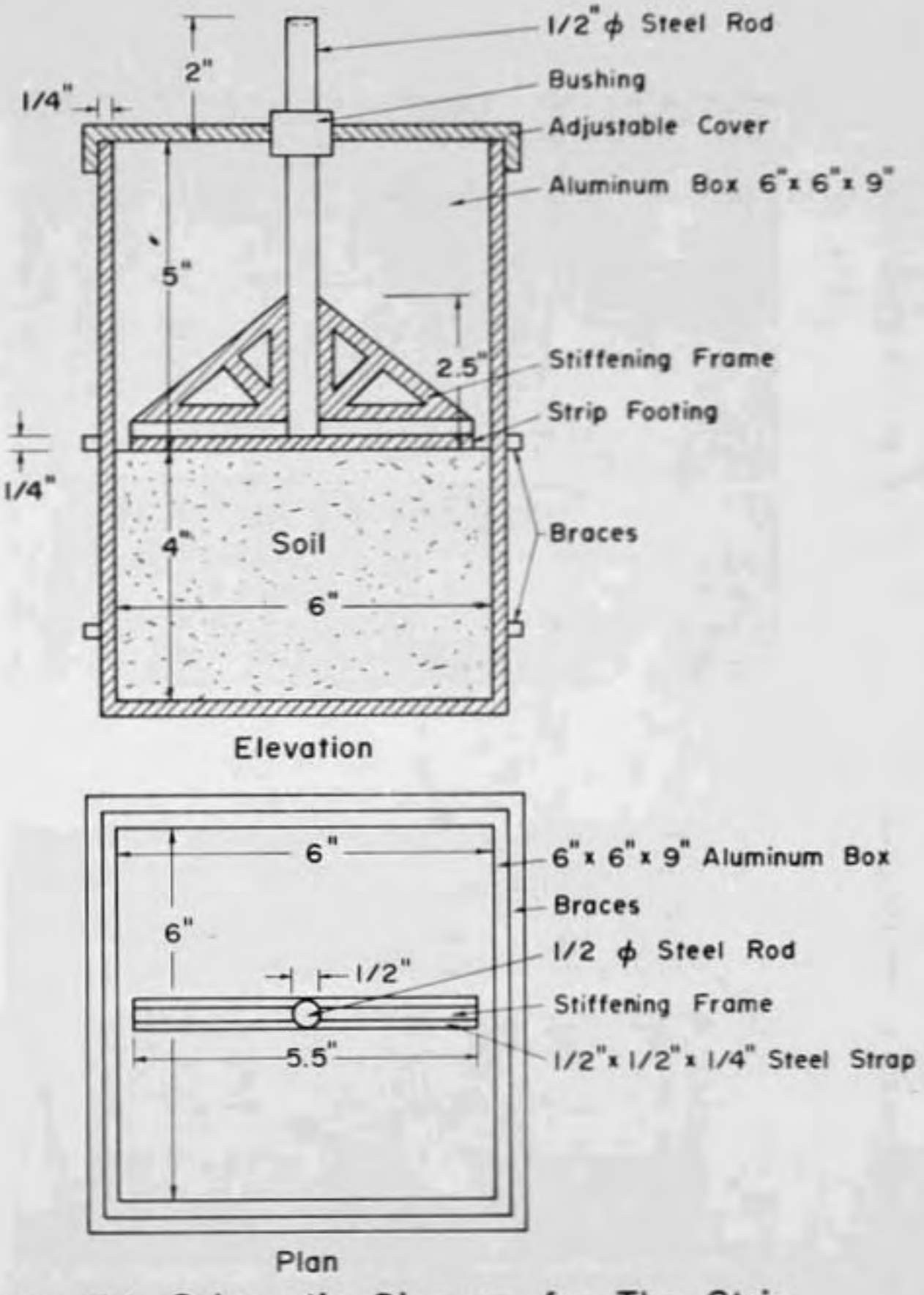

Figure 5.1 - Schematic Diagram for The Strip Footing Test

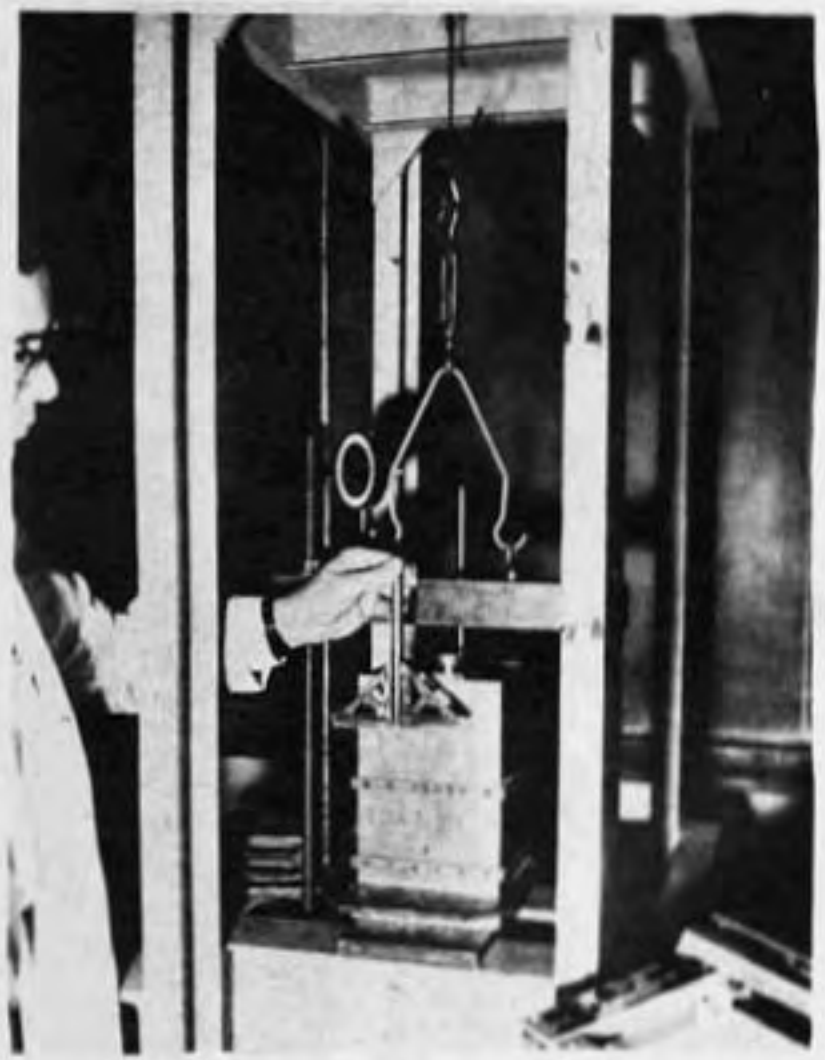

Figure 5-2. Details of Strip Footing.

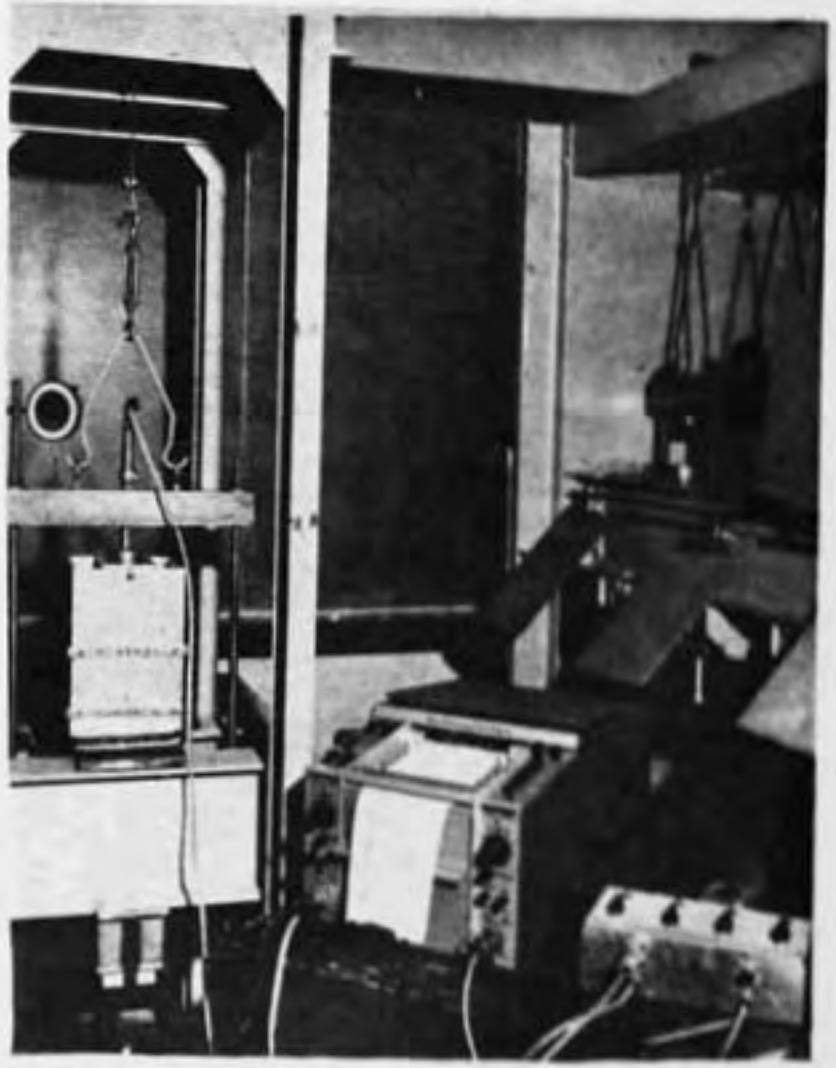

Figure 5-3. Strip Footing Test Setup.

5.3 Material Used

The soil used in this investigation was grundite. The pertinent characteristics of this soil are described in Chapters 3 and 4.

The moisture content used for the preparation of the soil was less than the optimum moisture content for standard Proctor compaction.

5.4 Test Procedure

The soil mass for the strip footing test was compacted statically. The required amount of soil was weighed and poured into the box. The top surface was made approximately level by light tamping prior to compaction. Entrapped air was removed by shaking the box. A cover plate was then placed on top of the soil and levelled. The required amount of loading was then applied by means of a screw loading universal testing machine at the rate of .07 inches per mt., care being taken to keep the top plate horizontal during loading. The compaction pressure used was 150 pounds per square inch. The maximum load for the static compaction was maintained for about a minute. The maximum variation in wet density was found to be slightly greater than one per cent between trimmed samples obtained from different positions in the box.

After releasing the load the box was transferred to the consolidation frame, the cover plate removed and the strip

footing placed on top of the soil. The steel plate with the bushing was adjusted so that the entire assembly was vertical. Then the desired load was applied carefully as an approximately instantaneous step load on the footing. The displacement of the footing with time was recorded by both the dial gage and the LVDT. The applied load was sufficient to neglect the weight of entire loading assembly. The creep loading was kept on for an hour and the soil allowed to relax for half an hour. The loading and unloading cycles were repeated once more. During both the cycles the footing displacement with time was recorded continuously. The results of the second loading cycle were used for comparison with the analysis.

5.5 Determination of Material Parameters

Creep parameters for the analysis were obtained from the triaxial creep tests conducted on the samples taken from the footing test box. After the strip footing test was completed the box was dismantled by unscrewing the plates. The cubical block of soil was then cut into six pieces each of which was trimmed into a cylindrical specimen approximately 1.3 inches in diameter and 2.8 inches high. A soil lathe as shown in Figure 5-4 was modified for this purpose. Confined creep and recovery tests were conducted under different confining pressures. The strength of each specimen was determined after each creep test. The load during the

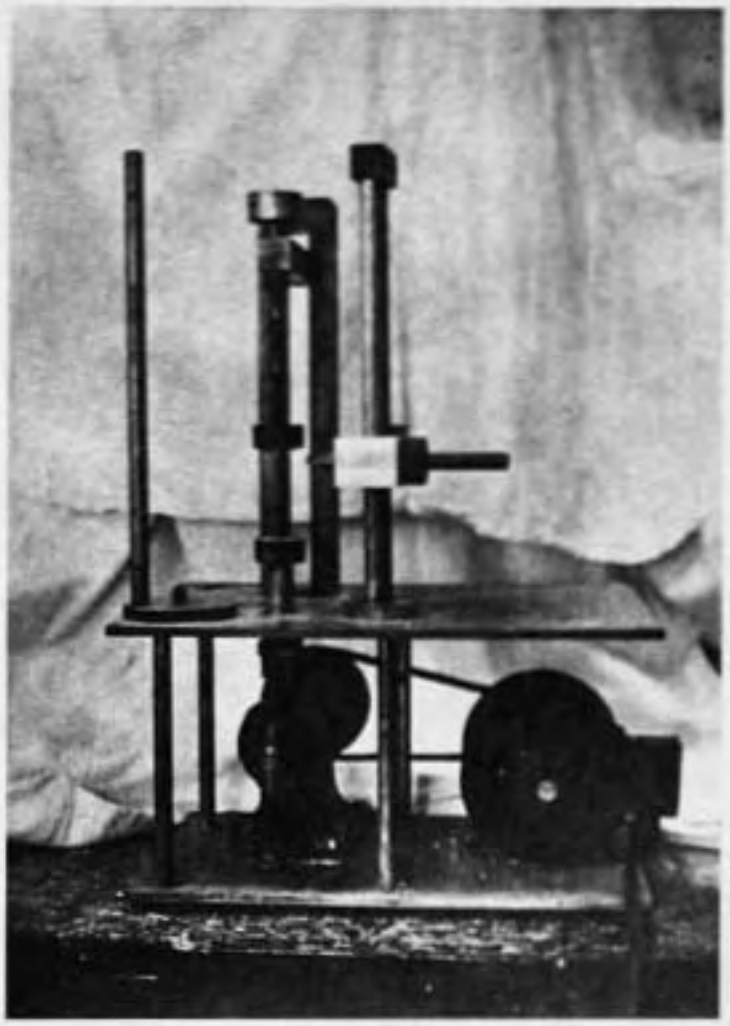

Figure 5-4. Soil Lathe Modified for Trimming Samples.

creep test was applied in the same direction to the sample as in the original footing tests. The relation between octahedral shear stress at failure and octahedral normal stress at failure, the variation of a_σ, g_2 and g_1 with stress-strength ratio and the linear relation between equivalent Poisson's ratio and stress-strength ratio were obtained from these tests. The results are discussed in the next chapter.

6. FINITE ELEMENT ANALYSIS

6.1 Introduction

In recent years the finite element method has been extensively dealt with in the literature (Clough, 1960; Wilson, 1963; Zienkiewicz and Cheung, 1967). It has been applied to many soil mechanics boundary value problems, as indicated before. The formulation of the method is sufficiently general so that it may be used for analysis of stress and strain in a soil mass with complex boundary and loading conditions.

The basic concept of the finite element method is that a continuum may be represented by an assemblage of a finite number of elements interconnected at the element nodal points. The exact displacement field throughout the element is approximated by functions with a number of coefficients equal to the number of degrees of freedom of the node points. The order of the polynomials is selected so that displacements within each of the elements satisfy compatibility at the element boundaries. Assuming elastic behavior of the elements, stiffness values, which relate nodal point forces and displacements are calculated for each element using the principle of minimum potential energy. The stiffness matrix for the entire structure is

assembled by superimposing the appropriate stiffness coefficients of the individual elements. A system of equilibrium equations can be written expressing the nodal point displacements in terms of the stiffnesses and applied loads, taking into account the boundary conditions, applied loads and the stiffness of each element. This system of equilibrium equations is solved for the unknown nodal point displacements by a suitable numerical solution procedure. The desired stresses and strains are then calculated from the known node point displacements.

The computer program developed for the analysis of strip footing resting on compacted cohesive soil was a modification of that described by Wilson (1963). In this program the stiffness matrix for rectangular elements was obtained by combining the stiffness coefficients of the four associated triangles. Major changes were made in the original program to include the non-linearity and time-dependency of the soil parameters. A listing of the modified computer program is given in Appendix A.

6.2 Idealization of the Continuum and Boundary Conditions

In the present analysis square elements have been used except where triangular elements are required to provide a transition between element sizes. Smaller elements were used in zones of high stress gradient. Only one half of the total system was analyzed because the load and geometry

were symmetric. Figure 6-1 illustrates the two-dimensional view of the idealized system.

In the laboratory footing test, the soil at the side boundary can move vertically, while no lateral movement is possible; soil at the bottom boundary can move horizontally while no vertical movement can occur. Since the two bottom corners cannot move in any direction they are kept fixed. There is no shear stress on the axis of symmetry and there will be only vertical movement along it. These boundary conditions are included in the analysis and are indicated schematically in Figure 6-1 by the rollers and pins shown at the boundaries. The rollers are intended to depict allowable movement parallel to the rolling plane only.

6.3 Method of Non-Linear Analysis

Major changes were made in the original program to incorporate the nonlinear viscoelastic behavior of compacted cohesive soil. The inclusion of nonlinear behavior was achieved by an iteration method similar to that used by Girijavallabhan and Reese (1968) and Duncan, et al, (1968). In this approach each discrete element within the idealized assembly was considered as a different, homogeneous, isotropic and elastic material whose properties could be described by two equivalent elastic constants, modulus of elasticity E, and Poisson's ratio ν, both of which depend on the state of stress within the element and the elapsed

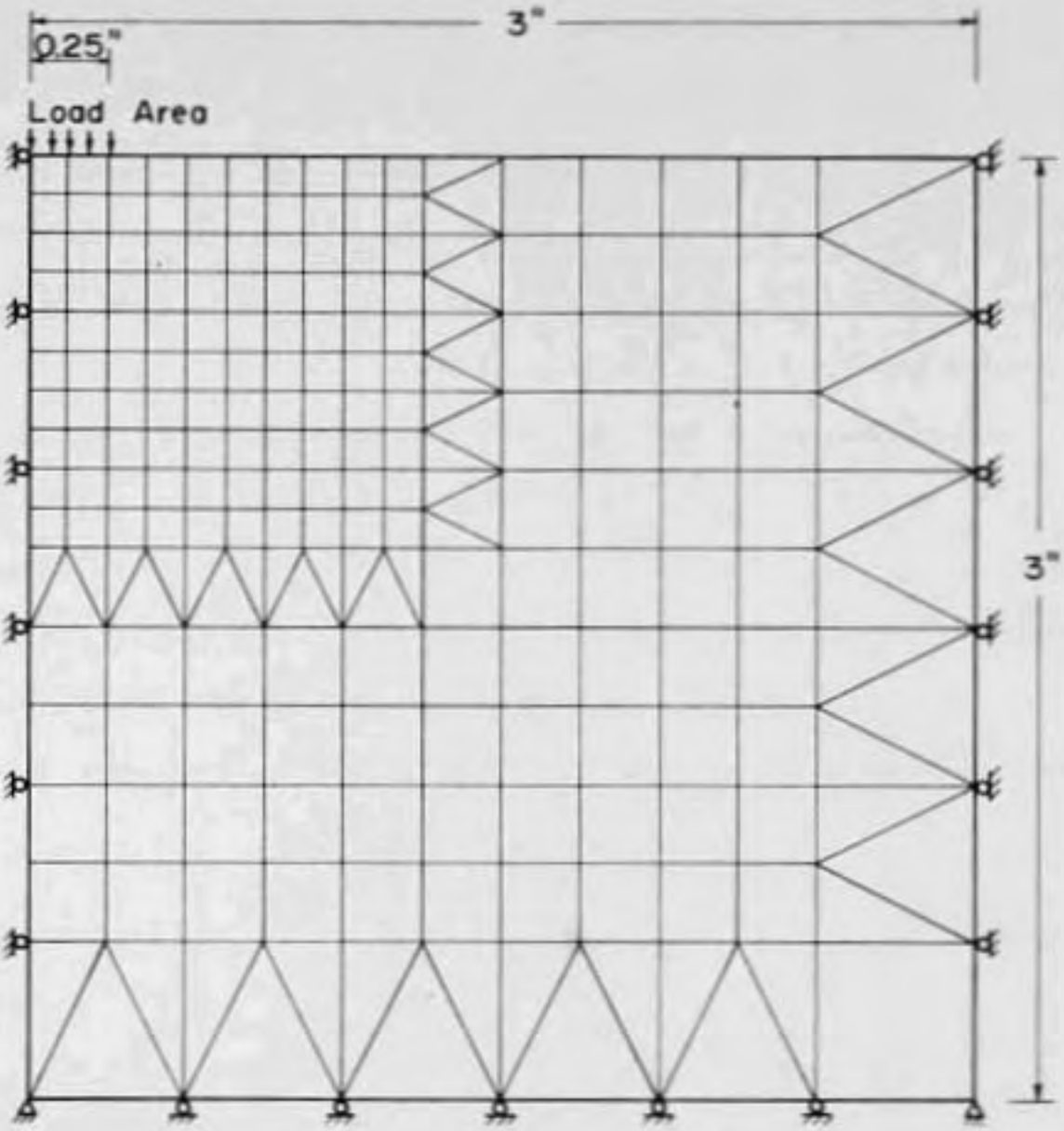

Figure 6.1 - Idealized Scheme for Two Dimensional Finite Element Analysis

time after loading. The equivalent elastic constants E and ν were assumed constant within the element for the particular stress level and time.

Because of the nonlinearity, the analysis should be started at zero time. However, due to the fact that J(0)=0, the initial time was taken to be 0.01 minute. It was necessary to assume initial values of the equivalent elastic constants. By applying the necessary boundary conditions and using the assumed elastic constants, the stresses and strains at the center of each element within the assemblage were computed. Assuming the stress remained constant during the small increment of time, new values of the stress dependent viscoelastic constants were obtained by,

$$J'(t) = \frac{\varepsilon_1 \varepsilon_2}{a_\sigma^n} \; (J_o') \; t^n \qquad (6\text{-}1)$$

where

$\varepsilon_1, \varepsilon_2, a_\sigma, J_o'$ and n = the viscoelastic parameters obtained from creep tests conducted on samples obtained from the footing test soil mass;

t = 0.01 minute .

$$J(t) = \frac{J'(t)}{(\tau_{oct})_f} \qquad (6\text{-}2)$$

where

$J(t)$ = shear creep compliance,

$(\tau_{oct})_f$ is a function of the octahedral normal stress; when octahedral normal stress becomes tensile during the program it is set equal to zero.

Then

$$G = 1/J(t) \tag{6-3}$$

where

G = the equivalent elastic shear modulus at the time t.

The equivalent Poisson's ratio ν, is

$$\nu = k_o + k_1 \left[\frac{\tau_{oct}}{(\tau_{oct})_f}\right] \tag{6-4}$$

where

k_o and k_1 are constants obtained from creep tests.

And so, the equivalent Young's modulus for the stress increment is

$$E = G\ [2(1+\nu)]$$

These new equivalent elastic constants were then used to evaluate the stresses and displacements in the soil mass, leading to another set of equivalent elastic parameters. The iteration process was continued until the differences between the new and the previous values of elastic parameters were less than specified quantities. When proper convergence on the values of E and ν were obtained, the

iteration was stopped and the value of time increased by the desired increment.

In the finite element analysis the strip footing can be considered either flexible or rigid. Uniform pressure is applied over the footing area in the case of flexible footing, while rigid footing conditions can be simulated by imposing equal displacements to the surface points under the footing. The load-settlement curves obtained by either analysis are essentially the same, while the stress pattern under the edge of the footing is different (Hoeg, et. al., 1968; Radhakrishnan and Reese, 1969; Desai and Reese, 1970; Kinner and Ladd, 1970). In the present investigations, a given total load is applied as a step load on a rigid footing, which is difficult to simulate in the analysis. Since the main objective of the analysis was to determine the settlement of the footing, it was decided to consider the strip footing as flexible, with uniform pressure applied over the footing area.

The effect of a change in Poisson's ratio on the stresses and displacements within the soil mass have been investigated for an earth embankment resting on a rigid foundation (Clough and Woodward, 1960), and for a strip footing resting on an idealized elasto-plastic soil (Hoeg, et. al., 1968). An increase in Poisson's ratio decreases the vertical settlement, but only the horizontal stresses are affected significantly by changes in Poisson's

ratio. In the present investigation, changes in equivalent Poisson's ratio with time (for a particular stress level for the duration of the test) are relatively small. The stress and displacement patterns are not expected to alter appreciably due to these small increases or decreases in magnitude. Hence a constant Poisson's ratio with time for a particular stress level was assumed for this analysis.

Certain modifications have to be made in the above procedure for non-linear finite element analysis, depending on the particular boundary value problem. The numerous investigations that have been made provide valuable guidance, even though they may lack the details about numerical values used in various operations. It is known that a finer mesh provides more accurate results than a coarse mesh (Zienkiewicz and Cheung, 1967); but the accuracy gained in increasing the fineness beyond a certain limit may not be commensurate with the increase in computer time. Also, results obtained by the relatively coarse meshes have shown good agreement with the analytical or predicted results (Girijavallabhan and Reese, 1968; Perumpral, 1969). Generally, triangular elements are used to increase the fineness of mesh. But Kinner and Ladd (1970) concluded that triangular elements adversely affected the stress distribution, and recommended that triangular elements, if used for transition zones between elements of different sizes, should be located as far as possible from zones of

high stress gradients. Duncan, et al, (1968) and Barksdale (1969) came to the conclusion that a larger number of iterations will be required when the material properties are strongly stress-dependent, and in some cases it may be practically impossible to obtain convergence.

Some initial runs were made to decide on the procedures to be adopted in this present investigation and it was concluded that,

1. The convergence of a coarse mesh was faster than that of a fine mesh;
2. The difference in the vertical settlement between using a fine mesh (four elements under the load) and a coarse mesh (two elements under the load) did not exceed two per cent for the boundary value problems analyzed;
3. Even when convergence was not obtained after about six iterations, the vertical displacement for successive cycles did not alter by more than one per cent;
4. The nonconvergence was due to a few elements, generally one or two, where the modulus values converged very slowly, oscillating between two values;
5. It is found that most of the elements did not show any significant difference between successive moduli after five to six iterations.

Based on the above results and keeping in mind that the main aim in the analysis is to predict the vertical displacement of the footing, the following procedures were adopted. It was assumed that convergence is obtained when the difference between successive moduli was less than ten per cent of the initial modulus. It is to be pointed out that this large value was used mainly because of the very few elements where the difference between successive moduli remained large after a few iterations; most of the elements did not show any significant difference after five to six iterations. The limits of convergence of Poisson's ratio was chosen arbitrarily to be 0.025. Also, the program was stopped after eight iterations or so, when the difference between successive vertical displacements was generally less than one per cent. The coarse mesh was used in the non-linear viscoelastic program, while the fine mesh was used to check the above by running a nonlinear elastic program. The difference as indicated was less than two per cent.

6.4 Extension to Nonlinear Viscoelasticity

Non-linear viscoelastic boundary value problems have been solved by either a stepwise incremental approach (Zienkiewicz, et. al., 1968; Greenbaum and Rubinstein, 1968) or using the correspondence principle and inverting the solution to the time plane by using the method

suggested by Schapery (Barksdale, 1969). In this investigation the incremental approach has been modified and a procedure similar to the quasielastic method had been used.

In the stepwise incremental method (Zienkiewicz, et. al., 1968) the non-linear elastic solution is obtained at time t=0 by either an iterative method or an incremental method. Assuming that the stresses and the initial equivalent elastic parameters remain unchanged during a short time interval Δt, the creep strain εc_1 at the end of the interval the properties are assumed to change abruptly. Now considering εc_1 as an imposed initial strain, the elastic problem is solved again, resulting in a new stress system $(\sigma)_1$. Assuming again that the new stress system and material properties remain constant during the second interval of time, the total creep strain at the end of this interval is found εc_2. This procedure is carried on to the time for which the solution is needed. It is obvious that the errors involved in this assumption will be extremely small for infinitesimal time intervals.

In the present analysis it is assumed that the stress change induced by the creep deformation in the time interval Δt is not large enough to significantly affect the value of the elastic parameters. This assumption is valid for linear viscoelastic materials; it is known that for a homogeneous material with time-independent Poisson's

ratio, no change in stress distribution occurs under time-independent loading (Zienkiewicz, 1961). The loading in the plane strain footing is time independent and Poisson's ratio for the compacted cohesive soil is found to be approximately independent of time. But the material properties are dependent on the stresses induced and hence the assumption is not strictly valid. Therefore, some error will be introduced in the analysis due to this assumption.

The procedure followed in the finite element analysis was: the induced stresses and strains due to the instantaneously applied loads were determined at time t = 0.01 minute. Then the time was increased to 0.1 minute and the material properties were assumed to change abruptly. With the strain at 0.01 minute as the initial imposed strain and the new material properties, the problem was solved by use of an iterative technique, as in the initial elastic solution. In a similar way, the solutions were obtained at time t = 1, 10, and 100 minutes. The time intervals 0.01, 0.1, 1.0, 10 and 100 minutes were chosen, since the creep compliance for the compacted cohesive soil is a power function of time.

6.5 Material Characterization for Analysis

The static compaction used for preparing the material in the strip footing test may induce initial residual stresses

in the compacted cohesive soil. An estimate has to be made as to their influence in the evaluation of the parameters for the analysis.

The constraints imposed by the footing box will induce residual stresses in the soil after the compaction pressure is released (Brooker and Ireland, 1965; Sherif and Koch, 1970). The distribution of residual stress will vary with depth and is likely to be much smaller in the top portion of the soil mass than at some depth. The influence of confining stresses is much greater at high stress-strength ratios than for small values, as indicated in Chapter 4. In the footing test, the stress-strength ratio and σ_{oct} induced by the applied loads are high near the loaded surface; but the magnitude of residual stresses is small. In the lower portion of the soil mass the initial stresses will be larger in relation to the induced σ_{oct}; but the contribution to the total settlement of this portion of soil mass is small. In the experiment described, 75 per cent of the settlement occurred in the top one inch of the soil mass. Hence the initial residual stresses were not included in the analysis; the compacted cohesive soil was assumed to be as an initially unstressed body.

Grundite was used for conducting the footing test. The moisture content used was one per cent less than the optimum moisture content obtained for standard Proctor compaction. Figure 6-2 indicates the variation in strength

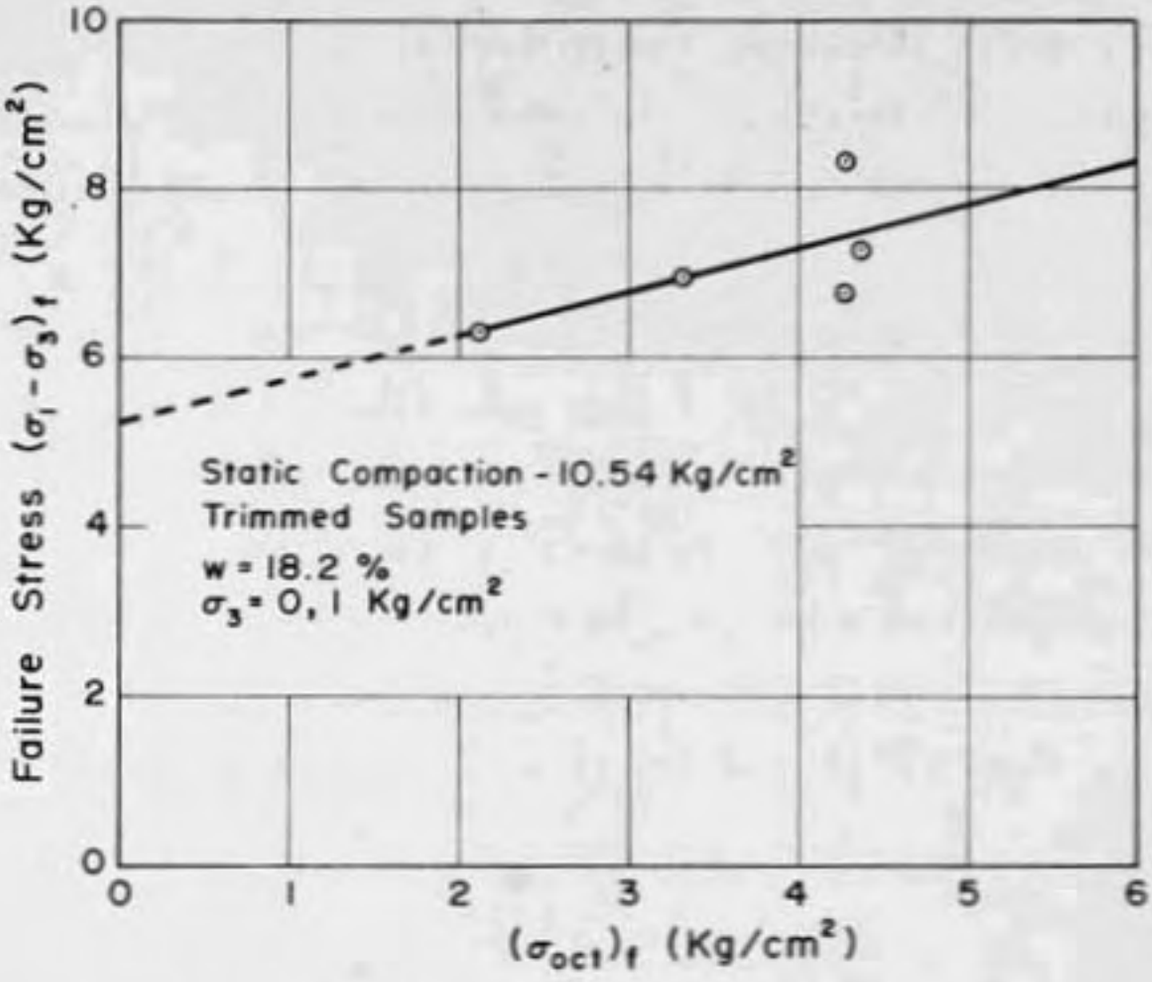

Figure 6.2 - Effect of Octahedral Normal Stress on Failure Strength for Grundite

with octahedral normal stress for the trimmed samples taken out of the footing box. The conventional Mohr failure envelope for the soil is shown in Figure 6-3. The strength intercept is 2.5 kilograms per square centimeter while the angle of shearing resistance is 13 degrees. Using the Terzaghi equation, the ultimate bearing capacity was found to be 25.0 kilograms per square centimeter. The footing load during the test was 9 kilograms per square centimeter. Hence the factor of safety was about 2.75.

Figure 6-4 indicates the effect of the stress-strength ratio on creep parameters for grundite. The normalized creep recovery curve used for determining the magnitudes of the shift factors a_σ and g_1 is shown in Figure 6-5. The values of g_2 and J_o' were then obtained from Figure 6-4 using the equation

$$(\varepsilon_1-\varepsilon_3) = \frac{3}{2\sqrt{2}}\gamma_{oct} = \frac{3}{2\sqrt{2}}\frac{g_1 g_2}{a_\sigma^n} J_o' R_1 \qquad (6\text{-}6)$$

Figure 6-6 shows the nonlinear viscoelastic parameters g_1, g_2 and a_σ as a function of the stress-strength ratio. The data from Figures 6-6 and 6-2 were used to characterize the material for the finite element analysis of the footing test. The variation of equivalent Poisson's ratio was taken to be linear with stress-strength ratio as in Equation 6-4, while n was the average from the tests.

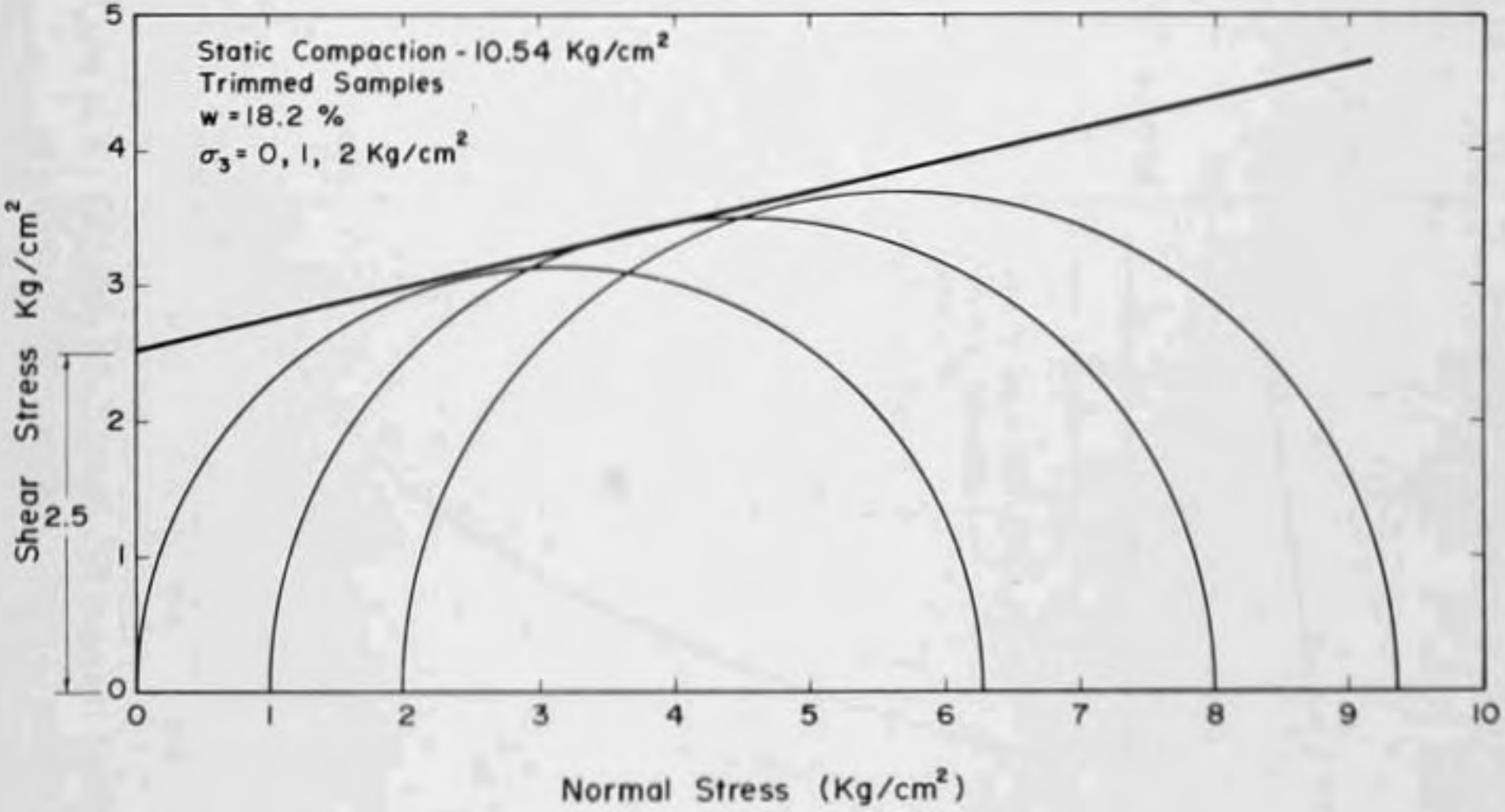

Figure 6.3 - Failure Envelope for Grundite

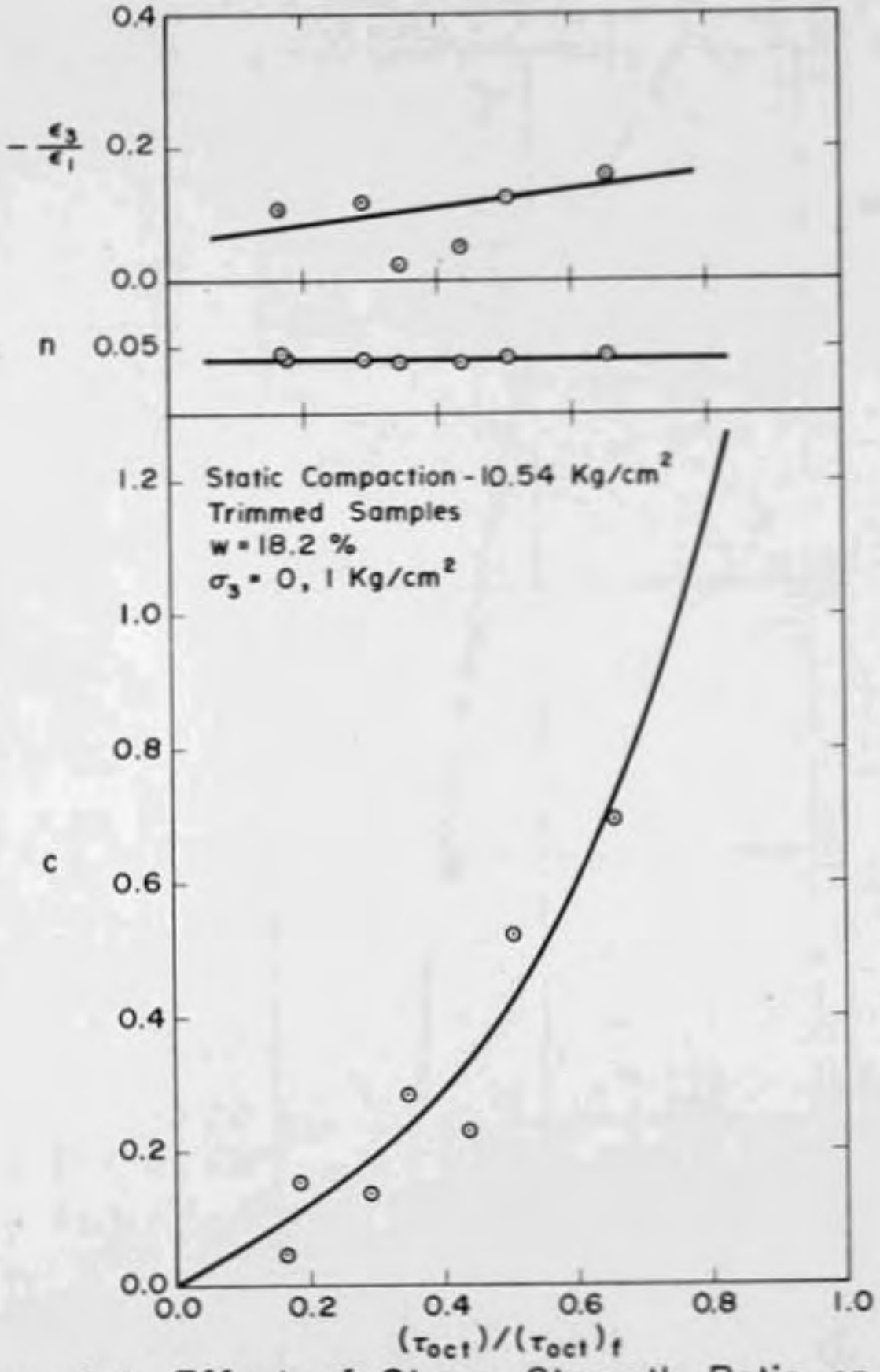

Figure 6.4 - Effect of Stress - Strength Ratio on Creep Parameters for Grundite

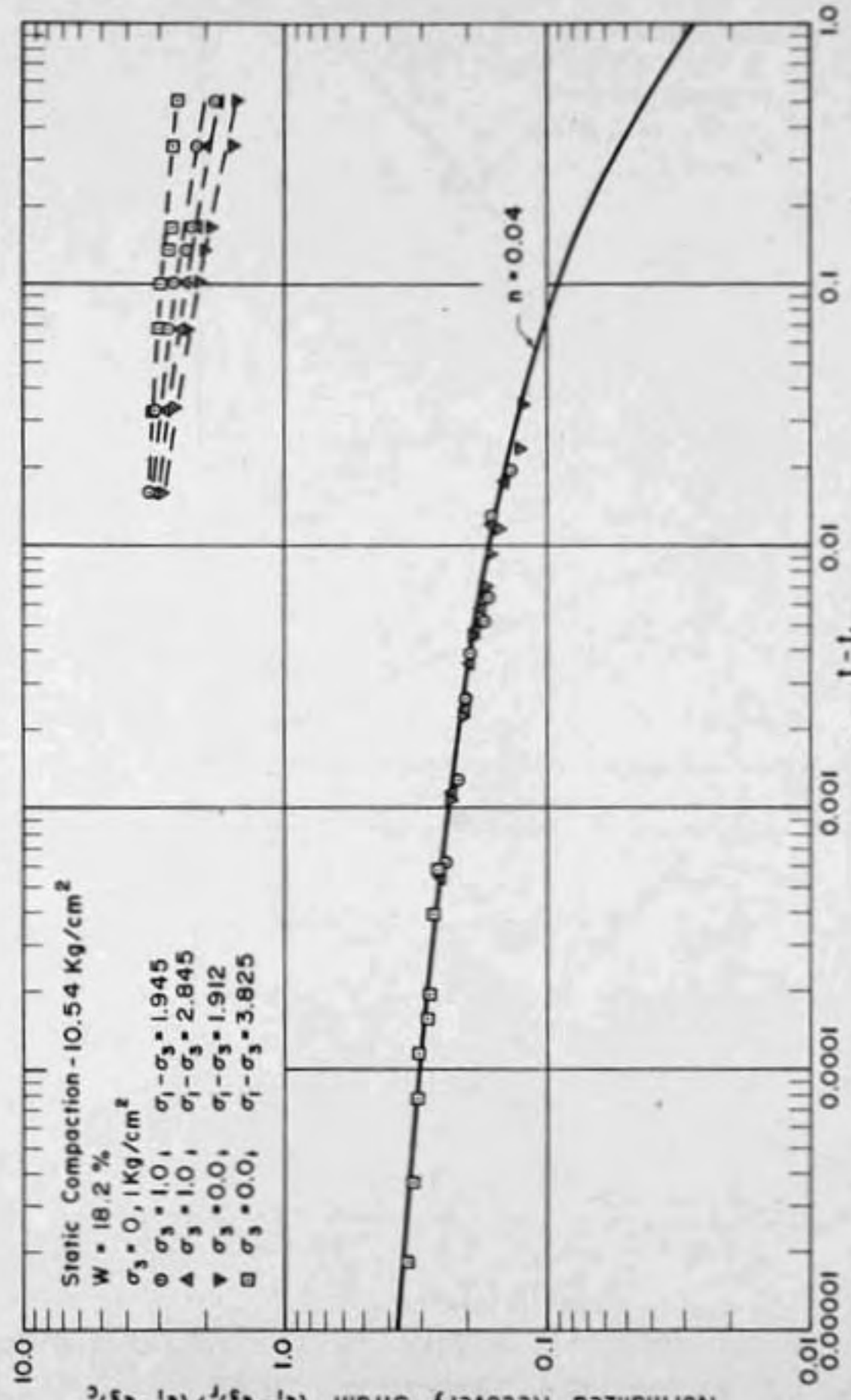

Figure 6.5 - Determination of Shift Factors a_σ and g_1 for Grundite

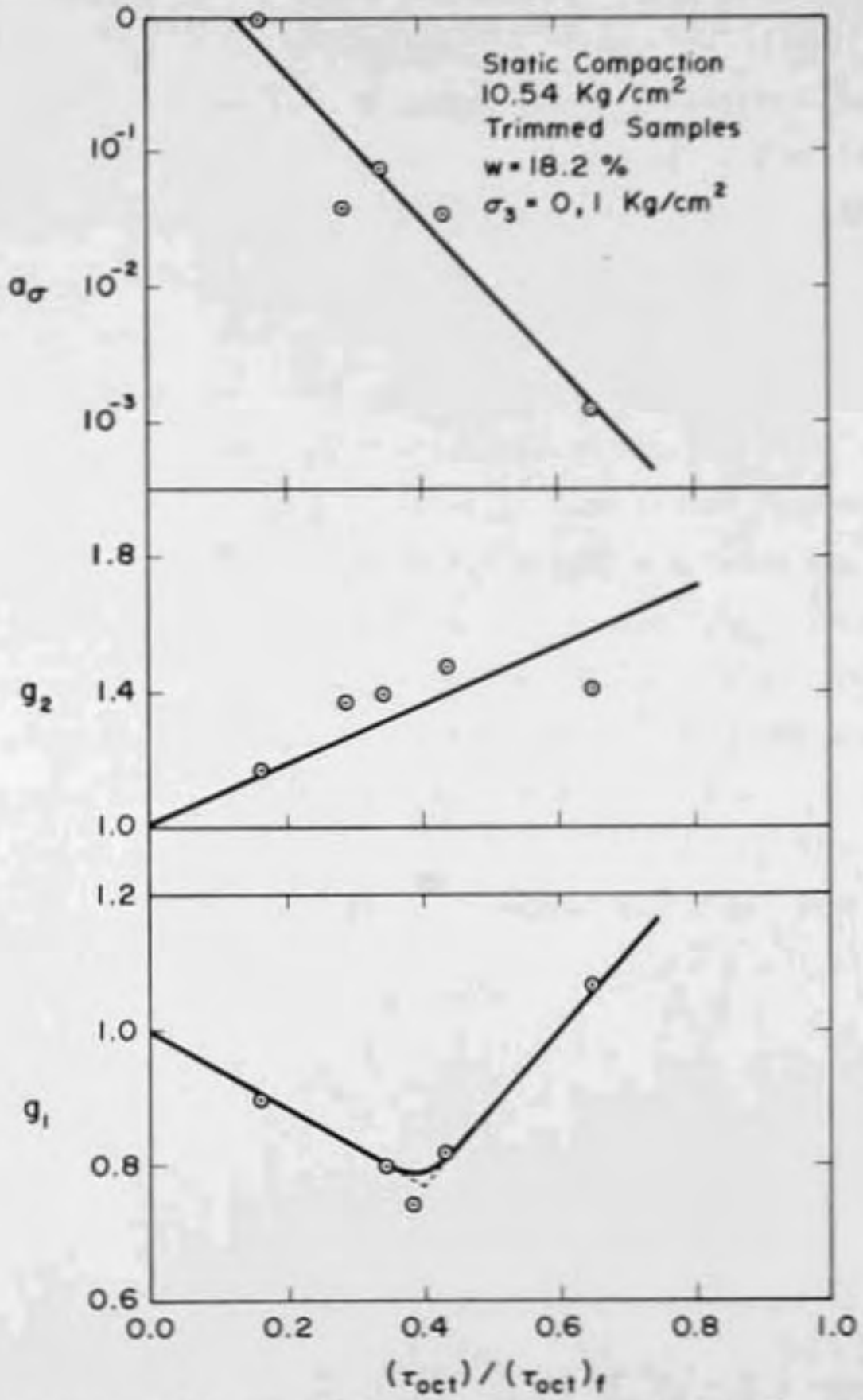

Figure 6.6 - Effect of Stress - Strength Ratio on Non-linear Viscoelastic Parameters for Grundite

6.6 Results

Figure 6-7 shows the measured displacement of the footing with time for the second loading cycle and the predicted response obtained from the finite element a analysis. The figure indicates that the measured rate of displacement is the same as the predicted rate of displacement, and the predicted vertical displacements agree very closely with the actual measured response. It is to be pointed out that initial residual stresses are neglected in the analysis. Also the exact relation between ε_1, ε_2 and the logarithm of a_σ and stress-strength ratio is not known and a linear relation has been used. It was found that the ratio between the octahedral shear stress and octahedral shear stress at failure was less than one in all the elements.

These results suggest that the proposed non-linear viscoelastic characterization is approximately valid for general stress conditions.

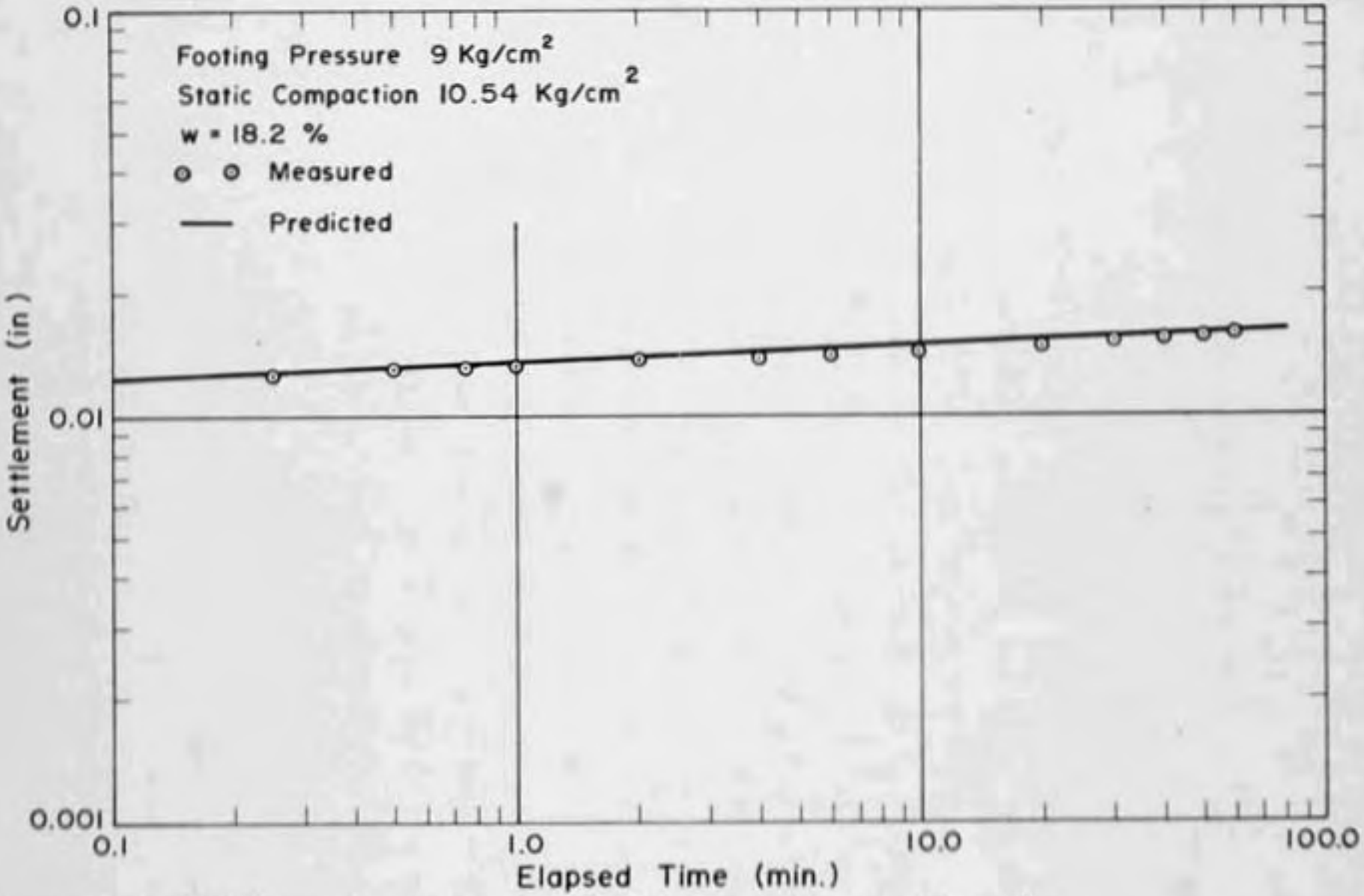

Figure 6.7 - Settlement Curve for Strip Footing on Grundite

7. CONCLUSIONS AND RECOMMENDATIONS

7.1 Conclusions

From the results discussed in the preceding sections the following conclusions concerning the creep behavior of compacted clays of the types tested are drawn:

1. When a compacted clay is subjected to a series of load and unload cycles of given stress level, the difference in response between the second and subsequent cycles is much less than between the first and second cycles. For second and subsequent loadings, the mechanical behavior of compacted clay can be described by a non-linear viscoelastic constitutive relation based upon the principles of irreversible thermodynamics.

   a. Non-linear effects can be accounted for by time-independent parameters which are functions of the stress-strength ratio, i.e., the ratio between octahedral shear stress and the octahedral shear stress at failure corresponding to the existing octahedral normal stress.

   b. A power-law representation is valid to represent time-dependent effects.

c. The effects of moisture content and confinement are approximately accounted for by this constitutive law.

d. The validity of the constitutive relation is independent of the scale of problem considered, provided the compaction conditions are such that the effective stresses approximate the applied total stresses. In many clays this requirement will be satisfied if the compaction moisture content is below Proctor optimum and the confining pressure is less than 8 kg/cm^2.

2. The applicability of the constitutive relation, determined from triaxial tests, was examined by predicting the displacements (on second loading) of a model footing loaded under plane strain conditions. The agreement with experimental results was exceptionally good.

3. Laboratory compacted clays exhibit anisotropic mechanical behavior. The importance of this anisotropy to the prediction of the behavior of compacted embankments remains to be assessed.

7.2 Recommendations

The following suggestions are offered for extension of this study with the goal of improving the knowledge of time-dependent behavior of cohesive soils.

1. The functional form of the variation of the stress dependent parameters a_σ, g_1 and g_2 with stress level needs to be clarified.

2. The non-linear viscoelastic characterization should be modified to permit description of the time-dependent behavior of saturated soils.

3. Experimental techniques can be developed for determining the anisotropic parameters of soils, so that the significance of material anisotropy can be more definitively ascertained.

BIBLIOGRAPHY

BIBLIOGRAPHY

Alpan, I. (1961), "The Dissipation Function for Unsaturated Soils", Proceedings, Fifth International Conference of Soil Mechanics and Foundation Engineering, Vol. I, Paris, pp. 3-5.

Andresen, A., and Simons, N. E. (1960), "Norwegian Triaxial Equipment and Technique," Proceedings, ASCE Research Conference on Shear Strength of Soils, Boulder, Colorado, pp. 695-709.

Barden, L., (1963), "Stresses and Displacements in a Cross-Anisotropic Soil," Geotechnique, Vol. 13, No. 3, pp. 198-210.

Barden, L. (1965), "Consolidation of Compacted and Unsaturated Clays," Geotechnique, Vol. 15, No. 3, pp. 267-286.

Barden, L. and Sides, G. R. (1970), "Engineering Behavior and Structure of Compacted Clay," Journal of Soil Mechanics and Foundations Division, ASCE, Vol. 96, SM4, pp. 1171-1200.

Barksdale, R. D. (1969), "Analysis of Layered Systems," Final Report, Project B-607, School of Civil Engineering, Georgia Institute of Technology, Atlanta, Georgia.

Bell, J. M. (1968), "Correspondence on 'A New Soil Testing Apparatus' by Ko, H. Y., and Scott, R. F.," Geotechnique, Vol. 18, No. 2, pp. 267-271.

Biot, M. A. (1958), "Linear Thermodynamics and the Mechanics of Solids," Proceedings, Third U.S. National Congress of Applied Mechanics, A.S.M.E., pp. 1-18.

Bishop, A. W. (1966), "The Strength of Soils as Engineering Materials," Geotechnique, Vol. 16, No. 2, pp. 99-128.

Bishop, A. W., and Green, G. E. (1965), "The Influence of End Restraint on the Compression Strength of a Cohesionless Soil," Geotechnique, Vol. 15, No. 3, pp. 243-266.

Bishop, A. W. and Henkel, D. J. (1962), The Measurement of Soil Properties in the Triaxial Test, Edwin Arnold, London.

Bishop, A. W., and Lovenbury, H. T. (1969), "Creep Characteristics of Undisturbed Clays," Proceedings, Seventh International Conference on Soil Mechanics and Foundation Engineering, Mexico, Vol. 1, pp. 29-37.

Brooker, E. W., and Ireland, H. O., (1965), "Earth Pressure at Rest Related to Stress History," Canadian Geotechnical Journal, Vol. 2, No. 1, pp. 1-15.

Casagrande, A., and Hirschfield, R. C. C. (1960), "Stress Deformation and Strength Characteristics of a Clay Compacted to a Constant Dry Unit Weight," Proceedings, A.S.C.E. Research Conference on Shear Strength of Cohesive Soils, Boulder, Colorado, pp. 359-418.

Christensen, R. W. and Wu, T. H. (1964), "Analysis of Clay Deformation as a Rate Process," Journal of Soil Mechanics and Foundations Division, ASCE, Vol. 90, No. SM6, pp. 125-157.

Clough, R. W., (1960), "The Finite Element Method in Plane Stress Analysis," Proceedings, Second American Society of Civil Engineers Conference on Electronic Computation, Pittsburgh, Pennsylvania, pp. 345-378.

Clough, R. W. and Woodward, R. J., III, (1967), "Analysis of Embankment Stresses and Deformations," Journal of Soil Mechanics and Foundations Division, ASCE, Vol. 93, No. SM 4, pp. 529-549.

Drucker, D. C. and Prager, W. (1952), "Soil Mechanics and Plastic Analysis or Limit Design," Quarterly of Applied Mathematics, Vol. 10, 1952, pp. 157-165.

Danielson, J. A. (1963), "Consolidation of Unsaturated Clay-Soils," Ph.D. Thesis, Colorado State University, Fort Collins, Colorado.

D'Appolonia, D. J., and Lambe, T. W., (1970), "Method for Predicting Initial Settlement," Journal of Soil Mechanics and Foundations Division, ASCE, Vol. 96, No. SM2, pp. 523-544.

Desai, C. S., and Reese, L. C. (1970), "Analysis of Circular Footings on Layered Soils," Journal of Soil Mechanics and Foundations Division, ASCE, Vol. 96, No. SM 4, pp. 1289-1310.

Duncan, J. M., and Dunlop, P. (1968), "The Significance of Cap and Base Restraint," Journal of Soil Mechanics and Foundations Division, ASCE, Vol. 94, No. SM1, pp. 271-290.

Duncan, J. M., Monismith, C. L., and Wilson, E. L. (1968), "Finite Element Analysis of Pavements," Highway Research Record 228, Highway Research Board, pp. 18-33.

Gibbs, H. J., Hilf, J. W., Holtz, W. G., and Walker, F. C., (1960), "Shear Strength of Cohesive Soils," Proceedings, ASCE Research Conference on Shear Strength of Cohesive Soils, Boulder, Colorado, pp. 33-162.

Girijavallaban, C. V. and Reese, L. C. (1968), "Finite Element Method for Problems in Soil Mechanics," Journal of Soil Mechanics and Foundations Division, ASCE, Vol. 94, No. SM 2, pp. 473-496.

Gould, J. P. (1959), "Construction Pore Pressures Observed in Rolled Earth Dams," Technical Memorandum 650, U. S. Department of Interior, Bureau of Reclamation, Denver, Colorado.

Green, A. E. and Rivlin, R. S. (1957), "The Mechanics of Nonlinear Materials with Memory, Part I," Arch. Rational Mech. Anal., 1, pp. 1-34.

Greenbaum, G. A., and Rubinstein, M. F. (1968), "Creep Analysis of Axisymmetric Bodies Using Finite Elements," Nuclear Engineering and Design, Vol. 7, pp. 379-397.

Hilf, J. W., (1956), "An Investigation of Pore Water Pressure in Compacted Cohesive Soils," Technical Memorandum 654, United States Department of the Interior, Bureau of Reclamation, Denver, Colorado.

Hilf, J. W., (1957), "Compacting Earth Dams with Heavy Tamping Rollers," Journal of Soil Mechanics and Foundations Division, ASCE, Vol. 83, No. SM 2, pp. 1205-1-27.

Hoeg, K., Christian, J. T., and Whitman, R. V. (1968), "Settlement of Strip Load on Elastic-Plastic Soil," Journal of Soil Mechanics and Foundations Division, ASCE, Vol 94, No. SM 1, pp. 430-445.

Holtz, W. G. and Ellis, W. (1963), "Comparison of the Shear Strengths of Laboratory and Field Compacted Soils," ASTM Special Technical Publication 361, Ottawa, pp. 471-480.

Januskevicius, C. K., and Vey, E. (1965), "Stresses and Strains in Triaxial Specimens Using Embedded Gauges," ASTM Special Technical Publication No. 392.

Johnson, A. W. and Sallberg, J. R. (1960), "Factors that Influence Field Compaction of Soils," Highway Research Board Bulletin No. 272, Highway Research Board.

Kinner, E. B., and Ladd, C. C. (1970), "Load Deformation Behavior of Saturated Clay During Undrained Shear," MIT Research Report R70-27, Soils Publication No. 259, MIT, Cambridge, Mass.

Kirkpatrick, M. W. (1957), "The Condition of Failure for Sands," Proceedings, Fourth International Conference on Soil Mechanics and Foundation Engineering, London, Vol. 1, pp. 172-178.

Kirkpatrick, W. M. and Belshaw, D. J. (1968), "On the Interpretation of the Triaxial Test," Geotechnique, Vol. 18, No. 3, pp. 336-350.

Ko, H. Y., and Scott, R. F. (1967), "A New Soil Testing Apparatus," Geotechnique, Vol. 17, No. 1, pp. 40-57.

Ko, H. Y. and Scott, R. F. (1968), "Deformation of Sand at Failure," Journal of Soil Mechanics and Foundations Division, ASCE, Vol. 94, No. SM 4, pp. 883-898.

Kraft, L. M. (1965), "The Effect of Cyclic Loading on the Stress-Strain Properties of a Cohesive Soil," M.S. Thesis, The Ohio State University, Columbus.

Lambe, T. W. (1961), "Residual Pore Pressure in Compacted Clay," Proceedings, Fifth International Conference on Soil Mechanics and Foundation Engineering, Vol. I, Paris, pp. 201-211.

Langfelder, L. J., Chen, C. F., and Justice, J. A. (1968), "Air Permeability of Compacted Cohesive Soils," Journal of Soil Mechanics and Foundations Division, ASCE, Vol. 94, No. SM 4, pp. 981-1001.

LaraTomas, M., (1962), "Time-Dependent Deformation of Clay Soils Under Shear Stress," Proceedings, First International Conference on the Structural Design of Asphalt Pavements, Ann Arbor, Michigan.

Larew, H. G., and Leonards, G. A. (1962), "A Strength Criterion for Repeated Loads," Proceedings, Highway Research Board, Vol. 41, pp. 529-556.

Leaderman, H. (1962), "Large Longitudinal Retarded Elastic Deformation of Rubberlike Network Polymers," Transactions, Society of Rheology, Vol. 6, 1962, pp. 361-382.

Lee, E. H. (1956), "Stress Analysis in Viscoelastic Materials," Journal of Applied Physics, Vol. 27, No. 7, pp. 665-672.

Leonards, G. A. (1955), "Strength Characteristics of Compacted Clays," Transactions, ASCE, Vol. 120, pp. 1420-1455.

Leonards, G. A., and Narain, J. A. (1964), "Flexibility of Clay and Cracking of Earth Dams," Journal of the Soil Mechanics and Foundations Division, ASCE, Vol. 89, SM 2, pp. 47-97.

Lou, Y. C. and Schapery, R. A. (1969), "Viscoelastic Behavior of a Nonlinear Fiber - Reinforced Plastic," Technical Report AFML-TR-68-90, Part II, Purdue University, Lafayette, Indiana.

Matyas, E. L. (1969), Discussion on "Air Permeability of Compacted Cohesive Soils"by Langfelder et al., Journal of Soil Mechanics and Foundations Division, ASCE, Vol. 95, No. SM 3, pp. 924-926.

Matyas, E. L. and Radhakrishna, H. S. (1968), "Volume Change Characteristics of Partially Saturated Soils," Geotechnique, Vol. 18, No. 4, pp. 432-448.

Mitchell, J. K. (1968), "Shearing Resistance of Soils as a Rate Process," Journal of the Soil Mechanics and Foundations Division, ASCE, Vol. 94, No. SM 1, pp. 231-253.

Mitchell, J. K. and Campanella, R. G. (1963), "Creep Studies on Saturated Clays," ASTM Special Technical Publication No. 361, pp. 90-103.

Mitchell, J. K., Singh, A., and Campanella, R. G., (1969), "Bonding, Effective Stresses, and Strength of Soils," Journal of Soil Mechanics and Foundations Division, ASCE, Vol. 95, No. SM 5, pp. 1219-1246.

Mitchell, J. K., Campanella, R. G., and Singh, A. (1968), "Soil Creep as a Rate Process," Journal of Soil Mechanics and Foundations Division, ASCE, Vol. 94, No. SM 1, pp. 231-254.

Murayama, S., and Shibata, T. (1961), "Rheological Properties of Clays," Proceedings, Fifth International Conference on Soil Mechanics and Foundation Engineering, Paris, Vol. 1, pp. 269-273.

Olsen, R. E., and Langfelder, L. J., (1965), "Pore-Water Pressures in Unsaturated Soils," Journal of Soil Mechanics and Foundations Division, ASCE, Vol. 91, No. SM 4, pp. 127-150.

Pagen, C. A., and Jagannath, B. N., (1967), "Evaluation of Soil Compaction by Rheological Techniques," Highway Research Record 177, Highway Research Board, pp. 22-42.

Pagen, C. A., and Jagannath, B. N., (1968), "Mechanical Properties of Compacted Soils," Highway Research Record 235, Highway Research Board, pp. 12-26.

Perloff, W. H. (1966), "Study of Long Term Deformation of Compacted Cohesive Soil Embankments," Plan of Study, Joint Highway Research Project, Project No. C-36-5F, File No. 6-6-6, Purdue University, Lafayette, Indiana.

Perloff, W. H. (1969), "Finite Element Analysis of Underground Openings," Strain Distribution Around Underground Openings, Technical Report No. 1, Contract No. DACA 73-68-C-0002 (P002), Advanced Research Projects Agency, Department of Defense.

Perloff, W. H., Baladi, G. Y., and Harr, M. E. (1967), "Stress Distribution Within and Under Long Elastic Embankments," Highway Research Record No. 181, Highway Research Board, pp. 12-40.

Perloff, W. H., and Pombo, L. E. (1969), "End Restraint Effects in the Triaxial Test," Proceedings, Seventh International Conference on Soil Mechanics and Foundation Engineering, Mexico, pp. 327-334.

Pickering, D. J., (1970), "Anisotropic Elastic Parameters For Soil," Geotechnique, Vol. 20, No. 3, pp. 271-276.

Ramaswamy, S. V., and Perloff, W. H. (1970), "Time Dependent Deformation Characteristics of Compacted Cohesive Soils," Progress Report, Joint Highway Research Project, Project: C-36-5F, File: 6-6-6, Purdue University, Lafayette, Indiana.

Radhakrishnan, N. and Reese, L. C. (1969), "Behavior of Strip Footings on Layered Cohesive Soils," Proceedings, Symposium on Application of Finite Element Methods in Civil Engineering, Vanderbilt University, Nashville, pp. 690-728.

Roscoe, K. H. (1970), "Influence of Strains in Soil Mechanics," Geotechnique, Vol. 20, No. 2, pp. 129-170.

Roscoe, K. H., Schofield, A. N., and Wroth, C. P. (1958), "On the Yielding of Soils," Geotechnique, Vol. 8, No. 1, pp. 22-53.

Roscoe, K. H., Schofield, A. N., and Thurairajah, A. C. (1963), "An Evaluation of Test Data for Selecting a Yield Criterion for Soils," ASTM Special Technical Publication 361, Ottawa, pp. 111-128.

Rowe, P. W., (1963), "Stress-Dilatancy, Earth Pressures, and Slopes," Journal of Soil Mechanics and Foundations Division, ASCE, Vol. 89, No. SM 3, pp. 37-61.

Rowe, P. W., and Barden, L. (1964), "Importance of Free Ends in Triaxial Testing," Journal of the Soil Mechanics and Foundations Division, ASCE, Vol. 90, No. SM 1, pp. 1-28.

Sankaran, K. S., (1966), "Time Dependent Deformation of Partially Saturated Cohesive Soils," Unpublished Ph.D. Thesis, Indian Institute of Technology, Madras, India.

Schapery, R. A. (1964), "Application of Thermodynamics to Thermomechanical, Fracture and Birefringent Phenomena in Viscoelastic Media," Journal of Applied Physics, Vol. 5, pp. 1451-1456.

Schapery, R. A., (1966a), "An Engineering Theory of Non-linear Viscoelasticity with Applications," International Journal of Solids Structures, Vol. 2, pp. 407-425.

Schapery, R. A. (1966b), "A Theory of Non-Linear Thermo-viscoelasticity Based on Irreversible Thermodynamics," Proceedings, Fifth U. S. National Congress of Applied Mechanics, ASME, pp. 511-530.

Schapery, R. A., (1969a), "Further Development of a Thermo-dynamic Constitutive Theory: Stress Formulation," A & E S Report No. 69-2, Purdue University, Lafayette, Indiana.

Schapery, R. A., (1969b), "On the Characterization of Non-Linear Viscoelastic Materials," Polymer Engineering and Science, Vol. 9, No. 4, pp. 295-310.

Schuurmann, Ir. E., (1966), "The Compressibility of an Air Water Mixture and a Theoretical Relation Between Air and Water Pressures," Geotechnique, Vol. 16, No. 4, pp. 269-281.

Seed, H. B., Chan, C. K., and Monismith, C. L. (1955), "Effects of Repeated Loadings on the Strength and Deformation of Compacted Clay," Proceedings, Highway Research Board, Vol. 34, pp. 541-558.

Seed, H. B., and Chan, C. K., (1958), "Effect of Stress History and Frequency of Stress Application on Deformation of Clay Subgrades Under Repeated Loading," Proceedings, Highway Research Board, Vol. 37, pp. 555-575.

Seed, H. B., Mitchell, J. K., and Chan, C. K., (1960), "The Strength of Compacted Cohesive Soils," Proceedings, ASCE Research Conference on Shear Strength of Cohesive Soils, Boulder, Colorado, pp. 877-964.

Sherif, M. A., and Koch, D. E., (1970), "Coefficient of Earth Pressure at Rest as Related to Soil Precompression Ratio and Liquid Limit," Highway Research Record No. 323, Highway Research Board, pp. 39-48.

Shockley, W. G., and Ahlvin, R. G. (1960), "Nonuniform Conditions in Triaxial Test Specimens," Proceedings, ASCE Research Conference on Shear Strength of Cohesive Soils, Boulder, Colorado, pp. 341-358.

Singh, A. and Mitchell, J. K., (1968), "General Stress-Strain-Time Function for Soils," Journal of Soil Mechanics and Foundations Division, ASCE, Vol. 94, No. SM 1, pp. 21-46.

Singh, A., and Mitchell, J. K., (1969), "Creep Potential and Creep Rupture of Soils," Proceedings, Seventh International Conference on Soil Mechanics and Foundation Engineering, Mexico, Vol. 1, pp. 379-384.

Soussou, J. E. and Moavenzadeh, F., (1970), "Classical and Statistical Theories for the Determination of Constitutive Equations," Department of Civil Engineering, Massachusetts Institute of Technology, Cambridge.

Sowers, G. F. (1963), "Strength Testing of Soils," ASTM Special Technical Publication 361, Ottawa, pp. 3-21.

Sowers, G. F., and Gulliver, J. G. (1955), "Effect of Varying Tamping-Foot Width on Compaction of Cohesive Soil," Proceedings, Highway Research Board, Vol. 34, pp. 598-601.

Teerawong, P., (1963), "One Dimensional Consolidation of Unsaturated Clay," Ph.D. Thesis, Colorado State University, Fort Collins, Colorado.

Thorkildsen, R. L., (1964), "Mechanical Behavior," Chapter 5 in Engineering Design for Plastics, Edited by E. Baer, Reinhold, pp. 277-392.

Toriyama, K., and Sawada, T., (1968), "On the Consolidation of Partly Saturated Soils Compacted Wet of Optimum Moisture Content," Soils & Foundations, Vol. 8, No. 3, pp. 62-86.

Truesdale, W. B., and Rusin, R. W. (1963), "Discussion on 'An Evaluation of Test Data for Selecting a Yield Criterion for Soils' by Roscoe et. al.," ASTM Special Technical Publication 361, Ottawa, pp. 129-133.

Wahls, H. E., and Langfelder, L. J. (1967), "The Influence of Compaction Methods and Conditions on the Structural Behavior of Compacted Subgrades," Proceedings, Second International Conference on Structural Design of Asphaltic Pavements, Ann Arbor, Michigan, pp. 373-379.

Walker, F. C., and Holtz, W. G. (1951), "Control of Embankment Material by Laboratory Testing," Transactions, ASCE, Vol. 118, pp. 1-25.

Walker, L. K. (1969), Discussion on "General Stress-Strain-Time Function for Soils," Journal of Soil Mechanics and Foundations Division, ASCE, Vol. 95, No. SM 1, pp. 409-415.

Waterways Experiment Station (1949), "Soil Compaction Investigation: Compaction Studies on Silty Clay," Report No. 2, Tech. Memo No. 3-271, U. S. Corps of Engineers, Vicksburg, Mississippi.

Wilson, E. L., (1963), "Finite Element Analysis of Two Dimensional Structures," Dissertation, Doctor in Engineering, University of California, Berkeley, California.

Wilson, E. L., (1965), "Structural Analysis of Axisymmetric Solids," American Institute of Aerospace and Aeronautics, Vol. 3, No. 12, pp. 1-32.

Wu, T. H., Loh, A. K., and Malvern, L. E., (1963), "Study of Failure Envelope of Soils," Journal of Soil Mechanics and Foundations Division, ASCE, Vol. 89, No. SM 1, pp. 145-182.

Yoshimi, Y., and Osterberg, J. O. (1963), "Compression of Partially Saturated Soils," Journal of Soil Mechanics and Foundations Division, ASCE, Vol. 89, No. SM 4, pp. 1-24.

Zienkiewicz, O. C. (1961), "Analysis of Viscoelastic Behavior of Concrete Structure with Particular Reference to Thermal Stresses," Proceedings, American Concrete Institute, Vol 58, pp. 383-393.

Zienkiewicz, O. C., and Cheung, Y. K. (1967), The Finite Element Method in Structural and Continuum Mechanics, McGraw Hill, London, England.

Zienkiewicz, O. C., Watson, M., and King, I. P. (1968), "A Numerical Method of Viscoelastic Stress Analysis," International Journal of Mechanical Sciences, Vol. 10, pp. 807-827.

APPENDIX A

FINITE ELEMENT PROGRAM

1. COMPUTER PROGRAM INPUT:

   i. Identification Card (1A6)
   Columns 1-6 HED (1)

   ii. CONTROL CARD (4I5, 3F10.2, 2I5)
   Columns 1-5 Number of nodal points;
   6-10 Number of elements;
   11-15 Number of different materials;
   = Number of elements;
   16-20 Number of boundary pressure cards;
   21-30 Axial acceleration in the z direction;
   31-40 Angular velocity;
   41-50 Reference temperature;
   51-55 Number of approximations - not used in this program - Print 1;
   55-60 A positive number for solution of plane strain structure.

   iii. NODAL POINT CARDS (2I5, F5.0, 5F10.4)
   One card for each nodal point with the following information:
   Columns 1-6 Nodal point number;
   6-10 Number which indicates if displacements or forces are to be specified;
   11-20 X-ordinate
   21-30 Z-ordinate
   31-40 XR
   41-50 XZ
   51-60 Temperature
   If the number in column 10 is
   0 XR is the specified R-Load and
   XZ is the specified Z-Load.
   1 XR is the specified R-displacement and
   XZ is the specified Z-load.
   2 XR is the specified R-load and
   XZ is the specified Z-displacement.
   3 XR is the specified R-displacement and
   XZ is the specified Z-displacement.

Nodal point cards must be in numerical sequence. If cards are omitted, the omitted nodal points are generated at equal intervals along a straight line between the defined nodal points. The necessary temperatures are determined by linear interpolation. The boundary code (Column 10), XR and XZ are set equal to zero.

iv. ELEMENT CARDS (6I5)

One card for each element:

Columns 1- 5 Element number;
6-10 Nodal Point I;
11-15 Nodal Point J;
16-20 Nodal Point K;
21-25 Nodal Point L;
26-30 Material Identification.

The nodal points should be ordered counterclockwise around the element. The maximum difference between adjacent nodal points must be less than 28.

Element cards must be in element number sequence. If element cards are omitted, the program automatically generates the omitted information by incrementing by one the preceding I, J, K and L. The material identification code for the generated cards is set equal to the value given on the last card. The last element card must always be supplied.

Triangular elements are also permitted and are identified by repeating the last nodal point number (i.e. I, J, K, k)

v. PRESSURE CARDS (2I5, F10.2)

One card for each boundary element which is subjected to a normal pressure:

Columns 1- 5 Nodal Point I;
6-10 Nodal Point J;
11-20 Normal Pressure

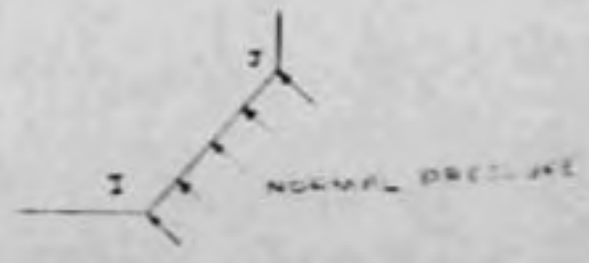

As shown above, the boundary element must be on the left as one progresses from I to J. Surface tnesile force is input as a negative pressure.

2. OUTPUT INFORMATION:

The following information is developed and printed by the program:

1. Reprent of the input data;
2. Nodal point displacements;
3. Stresses at the center of each element;
4. The ratio between octahedral shear stress and the octahedral shear stress at failure.
5. The stress dependent elastic parameters at the start and at the end of the analysis.

3. ADDITIONAL INFORMATION

1) The nonlinear elastic analysis can be stopeed either after the convergence has been achieved or after a certain specified number of iterations. Similar facility is available for each time increment.

```
15073,RAMASWAMY,T500,CM77777,P5,L30000,C100,TP4.
RUN(S)
MAP(ON)
LGO.
*
      PROGRAM MAIN(INPUT,OUTPUT,PUNCH,TAPE1,TAPE2,
     1       TAPE5=INPUT,TAPE6=OUTPUT)
C     ******************************************************************
C     ******************************************************************
C     ******************************************************************
C     SYSTEM PARAMETERS
      COMMON NUMNP,NUMEL,NUMMAT,NUMPC,ACELZ,ANGFQ,N,VOL,TEMP,MTYPE,Q,NP,
     1HED, E(1,8,500),RO(500),XXNN(12),R(500),Z(500),UR(500),UZ(500),
     2 CODE(500),T(500),IBC(500),JHC(500),PR(500),ANGLE(4)
      COMMON /ARG/ RRR(5),ZZZ(5),S(10,10),P(10),TT(4),LM(4),DD(3,3),
     1 HH(6,10),RR(4),ZZ(4),C(4,4),H(6,10),D(6,6),F(6,10),TP(6),X1(10)
     2 ,EE(7),IX(700,5),FPS(700),MTAG(700),SIG(10)
      COMMON /MANARG/ MBAND,NUMBLK,B(108),A(108,54)
      COMMON/PLANE/NPP
      COMMON  EXX(500),POIS(500)
      COMMON  TIME
C
C  READ INITIAL  PARAMETERS
C
   50 READ(5,1000) HED,NUMNP,NUMEL,NUMMAT,NUMPC,ACELZ,ACEFQ,Q,NP,NPP
      WRITE(6,2000)HED,NUMNP,NUMEL,NUMMAT,NUMPC,ACELZ,ACEFQ,Q,NP
      IF(NPP) 54,56,54
   54 WRITE(6,2008)
   56 DO59M=1,NUMMAT
      RO(M)= 0.0
      E(1,1,M) = 29.0
      E(1,2,M) = 19000.0
      E(1,3,M) = 0.13
      E(1,4,M) = E(1,2,M)
      E(1,5,M) = E(1,3,M)
      E(1,6,M) = 0.0
      E(1,7,M) = 0.0
   59  CONTINUE
      NUMTC = 1
      MTYPE = NUMMAT
C
C     READ AND PRINT OF NODAL POINT DATA
C
      WRITE(6,2004)
      L=0
   60 READ(5,1002) N,CODE(N),R(N),Z(N),UR(N),UZ(N),T(N)
      NL=L+1
      ZX=N-L
   70 L=L+1
      DR=(R(N)-R(L))/ZX
      DZ=(Z(N)-Z(L))/ZX
      DT=(T(N)-T(L))/ZX
      IF(N-L) 100,90,80
   80 CODE(L)=0.0
      R(L)=R(L-1)+DR
      Z(L)=Z(L-1)+DZ
      UR(L)=0.0
      UZ(L)=0.0
```

```
      T(L)=T(L-1)+DT
      GO TO 70
   90 WRITE (6,2002) (K,CODE(K),R(K),Z(K),UR(K),UZ(K),T(K),K=NL,N)
      IF(NUMNP-N)100,110,60
  100 WRITE(6,2009)N
      CALL EXIT
  110 CONTINUE
C
C     READ AND PRINT ELEMENT PROPERTIES
C
      WRITE(6,2001)
      N=0
  130 READ(5,1003) M, (IX(M,I),I=1,5)
  140 N=N+1
      IF (M-N) 170,170,150
  150 IX(N,1)=IX(N-1,1)+1
      IX(N,2)=IX(N-1,2)+1
      IX(N,3)=IX(N-1,3)+1
      IX(N,4)=IX(N-1,4)+1
      IX(N,5)=IX(N-1,5)
  170 WRITE (6,2003) N,(IX(N,I),I=1,5)
      IF (M-N) 180,180,140
  180 IF (NUMEL-N) 190,190,130
  190 CONTINUE
C
C     READ AND PRINT OF PRESSURE BOUNDARY CONDITIONS
C
      IF(NUMPC)290,310,290
  290 WRITE(6,2005)
      DO300L=1,NUMPC
      READ(5,1004)IBC(L),JBC(L),PR(L)
  300 WRITE(6,2007)IBC(L),JBC(L),PR(L)
  310 CONTINUE
C
C     DETERMINE BAND WIDTH
C
      J=0
      DO 340 N=1,NUMEL
      DO 340 I=1,4
      DO 325 L=1,4
      KK=IABS(IX(N,I)-IX(N,L))
      IF (KK-J) 325 ,325 ,320
  320 J=KK
  325 CONTINUE
  340 CONTINUE
      MBAND=2*J+2
      WRITE (6,2012) MBAND
 2012 FORMAT (I12)
C
C     SOLVE NON-LINEAR STRUCTURE BY SUCCESSIVE APPROXIMATION
C
      DO 350 N=1,NUMEL
  350 EPS(N)=0.0
C
      TIME = 0.01
  362 K = 1
      KKK=1
  360 CONTINUE
C     FORM STIFFNESS MATRIX
      CALL STIFF
      WRITE (6,2013) NUMBLK
```

```
 2013 FORMAT(I5)
C      SOLVE FOR DISPLACEMENTS
       CALL FINSOL
       WRITE(6,2006) (N,B(2*N-1),B(2*N),N=1,NUMNP)
C
C
C      COMPUTE STRESSES
       CALL STRESS
       WRITE (6,11)
    11 FORMAT (1H1)
       WRITE (6,5002) TIME
 5002 FORMAT (6HTIME =,F14.8)
       IF(TIME.GT. 0.01) GO TO 460
       IF(K) 525,525,550
  550 K=0
C
C CHECK  FOR  CONVERGENCE  OF  YOUNG'S MODULUS AND POISSONS RATIO
C
       DO 510 M=1,NUMMAT
       CORFF = 0.1 * E(1,2,M)
       IF(ABS(E(1,2,M) -EXX(M)). GT. CORFF ) K=K+1
       E(1,2,M) = (E(1,2,M) + EXX(M))/2.
       E(1,4,M) = E(1,2,M)
       IF (ABS(POIS(M) - E(1,3,M)). GT. 0.025) K=K+1
       E(1,3,M) = POIS(M)
  510 E(1,5,M) = E(1,3,M)
       KKK = KKK+1
       WRITE (6,8011) KKK
 8011 FORMAT (5H KKK=,I5)
       IF (KKK- 5) 8012,8012,525
 8012 CONTINUE
       GO TO 360
C
  460 IF(K) 525,525,551
  551 K = 0
       DO 411 M= 1,NUMMAT
       CORFF = 0.05 * E(1,2,M)
       IF(ABS(EXX(M) -E(1,2,M)). GT. CORFF ) K=K+1
       E(1,2,M) = EXX(M)
       E(1,4,M) = E(1,2,M)
       IF (ABS(POIS(M) - E(1,3,M)). GT. 0.025) K=K+1
       E(1,3,M) = POIS(M)
  411 E(1,5,M) = E(1,3,M)
       KKK= KKK+ 1
       GO TO 360
C  TIME INCREMENT
C
  525 TIME = 10. *TIME
       IF (TIME. GT. 100.0) GO TO 625
       GO  TO  362
  625 GO TO 50
C
C  READING FORMAT
C
 1000 FORMAT (18A4/4I5,3F10.2,2I5 )
 1001 FORMAT (2I5,1F10.6)
 1002 FORMAT (I5,F5.0,2F10.4,2F10.4,F10.4 )
 1003 FORMAT (6I5)
 1004 FORMAT (2I5,F10.2)
 1005 FORMAT (5F10.2,F10.6,2F10.2)
C
```

```
C  WRITING FORMAT
C
 2000 FORMAT (1H1  1A6/
     1 29H0 NUMBER OF NODAL POINTS-----I3/
     2 29H0 NUMBER OF ELEMENTS          I3/
     3 29H0 NUMBER OF DIFF. MATERIALS   I3/
     4 29H0 NUMBER OF PRESSURE CARDS    I3/
     5 29H0 Y-ACCELERATION              F12.4/
     6 29H0 X-ACCELERATION              F12.4/
     7 29H0 REFERANCE TEMPRATURE        E12.4/
     8 29H0 NUMBER OF APPROXIMATIONS    I3)
 2001 FORMAT (49H1ELEMENT NO.     I     J     K     L     MATERIAL   I
 2002 FORMAT (I12,F12.2,2F12.3,2E24.7,F12.3)
 2003 FORMAT (I13,4I6,I12)
 2004 FORMAT (11?H1NODAL POINT      TYPE  X-ORDINATE  Y-ORDINATE
    1X LOAD OR DISPLACEMENT  Y LOAD OR DISPLACEMENT  TEMPRATURE)
 2005 FORMAT(29H0PRESSURE BOUNDRY CONDITIONS/ 24H     I     J     PRESSUR
    1E    )
 2006 FORMAT(12H1N.P. NUMBER 1RX 2HUX 1RY 2HUY / (I12,2E20.7))
 2007 FORMAT(2I6,F12.3)
 2008 FORMAT (23H0PLANE STRAIN STRUCTURE )
 2009 FORMAT(26H NODAL POINT CARD ERROR N= I5)
 2010 FORMAT(15H0  TEMPERATURE 1UX 5HE(C)  9X 6HNU      11X 4HF(I)
     1 10X 5HG/H2  10X 5HALPHA   9X 6HSTRESS   / (F15.2,6E15.5))
 2011 FORMAT(17H0MATERIAL NUMBER= I3, 30H, NUMBER OF TEMPERATURE CARDS=
     1 I3, 15H, MASS DENSITY= E12.4 )
      END
```

```
      SUBROUTINE STIFF
      COMMON NUMND,NUMEL,NUMMAT,NUMPC,ACEL2,ANGFC,NA,VOL,TEMP,MTYPE,C,NP,
     1MED, E(1,8,500),P(4000),XX(N(12),Q(1500),Z(500),UZ(500),
     2 CODE(5001,T(500),IPC(500),JPC(500),PP(500),ANGLE(4)
      COMMON //BC/ BB(6),ZZ(6),S(10,10),R(10),TT(4),LM(4),DD(3,3),
     1 WHEA,10),PP(4),ZZ(4),C(4,4),H(6,10),D(6,6),F(6,10),TP(6),KI(10)
     2 ,FE(7),IX(700,5),EPS(700),MAG(700),SIG(10)
      COMMON /RANBOC/ MRAND,NUMBLK,R(10P),A(10P,*4)
      COMMON/PLANE/NPP
C     ****************************************************************
C     INITIALIZATION
      REWIND 2
      NB=27
      ND=2*NB
      ND2=3*ND
      STOP=0.0
      NUMBLK=0
      DO50 N=1,ND2
      R(N)=0.0
      DO50M=1,ND
   50 A(N,M)=0.0
C     FORM STIFFNESS MATRIX IN BLOCKS
   60 NUMBLK=NUMBLK+1
      NH=NB*(NUMBLK+1)
      NM=NH-NB
      NL=NM-NB+1
      KSHIFT=2*NL-2
      DO210 N=1,NUMEL
      IF(IX(N,5))210,210,65
   65 DO 80 I=1,4
      IF(IX(N,I)-NL)80,70,70
   70 IF(IX(N,I)-NM)90,90,80
   80 CONTINUE
      GO TO 210
   90 CALL QUAD
      IX(N,5)=-IX(N,5)
      IF(VOL)142,142,144
  142 WRITE(6,2003) N
      STOP=1.0
  144 IF(IX(N,3)-IX(N,4)) 145,165,145
  145 DO 150 II=1,9
      CC=S(II,10)/S(10,10)
      P(II)=P(II)-CC*P(10)
      DO 150 JJ=1,9
  150 S(II,JJ)=S(II,JJ)-CC*S(10,JJ)
      DO 160 II=1,8
      CC=S(II,9)/S(9,9)
      P(II)=P(II)-CC*P(9)
      DO 160 JJ=1,8
  160 S(II,JJ)=S(II,JJ)-CC*S(9,JJ)
C     ADD ELEMENT STIFFNESS TO TOTAL STIFFNESS
  165 DO 166 I=1,4
  166 LM(I)=2*IX(N,I)-2
      DO 200 I=1,4
      DO 200 K=1,2
      II=LM(I)+K-KSHIFT
      KK=2*I-2+K
```

```
      R(I1)=R(I1)+P(KK)
      DO 200 J=1,4
      DO 200 L=1,2
      JJ=LM(J)+I-II+1-KSHIFT
      LL=2*J-2+L
      IF(JJ)200,200,175
  175 IF(ND-JJ)180,195,195
  180 WRITE(6,2004) N
      STOP=1.0
      GO TO 210
  195 A(I,JJ)=A(I,JJ)+S(KK,LL)
  200 CONTINUE
  210 CONTINUE
C     ADD CONCENTRATED FORCE WITH IN BLOCK
      DO 250 N=NL,NM
      K=2*N-KSHIFT
      IF (N-NUMND) 249,249,248
  248 U2(N)=0.0
      U2(N) = 0.0
  249 R(K) = R(K) + U2(N)
      R(K-1) = R(K-1) + U1(N)
 6001 FORMAT (2I5,2F14.2)
  250 CONTINUE
C     BOUNDARY CONDITIONS
C     1. PRESSURE B.C
      IF(NUMPC)260,310,260
  260 DO 300 L=1,NUMPC
      I=IRC(L)
      J=JRC(L)
      PP=PR(L)/6.0
      DZ=(Z(I)-Z(J))*PP
      DR=(R(J)-R(I))*PP
      RX=2.0*R(I)+R(J)
      ZX=R(I)+2.0*R(J)
      IF(NDP) 262,264,262
  262 RX=3.0
      ZX=3.0
  264 II=2*I-KSHIFT
      JJ=2*J-KSHIFT
      IF(II) 280,280,265
  265 IF(II-ND) 270,270,280
  270 SINA=0.0
      COSA=1.0
      IF(CODE(I)) 271,272,272
  271 SINA=SIN(CODE(I))
      COSA=COS(CODE(I))
  272 R(II-1)=R(II-1)+RX*(COSA*DZ+SINA*DR)
      R(II)=R(II)-RX*(SINA*DZ-COSA*DR)
  280 IF(JJ) 300,300,285
  285 IF(JJ-ND) 290,290,300
  290 SINA=0.0
      COSA=1.0
      IF(CODE(J)) 291,292,292
  291 SINA=SIN(CODE(J))
      COSA=COS(CODE(J))
  292 R(JJ-1)=R(JJ-1)+ZX*(COSA*DZ +SINA*DR
      R(JJ)=R(JJ)-ZX*(SINA*DZ-COSA*DR)
  300 CONTINUE
C       2. DISPLACEMENT BOUNDARY CONDITION
  310 DO 400 M=NL,NM
      IF (M-NUMND) 315,315,400
```

```
  315 U=UR(M)
      N=2**M-1-KSHIFT
      IF (CODE(M)) 390,400,316
  316 IF (CODE(M)-1.) 317,370,317
  317 IF (CODE(M)-2.) 318,390,318
  318 IF (CODE(M)-3.) 390,380,390
  370 CALL MODIFY(A,B,ND2,MBAND,N,U)
      GO TO 400
  380 CALL MODIFY(A,B,ND2,MBAND,N,U)
  390 U=UZ(M)
      N=N+1
      CALL MODIFY(A,B,ND2,MBAND,N,U)
  400 CONTINUE
C     WRITE BLOCK OF EQUATIONS ON TAPE AND SHIFT UP LOWER BLOCK
      WRITE (2) (B(N),(A(N,M),M=1,MBAND),N=1,ND)
      DO 420 N=1,ND
      K=N+ND
      B(N)=B(K)
      B(K)=0.0
      DO 420 M=1,ND
      A(N,M)=A(K,M)
  420 A(K,M)=0.0
C     CHECK FOR LAST BLOCK
      IF(NM-NUMNP) 60,480,480
  480 CONTINUE
      IF(STOP) 490,500,490
  490 CALL EXIT
  500 RETURN
 2003 FORMAT(26HONEGATIVE AREA ELEMENT NO. I4)
 2004 FORMAT(29HOBAND WIDTH EXCEEDS ALLOWABLE I4)
      END
```

```
      SUBROUTINE  QUAD
      COMMON NUMNP,NUMEL,NUMMAT,NUMPC,ACELZ,ANGFO,N,VOL,TEMP,MTYPE,O,NP,
     1HED, EL(6,500),RO(500),XXNN(12),R(500),Z(500),UR(500),UZ(500),
     2 CODE(500),T(500),IBC(500),JBC(500),PR(500),ANGLE(4)
      COMMON /ARG/ RRR(5),ZZZ(5),S(10,10),P(10),TT(4),LM(4),DD(3,3),
     1 HH(6,10),RR(4),ZZ(4),C(4,4),H(6,10),D(6,6),F(6,10),IP(6),XI(10)
     2 ,FE(7),IX(700,5),EPS(700),MTAG(700),SIG(10)
      COMMON /BANARG/     ND,NUMEL,A(108),A(108,54)
      COMMON/PLANE/NPP
C     ****************************************************************
      I=IX(N,1)
      J=IX(N,2)
      K=IX(N,3)
      L=IX(N,4)
C       FORM STRESS STRAIN RELATIONSHIP
      TEMP=(T(I)+T(J)+T(K)+T(L))/4.0
   71 DO 105 KK=1,7
  105 EE(KK) = EL( 1,KK+1,  N )
      TEMP=TEMP-0
      EE(1)=EE(3)
 5004 FORMAT(1H  ,F14.8)
      IF (NPP) 84,86,84
   84 XX=EE(1)/EE(3)
      YY=EE(2)/(XX-EE(2))
      ZZ=EE(1)/(1.0-EE(2)**2)
      COMM=ZZ/(XX-YY**2)
      C(1,1)=COMM*XX
      C(1,2)=COMM*YY
      C(1,3)=0.0
      C(3,1)=0.0
      C(3,2)=0.0
      C(3,3)=0.0
      C(2,1)=COMM*YY
      C(2,2)=COMM
      C(2,3)=0.0
      C(4,4)=0.5*ZZ/(XX+YY)
      GO TO 88
   86 C(1,1)=1.0/EE(1)
      C(1,2)=-EE(2)/EE(1)
      C(1,3)=-EE(4)/EE(3)
      C(2,1)=C(1,2)
      C(2,2)=C(1,1)
      C(2,3)=C(1,3)
      C(3,1)=C(1,3)
      C(3,2)=C(2,3)
      C(3,3)=1.0/EE(3)
      CALL SYMINV(C,3)
      C(4,4)=EE(1)/(2.0+2.0*EE(2))
   88 DO 110 M=1,4
  110 TT(M)=(C(M,1)*EE(5)+C(M,3)*EE(6))*TEMP
C     FORM QUADRILATERAL STIFFNESS MATRIX
      RRR(5)=(R(I)+R(J)+R(K)+R(L))/4.0
      ZZZ(5)=(Z(I)+Z(J)+Z(K)+Z(L))/4.0
      DO 94 M=1,4
      MM=IX(N,M)
      IF(NPP) 93,89,93
   89 IF(R(MM)) 93,91,93
   91 R(MM) =.01*RRR(5)
```

```
      IF (CODE(MM)) 93,92,93
   92 CODE(MM)=1.0
   93 RRR(M)=R(MM)
   94 ZZZ(M)=Z(MM)
      DO 100 II=1,10
      P(II)=4.0
      DO 95 JJ=1,6
   95 MM(JJ,II)=0.0
      DO 100 JJ=1,10
  100 S(II,JJ)=0.0
      DO 119 II=1,4
      JJ=IX(N,II)
  119 ANGLE(II)=CODE(JJ)/57.3
      IF(K-L) 125,120,125
  120 CALL TRISTF(1,2,3)
      RRR(5)=(RRR(1)+RRR(2)+RRR(3))/3.0
      ZZZ(5)=(ZZZ(1)+ZZZ(2)+ZZZ(3))/3.0
      VOL=XI(1)
      GO TO 130
  125 VOL=0.0
      CALL TRISTF(4,1,5)
      VOL=VOL+XI(1)
      CALL TRISTF(1,2,5)
      VOL=VOL+XI(1)
      CALL TRISTF(2,3,5)
      VOL=VOL+XI(1)
      CALL TRISTF(3,4,5)
      VOL=VOL+XI(1)
      DO 140 II=1,6
      DO 140 JJ=1,10
  140 MM(II,JJ)=MM(II,JJ)/4.0
  130 RETURN
      END
```

```
      SUBROUTINE TRISTF(II,JJ,KK)
      COMMON NUMNP,NUMEL,NUMMAT,NUMPC,ACELZ,ANGFQ,N,VOL,TEMP,MTYPE,Q,NP,
     1HED, F(1,8,500),RO(500),XXNN(12),R(500),Z(500),UR(500),UZ(500),
     2 CODE(500),T(500),IBC(500),JBC(500),PR(500),ANGLE(4)
      COMMON /ARG/ RRR(5),ZZZ(5),S(10,10),P(10),TT(4),LM(6),DD(3,3),
     1 HH(6,10),RR(4),ZZ(4),C(4,4),H(6,10),D(6,6),F(6,10),IP(6),XI(10)
     2 ,FF(7),IX(700,5),EPS(700),MTAG(700),SIG(10)
      COMMON/PLANE/NPP
C     ******************************************************************
C     1. INITIALIZATION
      LM(1)=II
      LM(2)=JJ
      LM(3)=KK
      RR(1)=RRR(II)
      RR(2)=RRR(JJ)
      RR(3)=RRR(KK)
      RR(4)=RRR(II)
      ZZ(1)=ZZZ(II)
      ZZ(2)=ZZZ(JJ)
      ZZ(3)=ZZZ(KK)
      ZZ(4)=ZZZ(II)
   85 DO 100 I=1,6
      DO 90 J=1,10
      F(I,J)=0.0
   90 H(I,J)=0.0
      DO 100 J=1,6
  100 D(I,J)=0.0
C     3. FORM INTEGRALS(IT*(C)*IG)
      CALL INTER (XI,RR,ZZ)
      D(2,6)=XI(1)*(C(1,2)+C(2,3))
      D(3,5)=XI(1)*C(4,4)
      D(5,5)=XI(1)*C(4,4)
      D(6,6)=XI(1)*C(2,2)
      IF(NPP) 104,106,104
  104 D(2,2)=XI(1)*C(1,1)
      D(3,3)=XI(1)*C(4,4)
      GO TO 108
  106 D(1,1)=XI(3)*C(3,3)
      D(1,2)=XI(2)*(C(1,3)+C (3,3))
      D(1,3)=XI(5)*C(3,3)
      MTYPE=IX(N,5)
      D(1,6)=X,(2)*C(2,3)
      D(2,2)=XI(1)*(C(1,1)+2.0*C(1,3)+C(3,3))
      D(2,3)=XI(4)*(C(1,3)+C(3,3))
      D(3,3)=XI(6)*C(3,3)+XI(1)*C(4,4)
      D(3,6)=XI(4)*C(2,3)
  108 DO 110 I=1,6
      DO 110 J=1,6
  110 D(J,I)=D(I,J)
C     4. FORM COEFFICIENT  DISPLASEMENT TRANFORMATION MATRIX
      COMM=RR(2)*(ZZ(3)-ZZ(1))+RR(1)*(ZZ(2)-ZZ(3))-RR(3)*(ZZ(1)-ZZ(2))
      DD(1,1)=(RR(2)*ZZ(3)-RR(3)*ZZ(2))/COMM
      DD(1,2)=(RR(3)*ZZ(1)-RR(1)*ZZ(3))/COMM
      DD(1,3)=(RR(1)*ZZ(2)-RR(2)*ZZ(1))/COMM
      DD(2,1)=(ZZ(2)-ZZ(3))/COMM
      DD(2,2)=(ZZ(3)-ZZ(1))/COMM
      DD(2,3)=(ZZ(1)-ZZ(2))/COMM
      DD(3,1)=(RR(3)-RR(2))/COMM
```

```
      DD(3,2)=(RR(1)-RR(3))/COMM
      DD(3,3)=(RR(2)-RR(1))/COMM
      DO 120 I=1,3
      J=2*LM(I)-1
      H(1,J)=DD(1,I)
      H(2,J)=DD(2,I)
      H(3,J)=DD(3,I)
      H(4,J+1)=DD(1,I)
C     ROTATE UNKNOWNS IF REQUIRED
      H(5,J+1)=DD(2,I)
  120 H(6,J+1)=DD(3,I)
      DO 125 J=1,2
      I=LM(J)
      IF(ANGLE(I)) 122,125,125
  122 SINA=SIN(ANGLE(I))
      COSA=COS(ANGLE(I))
      IJ=2*I
      DO 124 K=1,6
      TEM =H(K,IJ-1)
      H(K,IJ-1)=TEM*COSA+H(K,IJ)*SINA
  124 H(K,IJ)=-TEM*SINA+H(K,IJ)*COSA
  125 CONTINUE
C     5. FORM ELEMENT STIFFNESS MATRIX (H)T*(D)*(H)
      DO 130 J=1,10
      DO 130 K=1,6
      IF (H(K,J)) 128,130,128
  128 DO 129 I=1,6
  129 F(I,J)=F(I,J)+D(I,K)*H(K,J)
  130 CONTINUE
      DO 140 I=1,10
      DO 140 K=1,6
      IF (H(K,I))138,140,138
  138 DO 139 J=1,10
  139 S(I,J)=S(I,J)+H(K,I)*F(K,J)
  140 CONTINUE
C     6. FORM THERMAL LOAD MATRIX
      IF(NPP) 145,150,145
  145 TT(3)=0.0
      COMM=X(1)*EE(4)
      S(9,9)=S(9,9)+COMM
      S(10,10)=S(10,10)+COMM
  150 COMM=RO(MTYPE)*ANGFO**2
      TP(1)=COMM*X(7)+X(2)*TT(3)
      TP(2)=COMM*X(9)+X(1)*(TT(1)+TT(3))
      TP(3)=COMM*X(10)+X(4)*TT(3)
      COMM=+RO(MTYPE)*ACELZ
      TP(4)=COMM*X(1)
      TP(5)=COMM*X(7)
      TP(6)=COMM*X(8)+X(1)*TT(2)
      DO 160 I=1,10
      DO 160 K=1,6
  160 P(I)=P(I)+H(K,I)*TP(K)
C     FORM STRAIN TRANSFORMATION MATRIX
  400 DO 410 I=1,6
      DO 410 J=1,10
  410 HH(I,J)=HH(I,J)+H(I,J)
  500 RETURN
      END
```

```
      SUBROUTINE STRESS
      COMMON NUMNP,NUMEL,NUMMAT,NUMDC,ACEL2,ANGED,NL,VOL,TEMP,MTYPE,C,ND,
     1HED, E(1,8,500),RO(500),XX(N(17),R(500),Z(500),UR(500),UZ(500),
     2 CODE(500),T(500),IBC(500),JBC(500),PR(500),ANGLE(4)
      COMMON /ABC/ RRR(5),ZZZ(5),S(10,10),P(10),TT(4),LM(4),DD(3,3),
     1 MM(6,10),PP(6),Z(6),C(4,4),H(6,10),D(6,6),F(6,10),IP(6),X(10)
     2 ,EE(7),IX(770,5),EPS(700),MTAG(700),SIG(10)
      COMMON /PLANARG/     ND,NUMPLC,R(108),A(108,54)
      COMMON/PLANE/NPP
      COMMON  EXX(500),EPS(500)
      COMMON  TIME
C     ****************************************************************
C     COMPUTE ELEMENT STRESSES
      XKE=0.0
      XPE=0.0
      MPRINT=0
      DO 300 M=1,NUMEL
      N=M
      IX(N,5)=IABS(IX(N,5))
      MTYPE=IX(N,5)
      CALL  QUAD
      IX(N,5)=MTYPE
      DO 120 I=1,4
      II=2*I
      JJ=2*IX(N,I)
      P(II-1)=R(JJ-1)
  120 P(II)=R(JJ)
      DO 150 I=1,8
      RR(I)=P(I+8)
      DO 150 K=1,8
  150 RR(I)=RR(I)-S(I+8,K)*P(K)
      COMM=S(9,9)*S(10,10)-S(9,10)*S(10,9)
      IF(COMM) 155,160,155
  155 P(9)=(S(10,10)*RR(1)-S(9,10)*RR(2))/COMM
      P(10)=(-S(10,9)*RR(1)+S(9,9)*RR(2))/COMM
  160 DO 170 I=1,6
      TP(I)=0.0
      DO 170 K=1,10
  170 TP(I)=TP(I)+MM(I,K)*P(K)
      RR(1)=TP(2)
      RR(2)=TP(6)
      RR(3)=(TP(1)+TP(2)*RRR(5)+TP(3)*ZZZ(5))/RRR(5)
      RR(4)=TP(3)+TP(5)
  176 DO 180 I=1,3
      SIG(I)=-TT(I)
      DO 180 K=1,3
  180 SIG(I)=SIG(I)+C(I,K)*RR(K)
      SIG(3) = EE(2) * (SIG(1) + SIG(2))
      SIG(4)=C(4,4)*RR(4)
C
C     CALCULATE ENERGY TERM
C
      DO 250 I=1,10
      COMM=0.0
      DO 200 K=1,10
  200 COMM=COMM+S(I,K)*P(K)
  250 XPE=XPE+COMM*P(I)
      XKE=XKE+VOL*RO(MTYPE)*(P(9)**2+P(10)**2)
```

```
C     CALCULATE EFFECTIVE STRAIN
      IF(NPP) 251,252,251
  251 PP(3) = 0.0
  252 CC=(PP(1)+PP(2))/2.0
      CR=SQRT(((PP(2)-PP(1))/2.0)**2+(PP(4)/2.0)**2)
      PP(1)=CC+CR
      PP(2)=CC-CR
      EPS(N)=SQRT((PP(1)-PP(2))**2+(PP(1)-PP(3))**2+(PP(2)-PP(3))**2)
     1*.707/(1.0+EE(2))
C
C     OUTPUT STRESSES
C     CALCULATE PRINCIPAL STRESSES
C
      SIG(1) = -SIG(1)
      SIG(2) = -SIG(2)
      SIG(3) = -SIG(3)
      SIG(4) = -SIG(4)
      CC=(SIG(1)+SIG(2))/2.0
      RR=(SIG(1)-SIG(2))/2.0
      CR=SQRT(RR**2+SIG(4)**2)
      SIG(5)=CC+CR
      SIG(6)=CC-CR
      SIG(7)=28.648*ATAN2(2.0*SIG(4),RR)
C
C      STRESS  PARELLEL TO LINE I-J
      I=IX(N,1)
      J=IX (N,2)
      ANG=2.0*ATAN2((Z(J)-Z(I)),(R(J)-R(I)))
      COS2A=COS(ANG)
      SIN2A=SIN (ANG)
      CX=.5*(SIG(1)-SIG(2))
      SIG(8) = 0.0
      SIG(9) = 0.0
      SIG(10) = (SIG(5) - SIG(6))/2.0
  104 IF(MPRINT) 110,105,110
  105 WRITE (6,2002)
 2002 FORMAT (1H1)
      WRITE (6,2000)
      MPRINT=50
  110 MPRINT=MPRINT-1

C  CALCULATION  OF  YOUNGS  MODULUS

      SGY = EE(2) *(SIG(5) + SIG(6))
      TOC1 = (SIG(5) - SIG(6))**2
      TOC2 = (SIG(6) - SGY)**2
      TOC3 = (SGY - SIG(5))**2
      TOCT = (((TOC1 + TOC2 + TOC3 )**0.5)/ 3.
      SOCT = (SIG(5) + SIG(6) + SGY )/3.
      IF (SOCT. GT. 0.0) GO TO 7002
      XXF = 3.0
      GO TO 7003
 7002 XXF = SOCT

C  FAILURE  STRESS

 7003 TOCTF = (3.187 *14.2233 + 0.0576* XXF) *1.4142/3.
 7005 YYF = ABS (TOCT)
      RAT = YYF / TOCTF
      IF(RAT. GT. 0.1) GO TO 6123
      ASIG= 0.0
```

```
      GO TO 6124
 6123 ASIG = 0.5027 -5.0487 * RAT
 6124 ASIGMA = 10.**ASIG
      ONEG1=-0.8347*RAT+1.3988*(RAT**3.)-0.3504*(RAT**4.)
      G1 = 1. + ONEG1
      XJ1 = 0.0033789 * 1.4142 /1.58
      G2K = XJ1 * (1.58 * RAT + 1.01
      REMOD = G1 *G2K * ((TIME/ASIGMA)**0.0794)/TOCTF
      SHMOD = (1./REMOD)
      POIS(M) = 0.15 * RAT
      FXX(M) = 2. * SHMOD * (1.+ POIS(M))
  305 WRITE (6,2001) M,PPP(5),ZZZ(5),(SIG(I),I=1,4),SOCT,TOCT,TOCTF,
     1RAT,EE(2),POIS(M),EE(1),FXX(M)
  300 CONTINUE
      IF (XKE) 310,320,310
  310 W=SQRT(XPE/XKE)
      WRITE (6,2006) W
  320 RETURN
 2000 FORMAT (132H  ELE.    X       Z      R-STRESS    Z-STRESS    T-STRESS
     1RZ-STRESS  SIG-OCT.    TAU-OCT.    TAU-OCTF.  RAT   POISSONS.   INIT-
     2E   FINAL-E )
 2001 FORMAT (1H ,I4,2F8.3,7E11.4,F4.3,2F8.3,2F10.3)
 2006 FORMAT (25HOAPPROXIMATE FUNDAMENTAL FREQUENCY   E12.5)
      END
```

```
      SUBROUTINE MODIFY(A,B,NEQ,MBAND,N,U)
      DIMENSION A(108,54) ,B(108)
      DO 250 M=2,MBAND
      K=N-M+1
      IF(K) 235,235,230
  230 B(K)=B(K)-A(K,M)*U
      A(K,M)=0.0
  235 K=N+M-1
      IF(NEQ-K) 250,240,240
  240 B(K)=B(K)-A(N,M)*U
      A(N,M)=0.0
  250 CONTINUE
      A(N,1)=1.0
      B(N)=U
      RETURN
      END
```

```
      SUBROUTINE BANSOL
      COMMON /BANARG/     MM,NUMBLK,B(108),A(108,54)
C     ********************************************************
      REWIND 1
      REWIND 2
      NN=54
      NL=NN+1
      NH=NN+NN
      NB=0
      GO TO 150
C     REDUCE EQUATIONS BY BLOCKS
C     1. SHIFT BLOCK OF EQUATIONS
  100 NB=NB+1
      DO 125  N=1,NN
      NM=NN+N
      B(N)=B(NM)
      B(NM)=0.0
      DO 125 M=1,MM
      A(N,M)=A(NM,M)
  125 A(NM,M)=0.0
C     2. READ NEXT BLOCK OF EQUATIONS
      IF(NUMBLK-NB) 150,200,150
  150 READ(2) (B(N), (A(N,M),M=1,MM),N=NL,NH)
      IF(NB) 200,100,200
C     3. REDUCE BLOCK OF EQUATION
  200 DO 300 N=1,NN
      IF (A(N,1)) 225,300,225
  225 B(N)=B(N)/A(N,1)
      DO 275 L=2,MM
      IF(A(N,L)) 230,275,230
  230 C=A(N,L)/A(N,1)
      I=N+L-1
      J=0
      DO 250 K=L,MM
      J=J+1
  250 A(I,J)=A(I,J)-C*A(N,K)
      B(I)=B(I)-A(N,L)*B(N)
      A(N,L)=C
  275 CONTINUE
  300 CONTINUE
C     4. WRITE  BLOCK OF REDUCED EQUATIONS ON TAPE 2
      IF(NUMBLK-NB) 375,400,375
  375 WRITE(1) (B(N),(A(N,M),M=2,MM),N=1,NN)
      GO TO 100
C     BACK SUBSTITUTION
  400 DO 450 M=1,NN
      N=NN+1-M
      DO 425 K=2,MM
      L=N+K-1
  425 B(N)=B(N)-A(N,K)*B(L)
      NM=N+NN
      B(NM)=B(N)
  450 A(NM,NB)=B(N)
      NB=NB-1
      IF(NB) 475,500,475
  475 BACKSPACE 1
      READ(1)(B(N),(A(N,M),M=2,MM),N=1,NN)
      BACKSPACE 1
```

```
      GO TO 400
C     ORDER UNKNOWNS IN B ARRAY
  500 K=0
      DO 600 NB=1,NUMBLK
      DO 600 N=1,NN
      NM=N+NN
      K=K+1
  600 B(K)=A(NM,NB)
      RETURN
      END
```

```
      SUBROUTINE SYMINV(A,NMAX)
      DIMENSION A(4,4)
      DO 200 N=1,NMAX
      D=A(N,N)
      DO 100 J=1,NMAX
  100 A(N,J)=-A(N,J)/D
      DO 150 I=1,NMAX
      IF(N-I) 110,150,110
  110 DO 140 J=1,NMAX
      IF (N-J) 120,140,120
  120 A(I,J)=A(I,J)+A(I,N)*A(N,J)
  140 CONTINUE
  150 A(I,N)=A(I,N)/D
      A(N,N)=1.0/D
  200 CONTINUE
      RETURN
      END
```

```
      SUBROUTINE INTER(XI,RR,ZZ)
      DIMENSION RR(4),ZZ(4),XI(10),XM(6),R(6),Z(6),XX(6)
      COMMON/PLANE/NPP
      DATA (XX(I),I=1,6)/3*1.0,3*3.0/
      COMM=RR(2)*(ZZ(3)-ZZ(1))+RR(1)*(ZZ(2)-ZZ(3))+RR(3)*(ZZ(1)-ZZ(2))
      COMM=COMM/24.0
      R(1)=RR(1)
      R(2)=RR(2)
      R(3)=RR(3)
      R(4)=(R(1)+R(2))/2.0
      R(5)=(R(2)+R(3))/2.0
      R(6)=(R(3)+R(1))/2.0
C
      Z(1)=ZZ(1)
      Z(2)=ZZ(2)
      Z(3)=ZZ(3)
      Z(4)=(Z(1)+Z(2))/2.0
      Z(5)=(Z(2)+Z(3))/2.0
      Z(6)=(Z(3)+Z(1))/2.0
      IF (NPP) 10,30,10
   10 DO 20 I=1,6
   20 XM(I)=XX(I)
      GO TO 40
   30 DO 35 I=1,6
   35 XM(I)=XX(I)*R(I)
   40 DO 50 I=1,10
   50 XI(I)=0.0
      DO 100 I=1,6
      XI(1)=XI(1)+XM(I)
      XI(2)=XI(2)+XM(I)/R(I)
      XI(3)=XI(3)+XM(I)/(R(I)**2)
      XI(4)=XI(4)+XM(I)*Z(I)/R(I)
      XI(5)=XI(5)+XM(I)*Z(I)/(R(I)**2)
      XI(6)=XI(6)+XM(I)*Z(I)**2/(R(I)**2 )
      XI(7)=XI(7)+XM(I)*R(I)
      XI(8)=XI(8)+XM(I)      *Z(I)
      XI(9)=XI(9)+XM(I)*R (I)**2
      XI(8)=XI(8)+XM(I)      *Z(I)
      XI(9)=XI(9)+XM(I)*R (I)**2
      XI(10)=XI(10)+XM(I)*R(I)*Z(I)
  100 CONTINUE
      DO 150 I=1,10
  150 XI(I)=XI(I)*COMM
      RETURN
      END
```

APPENDIX B

SUMMARY OF EXPERIMENTAL RESULTS

Table 2

Effect of Stress-Strength Ratio on Creep Parameter for

Kaolin-Kneading Compaction,

60 lbs. Tamps - Drained

Specimen	Moisture Content	Confining Pressure kg/sq. cm.	Devr. Stress kg/sq. cm.	Failure Stress kg/sq. cm.	c	n	Equivalent Poisson's Ratio
8J	27.5	0.0	1.53	5.33	0.1640	0.0326	0.0927
8J	27.5	0.0	2.86	5.33	0.3860	0.0360	0.1451
8J	27.5	0.0	4.24	5.33	0.8427	0.0352	0.2191
2J	27.5	0.0	1.49	5.33	0.1752	0.0395	0.0944
2J	27.5	0.0	2.29	5.33	0.3096	0.0338	0.0913
2J	27.5	0.0	3.33	5.33	0.5185	0.0331	0.1392
2J	27.5	0.0	4.24	5.33	0.8131	0.0322	0.1751
2J	27.5	0.0	4.69	5.33	0.9671	0.0343	0.1927
13E	17.8	1.0	3.78	8.40	0.3736	0.0312	0.0337
13E	17.8	1.0	4.70	8.40	0.5001	0.0224	0.0711
13E	17.8	1.0	5.62	8.40	0.6995	0.0286	0.1060
13E	17.8	1.0	6.53	8.40	0.8998	0.0458	0.1312
14E	17.8	1.0	3.78	8.73	0.3359	0.0327	0.0804
14E	17.8	1.0	4.70	8.73	0.3830	0.0370	0.1067
14E	17.8	1.0	5.62	8.73	0.5427	0.0274	0.1364
14E	17.8	1.0	6.53	8.73	0.6946	0.0363	0.1587
8E	18.5	1.0	2.10	8.31	0.1345	0.0430	0.0349
8E	18.5	1.0	2.78	8.31	0.1754	0.0508	0.0337
7E	18.5	1.0	2.91	8.36	0.2079	0.0269	0.0517
7E	18.5	1.0	3.36	8.36	0.2535	0.0369	0.0528
7E	18.5	1.0	1.53	8.36	0.0795	0.0437	0.0322
7E	18.5	1.0	2.22	8.36	0.1426	0.0320	0.0458
14E	17.8	1.0	2.86	8.73	0.3018	0.0331	0.0447
3J	27.5	1.0	1.03	6.67	0.0689	0.0345	0.0561
3J	27.5	1.0	1.95	6.67	0.1563	0.0486	0.0610
3J	27.5	1.0	2.86	6.67	0.2796	0.0448	0.0986
3J	27.5	1.0	3.78	6.67	0.4921	0.0461	0.1420
3J	27.5	1.0	4.70	6.67	0.8587	0.0545	0.2342
10E	18.7	2.0	1.36	10.05	0.0606	0.0320	0.0584
10E	18.7	2.0	2.51	10.05	0.1525	0.0382	0.0611
10E	18.7	2.0	3.65	10.05	0.3003	0.0448	0.0565

Table 3

Effect of Stress-Strength Ratio on Creep Parameters for

Kaolinite-Impact Compaction,

45 blows - Drained

Specimen	Moisture Content	Confining Pressure kg/sq. cm.	Devr. Stress kg/sq. cm.	Failure Stress kg/sq. cm.	c	n	Equivalent Poisson's Ratio
6D	23.8	0.0	0.92	10.52	0.1212	0.0300	0.0193
6D	23.8	0.0	1.83	10.52	0.2179	0.0284	0.0577
6D	23.8	0.0	2.75	10.52	0.2937	0.0313	0.1093
6D	23.8	0.0	3.67	10.52	0.3551	0.0392	0.1727
12D	23.8	0.0	1.84	10.38	0.2753	0.0370	0.0756
12D	23.8	0.0	2.75	10.38	0.3463	0.0387	0.1286
14G	24.9	0.0	1.03	9.62	0.1097	0.0454	0.0179
14G	24.9	0.0	1.95	9.62	0.1803	0.0189	0.0584
14G	24.9	0.0	4.70	9.62	0.6210	0.0142	0.1815
14G	24.9	0.0	6.53	9.62	1.3421	0.0193	0.3119
16D	23.9	1.0	2.98	12.90	0.1738	0.0455	0.0697
16D	23.9	1.0	3.89	12.90	0.2433	0.0362	0.0999
16D	23.9	1.0	4.81	12.90	0.3460	0.0368	0.0492
14D	23.9	1.0	1.01	12.50	0.0760	0.0489	0.0397
14D	23.9	1.0	1.93	12.50	0.1350	0.0474	0.0595
14D	23.9	1.0	2.85	12.50	0.1733	0.0574	0.1157
14D	23.9	1.0	4.68	12.50	0.3350	0.0616	0.0558
12G	25.1	1.0	1.03	11.68	0.0464	0.0596	0.0960
9G	25.1	1.0	1.03	10.78	0.0385	0.0952	0.1412
3G	25.1	1.0	1.03	11.38	0.0376	0.0685	0.1005
3G	25.1	1.0	1.95	11.38	0.0927	0.0506	0.1551
3G	25.1	1.0	2.86	11.38	0.1652	0.0644	0.1969
3G	25.1	1.0	4.70	11.38	0.4523	0.0429	0.2687
3G	25.1	1.0	6.53	11.38	1.0263	0.0385	0.3248

Table 4

Effect of Stress-Strength Ratio on Creep Parameters for

Kaolinite - Impact Compaction,

45 Blows - Undrained and Partly Drained

Specimen	Moisture Content	Confining Pressure kg/sq. cm.	Devr. Stress kg/sq. cm.	Failure Stress kg/sq. cm.	c	n	Equivalent Poisson's Ratio
15G	24.9	0.0	1.03	9.48	0.1256	0.0368	0.0257
15G	24.9	0.0	1.95	9.48	0.2085	0.0399	0.0617
15G	24.9	0.0	2.86	9.48	0.3168	0.0360	0.1128
15G	24.9	0.0	4.70	9.48	0.5712	0.0411	0.1728
15G	24.9	0.0	6.53	9.48	1.1866	0.0358	0.2683
5G	25.1	1.0	1.03	10.43	0.0429	0.0458	0.0905
5G	25.1	1.0	1.95	10.43	0.1086	0.0474	0.1349
5G	25.1	1.0	2.86	10.43	0.2248	0.0484	0.1628
5G	25.1	1.0	4.70	10.43	0.7267	0.0314	0.2481
5G	25.1	1.0	6.53	10.43	1.4804	0.0456	0.3257

Table 5

Results of Tests Conducted on Grundite Specimens From

Footing Test - Static Compaction

10.54 kg/sq. cm. - Drained

Specimen	Moisture Content	Confining Pressure kg/sq. cm.	Devr. Stress kg/sq. cm.	Failure Stress kg/sq. cm.	c	n	Equivalent Poisson's Ratio
G1	18.3	0.0	0.96	6.30	0.1755	0.0406	0.0037
G1	18.3	0.0	1.91	6.30	0.2834	0.0391	0.0251
G1	18.3	0.0	2.87	6.30	0.5221	0.0414	0.1211
G1	18.3	0.0	3.82	6.30	0.6949	0.0443	0.1511
G5	17.1	1.50	1.04	8.33	0.0546	0.0405	0.1087
G5	17.1	1.50	1.95	8.33	0.1357	0.0400	0.1158
G5	17.1	1.50	2.85	8.33	0.2272	0.0394	0.0456
G2	19.0	1.00	-	6.96			
G6	18.1	2.00	-	7.29			
G4	18.7	2.00	-	6.78			

Table 6

Effect of Stress-Strength Ratio on Creep Parameters For

Kaolinite - Impact Compaction

45 Blows - Drained

Specimen	Moisture Content	Confining Pressure kg/sq. cm.	Devr. Stress kg/sq. cm.	Failure Stress kg/sq. cm.	c	n	Equivalent Poisson's Ratio
4H	26.4	1.0	1.95	11.06	0.1144	0.0543	0.0658
4H	26.4	1.0	3.32	11.06	0.2699	0.0456	0.0908
4H	26.4	1.0	4.70	11.06	0.4780	0.0406	0.1106
4H	26.4	1.0	6.07	11.06	0.7941	0.0356	0.1364
4H	26.4	1.0	7.45	11.06	1.1076	0.0347	0.1728
7D*	25.0	0.0	1.95	9.60	0.2276	0.0532	0.0618
7D*	25.0	0.0	6.51	9.60	1.1397	0.0445	0.3416

* 1 Loading duration was for 1 minute only.

Table 7

Results of Extension Creep Tests on Kaolinite -

Impact Compaction, 45 Blows

Specimen	Moisture Content	Confining Pressure kg/sq. cm.	Devr. Stress kg/sq. cm.	c	n	Equivalent Poisson's Ratio
8H	26.4	1.0	2.02	0.0857	0.0569	0.5147
8H	26.4	1.0	3.01	0.2564	0.0821	0.5836
8H	26.4	1.0	3.56	0.3367	0.0774	0.5613
8H	26.4	1.0	4.01	0.4970	0.0553	0.5808
8H	26.4	1.0	4.54	0.6923	0.0883	0.5875
5H	26.4	1.0	3.00	0.1441	0.0847	0.4041
5H	26.4	1.0	3.50	0.2505	0.0673	0.4742
5H	26.4	1.0	4.54	0.7277	0.0652	0.5635

Table 8

Results of Extension Creep Tests on Kaolinite -

Kneading Compaction, 60 lbs. Tamps

Specimen	Moisture Content	Confining Pressure kg/cm. sq.	Devr. Stress kg/cm. sq.	c	n	Equivalent Poisson's Ratio
10J	27.5	1.0	1.97	0.1904	0.0444	0.4371
10J	27.5	1.0	2.98	0.3756	0.0416	0.3960
10J	27.5	1.0	3.97	0.8264	0.0441	0.4483

Table 9

Effect of Stress Level on Creep Parameters for

Kaolinite - Impact Compaction,

45 Blows - Moisture Content 27.1 Per Cent - Drained

(Data from Perloff)

Specimen	Confining Pressure kg/sq. cm.	Devr. Stress kg/sq. cm.	c	n	Equivalent Poisson's Ratio
70	0.0	2.12	0.083	0.041	0.252
70	0.0	3.53	0.240	0.038	0.321
70	0.0	4.93	0.510	0.036	0.365
73	0.0	2.12	0.080	0.075	0.280
73	0.0	3.53	0.40	0.025	0.485
145	0.0	3.53	0.28	-	0.108
145	0.0	4.93	0.63	0.040	0.349
145	0.0	5.30	0.90	0.039	0.373
145	0.0	6.02	1.30	0.079	0.393
148	0.0	5.30	0.62	0.043	0.293
148	0.0	6.02	0.83	0.034	0.486
149	0.0	6.02	1.00	0.039	0.342
96	1.0	2.12	0.13	0.032	0.126
96	1.0	3.53	0.28	0.041	0.227
96	1.0	4.93	0.47	0.040	0.348
96	1.0	6.36	0.78	0.056	0.413
142	1.0	2.12	0.12	0.041	0.228
142	1.0	3.53	0.17	0.044	0.221
142	1.0	4.93	0.35	0.057	0.351
142	1.0	6.36	0.72	0.047	0.428
50	3.0	0.12	0.08	0.053	0.152
50	3.0	3.53	0.15	0.043	0.282
50	3.0	4.95	0.27	0.030	0.319
50	3.0	6.36	0.49	0.040	0.443
59	3.0	2.12	0.08	0.049	-
59	3.0	3.53	0.20	0.043	0.308
59	3.0	4.95	0.41	0.044	0.468
59	3.0	6.36	0.74	0.052	0.490
109	6.0	2.12	0.10	0.039	-
109	6.0	3.53	0.17	0.041	-
109	6.0	4.95	0.26	0.038	-
109	6.0	6.36	0.43	0.039	-
116	6.0	2.12	0.083	0.053	-
116	6.0	3.53	0.11	0.077	-
116	6.0	4.95	0.29	0.043	-

Table 10

Effect of Stress Level on Creep Parameters For Grundite -

Kneading Compaction, 45 lbs. Tamps - Moisture Content 19.5 Per Cent-

Drained (Data From Perloff)

Specimen	Confining Pressure kg/sq. cm.	Devr. Stress kg/sq. cm.	c	n	Equivalent Poisson's Ratio
133	0.0	1.71	0.15	0.078	0.358
133	0.0	2.86	0.41	0.057	0.300
133	0.0	4.00	0.76	0.055	0.337
133	0.0	5.14	1.55	0.061	0.297
132	0.0	1.71	0.19	0.100	0.276
132	0.0	2.86	0.39	0.057	0.332
132	0.0	4.00	0.78	0.052	0.348
132	0.0	5.14	1.48	0.056	0.424
110	1.0	1.71	0.14	0.060	0.283
110	1.0	2.86	0.33	0.060	0.399
110	1.0	4.00	0.66	-	0.477
110	1.0	5.14	0.94	0.095	0.305
135	1.0	1.71	0.14	0.078	0.214
135	1.0	2.86	0.25	0.067	0.297
135	1.0	4.00	0.45	0.077	0.267
135	1.0	5.14	1.04	0.060	0.305
81	3.0	1.71	0.11	0.057	0.262
81	3.0	2.86	0.25	0.071	-
81	3.0	4.00	0.43	0.049	0.322
81	3.0	5.14	0.76	0.050	0.414
86	3.0	1.71	0.19	0.032	-
86	3.0	2.86	0.24	0.065	-
86	3.0	4.00	0.58	0.061	0.347
86	3.0	5.14	0.95	0.077	0.405
136A	3.0	1.71	0.08	0.094	0.139
136A	3.0	2.86	0.24	0.091	0.237
136A	3.0	4.00	0.58	0.060	0.254
136A	3.0	5.14	1.10	0.055	0.285
141	4.0	1.71	0.19	0.072	-
141	3.0	2.86	0.40	0.091	0.167
141	3.0	4.00	0.60	0.066	0.122
141	3.0	5.14	1.04	0.062	0.117

Table 11

Effect of Moisture Content on Creep Parameters for Grundite-

Impact Compaction, 45 Blows - Confining Pressure

3 kg/sq. cm. - Drained (Date from Perloff)

Specimen	Moisture Content Per Cent	Devr. Stress kg/sq. cm.	c	n	Equivalent Poisson's Ratio
88	14.1	2.62	0.13	0.70	0.138
88	14.1	4.37	0.22	0.052	0.169
88	14.1	4.37	0.22	0.052	0.169
88	14.1	6.12	0.34	0.065	0.230
89	14.1	2.62	0.13	0.046	0.033
89	14.1	4.37	0.21	0.037	0.115
89	14.1	6.12	0.34	0.032	0.160
89	14.1	8.33	0.49	0.042	0.242
77	17.8	1.52	0.12	0.045	-
77	17.8	2.52	0.21	0.056	-
77	17.8	3.52	0.52	0.048	-
77	17.8	4.53	0.95	0.060	-
80	17.8	1.52	0.13	0.045	-
80	17.8	2.52	0.20	0.053	-
80	17.8	3.52	0.48	0.041	-
80	17.8	4.53	0.90	0.066	-
66	21.7	1.53	0.20	0.047	0.092
66	21.7	2.55	0.30	0.060	0.163
66	21.7	3.56	0.62	0.036	0.286
69	21.7	1.53	0.19	0.057	0.144
69	21.7	2.55	0.38	0.052	0.120
69	21.7	3.56	1.25	0.048	-
69	21.7	4.58	2.30	0.092	-

Table 12

Effect of Moisture Content on Creep Parameters for Grundite - Impact Compaction, 120 Blows - Confining Pressure 3.0 kg/sq. cm. - Drained (Data from Perloff)

Specimen	Moisture Content Per Cent	Devr. Stress kg/sq. cm.	c	n	Equivalent Poisson's Ratio
91	14.2	4.55	0.28	0.052	0.171
91	14.2	7.59	0.56	0.045	0.267
91	14.2	10.63	0.92	0.066	0.343
84	16.7	3.75	0.28	0.052	0.113
84	16.7	6.26	0.90	0.042	0.181
84	16.7	8.76	2.00	0.069	0.207
97	19.0	2.71	0.24	0.035	0.422
97	19.0	4.52	0.70	0.050	0.432
97	19.0	6.32	1.48	0.048	0.434
97	19.0	8.13	2.45	0.098	0.623
102	19.0	2.71	0.24	0.078	0.375
102	19.0	4.52	0.68	0.045	0.391
102	19.0	6.32	1.30	0.044	0.422
102	19.0	8.13	2.70	0.068	0.466

APPENDIX C

EXPERIMENTAL RESULTS

APPENDIX C

1. Kneading Compaction - 60 lbs. Tamps - Kaolinite

13E 12-26-68 COMP. CREEP
CONFP=1.0000 DEVP=3.7800
HIGHT=2.8125DIAMR=1.3125

TIME	AXL.STRN	RDL.STRN
.02	.00288	-.00018
.04	.00306	-.00018
.06	.00316	-.00018
.10	.00324	-.00019
.40	.00356	-.00020
1.00	.00373	-.00022
2.00	.00384	-.00022
4.00	.00388	-.00022
6.00	.00391	-.00022
10.00	.00395	-.00023
20.00	.00402	-.00024
40.00	.00416	-.00024
60.00	.00423	-.00025

13E 12-26-68 COMP. CREEP
CONFP=1.0000 DEVP=4.5300
HIGHT=2.8125DIAMR=1.3125

TIME	AXL.STRN	RDL.STRN
.02	.00604	-.00084
.04	.00702	-.00096
.06	.00711	-.00097
.10	.00738	-.00098
.40	.00773	-.00105
1.00	.00809	-.00106
2.00	.00827	-.00109
4.00	.00853	-.00113
6.00	.00862	-.00114
10.00	.00871	-.00120
20.00	.00880	-.00122
40.00	.00924	-.00129
60.00	.00960	-.00133

14E 1-6-69 COMPN. CREEP
CONFP=1.0000 DEVP=3.7800
HIGHT=2.8125DIAMR=1.3125

TIME	AXL.STRN	RDL.STRN
.02	.00256	-.00021
.04	.00281	-.00023
.06	.00286	-.00024
.10	.00292	-.00025
.40	.00306	-.00026
1.00	.00320	-.00026
2.00	.00324	-.00026
4.00	.00331	-.00027
6.00	.00334	-.00029
10.00	.00338	-.00029
20.00	.00338	-.00029
40.00	.00338	-.00032
60.00	.00338	-.00032

13E 12-26-68 COMP. CREEP
CONFP=1.0000 DEVP=4.7000
HIGHT=2.8125DIAMR=1.3125

TIME	AXL.STRN	RDL.STRN
.02	.00469	-.00036
.04	.00491	-.00037
.06	.00498	-.00037
.10	.00501	-.00038
.40	.00523	-.00038
1.00	.00533	-.00039
2.00	.00537	-.00039
4.00	.00540	-.00039
6.00	.00548	-.00040
10.00	.00558	-.00040
20.00	.00565	-.00041
40.00	.00569	-.00041
60.00	.00572	-.00043

14E 1-7-69 COMPN. CREEP
CONFP=1.0000 DEVP=4.5300
HIGHT=2.8125DIAMR=1.3125

TIME	AXL.STRN	RDL.STRN
.02	.00473	-.00072
.04	.00555	-.00081
.06	.00565	-.00083
.10	.00572	-.00088
.40	.00601	-.00091
1.00	.00608	-.00096
2.00	.00615	-.00098
4.00	.00629	-.00101
6.00	.00633	-.00103
10.00	.00640	-.00105
20.00	.00654	-.00110
40.00	.00672	-.00114
60.00	.00690	-.00119

14E 1-7-69 COMPN. CREEP
CONFP=1.0000 DEVP=4.7000
HIGHT=2.8125DIAMR=1.3125

TIME	AXL.STRN	RDL.STRN
.02	.00281	-.00028
.04	.00316	-.00030
.06	.00320	-.00032
.10	.00324	-.00033
.40	.00334	-.00035
1.00	.00356	-.00038
2.00	.00359	-.00039
4.00	.00370	-.00040
6.00	.00377	-.00041
10.00	.00377	-.00042
20.00	.00380	-.00045
40.00	.00380	-.00046
60.00	.00388	-.00048

13E 12-26-68 COMP. CREEP
CONFP=1.0000 DEVP=5.6200
HIGHT=2.8125DIAMR=1.3125

TIME	AXL.STRN	RDL.STRN
.02	.00565	-.00059
.04	.00572	-.00060
.06	.00583	-.00062
.10	.00601	-.00064
.40	.00615	-.00066
1.00	.00640	-.00068
2.00	.00644	-.00069
4.00	.00651	-.00071
6.00	.00661	-.00072
10.00	.00668	-.00074
20.00	.00683	-.00076
40.00	.00700	-.00079
60.00	.00711	-.00081

14E 1-5-69 COMPN. CREEP
CONFP=1.0000 DEVP=2.8600
HIGHT=2.8125DIAMR=1.3125

TIME	AXL.STRN	RDL.STRN
.02	.00249	-.00010
.04	.00260	-.00011
.06	.00263	-.00012
.10	.00277	-.00012
.40	.00284	-.00013
1.00	.00288	-.00013
2.00	.00295	-.00013
4.00	.00302	-.00014
6.00	.00306	-.00014
10.00	.00306	-.00015
20.00	.00306	-.00016
40.00	.00331	-.00016
60.00	.00334	-.00017

14E 1-7-69 COMPN. CREEP
CONFP=1.0000 DEVP=5.6200
HIGHT=2.8125DIAMR=1.3125

TIME	AXL.STRN	RDL.STRN
.02	.00434	-.00055
.04	.00441	-.00057
.06	.00448	-.00059
.10	.00452	-.00061
.40	.00462	-.00064
1.00	.00476	-.00065
2.00	.00480	-.00067
4.00	.00491	-.00068
6.00	.00498	-.00068
10.00	.00505	-.00071
20.00	.00516	-.00073
40.00	.00530	-.00077
60.00	.00537	-.00078

1. Kneading Compaction - 60 lbs. Tampa - Kaolinite, cont.

8E A-15-6A COMPN. CREEP
CONFP=1.0000 DEVP=2.7800
HIGHT=2.8125DIAMR=1.3125

TIME	AXL.STRN	RDL.STRN
.02	.00142	-.00005
.04	.00144	-.00005
.06	.00146	-.00005
.10	.00149	-.00005
.40	.00160	-.00005
1.00	.00167	-.00006
2.00	.00178	-.00005
4.00	.00181	-.00006
8.00	.00185	-.00006
10.00	.00196	-.00006
20.00	.00203	-.00007
40.00	.00204	-.00007
60.00	.00204	-.00007

7E A-18-6A COMPN. CREEP
CONFP=1.0000 DEVP=2.7700
HIGHT=2.8125DIAMR=1.3125

TIME	AXL.STRN	RDL.STRN
.02	.00111	-.00005
.04	.00124	-.00005
.06	.00126	-.00005
.10	.00132	-.00006
.40	.00136	-.00006
1.00	.00140	-.00006
2.00	.00141	-.00006
4.00	.00142	-.00006
8.00	.00144	-.00006
10.00	.00146	-.00006
20.00	.00149	-.00006
40.00	.00151	-.00006
60.00	.00155	-.00006

10E A-26-6A COMPN. CREEP
CONFP=2.0000 DEVP=3.6500
HIGHT=2.8125DIAMR=1.3125

TIME	AXL.STRN	RDL.STRN
.02	.00231	-.00011
.04	.00249	-.00013
.06	.00252	-.00013
.10	.00260	-.00013
.40	.00281	-.00015
1.00	.00294	-.00016
2.00	.00295	-.00017
4.00	.00302	-.00017
8.00	.00313	-.00018
10.00	.00316	-.00019
20.00	.00320	-.00019
40.00	.00327	-.00020
60.00	.00338	-.00021

8E A-15-6A COMPN. CREEP
CONFP=1.0000 DEVP=2.1000
HIGHT=2.8125DIAMR=1.3125

TIME	AXL.STRN	RDL.STRN
.02	.00110	-.00004
.04	.00114	-.00004
.06	.00116	-.00004
.10	.00117	-.00004
.40	.00121	-.00004
1.00	.00124	-.00004
2.00	.00142	-.00004
4.00	.00143	-.00005
8.00	.00144	-.00005
10.00	.00145	-.00005
20.00	.00149	-.00005
40.00	.00149	-.00005
60.00	.00150	-.00006

7E A-19-6B COMPN. CREEP
CONFP=1.0000 DEVP=2.9100
HIGHT=2.8125DIAMR=1.3125

TIME	AXL.STRN	RDL.STRN
.04	.00180	-.00010
.06	.00185	-.00010
.10	.00187	-.00010
.40	.00192	-.00010
1.00	.00199	-.00010
2.00	.00201	-.00010
4.00	.00203	-.00012
8.00	.00204	-.00012
10.00	.00208	-.00012
20.00	.00213	-.00013
40.00	.00218	-.00013
60.00	.00221	-.00013

10E A-25-6A COMPN. CREEP
CONFP=2.0000 DEVP=1.3000
HIGHT=2.8125DIAMR=1.3125

TIME	AXL.STRN	RDL.STRN
.04	.00052	-.00003
.06	.00053	-.00003
.10	.00053	-.00003
.40	.00055	-.00003
1.00	.00055	-.00003
2.00	.00059	-.00003
4.00	.00060	-.00003
8.00	.00061	-.00003
10.00	.00062	-.00003
20.00	.00062	-.00003
40.00	.00066	-.00003
60.00	.00067	-.00003

7E A-18-6A COMPN. CREEP
CONFP=1.0000 DEVP=1.5300
HIGHT=2.8125DIAMR=1.3125

TIME	AXL.STRN	RDL.STRN
.02	.00062	-.00002
.04	.00066	-.00002
.06	.00068	-.00002
.10	.00071	-.00003
.40	.00076	-.00003
1.00	.00080	-.00003
2.00	.00081	-.00003
4.00	.00082	-.00003
8.00	.00084	-.00003
10.00	.00085	-.00003
20.00	.00087	-.00003
40.00	.00089	-.00003
60.00	.00090	-.00003

7E A-19-6B COMPN. CREEP
CONFP=1.0000 DEVP=3.3600
HIGHT=2.8125DIAMR=1.3125

TIME	AXL.STRN	RDL.STRN
.02	.00204	-.00010
.04	.00213	-.00010
.06	.00217	-.00011
.10	.00226	-.00012
.40	.00235	-.00013
1.00	.00244	-.00013
2.00	.00247	-.00014
4.00	.00252	-.00015
8.00	.00258	-.00016
10.00	.00261	-.00016
20.00	.00267	-.00016
40.00	.00268	-.00017
60.00	.00274	-.00018

10E A-26-6A COMPN. CREEP
CONFP=2.0000 DEVP=2.5100
HIGHT=2.8125DIAMR=1.3125

TIME	AXL.STRN	RDL.STRN
.04	.00128	-.00007
.06	.00130	-.00007
.10	.00132	-.00008
.40	.00139	-.00008
1.00	.00142	-.00009
2.00	.00149	-.00010
4.00	.00151	-.00010
8.00	.00153	-.00010
10.00	.00155	-.00010
20.00	.00160	-.00010
40.00	.00167	-.00010
60.00	.00169	-.00010

1. Kneading Compaction - 60 lbs Tamps - Kaolinite, cont.

3J 1-20-70 COMPN. CREEP
CONFP=1.0000 DEVP=1.0300
HIGHT=2.8125DIAMR=1.3125

TIME	AXL.STRN	RDL.STRN
.02	.00057	-.00004
.04	.00059	-.00004
.06	.00060	-.00004
.10	.00061	-.00004
.40	.00062	-.00004
1.00	.00063	-.00004
2.00	.00065	-.00004
4.00	.00068	-.00004
6.00	.00069	-.00004
10.00	.00071	-.00004
20.00	.00072	-.00004
40.00	.00075	-.00004
60.00	.00076	-.00004

3J 1-21-70 COMPN. CREEP
CONFP=1.0000 DEVP=3.7900
HIGHT=2.8125DIAMR=1.3125

TIME	AXL.STRN	RDL.STRN
.02	.00345	-.00048
.04	.00377	-.00050
.06	.00388	-.00051
.10	.00395	-.00054
.40	.00423	-.00058
1.00	.00430	-.00061
2.00	.00452	-.00064
4.00	.00459	-.00067
6.00	.00462	-.00068
10.00	.00473	-.00071
20.00	.00491	-.00074
40.00	.00501	-.00079
60.00	.00508	-.00082

2J 1-15-70 COMPN. CREEP
CONFP=1.0000 DEVP=3.3300
HIGHT=2.8125DIAMR=1.3125

TIME	AXL.STRN	RDL.STRN
.02	.00395	-.00050
.04	.00416	-.00055
.06	.00420	-.00055
.10	.00427	-.00056
.40	.00444	-.00060
1.00	.00462	-.00064
2.00	.00466	-.00065
4.00	.00469	-.00067
6.00	.00480	-.00070
10.00	.00491	-.00072
20.00	.00498	-.00073
40.00	.00505	-.00076
60.00	.00516	-.00080

3J 1-20-70 COMPN. CREEP
CONFP=1.0000 DEVP=1.9500
HIGHT=2.8125DIAMR=1.3125

TIME	AXL.STRN	RDL.STRN
.02	.00124	-.00006
.04	.00125	-.00006
.06	.00131	-.00006
.10	.00134	-.00007
.40	.00142	-.00007
1.00	.00148	-.00009
2.00	.00151	-.00010
4.00	.00156	-.00010
6.00	.00160	-.00010
10.00	.00163	-.00010
20.00	.00168	-.00011
40.00	.00178	-.00012
60.00	.00180	-.00013

3J 1-21-70 COMPN. CREEP
CONFP=1.0000 DEVP=4.7900
HIGHT=2.8125DIAMR=1.3125

TIME	AXL.STRN	RDL.STRN
.02	.00565	-.00117
.04	.00594	-.00128
.06	.00604	-.00134
.10	.00629	-.00139
.40	.00672	-.00153
1.00	.00697	-.00163
2.00	.00718	-.00170
4.00	.00743	-.00182
6.00	.00750	-.00186
10.00	.00779	-.00193
20.00	.00804	-.00207
40.00	.00832	-.00217
60.00	.00853	-.00226

2J 1-15-70 COMPN. CREEP
CONFP=0.0000 DEVP=2.2900
HIGHT=2.8125DIAMR=1.3125

TIME	AXL.STRN	RDL.STRN
.02	.00244	-.00021
.04	.00254	-.00022
.06	.00258	-.00023
.10	.00268	-.00024
.40	.00279	-.00026
1.00	.00285	-.00026
2.00	.00293	-.00027
4.00	.00295	-.00028
6.00	.00300	-.00029
10.00	.00303	-.00029
20.00	.00310	-.00031
40.00	.00318	-.00032
60.00	.00321	-.00032

3J 1-20-70 COMPN. CREEP
CONFP=1.0000 DEVP=2.8600
HIGHT=2.8125DIAMR=1.3125

TIME	AXL.STRN	RDL.STRN
.02	.00212	-.00019
.04	.00220	-.00020
.06	.00225	-.00021
.10	.00233	-.00022
.40	.00247	-.00023
1.00	.00258	-.00025
2.00	.00267	-.00026
4.00	.00271	-.00027
6.00	.00276	-.00027
10.00	.00281	-.00029
20.00	.00287	-.00029
40.00	.00296	-.00032
60.00	.00302	-.00032

2J 1-15-70 COMPN. CREEP
CONFP=0.0000 DEVP=4.2400
HIGHT=2.8125DIAMR=1.3125

TIME	AXL.STRN	RDL.STRN
.02	.00604	-.00102
.04	.00629	-.00105
.06	.00640	-.00109
.10	.00644	-.00113
.40	.00676	-.00119
1.00	.00693	-.00121
2.00	.00711	-.00125
4.00	.00715	-.00129
6.00	.00722	-.00133
10.00	.00747	-.00134
20.00	.00750	-.00141
40.00	.00772	-.00143
60.00	.00782	-.00149

2J 1-15-70 COMPN. CREEP
CONFP=0.0000 DEVP=1.4900
HIGHT=2.8125DIAMR=1.3125

TIME	AXL.STRN	RDL.STRN
.02	.00133	-.00012
.04	.00140	-.00013
.06	.00144	-.00013
.10	.00149	-.00013
.40	.00158	-.00015
1.00	.00164	-.00015
2.00	.00168	-.00015
4.00	.00170	-.00015
6.00	.00171	-.00016
10.00	.00175	-.00016
20.00	.00178	-.00016
40.00	.00185	-.00017
60.00	.00188	-.00017

1. Kneading Compaction - 60 lbs. Tamps - Kaolinite, cont.

2J 1-15-70 COMPN. CREEP
CONFP=0.0000 DEVP=4.6900
HIGHT=2.8125DIAMR=1.3125

TIME	AXL.STRN	RDL.STRN
.02	.00490	-.00135
.04	.00736	-.00138
.06	.00743	-.00143
.10	.00754	-.00145
.40	.00789	-.00153
1.00	.00818	-.00158
2.00	.00828	-.00161
4.00	.00850	-.00165
6.00	.00857	-.00168
10.00	.00871	-.00170
20.00	.00889	-.00174
40.00	.00921	-.00181
60.00	.00928	-.00185

BJ 1-12-70 COMPN. CREEP
CONFP=0.0000 DEVP=1.5300
HIGHT=2.8125DIAMR=1.3125

TIME	AXL.STRN	RDL.STRN
.02	.00130	-.00013
.04	.00133	-.00013
.06	.00136	-.00013
.10	.00141	-.00013
.40	.00148	-.00014
1.00	.00152	-.00014
2.00	.00153	-.00014
4.00	.00156	-.00015
6.00	.00158	-.00015
10.00	.00160	-.00015
20.00	.00165	-.00016
40.00	.00169	-.00016
60.00	.00171	-.00016

BJ 1-12-70 COMPN. CREEP
CONFP=0.0000 DEVP=2.8600
HIGHT=2.8125DIAMR=1.3125

TIME	AXL.STRN	RDL.STRN
.02	.00284	-.00040
.04	.00302	-.00041
.06	.00309	-.00043
.10	.00320	-.00045
.40	.00327	-.00048
1.00	.00341	-.00050
2.00	.00348	-.00051
4.00	.00356	-.00052
6.00	.00359	-.00054
10.00	.00363	-.00055
20.00	.00370	-.00056
40.00	.00380	-.00058
60.00	.00388	-.00060

BJ 1-12-70 COMPN. CREEP
CONFP=0.0000 DEVP=4.2400
HIGHT=2.8125DIAMR=1.3125

TIME	AXL.STRN	RDL.STRN
.02	.00604	-.00125
.04	.00619	-.00132
.06	.00636	-.00135
.10	.00644	-.00138
.40	.00668	-.00145
1.00	.00690	-.00151
2.00	.00711	-.00153
4.00	.00718	-.00159
6.00	.00735	-.00162
10.00	.00747	-.00169
20.00	.00757	-.00174
40.00	.00782	-.00181
60.00	.00793	-.00185

2J 1-15-70 RECOVERY
CONFP=0.0000 DEVP=1.4400
HIGHT=2.8125DIAMR=1.3125

TIME	AXL.STRN	RDL.STRN
1.00	.00052	-.00007
2.00	.00042	-.00007
4.00	.00039	-.00006
6.00	.00032	-.00006
8.00	.00028	-.00005
10.00	.00027	-.00005
20.00	.00023	-.00005
30.00	.00019	-.00004

2J 1-15-70 RECOVERY
CONFP=0.0000 DEVP=2.2400
HIGHT=2.8125DIAMR=1.3125

TIME	AXL.STRN	RDL.STRN
1.00	.00082	-.00013
2.00	.00071	-.00012
4.00	.00060	-.00010
6.00	.00055	-.00010
8.00	.00052	-.00009
10.00	.00051	-.00009
20.00	.00045	-.00007
30.00	.00038	-.00007

2J 1-15-70 RECOVERY
CONFP=0.0000 DEVP=3.3300
HIGHT=2.8125DIAMR=1.3125

TIME	AXL.STRN	RDL.STRN
1.00	.00114	-.00031
2.00	.00103	-.00027
4.00	.00078	-.00023
6.00	.00075	-.00023
8.00	.00071	-.00022
10.00	.00071	-.00020
20.00	.00057	-.00018
30.00	.00043	-.00015

2J 1-16-70 RECOVERY
CONFP=0.0000 DEVP=4.2400
HIGHT=2.8125DIAMR=1.3125

TIME	AXL.STRN	RDL.STRN
1.00	.00210	-.00051
2.00	.00178	-.00045
4.00	.00149	-.00043
6.00	.00142	-.00039
8.00	.00139	-.00037
10.00	.00135	-.00036
20.00	.00117	-.00033
30.00	.00110	-.00031

2J 1-16-70 RECOVERY
CONFP=0.0000 DEVP=4.6900
HIGHT=2.8125DIAMR=1.3125

TIME	AXL.STRN	RDL.STRN
1.00	.00245	-.00049
2.00	.00204	-.00046
4.00	.00178	-.00040
6.00	.00171	-.00038
8.00	.00153	-.00035
10.00	.00142	-.00032
20.00	.00139	-.00031
30.00	.00135	-.00027

BJ 1-12-70 RECOVERY
CONFP=0.0000 DEVP=1.5300
HIGHT=2.8125DIAMR=1.3125

TIME	AXL.STRN	RDL.STRN
1.00	.00034	-.00001
2.00	.00027	-.00000
4.00	.00021	0.00000
6.00	.00018	0.00000
8.00	.00017	0.00000
10.00	.00017	0.00000
20.00	.00014	0.00000
30.00	.00001	0.00000

BJ 1-12-70 RECOVERY
CONFP=0.0000 DEVP=4.2400
HIGHT=2.8125DIAMR=1.3125

TIME	AXL.STRN	RDL.STRN
1.00	.00220	-.00056
2.00	.00206	-.00048
4.00	.00181	-.00042
6.00	.00178	-.00040
8.00	.00171	-.00039
10.00	.00160	-.00035
20.00	.00146	-.00031
30.00	.00142	-.00029

1. Kneading Compaction - 60 lbs. Tamps - Kaolinite, cont.

3J 1-20-70 RECOVERY
CONFP=1.0000 DEVP=2.8600
HIGHT=2.8125DIAMR=1.3125

TIME	AXL.STRN	RDL.STRN
1.00	.00071	-.00009
2.00	.00060	-.00007
4.00	.00052	-.00006
6.00	.00049	-.00005
8.00	.00045	-.00005
10.00	.00044	-.00004
20.00	.00036	-.00004
30.00	.00035	-.00003

[illegible]

[illegible]

[illegible]

2. Impact Compaction - 45 Blown - Kaolinite

6D 7-18-68 COMPN. CREEP
CONFP=0.0000 DEVP= .9170
HIGHT=2.8125DIAM=1.3125

TIME	AXL.STRN	RUL.STRN
.02	.00107	-.00016
.04	.00108	-.00002
.06	.00110	-.00002
.10	.00112	-.00002
.40	.00116	-.00002
1.00	.00117	-.00002
2.00	.00119	-.00002
4.00	.00124	-.00003
6.00	.00125	-.00003
10.00	.00126	-.00003
20.00	.00130	-.00003
40.00	.00133	-.00003
60.00	.00134	-.00003

6D 7-19-68 COMPN. CREEP
CONFP=0.0000 DEVP=3.6700
HIGHT=2.8125DIAM=1.3125

TIME	AXL.STRN	RUL.STRN
.02	.00249	-.00039
.04	.00267	-.00045
.06	.00274	-.00046
.10	.00284	-.00048
.40	.00295	-.00051
1.00	.00313	-.00054
2.00	.00320	-.00055
4.00	.00324	-.00057
6.00	.00325	-.00058
10.00	.00327	-.00059
20.00	.00329	-.00061
40.00	.00341	-.00061
60.00	.00348	-.00062

14D 7-27-68 COMPN. CREEP
CONFP=1.0700 DEVP=1.4100
HIGHT=2.8125DIAM=1.3125

TIME	AXL.STRN	RUL.STRN
.02	.00153	-.00027
.04	.00164	-.00027
.06	.00166	-.00027
.10	.00171	-.00027
.40	.00177	-.00027
1.00	.00173	-.00027
2.00	.00175	-.00027
4.00	.00178	-.00027
6.00	.00178	-.00027
10.00	.00182	-.00027
20.00	.00185	-.00028
40.00	.00185	-.00028
60.00	.00189	-.00028

6D 7-18-68 COMPN. CREEP
CONFP=0.0000 DEVP=1.8300
HIGHT=2.8125DIAM=1.3125

TIME	AXL.STRN	RUL.STRN
.02	.00185	-.00010
.04	.00188	-.00010
.06	.00192	-.00010
.10	.00196	-.00010
.40	.00203	-.00011
1.00	.00206	-.00012
2.00	.00208	-.00012
4.00	.00212	-.00013
6.00	.00212	-.00013
10.00	.00215	-.00013
20.00	.00228	-.00013
40.00	.00229	-.00014
60.00	.00235	-.00015

12D 7-20-68 COMPN. CREEP
CONFP=0.0000 DEVP=1.8350
HIGHT=2.8125DIAM=1.3125

TIME	AXL.STRN	RUL.STRN
.02	.00089	-.00014
.04	.00160	-.00020
.06	.00178	-.00022
.10	.00185	-.00022
.40	.00213	-.00023
1.00	.00217	-.00023
2.00	.00220	-.00024
4.00	.00222	-.00025
6.00	.00228	-.00025
10.00	.00231	-.00026
20.00	.00238	-.00026
40.00	.00242	-.00026
60.00	.00249	-.00273

14D 7-27-68 COMPN. CREEP
CONFP=1.0700 DEVP=1.4300
HIGHT=2.8125DIAM=1.3125

TIME	AXL.STRN	RUL.STRN
.02	.00100	-.00015
.04	.00107	-.00016
.06	.00110	-.00016
.10	.00114	-.00017
.40	.00132	-.00017
1.00	.00135	-.00018
2.00	.00139	-.00018
4.00	.00140	-.00019
6.00	.00140	-.00019
10.00	.00142	-.00019
20.00	.00142	-.00019
40.00	.00144	-.00019
60.00	.00146	-.00019

6D 7-18-68 COMPN. CREEP
CONFP=0.0000 DEVP=2.7500
HIGHT=2.8125DIAM=1.3125

TIME	AXL.STRN	RUL.STRN
.02	.00231	-.00024
.04	.00245	-.00025
.06	.00247	-.00026
.10	.00249	-.00026
.40	.00258	-.00028
1.00	.00265	-.00029
2.00	.00267	-.00030
4.00	.00268	-.00032
6.00	.00274	-.00032
10.00	.00280	-.00032
20.00	.00292	-.00034
40.00	.00299	-.00035
60.00	.00302	-.00037

12D 7-20-68 COMPN. CREEP
CONFP=0.0000 DEVP=2.7500
HIGHT=2.8125DIAM=1.3125

TIME	AXL.STRN	RUL.STRN
.02	.00160	-.00019
.04	.00249	-.00032
.06	.00277	-.00034
.10	.00284	-.00035
.40	.00313	-.00039
1.00	.00320	-.00041
2.00	.00324	-.00042
4.00	.00327	-.00043
6.00	.00329	-.00045
10.00	.00330	-.00045
20.00	.00338	-.00046
40.00	.00345	-.00046
60.00	.00345	-.00048

14D 7-27-68 COMPN. CREEP
CONFP=1.0700 DEVP=2.8500
HIGHT=2.8125DIAM=1.3125

TIME	AXL.STRN	RUL.STRN
.02	.00114	-.00013
.04	.00132	-.00014
.06	.00139	-.00015
.10	.00139	-.00015
.40	.00142	-.00015
1.00	.00153	-.00016
2.00	.00174	-.00019
4.00	.00178	-.00019
6.00	.00178	-.00019
10.00	.00181	-.00020
20.00	.00181	-.00021
40.00	.00185	-.00022
60.00	.00185	-.00023

2. Impact Compaction - 45 Blows - Kaolinite, cont.

14D 7-28-68 COMPN. CREEP
CONFP=1.0000 DEVP=4.9800
HIGHT=2.8125DIAMR=1.3125

TIME	AXL.STRN	RDL.STRN
.02	.00124	-.00008
.04	.00231	-.00013
.06	.00267	-.00014
.10	.00294	-.00014
.40	.00420	-.00017
1.00	.00334	-.00019
2.00	.00348	-.00019
4.00	.00356	-.00019
6.00	.00356	-.00019
10.00	.00359	-.00021
20.00	.00377	-.00021
40.00	.00388	-.00023
60.00	.00391	-.00023

16D 8-3-68 COMPN. CREEP
CONFP=1.0000 DEVP=4.8100
HIGHT=2.8125DIAMR=1.3125

TIME	AXL.STRN	RDL.STRN
.02	.00281	-.00012
.04	.00292	-.00014
.06	.00302	-.00014
.10	.00309	-.00014
.40	.00320	-.00016
1.00	.00327	-.00016
2.00	.00338	-.00018
4.00	.00348	-.00018
6.00	.00352	-.00018
10.00	.00356	-.00019
20.00	.00363	-.00021
40.00	.00373	-.00023
60.00	.00380	-.00023

3G 5-1-69 COMPN. CREEP
CONFP=1.0000 DEVP=1.0300
HIGHT=2.8125DIAMR=1.3125

TIME	AXL.STRN	RDL.STRN
.02	.00026	-.00003
.04	.00027	-.00003
.06	.00028	-.00003
.10	.00028	-.00003
.40	.00032	-.00003
1.00	.00036	-.00003
2.00	.00037	-.00003
4.00	.00037	-.00003
6.00	.00038	-.00003
10.00	.00040	-.00003
20.00	.00043	-.00003
40.00	.00044	-.00003
60.00	.00048	-.00003

16D 8-3-68 COMPN. CREEP
CONFP=1.0000 DEVP=2.9800
HIGHT=2.8125DIAMR=1.3125

TIME	AXL.STRN	RDL.STRN
.02	.00128	-.00008
.04	.00139	-.00009
.06	.00142	-.00010
.10	.00153	-.00010
.40	.00160	-.00011
1.00	.00171	-.00012
2.00	.00174	-.00012
4.00	.00176	-.00012
6.00	.00176	-.00013
10.00	.00178	-.00014
20.00	.00181	-.00014
40.00	.00185	-.00016
60.00	.00187	-.00016

12G 3-4-69 COMPN. CREEP
CONFP=1.0000 DEVP=1.0300
HIGHT=2.8125DIAMR=1.3125

TIME	AXL.STRN	RDL.STRN
.02	.00031	-.00003
.04	.00036	-.00003
.06	.00036	-.00003
.10	.00038	-.00004
.40	.00041	-.00004
1.00	.00044	-.00004
2.00	.00045	-.00004
4.00	.00046	-.00004
6.00	.00047	-.00004
10.00	.00048	-.00004
20.00	.00049	-.00005
40.00	.00052	-.00005
60.00	.00055	-.00005

3G 5-1-69 COMPN. CREEP
CONFP=1.0000 DEVP=1.9500
HIGHT=2.8125DIAMR=1.3125

TIME	AXL.STRN	RDL.STRN
.02	.00065	-.00010
.04	.00068	-.00010
.06	.00071	-.00010
.10	.00072	-.00010
.40	.00080	-.00012
1.00	.00081	-.00013
2.00	.00084	-.00013
4.00	.00088	-.00013
6.00	.00089	-.00013
10.00	.00090	-.00014
20.00	.00091	-.00014
40.00	.00097	-.00015
60.00	.00099	-.00015

16D 8-3-68 COMPN. CREEP
CONFP=1.0000 DEVP=3.8900
HIGHT=2.8125DIAMR=1.3125

TIME	AXL.STRN	RDL.STRN
.02	.00196	-.00008
.04	.00206	-.00008
.06	.00210	-.00008
.10	.00220	-.00008
.40	.00231	-.00010
1.00	.00242	-.00010
2.00	.00245	-.00010
4.00	.00245	-.00011
6.00	.00249	-.00012
10.00	.00249	-.00012
20.00	.00262	-.00014
40.00	.00267	-.00014
60.00	.00274	-.00014

9G 3-21-69 COMPN. CREEP
CONFP=1.0000 DEVP=1.0300
HIGHT=2.8125DIAMR=1.3125

TIME	AXL.STRN	RDL.STRN
.02	.00019	-.00004
.04	.00025	-.00004
.06	.00027	-.00004
.10	.00029	-.00004
.40	.00033	-.00004
1.00	.00036	-.00005
2.00	.00037	-.00005
4.00	.00038	-.00005
6.00	.00040	-.00005
10.00	.00044	-.00005
20.00	.00044	-.00005
40.00	.00046	-.00005
60.00	.00050	-.00005

3G 5-1-69 COMPN. CREEP
CONFP=1.0000 DEVP=2.8600
HIGHT=2.8125DIAMR=1.3125

TIME	AXL.STRN	RDL.STRN
.02	.00107	-.00021
.04	.00112	-.00022
.06	.00116	-.00023
.10	.00119	-.00023
.40	.00131	-.00026
1.00	.00140	-.00028
2.00	.00144	-.00029
4.00	.00150	-.00031
6.00	.00153	-.00032
10.00	.00160	-.00033
20.00	.00165	-.00034
40.00	.00172	-.00036
60.00	.00176	-.00038

2. Impact Compaction - 45 Blows - Kaolinite, cont.

30 5-1-69 COMPN. CREEP
CONFP=1.0000 DEVP=4.7000
HIGHT=2.8125DIAMR=1.3125

TIME	AXL.STRN	RDL.STRN
.02	.00295	-.00080
.04	.00309	-.00084
.06	.00320	-.00086
.10	.00324	-.00087
.40	.00348	-.00093
1.00	.00359	-.00096
2.00	.00363	-.00100
4.00	.00377	-.00103
6.00	.00384	-.00105
10.00	.00391	-.00109
20.00	.00395	-.00113
40.00	.00405	-.00117
60.00	.00427	-.00121

14G 5-11-69 COMPN. CREEP
CONFP=1.0000 DEVP=1.9500
HIGHT=2.8125DIAMR=1.3125

TIME	AXL.STRN	RDL.STRN
.02	.00144	-.00009
.04	.00152	-.00009
.06	.00156	-.00010
.10	.00160	-.00010
.40	.00168	-.00010
1.00	.00171	-.00010
2.00	.00177	-.00011
4.00	.00179	-.00011
6.00	.00182	-.00011
10.00	.00184	-.00012
20.00	.00184	-.00012
40.00	.00187	-.00013
60.00	.00195	-.00013

8H 10-28-69 [illegible]
CONFP=1.0000 DEVP=3.0100
HIGHT=2.8125DIAMR=1.3125

TIME	AXL.STRN	RDL.STRN
.02	-.33[illegible]	.0[illegible]
.04	-.33[illegible]	.0[illegible]
.06	-.33[illegible]	.0[illegible]
.10	-.33[illegible]	.0[illegible]
.40	-.33[illegible]	.0[illegible]
1.00	-.33[illegible]	.0[illegible]
2.00	-.33[illegible]	.0[illegible]
4.00	-.33[illegible]	.0[illegible]
6.00	-.33[illegible]	.0[illegible]
10.00	-.33[illegible]	.0[illegible]
20.00	-.33[illegible]	.0[illegible]
40.00	-.33[illegible]	.0[illegible]
60.00	-.33[illegible]	.0[illegible]

30 5-1-69 COMPN. CREEP
CONFP=1.0000 DEVP=4.5300
HIGHT=2.8125DIAMR=1.3125

TIME	AXL.STRN	RDL.STRN
.02	.00651	-.00009
.04	.00683	-.00010
.06	.00700	-.00010
.10	.00715	-.00010
.40	.00750	-.00010
1.00	.00782	-.00010
2.00	.00796	-.00010
4.00	.00814	-.00010
6.00	.00818	-.00010
10.00	.00836	-.00010
20.00	.00853	-.00011
40.00	.00878	-.00011
60.00	.00892	-.00011

14G 5-11-69 COMPN. CREEP
CONFP=1.0000 DEVP=4.7000
HIGHT=2.8125DIAMR=1.3125

TIME	AXL.STRN	RDL.STRN
.02	.00459	-.00081
.04	.00491	-.00087
.06	.00498	-.00089
.10	.00505	-.00091
.40	.00512	-.00094
1.00	.00533	-.00097
2.00	.00537	-.00099
4.00	.00544	-.00100
6.00	.00548	-.00101
10.00	.00558	-.00103
20.00	.00565	-.00105
40.00	.00569	-.00106
60.00	.00572	-.00108

8H 10-28-69 [illegible]
CONFP=1.0000 DEVP=3.0100
HIGHT=2.8125DIAMR=1.3125

TIME	AXL.STRN	RDL.STRN
.02	-.33[illegible]	.0[illegible]
.04	-.33[illegible]	.0[illegible]
.06	-.33[illegible]	.0[illegible]
.10	-.33[illegible]	.0[illegible]
.40	-.33[illegible]	.0[illegible]
1.00	-.33[illegible]	.0[illegible]
2.00	-.33[illegible]	.0[illegible]
4.00	-.33[illegible]	.0[illegible]
6.00	-.33[illegible]	.0[illegible]
10.00	-.33[illegible]	.0[illegible]
20.00	-.33[illegible]	.0[illegible]
40.00	-.33[illegible]	.0[illegible]
60.00	-.33[illegible]	.0[illegible]

14G 5-11-69 COMPN. CREEP
CONFP=1.0000 DEVP=1.0300
HIGHT=2.8125DIAMR=1.3125

TIME	AXL.STRN	RDL.STRN
.02	.00089	-.00002
.04	.00092	-.00002
.06	.00095	-.00002
.10	.00099	-.00002
.40	.00106	-.00002
1.00	.00108	-.00002
2.00	.00111	-.00002
4.00	.00115	-.00002
6.00	.00116	-.00003
10.00	.00117	-.00003
20.00	.00122	-.00003
40.00	.00126	-.00003
60.00	.00131	-.00003

14G 5-11-69 COMPN. CREEP
CONFP=1.0000 DEVP=4.5300
HIGHT=2.8125DIAMR=1.3125

TIME	AXL.STRN	RDL.STRN
.02	.00907	-.00254
.04	.00924	-.00267
.06	.00946	-.00283
.10	.00964	-.00289
.40	.00992	-.00302
1.00	.01031	-.00322
2.00	.01052	-.00325
4.00	.01070	-.00338
6.00	.01088	-.00344
10.00	.01106	-.00351
20.00	.01134	-.00354
40.00	.01141	-.00367
60.00	.01170	-.00373

8H 10-28-69 [illegible]
CONFP=1.0000 DEVP=4.5300
HIGHT=2.8125DIAMR=1.3125

TIME	AXL.STRN	RDL.STRN
.02	-.33[illegible]	.0[illegible]
.04	-.33[illegible]	.0[illegible]
.06	-.33[illegible]	.0[illegible]
.10	-.33[illegible]	.0[illegible]
.40	-.33[illegible]	.0[illegible]
1.00	-.33[illegible]	.0[illegible]
2.00	-.33[illegible]	.0[illegible]
4.00	-.33[illegible]	.0[illegible]
6.00	-.33[illegible]	.0[illegible]
10.00	-.33[illegible]	.0[illegible]
20.00	-.33[illegible]	.0[illegible]
40.00	-.33[illegible]	.0[illegible]
60.00	-.33[illegible]	.0[illegible]

2. Impact Compaction - 45 Blows - Kaolinite, cont.

[illegible] 10-28-69 EXTR. CREEP
CONFP=1.0000 DEVP=4.5000
HIGHT=2.8125DIAMR=1.3125

TIME	AXL.STRN	RDL.STRN
.10	-.33418	.03119
.20	-.33389	.03141
.40	-.33365	.03170
.60	-.33347	.03191
1.00	-.33323	.03213
2.00	-.33303	.03239
4.00	-.33286	.03264
6.00	-.33276	.03285
10.00	-.33261	.03301
20.00	-.33237	.03347
30.00	-.33227	.03378
40.00	-.33220	.03401
60.00	-.33205	.03440

[illegible] 10-29-69 EXTR. CREEP
CONFP=1.0000 DEVP=4.5000
HIGHT=2.8125DIAMR=1.3125

TIME	AXL.STRN	RDL.STRN
.10	-.33387	.02981
.20	-.33355	.03004
.40	-.33344	.03026
.60	-.33356	.03047
1.00	-.33364	.03061
2.00	-.33367	.03080
4.00	-.33371	.03107
6.00	-.33374	.03119
10.00	-.33385	.03133
20.00	-.33394	.03159
30.00	-.33394	.03175
40.00	-.33403	.03188
60.00	-.33412	.03210

4H 11-10-69 COMPN. CREEP
CONFP=1.0000 DEVP=7.4500
HIGHT=2.8125DIAMR=1.3125

TIME	AXL.STRN	RDL.STRN
.02	.00825	-.00132
.04	.00843	-.00135
.06	.00868	-.00142
.10	.00889	-.00148
.40	.00921	-.00161
1.00	.00949	-.00164
2.00	.00964	-.00167
4.00	.00985	-.00180
6.00	.00996	-.00187
10.00	.01006	-.00193
20.00	.01031	-.00196
40.00	.01056	-.00199
60.00	.01067	-.00203

[illegible] 10-28-69 EXTR. CREEP
CONFP=1.0000 DEVP=4.5000
HIGHT=2.8125DIAMR=1.3125

TIME	AXL.STRN	RDL.STRN
.10	-.33416	.03154
.20	-.33392	.03163
.40	-.33373	.03186
.60	-.33387	.03197
1.00	-.33412	.03184
2.00	-.33433	.03198
4.00	-.33462	.03208
6.00	-.33487	.03219
10.00	-.33613	.03222
20.00	-.33665	.03243
30.00	-.33693	.03244
40.00	-.33711	.03254
50.00	-.33737	.03260
60.00	-.33746	.03267

[illegible] 10-29-69 EXTR. CREEP
CONFP=1.0000 DEVP=4.5000
HIGHT=2.8125DIAMR=1.3125

TIME	AXL.STRN	RDL.STRN
.10	-.33382	.02980
.20	-.33362	.02963
.40	-.33356	.03020
.60	-.33360	.03073
1.00	-.33364	.03042
2.00	-.33367	.03092
4.00	-.33378	.03096
6.00	-.33385	.03096
10.00	-.33394	.03038
20.00	-.33403	.03086
30.00	-.33414	.03089
40.00	-.33423	.03086
50.00	-.33428	.03084
60.00	-.33433	.03086

4H 11-10-69 COMPN. CREEP
CONFP=1.0000 DEVP=6.0700
HIGHT=2.8125DIAMR=1.3125

TIME	AXL.STRN	RDL.STRN
.02	.00594	-.00077
.04	.00626	-.00081
.06	.00640	-.00084
.10	.00651	-.00086
.40	.00686	-.00093
1.00	.00708	-.00096
2.00	.00715	-.00103
4.00	.00736	-.00106
6.00	.00747	-.00106
10.00	.00750	-.00109
20.00	.00772	-.00109
40.00	.00782	-.00113
60.00	.00793	-.00116

[illegible] 10-28-69 EXTR. CREEP
CONFP=1.0000 DEVP=4.0000
HIGHT=2.8125DIAMR=1.3125

TIME	AXL.STRN	RDL.STRN
.10	-.33371	.03154
.20	-.33375	.03154
.40	-.33376	.03157
.60	-.33378	.03157
1.00	-.33387	.03160
2.00	-.33384	.03164
4.00	-.33386	.03167
6.00	-.33394	.03176
10.00	-.33397	.03183
20.00	-.33414	.03186
30.00	-.33417	.03186
40.00	-.33417	.03194
50.00	-.33416	.03189
60.00	-.33419	.03189

[illegible] 10-29-69 EXTR. CREEP
CONFP=1.0000 DEVP=4.5000
HIGHT=2.8125DIAMR=1.3125

TIME	AXL.STRN	RDL.STRN
.10	-.33420	.03177
.20	-.33435	.03187
.40	-.33434	.03200
.60	-.33436	.03206
1.00	-.33443	.03209
2.00	-.33453	.03209
4.00	-.33464	.03213
6.00	-.33472	.03216
10.00	-.33477	.03229
20.00	-.33496	.03229
30.00	-.33465	.03232
40.00	-.33483	.03245
50.00	-.33493	.03248
60.00	-.33489	.03242

4H 11-10-69 COMPN. CREEP
CONFP=1.0000 DEVP=4.7000
HIGHT=2.8125DIAMR=1.3125

TIME	AXL.STRN	RDL.STRN
.02	.00366	-.00038
.04	.00373	-.00039
.06	.00388	-.00041
.10	.00395	-.00042
.40	.00423	-.00045
1.00	.00430	-.00048
2.00	.00452	-.00049
4.00	.00459	-.00050
6.00	.00462	-.00052
10.00	.00466	-.00054
20.00	.00476	-.00055
40.00	.00498	-.00058
60.00	.00505	-.00059

2. Impact Compaction - 45 Blows - Kaolinite, cont.

AM 11-10-69 COMPN. CREEP		
CONFP=1.0000 DEVP=3.3200		
HIGHT=2.8125DIAMR=1.3125		
TIME	AXL.STRN	RDL.STRN
.02	.00205	-.00012
.04	.00213	-.00019
.06	.00220	-.00020
.10	.00226	-.00020
.40	.00240	-.00022
1.00	.00252	-.00023
2.00	.00258	-.00023
4.00	.00266	-.00023
6.00	.00268	-.00025
10.00	.00275	-.00025
20.00	.00281	-.00026
40.00	.00289	-.00027
60.00	.00294	-.00028

AM 11-10-69 COMPN. CREEP		
CONFP=1.0000 DEVP=1.9500		
HIGHT=2.8125DIAMR=1.3125		
TIME	AXL.STRN	RDL.STRN
.02	.00085	-.00006
.04	.00090	-.00006
.06	.00092	-.00007
.10	.00095	-.00007
.40	.00102	-.00007
1.00	.00108	-.00007
2.00	.00112	-.00007
4.00	.00115	-.00007
6.00	.00116	-.00008
10.00	.00122	-.00009
20.00	.00124	-.00009
40.00	.00132	-.00010
60.00	.00133	-.00010

3. Impact Compaction, 45 Blows - Kaolinite - Undrained and Partly Drained Tests.

15G 5-14-70 COMPN. CREEP
CONFP=0.0000 DEVP=1.0300
HIGHT=2.8125DIAMR=1.3125

TIME	AXL.STRN	RDL.STRN
.02	.00103	-.00003
.04	.00106	-.00003
.06	.00109	-.00003
.10	.00115	-.00003
.40	.00120	-.00003
1.00	.00125	-.00003
2.00	.00127	-.00003
4.00	.00132	-.00003
6.00	.00132	-.00003
10.00	.00133	-.00003
20.00	.00134	-.00003
40.00	.00138	-.00003
60.00	.00141	-.00003

15G 5-14-69 COMPN. CREEP
CONFP=0.0000 DEVP=4.7000
HIGHT=2.8125DIAMR=1.3125

TIME	AXL.STRN	RDL.STRN
.02	.00412	-.00071
.04	.00427	-.00072
.06	.00430	-.00073
.10	.00448	-.00079
.40	.00466	-.00081
1.00	.00498	-.00086
2.00	.00501	-.00088
4.00	.00512	-.00095
6.00	.00519	-.00096
10.00	.00526	-.00098
20.00	.00533	-.00100
40.00	.00565	-.00104
60.00	.00569	-.00107

5G 5-6-69 COMPN. CREEP
CONFP=1.0000 DEVP=1.9500
HIGHT=2.8125DIAMR=1.3125

TIME	AXL.STRN	RDL.STRN
.02	.00076	_.00011
.04	.00080	_.00012
.06	.00082	_.00012
.10	.00087	_.00013
.40	.00093	_.00013
1.00	.00098	_.00013
2.00	.00099	_.00014
4.00	.00104	_.00014
6.00	.00106	_.00014
10.00	.00107	_.00014
20.00	.00108	_.00014
40.00	.00114	_.00015
60.00	.00115	_.00015

15G 5-14-69 COMPN. CREEP
CONFP=0.0000 DEVP=1.9500
HIGHT=2.8125DIAMR=1.3125

TIME	AXL.STRN	RDL.STRN
.02	.00164	-.00012
.04	.00169	-.00012
.06	.00173	-.00012
.10	.00180	-.00012
.40	.00192	-.00012
1.00	.00198	-.00012
2.00	.00204	-.00012
4.00	.00212	-.00013
6.00	.00212	-.00013
10.00	.00214	-.00013
20.00	.00220	-.00014
40.00	.00221	-.00015
60.00	.00229	-.00015

15G 5-14-69 COMPN. CREEP
CONFP=0.0000 DEVP=6.5300
HIGHT=2.8125DIAMR=1.3125

TIME	AXL.STRN	RDL.STRN
.02	.00793	-.00207
.04	.00846	-.00220
.06	.00857	-.00225
.10	.00878	-.00233
.40	.00921	-.00241
1.00	.00935	-.00251
2.00	.00960	-.00257
4.00	.00971	-.00265
6.00	.00985	-.00273
10.00	.01006	-.00281
20.00	.01020	-.00297
40.00	.01045	-.00310
60.00	.01060	-.00317

5G 5-6-69 COMPN. CREEP
CONFP=1.0000 DEVP=2.8600
HIGHT=2.8125DIAMR=1.3125

TIME	AXL.STRN	RDL.STRN
.02	.00156	_.00024
.04	.00166	_.00027
.06	.00169	_.00028
.10	.00174	_.00028
.40	.00187	_.00030
1.00	.00196	_.00032
2.00	.00203	_.00032
4.00	.00206	_.00033
6.00	.00210	_.00034
10.00	.00214	_.00034
20.00	.00222	_.00038
40.00	.00229	_.00038
60.00	.00233	_.00041

15G 5-14-69 COMPN. CREEP
CONFP=0.0000 DEVP=2.8600
HIGHT=2.8125DIAMR=1.3125

TIME	AXL.STRN	RDL.STRN
.02	.00240	-.00026
.04	.00249	-.00028
.06	.00260	-.00029
.10	.00270	-.00030
.40	.00284	-.00031
1.00	.00288	-.00032
2.00	.00295	-.00033
4.00	.00299	-.00033
6.00	.00299	-.00035
10.00	.00302	-.00036
20.00	.00302	-.00036
40.00	.00331	-.00038
60.00	.00334	-.00039

5G 5-6-69 COMPN. CREEP
CONFP=1.0000 DEVP=1.0300
HIGHT=2.8125DIAMR=1.3125

TIME	AXL.STRN	RDL.STRN
.02	.00030	_.00004
.04	.00034	_.00004
.06	.00036	_.00004
.10	.00036	_.00004
.40	.00037	_.00004
1.00	.00039	_.00004
2.00	.00041	_.00004
4.00	.00042	_.00004
6.00	.00043	_.00004
10.00	.00044	_.00004
20.00	.00044	_.00004
40.00	.00047	_.00004
60.00	.00049	_.00004

5G 5-6-69 COMPN. CREEP
CONFP=1.0000 DEVP=4.7000
HIGHT=2.8125DIAMR=1.3125

TIME	AXL.STRN	RDL.STRN
.02	.00501	_.00125
.04	.00530	_.00132
.06	.00537	_.00134
.10	.00548	_.00137
.40	.00569	_.00141
1.00	.00583	_.00145
2.00	.00597	_.00149
4.00	.00604	_.00150
6.00	.00612	_.00152
10.00	.00626	_.00156
20.00	.00640	_.00161
40.00	.00647	_.00165
60.00	.00658	_.00170

3. Impact Compaction, 45 Blows - Kaolinite - Undrained and Partly Drained Tests, cont.

50 5-6-69 COMPN. CREEP
CONFP=1.0000 DEVP=6.5360
HIGHT=2.8125DIAMP=1.3125

TIME	AXL.STRN	RDL.STRN
.02	.00935	-.00300
.04	.00974	-.00318
.06	.00988	-.00327
.10	.01006	-.00328
.40	.01063	-.00354
1.00	.01106	-.00360
2.00	.01138	-.00370
4.00	.01173	-.00383
6.00	.01195	-.00392
10.00	.01227	-.00408
20.00	.01273	-.00434
40.00	.01316	-.00450
60.00	.01351	-.00470

4. Impact Compaction, 45 Blows - Kaolinite - First Loading Period of One Minute.

TG 4-30-63 COMPR. CREEP
CONFP=0.0000 DEVP=.5388
HIGHT=7.8125 DIAM=1.3125

TIME	AXI. STRN	VOL. STRN
.02	.00715	-.00241
.04	.00743	-.00249
.06	.00757	-.00255
.10	.00779	-.00260
.40	.00818	-.00277
1.00	.00859	-.00289
2.00	.00883	-.00297
4.00	.00906	-.00313
6.00	.00896	-.00322
10.00	.00924	-.00334
20.00	.00947	-.00347
40.00	.00974	-.00364
60.00	.00999	-.00388

TG 4-30-63 COMPR. CREEP
CONFP=0.0000 DEVP=1.9588
HIGHT=7.8125 DIAM=1.3125

TIME	AXI. STRN	VOL. STRN
.02	.00173	-.00418
.04	.00181	-.00011
.06	.00186	-.00011
.10	.00191	-.00012
.40	.00204	-.00013
1.00	.00213	-.00013
2.00	.00222	-.00013
4.00	.00229	-.00014
6.00	.00233	-.00015
10.00	.00241	-.00014
20.00	.00249	-.00014
40.00	.00247	-.00017
60.00	.00258	-.00018

5. Static Compaction - 10.54 kg/sq. cm. - Specimens from Footing Tests - Grundite.

G1 12-22-70 COMPN. CREEP
CONFP=0.0000 DEVP= .9600
HIGHT=2.8250DIAMR=1.2850

TIME	AXL.STRN	RDL.STRN
.02	.00147	-.00001
.04	.00155	-.00001
.06	.00158	-.00001
.10	.00160	-.00001
.40	.00168	-.00001
1.00	.00175	-.00001
2.00	.00178	-.00001
4.00	.00183	-.00001
6.00	.00186	-.00001
10.00	.00191	-.00001
20.00	.00196	-.00001
40.00	.00204	-.00001
60.00	.00212	-.00001

G1 12-22-70 COMPN. CREEP
CONFP=0.0000 DEVP=3.8250
HIGHT=2.8250DIAMR=1.2850

TIME	AXL.STRN	RDL.STRN
.02	.00499	-.00039
.04	.00535	-.00057
.06	.00552	-.00069
.10	.00566	-.00076
.40	.00598	-.00084
1.00	.00609	-.00092
2.00	.00630	-.00094
4.00	.00637	-.00100
6.00	.00644	-.00101
10.00	.00665	-.00105
20.00	.00673	-.00110
40.00	.00697	-.00117
60.00	.00708	-.00123

G5 12-29-70 COMPN. CREEP
CONFP=1.5000 DEVP=2.8450
HIGHT=2.8130DIAMR=1.3260

TIME	AXL.STRN	RDL.STRN
.02	.00184	-.00009
.04	.00187	-.00010
.06	.00196	-.00011
.10	.00201	-.00011
.40	.00212	-.00011
1.00	.00216	-.00011
2.00	.00222	-.00011
4.00	.00228	-.00011
6.00	.00231	-.00011
10.00	.00236	-.00011
20.00	.00243	-.00011
40.00	.00252	-.00011
60.00	.00258	-.00011

G1 12-22-70 COMPN. CREEP
CONFP=0.0000 DEVP=1.9120
HIGHT=2.8250DIAMR=1.2850

TIME	AXL.STRN	RDL.STRN
.02	.00234	-.00004
.04	.00248	-.00004
.06	.00250	-.00004
.10	.00257	-.00005
.40	.00265	-.00006
1.00	.00275	-.00007
2.00	.00283	-.00007
4.00	.00290	-.00007
6.00	.00292	-.00008
10.00	.00301	-.00009
20.00	.00310	-.00011
40.00	.00319	-.00011
60.00	.00324	-.00011

G5 12-29-70 COMPN. CREEP
CONFP=1.5000 DEVP=1.9440
HIGHT=2.8130DIAMR=1.3260

TIME	AXL.STRN	RDL.STRN
.02	.00043	-.00004
.04	.00044	-.00004
.06	.00044	-.00005
.10	.00044	-.00005
.40	.00046	-.00005
1.00	.00050	-.00005
2.00	.00051	-.00005
4.00	.00052	-.00005
6.00	.00053	-.00005
10.00	.00053	-.00005
20.00	.00054	-.00006
40.00	.00058	-.00006
60.00	.00061	-.00006

G1 12-22-70 RECOVERY
HIGHT=0.0000 DEVP= .9600
HIGHT=2.8125DIAMR=1.3125

TIME	AXL.STRN	RDL.STRN
1.00	.00080	0.00000
2.00	.00071	0.00000
4.00	.00065	0.00000
6.00	.00062	0.00000
8.00	.00059	0.00000
10.00	.00054	0.00000
20.00	.00050	0.00000
30.00	.00044	0.00000

G1 12-22-70 RECOVERY
HIGHT=0.0000 DEVP=1.9120
HIGHT=2.8125DIAMR=1.3125

TIME	AXL.STRN	RDL.STRN
1.00	.00101	0.00000
2.00	.00090	0.00000
4.00	.00079	0.00000
6.00	.00072	0.00000
8.00	.00070	0.00000
10.00	.00066	0.00000
20.00	.00054	0.00000
30.00	.00053	0.00000

G1 12-22-70 COMPN. CREEP
CONFP=0.0000 DEVP=2.8650
HIGHT=2.8250DIAMR=1.2850

TIME	AXL.STRN	RDL.STRN
.02	.00389	-.00045
.04	.00411	-.00047
.06	.00421	-.00049
.10	.00424	-.00051
.40	.00457	-.00055
1.00	.00464	-.00056
2.00	.00478	-.00059
4.00	.00488	-.00062
6.00	.00496	-.00065
10.00	.00499	-.00066
20.00	.00520	-.00069
40.00	.00531	-.00074
60.00	.00552	-.00076

G5 12-29-70 COMPN. CREEP
CONFP=1.5000 DEVP=1.9450
HIGHT=2.8130DIAMR=1.3260

TIME	AXL.STRN	RDL.STRN
.02	.00105	-.00012
.04	.00107	-.00013
.06	.00110	-.00013
.10	.00112	-.00013
.40	.00116	-.00014
1.00	.00118	-.00014
2.00	.00124	-.00014
4.00	.00127	-.00014
6.00	.00130	-.00015
10.00	.00133	-.00015
20.00	.00137	-.00015
40.00	.00143	-.00016
60.00	.00149	-.00016

G1 12-22-70 RECOVERY
HIGHT=0.0000 DEVP=2.8650
HIGHT=2.8125DIAMR=1.3125

TIME	AXL.STRN	RDL.STRN
1.00	.00178	-.00029
2.00	.00174	-.00029
4.00	.00171	-.00029
6.00	.00164	-.00029
8.00	.00149	-.00029
10.00	.00146	-.00029
20.00	.00142	-.00029
30.00	.00135	-.00029

5. Static Compaction - 10.54 kg/sq. cm. - Specimens from Footing Tests - Grundite, cont.

G1 12-22-70 RECOVERY
HIGHT=0.0000 DEVP=3.8250
HIGHT=2.8125DIAMR=1.3125

TIME	AXL.STRN	RDL.STRN
1.00	.00188	-.00056
2.00	.00171	-.00055
4.00	.00146	-.00055
6.00	.00142	-.00055
8.00	.00135	-.00055
10.00	.00121	-.00054
20.00	.00110	-.00053
30.00	.00107	-.00053

G5 12-29-70 RECOVERY
CONFP=1.5000 DEVP=1.0440
HIGHT=2.8130DIAMR=1.3260

TIME	AXL.STRN	RDL.STRN
1.00	.00009	-.00001
2.00	.00009	-.00001
4.00	.00008	-.00001
6.00	.00007	-.00000
8.00	.00005	-.00000
10.00	.00005	-.00000
20.00	.00003	-.00000
30.00	.00001	-0.00000

G5 12-29-70 RECOVERY
CONFP=1.5000 DEVP=1.9450
HIGHT=2.8130DIAMR=1.3260

TIME	AXL.STRN	RDL.STRN
1.00	.00052	-.00003
2.00	.00047	-.00003
4.00	.00044	-.00003
6.00	.00042	-.00003
8.00	.00037	-.00003
10.00	.00036	-.00003
20.00	.00035	-.00003
30.00	.00029	-.00003

G5 12-29-70 RECOVERY
CONFP=1.5000 DEVP=2.8450
HIGHT=2.8130DIAMR=1.3260

TIME	AXL.STRN	RDL.STRN
1.00	.00079	-.00005
2.00	.00071	-.00004
4.00	.00064	-.00004
6.00	.00062	-.00004
8.00	.00059	-.00004
10.00	.00055	-.00004
20.00	.00051	-.00003
30.00	.00044	-.00003

VITA

VITA

S. V. Ramaswamy was born on August 18, 1937, in Madras, India. He had his high school education in Sir. M. Ct. Muthiah Chettiar High School (1953) followed by the Intermediate in Science at Loyola College (1955), Madras. He then entered Government College of Engineering, Guindy, Madras and received his Bachelor's degree in Civil Engineering from Madras University in 1959.

He joined the technical teacher's program sponsored by government of India in September, 1959. He spent a total of six months in Parambikulam-Aliyar project during the summers of 1960 and 1962 and obtained his Master of Science degree in soil mechanics and foundation engineering from Madras University in 1961, as part of the program. At the conclusion of the training, he was appointed Lecturer in Civil Engineering in the same college in 1962 and was subsequently promoted to Assistant Professor in 1965. He received a study leave in September 1966 to attend Purdue University for his Ph.D. studies. He was working as a graduate research instructor during his stay at Purdue.

Mr. Ramaswamy is a Registered Professional Engineer in Indiana; Associate Member of Institution of Engineers, India; Associate Member of American Society of Civil Engineers; and

Member, International Society of Soil Mechanics and Foundation Engineering.

His writing activity includes publications both in India and United States.

He is unmarried and a citizen of India.